ISSN: 1945-3094 Volume 2, Number 6, June 2010

Scientific Research

Journal of Water Resource and Protection

Editor-in-Chief : Jian Shen

ISSN: 1945-3094

9 771945 309008 06

www.scirp.org/journal/jwarp

ISSN: 1945-3094 (Print) ISSN: 1945-3108 (Online)

http://www.scirp.org/journal/jwarp

J. Water Resource and Protection, **2010, 2, 501-608**
Published Online June 2010 in SciRes (http://www.SciRP.org/journal/jwarp/)

TABLE OF CONTENTS

Volume 2 Number 6 June 2010

Journal of Water Resource and Protection (JWARP)

Journal Information

SUBSCRIPTIONS

The *Journal of Water Resource and Protection* (Online at Scientific Research Publishing, www.SciRP.org) is published monthly by Scientific Research Publishing, Inc., USA.

Subscription rates:

Print: $50 per issue.
To subscribe, please contact Journals Subscriptions Department, E-mail: sub@scirp.org

SERVICES

Advertisements
Advertisement Sales Department, E-mail: service@scirp.org

Reprints (minimum quantity 100 copies)
Reprints Co-ordinator, Scientific Research Publishing, Inc., USA.
E-mail: sub@scirp.org

COPYRIGHT

Statements and opinions expressed in the articles and communications are those of the individual contributors and not the statements and opinion of Scientific Research Publishing, Inc. We assumes no responsibility or liability for any damage or injury to persons or property arising out of the use of any materials, instructions, methods or ideas contained herein. We expressly disclaim any implied warranties of merchantability or fitness for a particular purpose. If expert assistance is required, the services of a competent professional person should be sought.

PRODUCTION INFORMATION

For manuscripts that have been accepted for publication, please contact:
E-mail: jwarp@scirp.org

J. Water Resource and Protection, 2010, 2, 501-506
doi:10.4236/jwarp.2010.26057 Published Online June 2010 (http://www.SciRP.org/journal/jwarp)

Increasing the Efficiency of Transboundary Water Management: A Regionalization Approach

Dirk Huchtemann[1], Manuel Frondel[2]
[1]*Forschungszentrum Juelich GmbH, Juelich, Germany*
[2]*Rheinisch-Westfälisches Institut für Wirtschaftsforschung, Essen, and Ruhr-Universität Bochum, Bochum, Germany*
E-mail: *d.huchtemann@fz-juelich.de, frondel@rwi-essen.de*
Received December 18, 2009; *revised April* 23, 2010; *accepted May* 6, 2010

Abstract

In this paper, we develop a methodological approach to increase the efficiency of watershed management approaches that focuses on the reduction of diffuse water pollution. The basic idea is that the efficiency may be improved by identifying and constituting homogenous groups of contiguous administrative units of a watershed, which jointly implement water pollution reduction measures. Homogeneity means similarity of group members with respect to a set of local and environmental characteristics, such as the degree of pollution and abatement costs. We empirically apply our methodology to the watershed of the German river Ems and identify homogenous groups of contiguous administrative units using cluster analysis methods implemented in a Geographical Information System.

Keywords: Diffuse Water Pollution, Environmental Federalism, Cluster Analysis, EU Water Framework Directive

1. Introduction

Nitrate and phosphorus entry into surface water mainly originates from mineral and organic fertilizers employed in the agricultural sector. This sector is responsible for the vast majority of diffuse—or non-point-source—water pollution in Germany. Within the period 1993 to 1997, the average contribution of the agricultural sector to the overall nitrate and phosphorus entry from non-point sources was as large as 94.1% and 83.7%, respectively [1]. In contrast to pollutants originating from point sources, such as sewage disposal systems and livestock facilities, pollutants from non-point sources, such as agricultural drainage, are difficult to combat.

Diffuse water pollution disperses, thereby affecting less polluted areas and, specifically, potable water resources. Nitrate and phosphorus entries, the two most significant water pollutants, lead to the turbidity and malodor of surface water, as well as its accelerated eutrophication. Given all these undesirable effects, the further reduction of diffuse pollution is a major goal of the EU Water Framework Directive 2000/60/EC (Article 10), although the level of diffuse pollution has been significantly reduced during the past twenty years [2].

Article 3 of this directive demands the coordination of water management within river basin districts, which usually belong to several administrative units such as federal states. As a result, watersheds are affected by frequently distinct and simultaneous actions of several administrations, and possible deficiencies in coordination may create inefficiencies [3].

In this paper, we develop a methodological approach to improve the economic efficiency in the reduction of diffuse water pollution. It rests on the identification and formation of homogenous groups of contiguous administrative units of a watershed. By jointly implementing pollution reduction measures, these homogenous groups are able to diminish negative spillover effects and externalities. Homogeneity refers to characteristics such as willingness-to-pay for pollution reduction, abatement costs, and the degree of pollution, which varies with, e.g., agricultural production.

Our methodology proposed, commonly referred to as a *regionalization approach* [4], is exemplified here by an application to the German side of the watershed of the river Ems. To identify homogenous groups of administrative units within this watershed, we use cluster analysis methods implemented in a Geographical Information System (GIS). As the implementation of joint pollution mitigation measures is only sensible and manageable in contiguous areas, the spatial relationship among administrative units is an essential variable for this cluster analysis.

In the following section, we explain our regionalization approach. Section 3 provides a concise description of our sample region. Empirical results for our sample region are presented in Section 4. The last section summarizes our findings and provides conclusions.

2. Methodological Framework

To avoid negative spill-over effects and inefficiencies due to the divergence between natural watershed areas and districts, the prevailing administration units, we suggest designing new artificial administrative structures consisting of contiguous sets of communities that are – in terms of diffuse water pollution, abatement costs, etc. – more homogeneous than the districts For this purpose, we must address two methodological issues: 1) the definition of a set of homogeneity criteria and 2) the measurement of homogeneity levels.

In our example of the Ems watershed, the German stretch of which covers 227 communities and 22 districts, the set of homogeneity criteria consists of two variables: *abatement cost* and *discharge rates of nitrate.* Assuming that the livestock density in the agricultural sector is limited to only one animal unit per hectare, the abatement cost data originates from an agro-economic forecast model called RAUMIS [5], which was applied within the interdisciplinary research project REGFLUD[1]. This project is also the source for the data on *discharge rates of nitrate*, which was determined using a GIS-based model developed at Forschungszentrum Jülich.

Given that the implementation of joint water pollution mitigation measures is only sensible and manageable for contiguous administrative units, our clustering approach takes particular account of the spatial relationships of the communities (on cluster analysis and other regionalization approaches see [8] and [9]). Our approach is therefore embedded in a Geographic Information System (GIS). To show the importance of taking spatial relationships into account, **Figure 1** displays the outcome of an artificial clustering example when spatial distances among communities are either neglected or accounted for.

This illustrative example, inspired by [10], comprises 16 communities and two variables: discharge rates of nitrate and abatement costs. If spatial relationships are ignored, the resulting clusters, called classes, are usually not contiguous and exhibit conjoint borderlines only by chance, as indicated by the left-hand side of the lower part of **Figure 1**. In contrast, taking account of spatial relationships leads to so-called regions, that is, clusters that exclusively consist of contiguous administrative units, as shown on the right-hand side of the lower part of **Figure 1**.

In contrast to e.g. [11], who employ a contiguity matrix to capture spatial relationships, we proceed by determining artificial epicenters for each unit − called centroids − and including their x- and y-coordinates to our cluster analysis. The advantage of our method compared to approaches using a contiguity matrix is the parsimonious number of variables: We only need to add two additional variables, CX and CY, indicating the x- and y-positions of all centroids, rather than a matrix containing the information about spatial relationships among all administrative units, which, in practice, requires hundreds of variables [11].

In short, we are left with merely four variables − abatement costs, discharge rates of nitrate, CX, and CY − for our cluster analysis, rather than several hundred variables. For operational convenience, we simply assign equal weights to these four variables. Any unequal weighting scheme − for instance, by assigning lower weights to the geographical variables CX, and CY because the other variables are regarded as more important − would be arbitrary.

Additionally, we need a measure that helps us to decide whether two communities, say, *p* and *q*, are similar to each other regarding the set of selected variables. Among a variety of such measures (see [12]), we choose the *Squared Euclidian metric*:

$$d_{pq} = \sum_{j=1}^{N} (x_j^p - x_j^q)^2 , \qquad (1)$$

with x_j^p and x_j^q denoting the concrete realizations of variable X_j for community *p* and *q*, respectively. Before calculating the Squared Euclidian distances d_{pq}, one has to standardize the variables. Upon standardization, each of the transformed variables displays zero mean and a uniform standard deviation of 1.

The more similar two communities are the closer to zero is the Squared Euclidian metric. Eventually, we come up with a symmetric (227 × 227) matrix (d_{pq}), representing the basis for the clustering procedure. We then need to choose among several clustering algorithms that help us to identify the ultimate number of clusters such that the heterogeneity across, and the homogeneity within, all clusters is maximized. For this purpose, we have chosen the centroid method[2] (see [13] for other methods).

The second methodological issue refers to the measurement of the homogeneity of our cluster analysis out

[1]The overall objective of REGFLUD was the development and application of multi-criteria scientific methods to set up a Decision Support System aimed at reducing nonpoint source pollution in river catchments subject to economic feasibility and social acceptability. The project was funded by the Federal Ministry of Education and Research (BMBF) [6,7].

[2]The centroids used in this clustering algorithm must not be confused with geographic centroids: These centroid vectors include the coordinates of geographic centroids, but also the respective values of the variables *abatement cost* and *discharge rates of nitrate*.

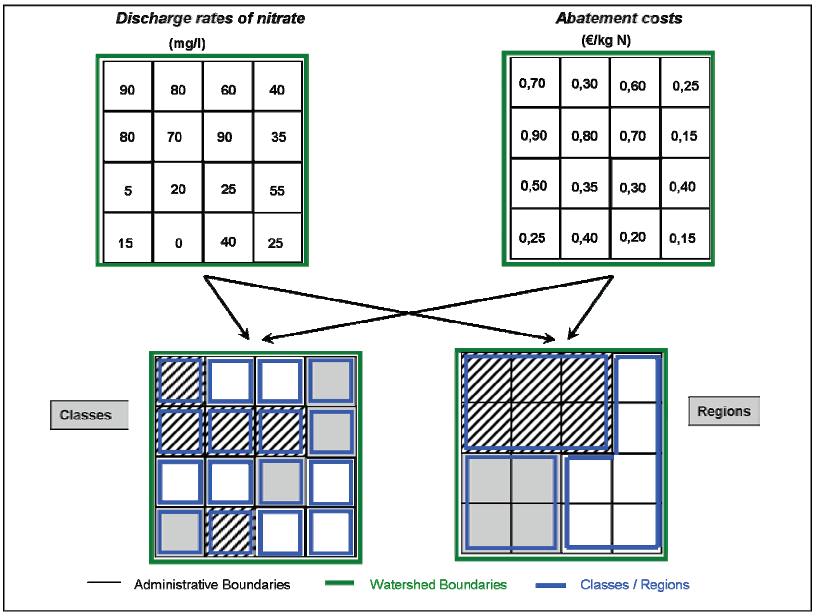

Figure 1. Clustering with and without incorporating spatial distances of communities.

comes — the set of output clusters. Commonly, homogeneity is examined for each criteria variable X_j individually. Homogeneity tests are based on a statistical measure defined as the ratio of the within-cluster variance $Var^G(X_j)$ of a given cluster G and the between-cluster variance $Var(X_j)$:

$$F := \frac{Var^G(X_j)}{Var(X_j)}. \quad (2)$$

The letter F indicates that the probability distribution of this test statistic is the F-distribution. While the F-value of a cluster that is perfectly homogeneous with respect to criteria variable X_j is zero, such desirable values do not occur in practice. In contrast, an F value equaling, or even exceeding, unity is not desirable. In this case, the within-cluster variance equals, or is even larger than, the respective between-cluster variance, which contradicts the inherent idea of clustering. Of course, the preferred result of any clustering approach is that all the clusters' F-values are substantially smaller than unity for *all* criteria variables. In this case, the clusters are called *totally homogeneous.*

For interpretational purposes, another test statistic is frequently employed. It is based on the relative difference of the within-cluster means $\bar{X}_j^G$ for a given cluster G and $\bar{X}_j$, which is the sample mean of criteria variable X_j:

$$t = \frac{\bar{X}_j^G - \bar{X}_j}{std(X_j)}, \quad (3)$$

with $std(X_j)$ denoting the sample standard deviation of variable X_j. This test statistic, which follows Student's t distribution, reflects the relative deviation of a cluster G from the respective sample means. A large t-value indicates that a cluster G differs strongly from the sample average of variable X_j.

3. Sample Region

Our approach is applied to the German side of the watershed of the river Ems, the region displayed in green in **Figure 2**. The major part of this watershed is located in the North-West of Germany and stretches across the boundaries of two federal states, North-Rhine Westphalia and Lower Saxony. 227 German communities are either completely located in this watershed or share a significant part of it. The Dutch side of the watershed - displayed in light green in **Figure 2 -** must be ignored in our application due to the lack of data.

The Ems watershed covers a wide range of different landscapes, exhibiting different hydrological, hydrogeological, and socio-economic characteristics. Agricultural production, particularly livestock farming, dominates the north-eastern part of this region, which is characterized by meagre, sandy soils. The dominance of livestock farming causes an abundance of organic fertilizers in the form of liquid manure. Generally, this liquid manure, commonly distributed to agricultural acreage, leads to nitrate entry into surface water and, hence, diffuse water pollution. Its degree depends upon the type of soil and the varying nitrate retention and degradation ability.

4. Regionalization of the Ems Watershed

In this section, we apply our regionalization approach to

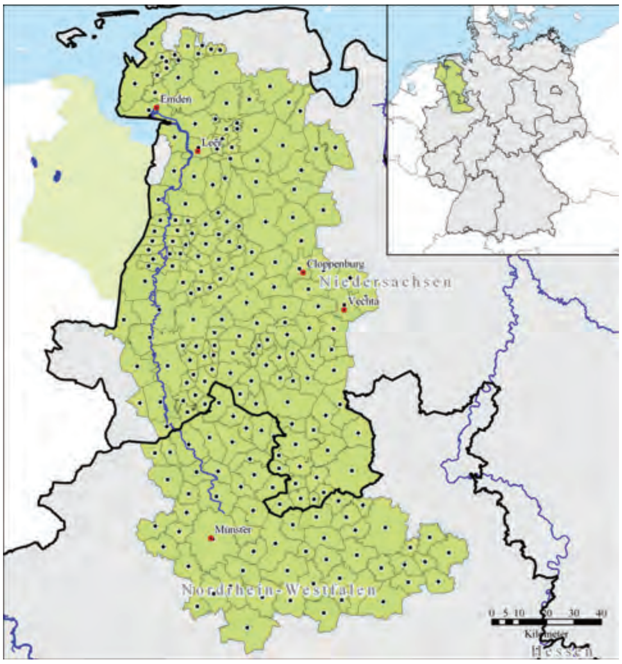

Figure 2. The Ems watershed and its communities in Germany.

the communities of the German side of the watershed of the river Ems. Our aim is to identify contiguous clusters among the 227 communities that are more homogeneous with respect to *abatement costs* and *discharge rates of nitrate* than the prevailing administrative units (districts). Using the method described in Section 2, we end up with 22 clusters, which is only by chance equal to the number of districts. All outcome clusters displayed in **Figure 3** are indeed contiguous groups of communities and most of these clusters are substantially different from the prevailing districts, although there are some similarities.

As a major result, the incongruity of district and cluster borderlines shown in **Figure 3** indicates that the homogeneity among communities with respect to abatement cost and discharge rates of nitrate might be improved by re-grouping these communities along the lines of the outcome of our cluster analysis. F-values reported in **Table 1** are well below the critical value of 1 for all clusters, indicating that the clustering outcome is totally homogenous with respect to the variables *discharge rates of nitrate* and *abatement costs*.

It is somewhat surprising that, except for three heterogeneous groups of communities, the prevailing administrative structure given by the districts of the Ems watershed appears to be quite homogeneous.

The *t*-values reported in **Table 1** indicate that the abatement costs of clusters 8, 9, 10, 15, 16, 17, 21, and 22 are significantly larger than on average. With the exception of clusters 8 and 16, these clusters also display larger nitrate discharge rates than the sample average. Yet, there is no perfect positive correlation between nitrate

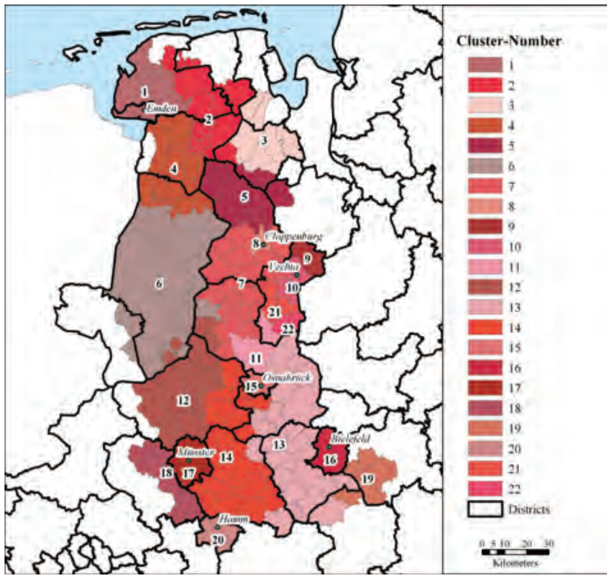

Figure 3. The outcome of a regionalization approach: Clusters of the Ems watershed.

entries and abatement cost, since the clusters 1, 4, 12, 13, 14, and 18 exhibit discharge rates of nitrate that are above the sample average, whereas the abatement costs of these clusters a below the average.

5. Summary and Conclusions

Current watershed management practices in Germany, as well as in other European countries, usually do not take particular account of the hydrological boundaries of watersheds. Yet, the fact that international and interregional watersheds are affected by the frequently distinct but simultaneous actions of several administrative units, such as districts, typically creates inefficiencies. Identifying and clustering adjacent communities of watersheds that are more homogeneous groups than the prevailing districts and that will then jointly implement pollution reduction measures has been suggested in this paper as a way to potentially increase the efficiency of watershed management.

Using cluster analysis methods, our regionalization approach is perfectly in line with Article 3 of the EU Water Framework Directive 2000/60/EC, which demands the coordination of the water management within river basin districts. Our approach is based on the theory of environmental federalism that deals with the efficient assignment of federal competencies − see, for example, [14]. Constitutional elements of this theory are the *principles* of *subsidiarity* and *fiscal equivalence* [15,16]. The principle of subsidiarity implies that competencies ought to be assigned to the lowest federal level that suffices to meet a certain task. The efficient provision of, specifically, the public good "clean water" requires the matching of the natural areas of watersheds with administra-

Table 1. Regionalization outcome.

Cluster	*Number of Communities*	*F-values abatement cost*	*t-values abatement cost*	*F-values nitrate*	*t-values nitrate*
1	12	0.009	-0.491	0.119	0.415
2	19	0.006	-0.426	0.285	-1.138
3	6	0.004	-0.245	0.239	-0.538
4	18	0.021	-0.297	0.422	1.235
5	7	0.832	0.808	0.733	1.066
6	51	0.036	-0.312	0.295	-0.897
7	22	0.298	0.078	0.172	-0.324
8	1	-	3.510	-	-0.495
9	2	0.001	2.214	0.005	1.139
10	2	0.440	7.285	0.032	0.699
11	3	0.795	0.886	0.222	0.987
12	18	0.062	-0.148	0.102	0.107
13	27	0.064	-0.149	0.179	0.231
14	21	0.040	-0.199	0.366	0.999
15	1	-	4.378	-	0.791
16	1	-	1.587	-	-0.764
17	1	-	1.341	-	0.222
18	6	0.003	-0.223	0.128	1.926
19	6	0.024	-0.245	0.662	-1.088
20	1	-	-0.413	-	-0.846
21	3	0.716	2.279	0.049	0.492
22	1	-	4.117	-	1.896

Note that for degenerated "clusters" including only one community *F*-values are undefined.

tive territories, and is in accordance with the principle of fiscal equivalence, which is also called perfect mapping.

According to [17], there are three criteria characterizing an ideal administrative unit: 1) Preferences for a public good, such as clean water, need to be homogenous among inhabitants of such a unit; 2) costs for the provision of this public good must be similar within the administrative unit, and 3) specific policy measures aimed at improving the provision of the public good must *only* affect this unit's area (*ideal geographical scope*).

Along the lines of these ideas, we have developed a regionalization approach that has been empirically applied to the communities belonging to the German side of the watershed of the river Ems. Since the implementation of joint pollution mitigation measures is only sensible and manageable in adjacent areas, it is critical to cluster this watershed's communities in such a way that the resulting clusters build contiguous areas. Hence, the spatial relationship among administrative units is an essential variable for any cluster analysis employed to identify more homogeneous clusters of communities than the prevailing districts within this watershed. We therefore use cluster analysis methods implemented in a Geographical Information System (GIS). Homogeneity means that communities are similar regarding a defined set of variables, such as the degree of pollution and abatement costs for water pollution reduction.

The results based on empirical data on abatement costs and average nitrate discharge rates of our sample communities demonstrate that the suggested methodological approach allows for creating regions that are more homogeneous than the prevailing districts, *i.e.*, the current administrative units. The resulting regionalization, however, represents only one possible spatial structure. Further research has to concentrate on determining and comparing the magnitude of the efficiency gains from different solutions.

Moreover, such reorganization might be problematic, because it might interfere with the current administrative structure and therefore may cause substantial legal problems that, ultimately, may hamper the desired watershed cooperation [18]. Nevertheless, the results of our regionalization approach may be useful when attempting to implement the EU Water Framework Directive.

6. Acknowledgments

We are grateful for invaluable comments and suggestions by Christoph M. Schmidt and Colin Vance. We also gratefully acknowledge funding by the Federal Ministry of Education and Research (BMBF) within the framework of the REGFLUD project.

7. References

[1] FME, “Water Resources Management: Emissions into Surface Waters and the Sea,” Federal Ministry for the Environment, Nature Conservation and Nuclear Safety, Berlin, 2001, pp. 49-51.

[2] FME, ibid, p. 58.

[3] T. Moss and H. J. Kujath, “Chancen und Grenzen des Institutionenwandels,” *Nachhaltige Entwicklung in der Wasserwirtschaft*: *Konzepte, Planung und Entscheidungsfindung, Schriftenreihe Wasserforschung,* B. Weigert and C. Steinberg, Eds., Berlin, Vol. 7, No. 1, 2001, pp. 305-324.

[4] R. J. Johnston, D. Gregory and D. M. Smith, Eds., “The Dictionary of Human Geography,” 3rd Edition, Oxford, 1997, pp. 71-87.

[5] H. Gömann, P. Kreins, R. Kunkel and F. Wendland, “Koppelung agrakökonomischer und Hydrologischer Modelle,” STE-Reprint 29/2003, Jülich, 2003.

[6] P. Kreins, H. Becker, D. Hecht, D. Huchtemann and F. Wendland, “Management regionaler Flusseinzugsgebiete in Deutschland (REGFLUG) – Rahmenbedingungen und Politikoptionen bei diffusen Nährstoffeinträgen (n und P) der Landwirtschaft in den Rhein und die Ems,” *Interdisziplinäre Methoden des Flussgebietmanagements*, J. Möltgen and D. Petry, Eds., IfGI Prints 21, University of Münster, Münster, 2004.

[7] http://www.faa-bonn.de/reghome.htm

[8] B. S. Everitt, S. Landau and M. Leese, “Cluster Analysis,” 4th Edition, Oxford University Press, Oxford, 2001.

[9] J. C. Duque, R. Ramos and J. Surinach, “Supervised Regionalization Methods: A Survey,” *International Regional Science Review*, Vol. 30, No. 3, 2007, pp. 195-220.

[10] G. Urfei, “Agrarumweltpolitik nach den Prinzipien der Ökonomischen Theorie des Föderalismus – Ein Regionalisierungsansatz zur Territorialen Abgrenzung Effizienter Politikaktionsräume,” Dunker und Humblot, Berlin, 1999.

[11] D. Martin, “Developing the Automated Zoning Procedures to Reconcile Incompatible Zoning Systems,” *Proceedings of the* 6*th* *International Conference on GeoComputation* 2001, University of Queensland, Brisbane, 2001.

[12] B. S. Everitt, S. Landau and M. Leese, ibid, pp. 35-45.

[13] B. S. Everitt, S. Landau and M. Leese, ibid, pp. 55-89.

[14] W. E. Oates, “A Reconsideration of Environmental Federalism,” *Recent Advances in Environmental Economics*, J. A. List and A. J. DeZeeuw, Eds., Edward Elgar, Cheltenham, 2002.

[15] A. Breton, “A Theory of Government Grants,” *Canadian Journal of Economics and Political Science*, Vol. 31, No. 2, 1965, pp. 175-187.

[16] J. Buchanan, “An Economic Theory of the Clubs,” *Economica*, Vol. 34, No. 3, 1965, pp. 1-14.

[17] M. Olson, “The Principle of ‘Fiscal Equivalence’: The Division of Responsibilities among Different Levels of Government,” *American Economic Review*, Vol. 59, No. 2, 1969, pp. 479-487.

[18] T. Moss, “Raumwissenschaftliche Perspektiverweiterung zur Umsetzung der EU-Wasserrahmenrichtlinie, Das Flussgebiet als Handlungsraum,” *Institutionenwandel durch die EU-Wasserrahmenrichtlinie aus raumwissenschaftlichen Perspektiven, Stadtund Regionalwissenschaften*, Bd. 3, Lit Verlag, Münster, 2003.

J. Water Resource and Protection, 2010, 2, 507-526
doi:10.4236/jwarp.2010.26058 Published Online June 2010 (http://www.SciRP.org/journal/jwarp)

The Upper Jordan River Algal Communities are Evidence of Long-Term Climatic and Anthropogenic Impacts

Sophia S. Barinova*, Eviatar Nevo
Institute of Evolution, University of Haifa, Mount Carmel, Israel
E-mail: *barinova@research.haifa.ac.il, nevo@research.haifa.ac.il*
Received March 25, 2010; *revised April* 23, 2010; *accepted May* 6, 2010

Abstract

Spatial and temporal algal diversity changes were studied in the major drinking water source of Israel - the Upper Jordan River. During 2006-2009, we found 232 species and infraspecies of algae and cyanobacteria: 85 of which were new for the Upper Jordan River Basin including three new for Israel. During many years of study of the Upper Jordan River, we collected information for the database of algal diversity. Historical analysis from 1883 to 2009 shows fluctuation of the whole algal diversity. Environmental indicator species show peaks in 1951, 1965, 1978, and 2009. Salinity impact was found in 1938 and 2000; acidification was detected in 1938, 1996, and 2000, and organic pollution, in 1996. Therefore, we can conclude that 1938, 1996, and 2000 were critical periods for the Upper Jordan River ecosystem. Indication of the trophic status shows stress of organic pollution since the 1970s, which was marked by dramatic increases in eutraphentic and hypereutraphentic species. The present analysis shows three peaks in the fluctuation in diversity throughout the river canal, which correlated with the organic pollution impact from the Masade village effluence in the middle reaches and near Lake Kinneret. Pollution was significant in rainy winters and stimulated species diversity development. The different approaches in comparing diversity in each river of the Upper Jordan Basin revealed that hydrology is a major regulating factor in species composition of the algal communities, which were formed under the influence of regional climatic factors. Therefore, the river can be highlighted as a natural system with high buffering and a self-purification capacity at the present time.

Keywords: Algal Communities, Bio-Indication, Climate Change, Comparative Floristic, Israel, Jordan River

1. Introduction

Biodiversity of algal communities in the Upper Jordan River formed according to natural climatic and anthropogenic impacts on various aquatic ecosystems. In the eastern Mediterranean region river algal diversity research is not very developed, whereas algal monitoring studies of aquatic systems on European coasts [1,2] have advanced rather well. In Israel, our knowledge of regional algal diversity is far from exhaustive, and algal communities of the rivers were not regularly studied till 2000 [3].

For many years, we have collected data on algal diversity for the Upper Jordan River. The data enables us to analyze the changes in community structure from the beginning of researches at the end of the 18th century till the present time. Moreover, we can most likely track the dynamics of species-indicators that can help us determine the time of impact and the direction of environmental influences on the algal communities.

Therefore, we decided to study spatial and temporal algal diversity changes in Israel's major drinking water resource – the Upper Jordan River, in respect to the fluctuation of water parameters affected by the anthropogenic impact and seasonal climate changes.

The main characteristic of Israeli climate is a short winter rainy season, which lasts from December till April. The Upper Jordan River water sources and their dynamics are similar to some of the same dynamics as those described from Southern Lebanon [4]. Algal communities as a basis for the trophic pyramid play a significant role in the water-quality forming process. Periphytonic communities show a strong potential for the recovery of ecosystems in the Mediterranean region [5-9]. Recently, we compared seasonal influences on Yarqon River communities in Israel [10]. Under similar climatic conditions and floristic realms, diatom algal communities were studied according to the same seasonal environmental factors as in the rivers of Egypt [11], Lebanon [12], and Turkey [13,14]. All of these mentioned rivers as well as the Upper Jordan River do not have a strong anthropogenic impact. Possible methods used to reveal the many influences of species indicators are: community structure fluctuation analysis, bio-indication of major influencing factors, calculations of integral density-diversity indices, and statistical approaches, which can be combined with community structure and environmental analyses as well.

2. Materials and Methods

2.1. Study Area Description

The Jordan River (320 km long) originates in the mountains of eastern Lebanon. As the Jordan River flows south through the entrance to the Great Syrian Rift Valley, it is fed from underground sources and small streams at various points in Jordan, Israel, Syria, and Lebanon [15]. Its tributaries are the Snir (Hasbani), which flows from Lebanon, Hermon (Banias), arising from a spring at Banias at the base of Mount Hermon, and the Dan and Saar, whose source is also at the base of Mount Hermon. They merge to form the Jordan River in northern Israel, near Kibbutz Sede Nehemya. The Jordan River used to drop rapidly in a 75-kilometer run into the swampy Lake Hula, which was slightly below sea level in the Rift Valley. Exiting the lake, it dropped much more, about 25 kilometers to Lake Kinneret. The last section has a lower gradient, and the river begins to meander before it enters the Dead Sea, which is about 400 meters below sea level and has no outlet. Two major tributaries enter from the East during this last phase: the Yarmouk River and Jabbok River.

The Jordan River is not only the largest and longest river that flows into Israel, but it is also the river that has a permanent flow year-round. The other major rivers in Israel are contaminated with agricultural and industrial sewage, which makes the Jordan River the only natural and clean river in the country.

It is important to emphasize that the Jordan River, in spite of its relatively large size in Israel, is actually a small river in international terms.

Data on the diversity of algal species in the Upper Jordan River Basin (including rivers, streams, lakes, wells, fishponds, and temporary water bodies) have been collected since 1883 [3,16-36] and contain 337 species and infraspecies. According to historical analyses (based on data collected from 1883-2009), we selected 227 species of algae and cyanobacteria that were found before our research in the Upper Jordan River and their tributaries from which we collected samples in 2006-2009. Our current research included analyses of the community structure dynamic and bio-indication.

2.2. Methods

Our research is based on 101 samples of planktonic and periphytonic algae that were collected at 21 sampling stations in the Upper Jordan River area. Samples were collected in March and May of 2006, April and August of 2007, July and April of 2008, and January, March, and April of 2009.

In 2006-2008, stations were selected in adjustment to water-quality monitoring stations used by “Mekorot” (Israel National Water Co.), most of which were located at the merging points of streams or at their outlets as follows: (1) Banias upstream; (2) Banias stream outlet; (3) Dan upstream; (4) Dan stream outlet; (5) Snir stream outlet; (6) Jordan River beginning at streams’ merger; (7) Ayun stream outlet; (8) Agmon pond; (9) Under Yosef bridge; (10) Jordan River outlet to Lake Kinneret; (11) Meshushim stream outlet; (12) Yeudiyya stream outlet, and (13) Daliyyot stream outlet.

Based upon research results obtained in 2006-2007, it became apparent that more research needed to be done on the chemical properties of the water flowing into the Upper Jordan River.

In order to reveal the influence of the upper part of the basin and to understand which parts of it are most critical, the basin’s structure was studied in detail. The basin’s structure was studied in the rainy winter period, since at that time water-flow increases from both rainfall and melting snow; the data collected in 2006-2007 made it clear that the winter period was more critical. The structural study of the Upper Jordan River Basin in winter 2009 led to the creation of a more precise map (**Figure 1**).

Stations added in 2009 were: (14) upper Ayun stream; (16) upper Saar stream; (17) Saar stream below station 16; (18) upper Meshushim stream pool; (20) Saar stream below Masade; (21) Saar stream above the confluence point with the Banias stream; (22) Saar stream near the confluence with the Banias stream; (23) Birkat Ram Lake, and (36, 37) two stations on the small wells placed near station 2.

Samples were obtained by scooping up phytoplankton and by scratching for periphyton, and then fixed in 3% formaldehyde. Part of the macrophyte algae was stored in the herbarium of the Institute of Evolution, University of Haifa. The algae were studied with a dissecting Swift microscope under magnifications of 740x–1850x and were photographed with the digital camera Inspector 1.

The diatoms were prepared with a peroxide technique [37] modified for glass slides [38]. In parallel with sampling for algae, the temperature, conductivity, TDS, and pH with the HANNA HI 9813 pH/EC/TDS Meter were measured. In addition to the sampling, data obtained from the chemical analyses regularly performed by the “Mekorot Water” company were used.

Taxonomy of our research along with the data list published for the last century was adopted under a modern

Figure 1. Basins and sampling stations' map of the Upper Jordan River in 2006-2009.

classification system [39]. The ecological data analysis of algal species diversity that was performed revealed the grouping of freshwater algae in respect to variables that were taken from the database compiled for freshwater algae in Israel [40]. Each group was separately assessed in respect to its bio-indication significance.

3. Results and Discussion

3.1. Chemical Analysis Data

Our results of chemical analysis data from field trips in 2006-2009 are shown in **Tables 1, 2** [41] and **3**.

Figure 2 is based on full screening data (Table 3) and displays changes in the major chemical parameters during the winter of 2009. The additional sampling stations were positioned from the headspring of the Saar stream under Mount Hermon peak (**Figure 1**, st. 16) all the way to the previously investigated stations on the Upper Jordan River (**Figure 1**, st. 2, 6, 9 and 10). Together, these stations comprise a longer water-flow path from the mountains into Lake Kinneret. Water temperature rises upon its approach to Lake Kinneret. The pH remains practically the same throughout the flow. Electrical conductivity and TDS both change similarly and generally increase upon their approach to the lake, yet have significant peaks at on stations 17 and 2. Station 17 is situated downstream from agricultural enterprises at the foot of Mount Hermon.

Station 2 is located after the confluence of the Banias stream. Stations 16-22 are of a mountainous-piedmont nature of effluence, whereas stations 2-10 are more planar. This difference in the effluence types might be the cause for the overall change in the quantity of ions (TDS, Conductivity) and phosphates, as illustrated in **Figure 2**.

The high chloride concentration could be a result of effluence from Masade before station 20. However, during the highly polluted winter period, the self-purification process in the river is also the highest as nitrate levels drop.

Table 1. Chemical analysis data, saprobity index (S), and number of species collected in December 2006.

No. of Station	1	6	10	11
N Kjeldahl, mg/l	0.10	0.13	0.27	0.26
T, C°	15.40	14.80	14.00	14.00
Electrical Conductivity, msm/cm	494.5	401.0	455.0	451.0
N org., mgN/l	0.10	0.11	0.25	0.25
NH_3, mg N/l	0.01	0.02	0.02	0.01
NO_3, mgN/l	1.32	1.89	1.88	2.25
N tot., mgN/l	1.43	1.60	2.10	2.53
pH	7.95	7.90	7.27	7.84
PO_4, mgP/l	0.06	0.02	0.05	0.0295
P tot., mgP/l	0.07	0.04	0.12	0.041
Cl, mg/l	13.0	10.0	13.0	29.0
Index of Saprobity (S)	1.47	1.74	1.60	1.73-1.87
No. of Species	8.00	42.00	28.00	24-25

Table 2. Chemical substance analysis data, saprobity index, and number of species collected in March 2006.

No. of Station	1	2	4	5	6	9	10	11
T, C°	17	18	20	20	18	19	21.5	20
Elect. Cond., msm/cm	349	389	336	391	371	413	406	452
N org., mg	0.11	0.10	0.01	0.09	0.08	0.15	0.20	0.08
NH_3, mg N/l	0.01	0.02	0.02	0.05	0.03	0.04	0.02	0.03
NO_3, mg N/l	1.04	1.27	1.08	1.55	1.29	1.61	1.54	1.96
N tot., mg N/l	1.09	1.34	1.45	1.71	1.38	1.79	1.62	2.03
pH	7.44	8.07	7.81	8.12	8.29	8.13	8.3	8.38
PO_4, mg P/l	0.02	0.02	0.01	0.01	0.02	0.02	0.03	0.05
P tot., mg P/l	0.03	0.04	0.01	0.03	0.03	0.04	0.07	0.06
Index Saprobity (S)	1.60	0.70	2.00	1.40	1.30	1.30	1.30	1.94
No. of Species	9	8	13	11	17	20	15	17

Table 3. Chemical substance analysis data, saprobity index, and number of species collected in February-April 2009.

Station no	1	2	3	4	5	6	9	10	11	12	13	14	16	17	18	20	21	22	23	36	37
N Kjeldahl, mg/l	1.7	1.7	1.7	1.7	2.3	1.1	0.5	2.4	0.2	0.2	1.4	1.1	1.7	1.7	0.5	1.9	2.4	2.3	3	1.7	1.7
T	14.8	15.3	14.8	14.2	17.5	14.4	17.4	15	16.1	16.4	16.5	11.8	14.6	11.4	20.2	15.5	15.3	12.4	10.9	15.0	13.1
Electrical Conductivity	0.42	0.42	0.31	0.34	0.41	0.34	0.35	0.61	0.4	0.44	0.53	0.54	0.30	0.42	0.37	0.31	0.3	0.34	0.28	0.52	0.26
TDS	294	297	217	244	287	240	248	431	281	310	374	378	216	185	264	215	215	209	162	366	188
N org., mg/l	1.7	1.7	1.7	1.7	2.3	1.1	0.5	2.4	0.2	0.2	1.4	1.1	1.7	1.7	0.5	1.9	2.4	2.3	3	1.7	1.7
NH3, mg/l	0	0	0	0	0	0	0	0	0	0	0	0	0	0	0	0	0	0	0	0	0
N-NO3, mg/l	2.3	2.9	1.8	2.2	2.1	1.9	2.5	1.3	1.7	1.7	1.2	1.7	4.0	4.2	2.7	3.7	3.8	2.3	0.8	6.5	1.8
N tot., mg/l	4	4.6	3.5	3.9	4.4	3	3	3.7	1.9	1.9	2.6	2.8	5.7	5.9	3.2	5.6	6.2	4.6	3.8	8.2	3.5
pH	7.5	8.3	8.3	8.3	8.4	8.3	8.2	8.4	8.4	8.3	8.5	8.0	8.1	8.5	8.3	8.8	8.9	8.1	8.7	7.9	8.2
PO4, mg/l	0	0	0	0	0	0	0	0	0	0	0	0	0	0	0	0	0	0	0	0	0
P tot., mg/l	0.1	0	0	0	0	0	0	0	0	0	0	0	0.1	0.2	0	0.1	0.1	0.1	0.3	0	0.1
Cl, mg/l	16.0	15.0	11.0	14.0	25.0	13.0	35.9	25.2	27	55	50.8	41.0	19.0	29.0	31.2	38	37	37.0	22.0	20.0	10.7
Index of Saprobity (S)	1.03	1.56	0.93	1.45	1.39	1.71	1.56	1.32	1.28	1.27	1.15	1.17	1.00	1.54	1.31	1.12	1.48	1.65	1.75	1.28	1.39

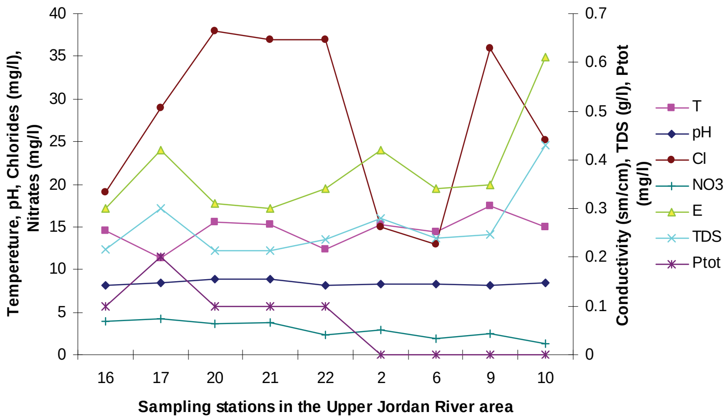

Figure 2. Chemical and physical parameters as measured in winter of 2009 at monitoring stations in the Upper Jordan River Basin.

Since the chemical monitoring by the Mekorot Company is performed only in sampling stations 1, 2, 6, and 10, samples had to be collected for a chemical analysis, parallel to the algological samples in other older and newer sampling stations.

3.2. The Last Century Dynamic of the Taxonomic Structure and Bioindicators in the Upper Jordan River Area, Historical Overview (1883-2009)

The following analysis includes our data collected in 2006-2009 as well as data from known international literature regarding species diversity in the Upper Jordan River [3,16-36]. Before our research in the Upper Jordan River area (including the river itself, tributaries, temporary streams, pools, fishponds, temporary water bodies, and lakes), there were 337 species and infraspecies of algae and cyanobacteria found. Therefore, the full species list now contains 467 taxa together with our findings of 232 taxa (for a total of 466 taxa, which includes our finding of 232 taxa) in 2006-2009. For our historical analysis, we selected taxa that were found during 1883-2000 only in the river and in their tributaries where we studied diversity, including 227 species and infraspecies. The diagram of the species diversity dynamics cover more than the past 100 years (**Figure 3**) and included our 2006-2009 findings.

As can be seen (**Figure 3**), species richness of the algal communities in the Upper Jordan River that was presented in mentioned references by 227 species and infraspecies fluctuated during the last century with peaks in 1951, 1965, 1978, and the present time. We significantly enriched the species list from 2006-2009 that was represented by 232 taxa of algae and cyanobacteria (**Table 4**) from which 85 taxa were new for the Upper Jordan River Basin, and three of them were mentioned for the first time in Israel. The revealed diversity belonged to seven taxonomic divisions. Bacillariophyta (Diatoms) were dominant but in order to clarify the change in algal communities' structure we constructed a percentage diagram (**Figure 4**), which shows some major periods when aquatic communities were impacted.

The first period showed a rather large increase in the number of species, which occurred in the middle of the last century. This was probably a result of mild organic

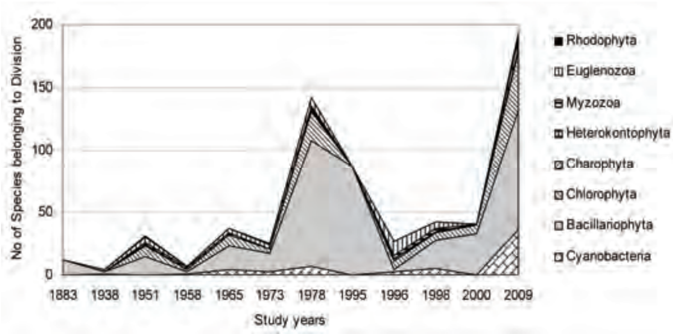

Figure 3. Species diversity dynamics in algal communities of the Upper Jordan River during the last century.

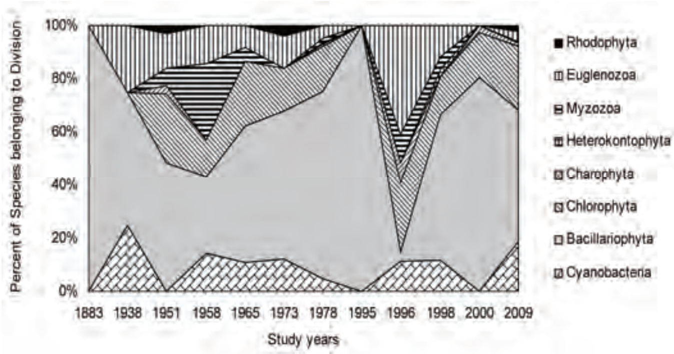

Figure 4. Historical overview (1883-2009) of the algal communities' structural changes in the Upper Jordan River.

pollution introduced primarily to this environment from 1951 and ended in 1965, as a result of the drying up the Hula Lake and the prevailing agriculture that replaced it [49]. Another climax in the number of species occurred during the period of 1973-1996; it seemed to reach its peak in 1978, but then in 1996 a dramatic decrease in the number of species occurred (about an 80% decrease), and instead, new species, previously unknown to this area, appeared in relatively high numbers. These newly emerged species are known indicators of organically polluted water with high temperatures and high salinity. With time, as the pollution decreased, the system started to return to its previous state (the state prior to pollution); by 2009, species common to the divisions typical to this area returned.

Figures 5-10 reveal the results of bioindication of major environmental parameters' fluctuation during the last century. As can be seen by species indicators from the figures, the algal community of the Upper Jordan River was stressed by temperature at a time when the taxonomic structure was changed in the middle of the last century and in 1996 (**Figure 5**). Water salinity stress was indicated in 1938 and 2000 (**Figure 6**). An impact of acidification was indicated in 1938, 1996, and 2000 (**Figure 7**). A dramatic decrease in the high-quality classes' indicators reflected an organic pollution impact in 1996 (**Figure 8**). The nitrogen uptake metabolism (photosynthetic) type indicators [48] changed in 1938 and 1996 with dominating facultatively nitrogen-heterotrophic taxa that needed periodically elevated concentrations of organically bound nitrogen (**Figure 9**). Their presence usually correlates with an impact of pollution.

The eutraphentic species indicators constituted the whole community in 1958 and 1996, whereas for 1995 and 2000 **Figure 10** shows two peaks of eutrophication marked by invasive high-trophic level indicators – hypereutraphentics [48].

It is interesting to note that the eutrophication trend can be seen from the 1970s till now, as indicated by the increase in eutraphentic and hypereutraphentic species.

3.3. Taxonomic Structure and Self-Purification Dynamic in the Upper Jordan River throughout the Sampling Stations in Winter 2009

As seen in **Figure 11**, the community of the Upper Jordan River Channel is comprised today mostly of Bacillariophyta (diatoms). There are three peaks in the fluctuation of diversity. The first peak is located at the Saar tributary above the Masade village (Stations 16-17), a community of 33-34 species. In addition to the diatoms, there are green algae and euglenoids, a result of the presence of organic pollution. At stations 20 and 21, after the Masade effluence, as a result of an anthropogenic influence, there is a sharp decrease in the number of species − to about 17-20 and an impoverishment of algal complexes. Afterwards, at stations 21 and 22, the com-

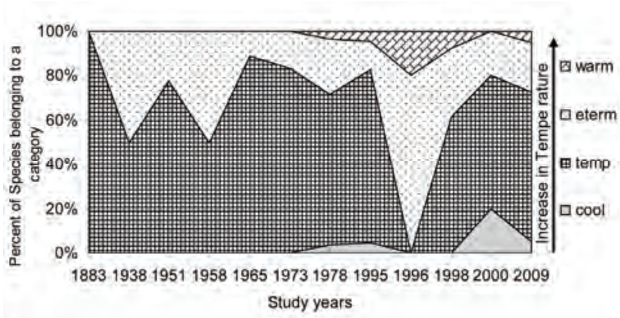

Figure 5. Historical overview (1883-2009) of the temperature indicator changes in the Upper Jordan River. Legend: warm – warm water, eterm – eurythermic, temp – temperate, cool – cool water.

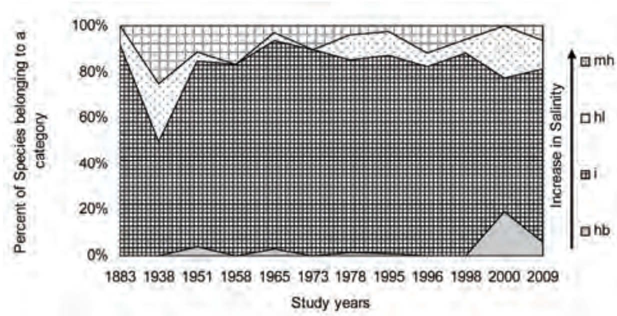

Figure 6. Historical overview (1883-2009) of the salinity indicator changes in the Upper Jordan River. Legend: halobity degree on Hustedt's scale [43] (hb – oligohalobes-halophobes, i – oligohalobes-indifferents, mh – mesohalobes, hl – halophiles).

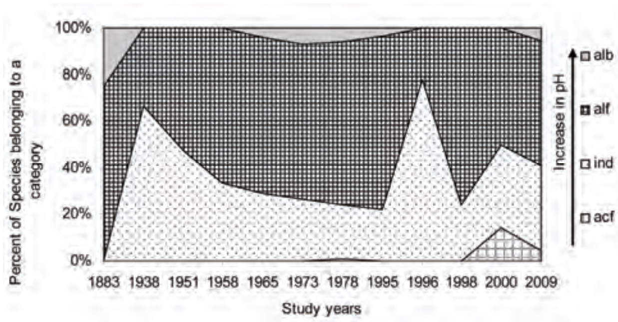

Figure 7. Historical overview (1883-2009) of the acidity (pH) indicator changes in the Upper Jordan River. Legend: pH degree on Hustedt's scale [44] (alb-alkalibiontes; alf – alkaliphiles, ind – indifferents; acf – acidophiles; neu – neutrophiles, which were mentioned in Table 4 affiliated with indifferents but have a narrower ecological specter).

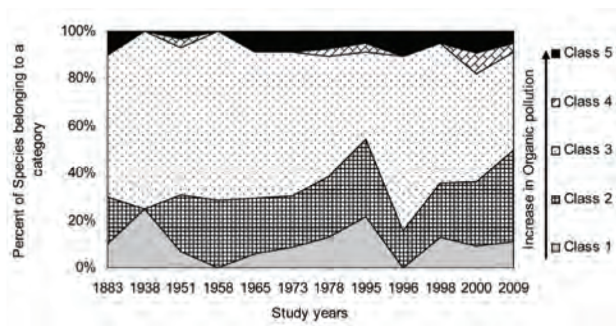

Figure 8. Historical overview (1883-2009) of the organic pollution indicator [45,46] changes in the Upper Jordan River. Legend: 1 Class – saprobity index is 0.0-0.5; 2 Class – saprobity index is 0.5-1.5; 3 Class – saprobity index is 1.5-2.5; 4 Class – saprobity index is 2.5-3.5; 5 Class – saprobity index is 3.5-4.0.

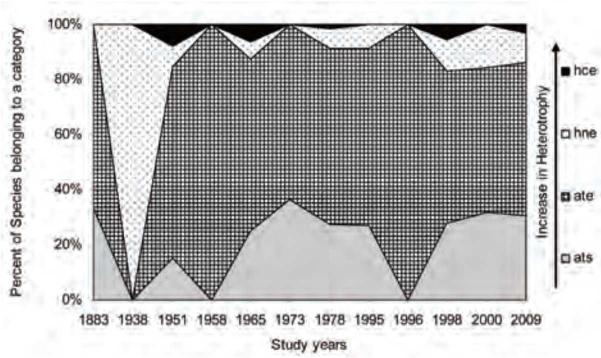

Figure 9. Historical overview (1883-2009) of the nitrogen uptake metabolism (photosynthetic) type indicator changes in the Upper Jordan River. Legend: Nitrogen uptake metabolism [48] (ats – nitrogen-autotrophic taxa, tolerating very small concentrations of organically bound nitrogen; ate – nitrogen-autotrophic taxa, tolerating elevated concentrations of organically bound nitrogen; hne – facultatively nitrogen-heterotrophic taxa, needing periodically elevated concentrations of organically bound nitrogen; hce – obligately nitrogen-heterotrophic taxa, needing continuously elevated concentrations of organically bound nitrogen).

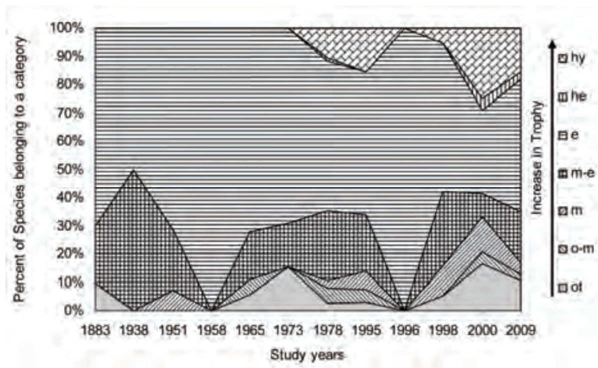

Figure 10. Historical overview (1883-2009) of the trophic status indicator changes in the Upper Jordan River. Legend: Trophic state [48] (ot – oligotraphentic; o-m – oligo-mesotraphentic; m – mesotraphentic; m-e – meso-eutraphentic; e – eutraphentic; he – hypereutraphentic; hy – oligo- to eutraphentic (hypereutraphentic)).

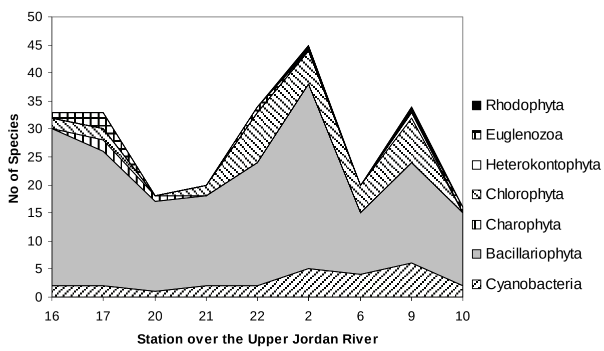

Figure 11. Algal species taxonomic structure changes in the sampling stations of the Upper Jordan River from upper reaches of the longest Saar tributary till the river mouth (winter 2009).

munities restored the diversity by means of self-purification and the addition of green algae and euglenoids. At the point of confluence with the clean waters of the Banias River (Station 2), the communities' composition reaches maximal diversity with 45 species. At this point, the red algae finally appear. At station 6, after the confluence with the three right-side tributaries (**Figure 1**), a drop in diversity occurs, however, it is again restored at station 9, where once again red algae enter the complex as indicators of self-purification. At the lower flow, near the entrance into Lake Kinneret, the community composition is less complex and includes diatoms, euglenoids, and cyanobacteria. Diversity is lowered to just 16 species accompanied by an impoverishment of the complex and the presence of euglenoids, which once more reflects the presence of anthropogenic factors affecting the algal community.

The fluctuations in diversity and the algal communities' composition at the basin confirm that, periodically, the presence of anthropogenic influences alters the formation of algal communities. However, these fluctuations are also related to the activity level of the self-purification process in the river. As can be seen in **Figure 12**, the fluctuation in species richness correlates with the saprobity index S value over the sampling stations in winter 2009. It can reflect the initial stage of the self-purification process, while the nutrient-enriched water gives a basis for diversity development in the community. This type of correlation can be related also with the oligotrophic status of the Upper Jordan River because the initial stage of eutrophication offers the best start for community development.

3.4. Taxonomic Composition Analysis in the Upper Jordan River Basin

Upon evidence of the species richness dynamic and its relationship with the trophic status of this river, we can see a highly significant role in algal diversity in the analysis of the river state. Species diversity in communities of each tributary reflects the state of their environments. Therefore, we can use the algal community composition structure in tributaries as an instrument for the clustering of species diversity of the Upper Jordan Basin as a whole. For this analysis, we divided all revealed species diversity for the studied period (2006-2009) into 11 species lists (**Table 4**) for each tributary, the river itself, and the two lakes, Hula and Ram (a volcanic crater lake between Majdel Shams and Masade). The taxonomic structure of each object was analyzed on the infraspecies level by the clustering methods in the "GRAPHS" program [50].

Clustering by the Serensen-Chekanovsky indices divided algal diversity into five different groups based on the similarity level, which was 40% (**Figure 13**). One cluster included the Mount Hermon piedmont streams: Saar, Banias, and Dan. The Upper Jordan (lower reaches) and Meshushim, flowing into Lake Kinneret close to each other, constitute the second cluster. More planer tributaries, such as the Daliyyot, Yehudiyya, Snir, and Ayun, located in the northern part of the river basin, formed the third cluster. Two different clusters included the two lakes, Hula and Ram volcanic crater lake with differences in hydrology from all of the rivers' tributaries. Therefore, river diversity was divided into five clusters, according to their hydrology.

The tree of taxonomic diversity clusters was constructed on the basis of revealed species diversity of the Upper Jordan River; the tributaries and lakes show (**Figure 14**) four different branches. As can be seen, the most similar (53%) diversity belonged to the Snir and Ayun rivers, located close to the northwest part of the river basin. This group also included the Yehudiyya River with similar hydrology. The second branch is formed by the mouth of the Upper Jordan River and the Meshushim River (49% similarity), both flowing into Lake Kinneret close to each other. The Saar, Banias, and Dan rivers were in the third group comprising 45% similarity. This group was located close to the northeastern part of the basin and has similar hydrology. The last group included the two lakes, Ram and Hula, as well as the Daliyyot River. The sampling station on this river was located in the lower pond of the river. Therefore, the hydrology of each river influenced species diversity significantly, and diversity can be used as a marker of hydrologically similar tributaries of the basin.

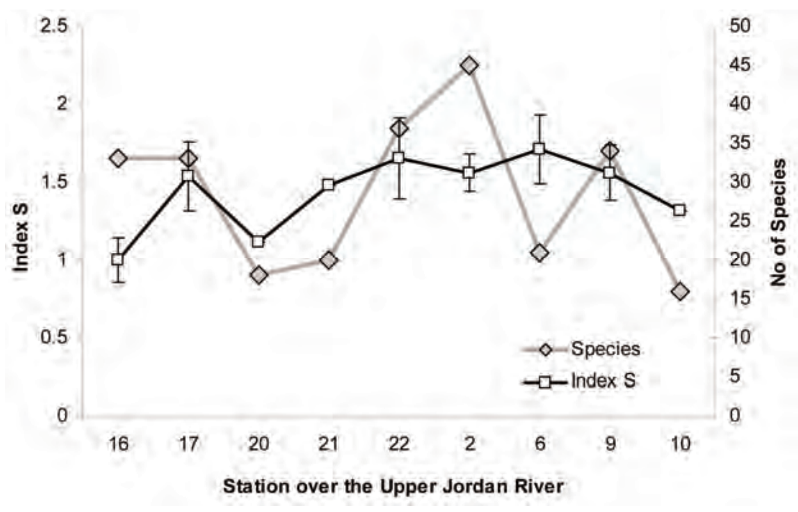

Figure 12. Algal species richness in communities and saprobity index S changes in the sampling stations of the Upper Jordan River in winter 2009.

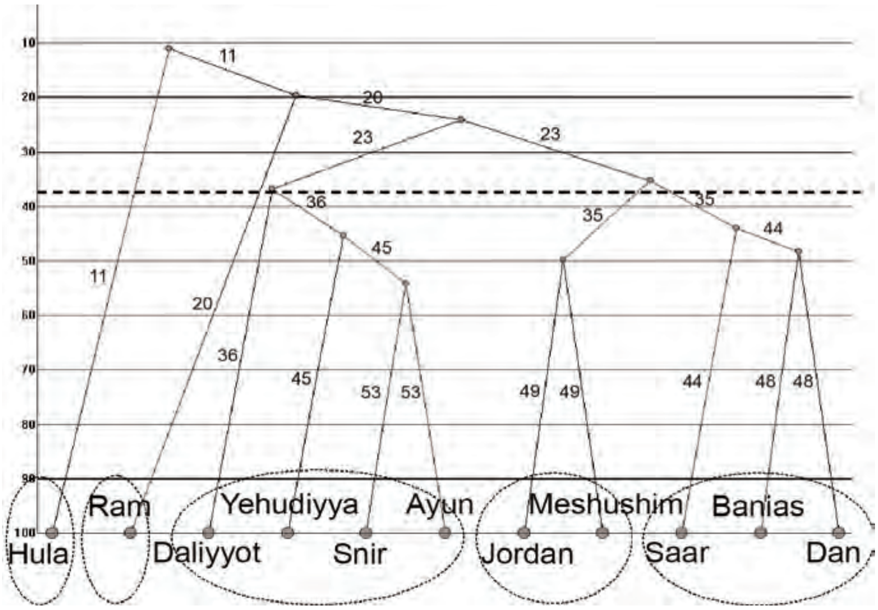

Figure 13. Clustering of the taxonomic structure in the rivers of the Upper Jordan River basin on the basis of Serensen-Chekanovsky indices.

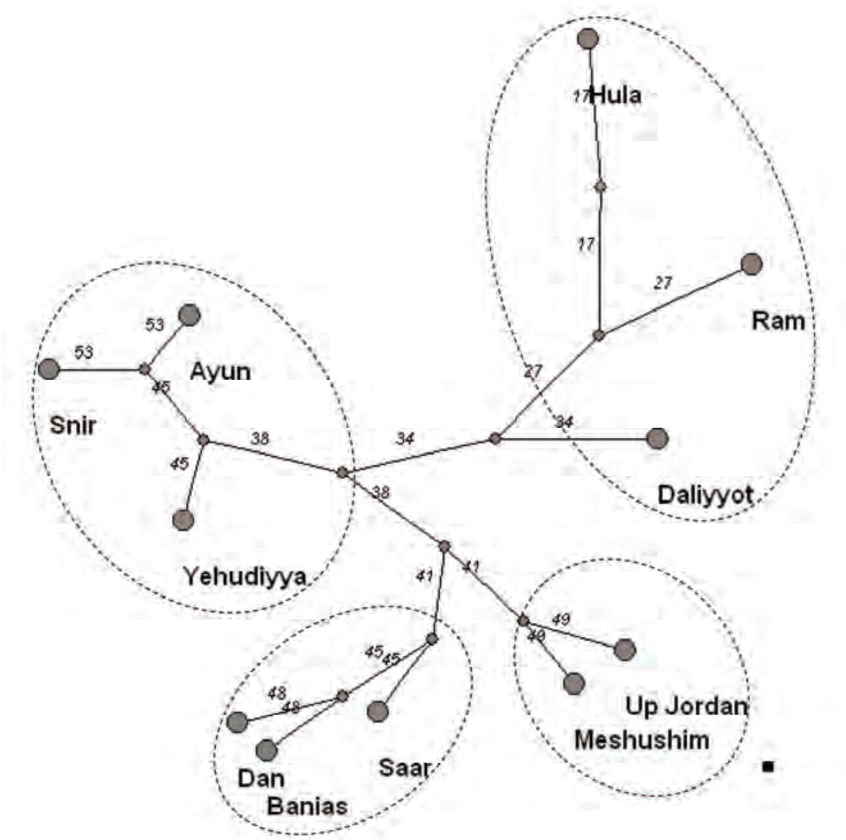

Figure 14. Tree of the taxonomic structure in the rivers of the Upper Jordan River basin on the basis of Serensen-Chekanovsky indices and brave calculation. The group of Banias, Dan, and Saar included cool piedmount streams; the group of Snir, Ayun, and Yehudiyya included piedmount streams that partly flow into the river plane; the group of Upper Jordan and Meshushim included plane streams; the group of Hula and Ram (lakes), and Daliyyot had ponded objects.

Table 4. Diversity and ecology of species in the Upper Jordan River communities in 2006-2009.

Taxon	Banias	Dan	Snir	Ayun	Jor-dan	Yehu-diyya	Meshu-shim	Daliy-yot	Saar	Ram	Hula	S	pH	Hal	Sap	Het	Tro
Cyanobacteria																	
Anabaena pseudoscillatoria Bory de Saint-Vincent	-	1	3	1	-	-	-	-	-	-	-	2.0	-	-	b	-	-
Anabaena sp.	-	1	-	-	-	-	-	-	-	-	-	-	-	-	-	-	-
**Anabaena spiroides* Klebahn	-	-	-	-	-	-	-	-	-	-	1	1.5	-	i	o-b	-	-
Aphanothece clathrata W. West & G.S. West	-	-	-	-	2	-	-	-	-	-	-	2.3	-	hl	b	-	-
Calothrix sp.	-	-	-	-	2	-	1	1	-	-	-		-	-	-	-	-
Chamaesiphon incrustans Grunow	1	4	-	-	-	-	2	-	-	-	-	1.0	-	-	o	-	-
Chamaesiphon sp.	-	-	-	2	-	-	-	-	-	-	-	-	-	-	-	-	-
Chlorogloea microcystoides Geitler	2	-	-	-	-	-	-	-	-	-	-	-	-	-	-	-	-
Chroococcidiopsis sp.	-	-	-	-	-	-	5	-	-	-	-	-	-	-	-	-	-
Chroococcus sp.	-	2	-	-	-	-	3	-	-	-	-	-	-	-	-	-	-
**Chroococcus turgidus* (Kützing) Nägeli	2	2	-	1	-	-	1	-	-	-	-	1.3	alf	hl	o	-	-
Coelosphaerium kuetzingianum Nägeli	-	-	-	-	1	-	-	-	-	-	-	1.6	-	i	b-o	-	-
Coelosphaerium sp.	-	-	-	-	4	-	-	-	-	-	-	-	-	-	-	-	-
***Cyanostylon microcystoides* Geitler	-	-	-	-	-	-	6	-	-	-	-	-	-	-	-	-	-
Gloeocapsopsis crepidinum (Thuret) Geitler ex Komàrek	-	2-3	1	1-2	-	-	1	-	-	-	-	-	-	hl	-	-	-
**Heteroleibleinia kossinskajae*(Elenkin) Anagnostidis & Komárek	-	-	6	-	-	-	-	-	-	-	-	-	-	-	-	-	-
Heteroleibleinia kuetzingii (Schmidle) Compère	-	4	3	-	-	-	-	-	-	-	2	1.5	-	-	o-b	-	-
Homoeothrix janthina (Bornet & Flahault) Starmach	-	-	-	6	-	6	5-6	-	-	-	-	0.8	-	-	x-b	-	-
Homoeothrix juliana (Meneghini) Kirchner	-	-	6	-	-	-	-	-	-	-	-	-	-	-	-	-	-
Homoeothrix sp.	-	-	6	-	-	-	6	-	-	-	-	-	-	-	-	-	-
Homoeothrix varians Geitler	6	-	4	6	1-6	-	4-5	-	-	-	-	1.0	-	-	o	-	-
Komvophoron constrictum (Szafer) Anagnostidis & Komárek	1	-	-	-	-	-	-	-	-	-	-	4.5	-	-	i	-	-
Leptochaete stagnalis Hans-girg	-	-	-	-	3	-	6	-	-	-	-	2.0	-	i	b	-	-
Lyngbya sp.	1-2	2-3	-	2-3	1-3	1	1-2	-	-	-	-	-	-	-	-	-	-
**Merismopedia minima* Beck	-	-	-	-	-	-	2	-	-	-	-	-	-	-	-	-	-
**Merismopedia punctata* Meyen	-	-	-	-	-	-	-	1	-	-	-	1.9	ind	i	o-a	-	-
Microcrocis sp.	1	-	-	-	-	-	-	-	-	-	-	-	-	-	-	-	-
**Microcystis aeruginosa* (Kützing) Kützing	-	-	-	-	2-3	-	-	-	-	-	-	1.8	-	hl	o-a	-	-
Nostoc linckia (Roth) Bornet ex Bornet & Flahault	-	-	-	6	-	-	-	-	-	-	-	1.8	-	-	o-a	-	-
Oscillatoria amoena (Kützing) Gomont	2-6	-	-	1-3	5	-	1	-	5-6	-	-	0.2	-	-	x	-	-
Oscillatoria sp.	1-3	3	-	3-4	-	-	3-6	-	2	-	-	-	-	-	-	-	-
***Phormidiochaete fusca* (Starmach) Komarek et Anagnostidis	-	-	2	4	-	-	-	-	-	-	-	-	-	-	-	-	-
**Phormidium ambiguum* Gomont	-	5	-	-	1	-	6	-	3-4	-	-	2.0	ind	i	b	-	-
Phormidium autumnale (C. Agardh) Trevisan	-	2	-	2	1-2	-	-	3	1	-	-	2.1	-	-	b	-	-

Table 4 - *Continued*

ex Gomont																
Phormidium breve (Kützing ex Gomont) Anagnostidis et Komárek	-	1-6	-	1-2	2-4	-	-	1	6	-	-	2.8	-	-	b-p	-	-
Phormidium limosum (Dillwyn) P.C. Silva	-	-	-	-	-	-	-	3	-	-	-	2.3	-	hl	b	-	-
Phormidium sp.	1-5	6	-	-	2	-	-	-	6	-	-	-	-	-	-	-	-
Phormidium subfuscum Kützing ex Gomont	6	-	-	-	-	-	-	-	-	-	-	2.0	-	-	b	-	-
**Phormidium uncinatum* (C. Agardh) Gomont ex Go-mont	-	-	-	-	-	-	1	-	-	-	-	2.1	-	i	b	-	-
**Planktothrix agardhii* (Gomont) Anagnostidis et Komárek	-	-	-	-	-	-	-	-	6	-	-	1.6	-	hl	b-o	-	-
Rivularia haematites (De Candolle) Bornet et Flahault	-	-	-	-	-	-	2	-	-	-	-	1.9	-	-	o-a	-	-
Synechococcus elongates (Nägeli) Nägeli	-	3	-	-	-	-	-	-	-	-	-	0.1	-	-	x	-	-
Synechococcus sp.	-	4	-	-	3	-	-	-	-	-	-	-	-	-	-	-	-
Euglenozoa																	
Colacium cyclopicola (Gicklh.) Bourr.	-	-	-	-	-	-	-	-	-	-	2	2.7	-	-	a-b	-	-
**Euglena deses* f. Klebsii (Lemmermann) T.G. Popova	-	-	-	-	-	-	-	-	1	-	-	-	-	-	-	-	-
Euglena limnophila Lemmermann	-	-	-	-	1	-	-	-	-	1	-	1.5	-	-	o-b	-	-
Euglena sp.	-	-	-	-	-	-	-	-	1	-	-	-	-	-		-	-
Euglena spathirhyncha H.L. Skuja	-	-	-	-	-	-	-	-	1	-	-	3.5	-	i	a-p	-	-
**Euglena tripteris* (Dujardin) Klebs	-	-	-	-	1	-	-	-	-	-	-	2.1	ind	mh	b	-	-
Lepocinclis ovum (Ehrenberg) Lemermann	-	1	-	-	-	-	-	-	-	1	-	2.7	ind	i	a-b	-	-
Phacus sp.	-	-	-	1	-	-	-	-	-	1	-	-	-	-	-	-	-
**Trachelomonas hispida* (Perty) F. Stein	-	-	-	-	-	-	-	-	1	-	1	2.0	-	i	b	-	-
Heterokontophyta																	
**Dinobryon divergens* O.E. Imhof	-	-	-	-	2	-	-	-	-	-	-	1.8	ind	i	o-a	-	-
**Ophiocytium majus* Nägeli	-	-	-	-	-	-	-	-	-	-	1	1.5	-	-	o-b	-	-
Bacillariophyta																	
Achnanthes inflata (Kützing) Grunow	-	-	-	-	-	-	1	-	-	-	-	-	-	i	-	-	-
Achnanthes sp.	-	-	-	-	3	-	-	-	-	-	-	-	-	-	-	-	-
**Achnanthidium minutissimum* (Kützing) Czarnecki	3-6	1-6	2-6	1-4	-	3	1-3	-	2-6	-	-	2.2	alf	i	b	ate	hy
Amphora coffeaeformis (C. Agardh) Kützing	-	-	-	-	-	-	-	-	-	1	-	-	alf	mh	a	ate	e
**Amphora ovalis* (Kützing) Kützing	2	1	1-2	1	1-2	-	1-3	1	1	2	-	2.7	alf	i	a-b	ate	e
**Amphora pediculus* (Kützing) Grunow ex A. Schmidt	2	1-3	1	1	1	-	1	-	2	3	-	1.8	alf	i	o-a	ate	e
Amphora sp.	-	-	2	-	-	-	-	-	1	-	-	-	-	-	-	-	-
**Amphora veneta* Kützing	1-2	-	-	-	-	-	-	-	2-3	-	-	1.0	alf	i	o	ate	e
**Aneumastus tuscula* (Ehrenberg) D.G. Mann & A.J. Stickle in Round et al.	-	-	-	-	1	-	-	-	-	-	-	0.7	alf	i	o-x	-	hy
**Anomoeoneis sphaerophora* E. Pfitzer	-	-	-	-	-	-	2	-	1	-	-	0.8	alb	hl	x-b	ate	e
**Aulacoseira granulata*	-	-	-	-	1	-	1	-	-	1	-	2.4	alf	i	b-a	ate	e

Table 4 - *Continued*

(Ehrenberg) Simonsen																	
**Bacillaria paradoxa* J.F. Gmelin	-	-	-	-	-	-	2	-	-	-	-	-	-	-	-	-	-
Brachysira brebissonii R. Ross	-	1	-	-	1	-	-	-	-	-	-	1.0	acf	oh	o	-	-
Campylodiscus hibernicus Ehrenberg	1	-	-	-	-	-	-	-	-	-	-	1.3	ind	i	o	-	e
**Cocconeis neodiminuta* Krammer	3	-	-	-	-	-	-	-	2	-	-	1.0	alb	i	o	-	-
**Cocconeis placentula* Ehrenberg	1-5	1-6	4-5	1-5	1-5	4-6	1-3	3-4	3	-	1-6	1.4	alf	i	o-b	ate	e
**Craticula cuspidata* (Kutzing) D.G. Mann in Round, Crawford & Mann	-	-	-	-	-	-	-	-	-	-	3	1.0	alf	i	o	-	-
Cyclotella antiqua W. Smith	-	-	-	-	-	-	-	-	1	-	-		acf	hb	o	ats	ot
**Cyclotella meneghiniana* Kützing	2	1	-	-	1-2	-	-	-	3-4	3-4	-	1.8	alf	hl	o-a	hne	e
**Cymatopleura elliptica* (Brébisson) W. Smith	1	-	-	-	1	-	-	1	-	-	-	1.7	alf	i	b-o	ate	e
**Cymatopleura solea* (Brébisson) W. Smith	1	-	-	-	1	1	-	-	-	-	-	1.0	alf	i	o	ate	e
**Cymbella affinis* Kützing	3	-	-	-	-	-	-	-	-	-	-	1.7	alf	i	b-o	ats	e
Cymbella lanceolata (Ehrenberg) Kirchner	-	-	-	-	1	3	3	-	-	-	-	1.3	alf	i	o	ats	hy
Cymbella naviculiformis (Auerswald) Cleve	-	2	-	-	-	-	-	-	-	-	-	1.3	ind	i	o	ate	e
Cymbella sp.	-	-	-	1-2	1	-	2	-	-	-	-	-	-	-	-	-	-
Cymbella tumida (Brébisson in Kützing) van Heurck	-	-	-	-	1-3	-	-	-	-	-	-	0.2	alf	i	x	ats	m-e
Cymbella turgidula Grunow in A. Schmidt et al.	-	1-2	-	1-2	-	1	-	-	2-5	-	-	-	ind	-	-	-	-
**Diatoma hyemale* (Roth) Heiberg	2	-	5	2-3	1-6	4	1	1-4	-	-	-	1.7	ind	hb	b-o	ats	-
**Diatoma vulgaris* Bory de Saint-Vincent	1-3	-	-	2-6	1-2	-	-	-	-	-	-	2.4	ind	i	b-a	ate	m-e
Diploneis oblongella (Nägeli in Kützing) Cleve-Euler in Cleve-Euler (& Osvald)	-	-	-	1	-	-	-	-	-	-	-	1.9	alf	i	o-a	ats	-
**Discostella stelligera* (Cleve & Grunow) Houk & Klee	-	-	-	-	-	-	-	-	-	3	-	0.1	ind	i	x	-	-
**Ellerbeckia arenaria* (Moore) R.M. Crawford	2	1	-	-	-	-	-	-	-	-	-	1.8	alf	i	o-a	ats	ot
Encyonema caespitosum Kützing	3	-	-	-	-	-	-	-	-	-	-	-	-	i	b-a		hy
**Encyonema minutum* (Hilse in Rabenhorst) D.G. Mann in Round, Crawford & Mann	1-2	-	-	-	1-2	2	2-3	-	1-3	-	-	1.3	ind	i	o	-	-
**Encyonema silesiacum* (Bleisch) D.G. Mann in Round, Crawford & Mann	-	-	-	-	-	-	2	-	-	-	-	1.33	ind	i	x-o	-	
Entomoneis costata (Hustedt) Reimer	-	-	-	-	1	-	-	-	-	-	-	-	alf	-	-	-	-
**Epithemia adnata* (Kützing) Brébisson	1	-	-	-	-	-	-	-	-	-	-	2.5	alb	i	b-a	ats	m-e
Epithemia argus (Ehrenberg) Kützing	-	-	-	-	-	-	-	1	-	-	-	1.8	ind	i	o	-	m
**Epithemia sorex* Kützing	-	-	-	-	-	-	1	1-3	-	-	-	1.9	alf	i	o-a	ats	e
Epithemia turgida (Ehrenberg) Kützing	-	3	-	-	1-2	-	-	1	-	-	-	1.1	alf	i	o	ats	m-e
Eucocconeis flexella (Kützing) Meister	-	-	-	-	-	1	-	-	-	-	-	1.5	ind	mh	o-b	ats	ot

Table 4 - *Continued*

**Fallacia pygmaea* (Kützing) A.J. Stickle & D.G. Mann in Round, Crawford & Mann	1	1	-	-	-	-	-	1	-	-	-	1.7	alf	mh	b-o	hne	e
Fallacia subhamulata (Grunow in van Heurck) D.G. Mann in Round, Crawford & Mann	-	-	-	3	-	-	-	-	-	-	-	-	-	-	-	-	-
**Fragilaria capucina* var. *vaucheriae* (Kützing) Lange-Bertalot	-	-	-	-	-	-	-	-	1	1	-	1.5	alf	i	o-b	-	-
Fragilariforma virescens (Ralfs) D.M. Williams & Round	-	1	-	-	-	-	-	-	2-3	-	-	1.3	neu	i	o	ats	o-m
Frustulia rhomboides (Ehrenberg) De Toni	-	-	-	-	-	-	1	-	-	-	-	0.9	acf	hb	x-b	ats	ot
**Frustulia vulgaris* (Thwaites) De Toni	-	1	-	-	2	-	-	-	-	-	-	0.9	alf	i	x-b	ate	m-e
**Gomphonema affine* Kützing	-	-	-	-	2	-	1-4	-	-	-	-	1.5	-	-	o-b	-	-
**Gomphonema angustatum* (Kützing) Rabenhorst	-	-	-	-	3-4	-	5-6	-	-	-	2	2.0	alf	i	b	-	-
**Gomphonema insigne* Gregory	3	-	-	-	-	-	-	-	-	-	-	-	-	i	-	-	-
Gomphonema intricatum Kützing	-	1	-	-	1	-	3	-	-	-	-	0.4	ind	i	x-o	-	-
**Gomphonema minutum* (C. Agardh) C. Agardh	-	-	-	-	1	-	-	-	-	-	-	-	alf	oh	o-b	-	e
**Gomphonema olivaceum* (Hornemann) Brébisson	3-6	-	-	-	-	-	-	-	2	1	-	2.5	alf	i	b-a	ate	e
**Gomphonema parvulum* (Kützing) Kützing	1-3	1-3	2-4	1-6	1-5	4	1-5	-	1-6	1-3	3-6	0.1	ind	i	x	hne	e
Gomphonema sp.	3	-	-	-	-	-	2-3	-	-	-	-	-	-	-	-	-	-
**Gomphonema truncatum* Ehrenberg	2	1	-	-	-	-	2	-	5	-	-	0.7	alf	i	o-x	ats	m-e
**Gomphonema vibrio* var. *intricatum* (Kützing) Playfair	3-4	-	-	2	1	4-5	4	-	-	-	-	1.4	ind	i	o-b	ats	ot
Gomphonemopsis exigua (Kützing) Medlin	-	-	-	-	-	-	1	-	-	-	-	-	-	hl	-	-	-
Gyrosigma acuminatum (Kützing) Rabenhorst	1	1-4	-	1-3	1-3	-	1-3	1	2	-	1	0.7	alf	i	o-x	ate	e
**Hantzschia amphioxys* (Ehrenberg) Grunow in Cleve & Grunow	-	1	-	1	-	-	-	-	2	4	-	1.7	neu	i	b-o	ate	hy
Luticola muticopsis (Van Heurck) D.G. Mann	-	-	-	-	4	-	-	-	-	-	-	-	-	-	-	-	-
**Melosira varians* C. Agardh	2-4	1-5	1	5	1-5	3	2-5	-	3-6	2	1	2.7	alf	hl	a-b	hne	e
**Meridion circulare* (Greville) C. Agardh	1	1-3	2	3	-	-	-	-	1-6	1	-	1.5	alf	i	o-b	ate	hy
**Navicula angusta* Grunow	-	-	-	-	4	4	-	-	-	-	-	-	acf	hl	o	ats	ot
**Navicula cryptocephala* Kützing	3	-	-	-	1-2	-	1	-	2-3	-	-	2.7	alf	i	a	ate	hy
Navicula exigua Gregory	1-2	1-2	3	-	3	-	2	2	2-6	3-4	-	0.5	alf	i	x-o	ats	e
Navicula gibbula Cleve	1	-	-	-	-	-	-	-	-	-	-	-	neu	i	-	-	-
Navicula pupula var. *rectangularis* (W. Gregory) Cleve & Grunov	-	-	4	-	-	-	-	-	-	-	-	-	ind	hl	-	ate	m-e
**Navicula radiosa* Kützing	3	-	-	-	-	-	-	-	-	-	-	1.1	ind	i	o	ate	m-e
Navicula recens (Lange-Bertalot) Lange-Bertalot in Krammer & Lange-Bertalot	3	1-4	3-4	3-6	2-6	4	1-4	2	3	5	-	-	alf	i	o-b	-	e
**Navicula rhynchocephala* Kützing	3-4	2-6	-	-	2-3	4	1-6	-	-	-	-	2.3	alf	hl	b	ate	hy

Table 4 - *Continued*

Navicula sp.	2-3	2-6	3-6	4-6	1-6	1	1-4	2	3-6	5	3	-	-	-	-	-	-
**Navicula tripunctata* (O.F. Müller) Bory	3	-	2	2-3	-	-	-	-	-	-	-	2.3	ind	i	b	ate	e
**Navicula veneta* Kützing	-	-	-	-	1	-	-	-	-	-	-	1.1	alf	hl	x-o	ate	e
**Navicula viridula* (Kützing) Kützing	3	-	-	-	-	-	-	-	-	-	-	1.3	alf	hl	o	ate	e
Neidium iridis (Ehrenberg) Cleve	-	-	1	-	-	-	-	-	1	-	-	0.6	ind	hb	o-x	ats	m
**Nitzschia acicularis* (Kützing) W. Smith	-	2	-	-	1	-	-	-	1-4	1	-	1.5	alf	i	o-b	hce	e
**Nitzschia amphibian* Grunow	-	-	-	-	1	-	-	-	-	-	-	1.3	alf	i	o	hne	e
**Nitzschia dissipata* (Kützing) Grunow	1	-	5	-	-	2	-	-	4-2	-	-	0.2	alf	i	x	ate	m-e
Nitzschia filiformis (W. Smith) Hustedt	2	-	3	3	1-5	-	2-4	-	1-6	-	-	0.3	alf	hl	x	hne	e
Nitzschia fonticola (Grunow) Grunow in Van Heurck	-	-	2	-	-	-	1	-	1	-	-	1.5	alf	oh	o-b	ate	m-e
**Nitzschia linearis* (Agardh) W. Smith	3	1	-	2	1-2	-	1-3	-	2	-	-	0.0	alf	i	x	ate	m-e
**Nitzschia palea* (Kützing) W. Smith	1-2	3-4	1-2	2-3	1-3	5	1-6	2	2-6	1	-	0.7	ind	i	o-x	hce	he
**Nitzschia sigmoidea* (Nitzsch) W. Smith	-	-	-	-	1	-	3	-	-	-	-	1.1	alf	i	o	ate	e
Nitzschia solita Hustedt	-	-	-	-	-	-	-	1	1-2	-	-	-	alf	mh	a-b	-	e
Nitzschia sp.	1-4	1	3	2-5	2-5	6	3	1-3	2-5	1	-	-	-	-	-	-	-
**Nitzschia umbonata* (Ehrenberg) Lange-Bertalot	-	-	-	-	3	-	-	-	-	-	-	1.7	-	-	b-o	-	-
**Nitzschia vermicularis* (Kützing) Hantzsch in Rabenhorst	1	1	-	-	1-4	-	4	-	-	-	-	1.3	alf	i	o	-	hy
**Planothidium lanceolatum* (Brébisson ex Kützing) Lange-Bertalot	1	1	-	-	2	-	1	-	1	-	-	0.75	alf	i	o-x	-	-
Pleurosira laevis (Ehrenberg) Compère	-	-	-	-	1-3	-	3	-	-	-	-	-	alf	mh	o	-	e
Reimeria sinuata (Gregory) Kociolek & Stoermer	-	-	-	-	1	-	1	-	-	-	-	-	ind	i	-	-	-
**Rhoicosphenia abbreviate* (C. Agardh) Lange-Bertalot	1-4	1-6	3-5	1-3	1-6	3-4	2-6	3	3	-	-	0.5	alf	i	x-o	ate	e
**Rhopalodia gibba* (Ehrenberg) O.F. Müller	-	-	-	-	-	-	-	2-4	-	-	-	0.4	alb	i	x-o	-	-
Rhopalodia musculus (Kützing) O.F. Müller	-	-	-	1	-	-	-	-	-	-	-	-	alb	mh	x	-	-
Sellaphora parapupula Lange-Bertalot	-	-	-	-	1	-	-	-	-	-	-	-	-	-	-	-	-
**Sellaphora pupula* (Kützing) Mereschkovsky	1	-	3	-	1	-	1	-	1	1	-	0.5	ind	hl	x-o	ate	m-e
Stauroneis anceps Ehrenberg	-	-	-	-	-	-	-	-	1	-	-	0.3	ind	i	x	ate	m-e
**Staurosira construens* Ehrenberg	1	-	-	-	-	-	-	-	-	-	-	1.3	alf	i	o	-	-
Staurosirella pinnata (Ehrenberg) D.M. Williams & Round	-	-	-	-	-	-	-	-	-	1	-	-	alf	hl	b-a	ate	o-e
**Stephanodiscus hantzschii* Grunow	-	-	-	-	1	-	-	-	-	-	-	2.7	alf	i	a-b	hne	he
**Surirella angusta* Kützing	1	-	-	-	1	-	-	-	2	-	-	1.1	alf	i	o	ate	e
Surirella linearis W. Smith	1	3	-	1-3	-	-	-	-	1-3	-	-	1.4	ind	i	o-b	-	o-m
**Surirella minuta* Brébisson in Kützing	2-3	1	-	-	1-2	1	-	-	2-6	2	-	1.85	ind	i	o-a	-	ot
**Surirella ovalis* Brébisson	-	-	-	1-4	1	-	1	-	1-3	-	-	-	alf	mh	o	ate	e
Surirella robusta Ehrenberg	-	-	-	-	1	-	-	1	-	-	-	1.7	ind	hb	b-o	-	hy

Table 4 - *Continued*

**Surirella spiralis* Kützing	1	-	-	-	-	-	-	-	-	-	-	1.0	neu	i	o	ats	ot
**Surirella splendida* (Ehrenberg) Kützing	-	-	-	-	-	-	1	-	-	-	-	1.5	alf	i	o-b	-	m-e
Surirella tenera W. Gregory	2	-	-	1	1	-	1	-	-	-	-	1.0	alf	i	o	-	e
**Tryblionella angustata* W. Smith	-	-	-	-	1	-	-	-	-	-	-	0.8	alf	i	x-b	ats	m
**Tryblionella apiculata* Gregory	1	-	-	-	-	-	-	-	-	-	-	2.2	alf	mh	b	ate	e
Tryblionella levidensis W. Smith	-	-	-	-	2	-	-	-	1	-	1	2.7	alf	hl	a-b	ate	e
**Ulnaria ulna* (Nitzsch) P. Compère in Jahn *et al.*	1-5	1-4	1	1-2	1-4	3-4	1-6	1-6	4-6	3	-	1.7	ind	i	b-o	ate	hy
Chlorophyta																	
Acutodesmus acuminatus (Lagerheim) Tsarenko	-	-	-	-	1	-	-	-	-	2-3	-	2.2	ind	i	b	-	-
**Ankistrodesmus falcatus* (Corda) Ralfs	-	-	-	-	1	-	-	-	-	-	-	2.1	-	hb	b	-	-
Chlamydomonas sp.	-	-	-	-	-	-	-	-	1	3	-	2.8	-	-	b-p	-	-
Chlamydopodium pluricoccum (O.A. Korshikov) H. Ettl et J. Komárek	-	-	-	1	-	-	1	-	-	-	3	-	-	-	-	-	-
**Cladophora glomerata* (Linnaeus) Kützing	6	2-6	6	2-6	2-6	4-6	2	1-6	3-4	6	3-5	1.7	alf	i	b-o	-	-
Closteriopsis acicularis (Chodat) J.H. Belcher & Swale	-	-	-	-	-	-	-	-	2	1	-	1.9	-	i	o-a	-	-
**Coelastrum astroideum* De Notaris	-	-	-	-	-	-	-	-	1	-	1-2	2.0	-	-	b	-	-
**Coelastrum microporum* Nägeli	-	-	-	-	1	-	-	-	-	1	1	2.1	ind	i	b	-	-
**Coelastrum sphaericu* Nägeli	-	-	-	-	1	-	-	-	-	3	-	1.0	-	i	o	-	-
**Crucigenia tetrapedia* (Kirchner) W. West & G.S. West	-	-	-	-	1	-	-	-	-	-	-	1.9	ind	i	o-a	-	-
**Desmodesmus abundans* (Kirchner) E. Hegewald	-	-	-	-	1	-	-	-	-	1	-	1.8	-	-	o-a	-	-
**Desmodesmus armatus* (R. Chodat) E. Hegewald var. *armatus*	-	-	-	-	2	-	-	-	1	-	1-2	1.9	-	-	o-a	-	-
**Desmodesmus armatus* var. *bicaudatus* (Guglielmetti) E. Hegewald	-	-	-	-	-	-	-	-	-	-	2	2.0	-	-	b	-	-
Desmodesmus armatus var. *spinosus* (Fritsch & Rich) E. Hegewald	-	-	-	-	-	-	-	-	1	-	-	-	-	-	b	-	-
**Desmodesmus intermedius* (R. Chodat) E. Hegewald	-	-	-	-	-	-	-	-	-	1	-	-	-	-	b	-	-
**Desmodesmus maximus* (W. West & G. S. West) E. Hegewald	1	-	-	-	11	-	-	-	-	-	-	2.0	-	-	b	-	-
**Desmodesmus opoliensis* (P. Richter) E. Hegewald	1	-	-	-	1	-	-	-	-	-	-	2.2	-	-	b	-	-
**Desmodesmus perforatus* (Lemmermann) E. Hegewald	-	-	-	-	-	-	-	-	-	-	1	-	-	-	-	-	-
**Dictyosphaerium Pulchellum* H.C. Wood	-	-	-	-	1	-	-	-	-	1-2	-	2.3	ind	i	b	-	-
Diplostauron sp.	-	-	-	-	-	-	-	-	-	1	-	-	-	-	-	-	-
Gloeocystis sp.	1	-	-	-	-	-	-	-	-	-	-	-	-	-	-	-	
**Golenkinia radiata* Chodat	-	-	-	-	1	-	-	-	-	-	-	1.9	-	i	o-a	-	-
**Monoraphidium arcuatum* (Korshikov) Hindák	-	-	-	-	-	-	-	-	-	1	-	2.1	-	-	b	-	-
**Monoraphidium contortum* (Thuret)	-	-	-	-	-	-	-	-	1	-	1	2.2	-	-	b	-	-

Table 4 - *Continued*

Komàrková-Legnerová																	
**Monoraphidium griffithii* (Berkeley) Komárk-ová-Legnerová	-	1	-	-	-	-	-	-	-	1-2	-	2.2	-	-	b	-	-
**Monoraphidium irregulare* (G.M.Smith) Komárk-ová-Legnerová	-	-	-	-	-	-	-	-	-	1	-	-	-	i	-	-	-
Monoraphidium obtusum (Korshikov) Komárková-Legnerová	-	-	-	-	1	-	-	-	-	-	-	1.2	-	-	o	-	-
Oedogonium sp.	-	4	-	-	1	-	1-4	1	1-2	-	-	-	-	-	-	-	-
**Oocystis submarina* Lagerheim	-	-	-	-	-	-	-	-	-	3	-	-	-	i	-	-	-
**Pandorina elegans* (Ehrenberg) Dujardin	-	-	-	-	1	-	-	-	-	-	-	2.2	-	i	b	-	-
**Pandorina mora* (O.F. Müller) Bory de Saint-Vincent	-	-	-	-	3	-	-	-	-	-	-	2.1	-	i	b	-	-
**Pediastrum duplex* Meyen	-	-	-	-	1-2	-	-	-	-	-	-	1.8	ind	i	o-a	-	-
**Pediastrum simplex* Meyen	-	-	-	-	1-2	-	-	-	-	-	1-2	1.5	-	-	o-b	-	-
Planctococcus sphaerocystiformis O. Korshikov	-	-	-	-	-	-	-	-	-	2	-	-	-	-	-	-	-
**Scenedesmus acuminatus* (Lagerheim) Chodat	1	-	-	-	1	-	-	-	-	3-4	-	-	-	-	-	-	-
Scenedesmus apiculatus (W. West & G.S. West) Chodat	-	-	-	-	1	-	-	-	-	-	-	-	-	-	-	-	-
Scenedesmus caudato-aculeolatus Chodat	2	-	-	-	-	-	-	-	-	-	-	-	-	-	-	-	-
Scenedesmus obliquus (Turpin) Kützing	-	-	-	-	-	-	-	-	2	-	-	2.0	-	i	b	-	-
Scenedesmus obtusus Meyen	1	-	-	-	1	-	-	-	-	-	-	2.0	-	-	b	-	-
Scenedesmus parvus (G.M. Smith) Bourrelly in Bourrelly et Manguin	-	-	-	-	1	-	-	-	-	-	-	-	-	-	-	-	-
Schroederia setigera (Schröder) Lemmermann	-	-	-	-	-	-	-	-	-	2	-	1.7	-	i	b-o	-	-
Stigeoclonium carolinianum Islam	-	-	-	-	1	-	-	-	-	-	-	-	-	-	-	-	-
**Stigeoclonium tenue* (C. Agardh) Kützing	-	-	-	-	-	-	-	-	3-6	-	-	2.8	-	-	b-p	-	-
**Tetraselmis cordiformis* (N. Carter) Stein	-	-	-	-	-	-	-	-	1	-	-	2.2	-	-	b	-	-
Tetrastrum elegans Playfair	-	-	-	-	-	-	-	-	-	2	1	1.5	-	i	o-b	-	-
**Tetrastrum staurogeniaeforme* (Schröder) Lemmermann	-	-	-	-	-	-	-	-	-	1	-	2.2	-	i	b	-	-
**Uronema confervicola* Lagerheim	-	-	-	-	1	-	-	-	3	-	2	1.8	-	-	o-a	-	-
Charophyta																	
Chara vulgaris Linnaeus	6	-	-	-	-	-	-	-	-	-	-	1.1	-	-	o	-	-
**Closterium acerosum* Ehrenberg ex Ralfs	-	-	-	-	-	1	1	1	1	-	-	2.6	ind	i	a-b	-	-
Closterium ehrenbergii Meneghini ex Ralfs	-	-	-	-	-	-	1	-	1	-	-	1.8	ind	hb	o-a	-	-
Closterium pronum Brébisson	-	-	-	-	-	-	1	-	-	-	-	-	-	i	-	-	-
**Closterium ruficeps* C.G. Ehrenberg	-	-	-	-	-	-	-	-	1	-	-	0.8	-	-	x-b	-	-
Closterium sp.	1	-	-	-	-	-	-	-	-	-	-	-	-	-	-	-	-
Coleochaete sp.	-	-	-	-	3	-	-	-	-	-	2	-	-	-	-	-	-
Cosmarium punctulatum Brébisson	-	-	-	-	2	-	-	-	-	-	-	1.3	acf	hb	o	-	-

Table 4 - *Continued*

Debarya sp.	-	-	-	-	1	-	-	-	-	-	-	-	-	-	-	-	-
**Koliella longiseta* (Vischer) Hindák	-	-	-	-	-	-	-	-	-	2	-	2.1	-	i	b	-	-
**Mougeotia* sp.	-	4-5	-	-	1	-	1-2	5-6	-	-	-	1.0	-	-	o	-	-
Nitella mucronata (A. Braun) Miquel in H.C. Hall	-	6	-	-	-	-	-	-	-	-	-	1.3	-	-	o	-	-
**Spirogyra* sp.	2-6	6	-	6	3	-	2	5	-	-	-	-	-	-	-	-	-
Rhodophyta																	
Audouinella pygmaea (Kützing) Weber-van Bosse	2-3	1-4	-	-	2-6	-	1-3	-	-	-	-	0.5	alf	-	x-o	-	-
***Batrachospermum gelatinosum* (Linnaeus) De Candolle	-	-	-	-	-	-	6	-	-	-	-	0.7	-	-	o-x	-	-
**Hildenbrandia rivularis* (Liebmann) J. Agardh	6	6	-	-	-	-	-	-	-	-	-	0.4	-	-	x-o	-	-
Total from our data 2006-2009 (232)	77	58	32	46	116	25	74	29	70	45	25						
Prevoiously recorded in references [3,16-36] for the objects listed in this Table (227)	8	53	12	6	216	4	19	1	0	7	111						
Totals for the objects studied in 1887-2009 in the Upper Jordan River Basin (altogether 466)	81	101	41	49	289	29	90	29	70	49	121						

Note: List of species found in the Upper Jordan River algal communities in 2006-2009 with abundance on the Korde scale [42] and autecological preferences. Hal–halobity degree on the Hustedt's [43] (hb–oligohalobes-halophobes, i–oligohalobes-indifferent, mh–mesohalobes, hl–halophiles; oh–oligohalobes of whide specter with optimum as indifferent); pH–pH degree on the Hustedt's [44] (alb-alkalibiontes; alf–alkaliphiles, ind–indifferents; acf–acidophiles; neu–neutrophiles); S–degree of saprobity on the Pantle-Buck's [45-47] (x–xenosaprobes, x-o–xeno-oligosaprobes, o-x– oligo-xenosaprobes, x-β–xeno-betamesosaprobes, o–oligosaprobes, o-β–oligo-betamesosaprobes, β-o–beta-oligosaprobes, β–betamesosaprobes, β-α –beta-alphamesosaprobes, β-p–beta-polysaprobes, o-α–oligo-alphasaprobes, α-β–alpha-betamesosaprobes, α–alphamesosaprobes, i–i-eusaprobes); Nitrogen uptake metabolism [48] (ats–nitrogen-autotrophic taxa, tolerating very small concentrations of organically bound nitrogen; ate–nitrogen-autotrophic taxa, tolerating elevated concentrations of organically bound nitrogen; hne–facultatively nitrogen-heterotrophic taxa, needing periodically elevated concentrations of organically bound nitrogen; hce–obligately nitrogen-heterotrophic taxa, needing continuously elevated concentrations of organically bound nitrogen); Trophic state [48] (ot–oligotraphentic; o-m–oligo-mesotraphentic; m–mesotraphentic; m-e–meso-eutraphentic; e–eutraphentic; he–hypereutraphentic; hy–oligo-to eutraphentic (hypereutraphentic)); *–taxa, previously mentioned in references for the Upper Jordan River and tributaries; **–first time finding taxa for Israel.

A dendrite (**Figure 15**), which was constructed by the paar-similarity calculating method, shows the closest cross-sections of the algal communities' diversity in the studied rivers. The bold connection lines of the Upper Jordan, Yehudiyya, and Meshushim rivers revealed the most similar communities. These rivers are very close to each other and to Lake Kinneret. The Daliyyot River community was included in the Upper Jordan River community, and the Banias was included in Yehudiyya.

The Saar and Ayun rivers' communities were included in the Snir community. The Hula and Ram Lakes' communities were not only the most different from the others, but also different between themselves. Ram is a volcanic crater lake and the Hula is a very different type of lake: see dramatic divergence in **Figure 15**. Therefore, the dendrite revealed the internal relatedness of communities of the rivers. This seems also connected with both hydrology and habitat height above sea level. Species-rich communities from the lower part of the basin were the most similar, and communities of the lakes were most different.

From the results of this investigation of the Upper Jordan River Basin communities, the species list of algae and cyanobacteria were significantly enriched from 327 to 467 species and infraspecies belonging to seven divisions. We found 232 taxa; 85 were mentioned for the first time for the Upper Jordan River basin and three of which were new for Israel. An historical analysis of the species richness dynamic in the Upper Jordan River algal communities shows that species richness has fluctuated during the last century with peaks in 1951, 1965, 1978, and 2009. Bio-indicators of major fluctuating environmental parameters revealed temperature stress at times when the taxonomic structure was changed – in the 1950s and in 1996. Salinity impacts occurred in 1938 and 2000; acidification in 1938, 1996, and 2000 and organic pollution in 1996. Therefore, we can conclude that 1938, 1996, and 2000 were critical years for the Upper Jordan River ecosystem. As a result, indicators of the trophic status [48] showed the stress of organic pollution since the 1970s, marked by dramatic increases in eutraphentic and hypereutraphentic species.

Present data analyses of spatial distribution of algal communities in the Upper Jordan River can be seen in

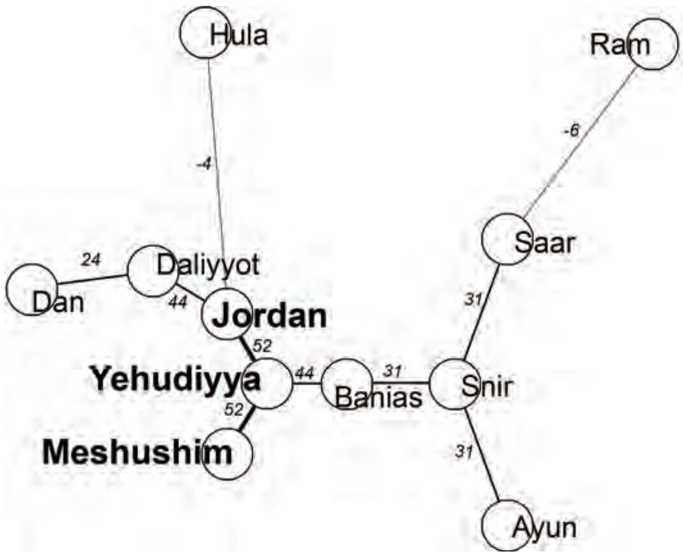

Figure 15. Dendrite of similar taxonomic structure on the rivers of the Upper Jordan basin constructed by the paar-similarity calculating method on the basis of Serensen-Chekanovsky indices. The floristic core of the Upper Jordan River algal diversity is marked by bold lines.

the three peaks of diversity fluctuation. This fluctuation correlates with the impact of organic pollution (revealed by the saprobity indices S) points on the river channel – after the Masade village effluence, after the confluence with three tributaries Snir, Banias and Ayun, and near the entrance to Lake Kinneret (see **Figure 1**). A significant amount of pollution was from the Masade village area in winter, whereas in the dry summer, the Saar tributary was desiccated. Organic pollution in the central and lower sections of the Upper Jordan basin is found year-round. It dose not damp, but rather stimulates the species diversity. This difference can be reflected in the orientation of each basin area: the Saar tributary is east-west, but the Upper Jordan is north-south. It is important in the arid and semi-arid environments of the Middle East [51].

4. Conclusions

The different approaches in comparing the diversity in each river of the Upper Jordan Basin pointed to hydrology as the most regulating factor in species composition of the algal communities. Using comparative floristic methods, we did not reveal any influence of the anthropogenic pollution on the structure of algal communities as a whole. However, it seems that streaming water, which influenced the hydrology of the river, can be marked as having a major impact, as was mentioned for the rivers in the Mediterranean region [52,53]. Dramatic seasonal changes in communities' structure also pointed to hydrology, which was different in dry and rainy seasons, as we revealed for the central Israel riverine communities [10]. On the other hand, the hydrology of the river basin is a conservative factor, which correlates with the climate and topography of the region [4], rather than with the effects of anthropogenic influence (especially for the oligotrophic river, such as the Upper Jordan). Statistical analysis shows indifferent relatedness of the algal species diversity forming process and the anthropogenic pollution influence in the Upper Jordan River Basin as a whole. Our results also show the relatedness to local climatic factors, which controlled species diversity distribution on all diversity levels in the Mediterranean climatic zone [54].

Therefore, since the algal species diversity of the Upper Jordan has been formed under the influence of regional climatic factors, it can be currently recognized as a natural system, with a high buffering and self-purification capacity.

5. Acknowledgements

We thank Moti Tavassi for his efforts in collecting algal samples from the Upper Jordan River. This work was partially funded by the Israel Ministry of Absorption and the Ancell Teicher Research Foundation.

6. References

[1] A. Dell'Uomo, "Use of Algae for Monitoring Rivers in Italy: Current Situation and Perspectives," In: J. Prygiel, B. A. Whitton, J. Buckowska, Eds., *Use of Algae for Monitoring Rivers III*, Agence de I'Eau Artois-Picardie Press, Douai Cedex, 1999.

[2] J. Prygiel, M. Coste and J. Buckowska, "Review of the Major Diatom-Based Techniques for the Quality Assessment of Rivers," *State of the Art in Europe*, In: J. Prygiel, B. A. Whitton, J. Buckowska, Eds., *Use of Algae*

for Monitoring Rivers III, Agence de I'Eau Artois-Picardie Press, Douai Cedex, 1999.

[3] E. Nevo and S. P. Wasser, Eds, "Biodiversity of Cyanoprocaryotes, Algae and Fungi of Israel," *Cyanoprocaryotes and Algae of Continental Israel*, A. R. G. Gantner Verlag, Ruggell, 2000.

[4] A. Shaban, C. Robinson and F. El-Baz, "Using MODIS Images and TRMM Data to Correlate Rainfall Peaks and Water Discharges from the Lebanese Coastal Rivers," *Journal of Water Resource and Protection*, Vol. 1, No. 4, 2009, pp. 227-236.

[5] É. Ács and K. T. Kiss, "Investigation of Periphytic Algae in the Danube at Göd (1669 river km, Hungary)," *Archive Hydrobiology - Algological Studies*, Vol. 62, No. (*Suppl.* 89), 1991, pp. 47-67.

[6] É. Ács, K. Szabó, K. T. Kiss and F. Hindák, "Benthic Algal Investigations in the Danube River and Some of its Main Tributaries from Germany to Hungary," Biologia, Vol. 58, No. 4, 2003, pp. 545-554.

[7] É. Ács, K. Szabó, B. Tóth and K. T. Kiss, "Investigations of Benthic Algal Community (with Special Attention to Bentic Diatoms) in Connection with Reference Conditions in WFD," *Acta Botanica Hungarica*, Vol. 46, 2004, pp. 255-278.

[8] É. Ács, K. Szabó, Á. K. Kiss, B. Tóth, Gy. Záray and K. T. Kiss, "Investigation of Epilithic Algae on the River Danube from Germany to Hungary and the Effect of a Very Dry Year on the Algae of the River Danube," *Archive Hydrobiology Large Rivers*, Vol. 16, No. (*Suppl.*), 2006, pp. 389-417.

[9] K. É. Szabó, K. T. Kiss, Gy. Taba and É. Ács, "Epiphytic Diatoms of the Tisza River, Kisköre Reservoir and Some Oxbows of the Tisza River after the Cyanide and Heavy Metal Pollution in 2000," *Acta Botanica Croatica*, Vol. 64, No. 1, 2005, pp. 1-46,

[10] S. S. Barinova, M. Tavassi and E. Nevo, "Study of Seasonal Influences on Algal Biodiversity in the Yarqon River (Central Israel) by Bio-Indication and Canonical Correspondence Analysis (CCA)," *Turkish Journal of Botany*, Vol. 33, 2009, pp. 353-372.

[11] A. A. El-Awamri, A. E. M. Shaaban and A. I. Saleh, "Floristic Study on Benthic Diatoms of the Groundwater Seepages at Kobri El-kobba (Cairo, Egypt)," *Journal of Applied Science Research*, Vol. 3, No. 12, 2007, pp. 1809-1818.

[12] L. E. Squires and N. S. Saoud, "Effects of Water Quality and Season on Diatom Community Structure in the Damour River, Lebanon," *Hydrobiologia*, Vol. 133, No. 1, 1986, pp. 127-141.

[13] Y. Aktan and G. Aykulu, "Colonisation of Epipelic Diatoms on the Littoral Sediments of Üzmit Bay," *Turkish Journal of Botany*, Vol. 29, No. 2, 2005, pp. 83-94.

[14] H. Gurbuz and E. Kivrak, "Use of Epilithic Diatoms to Evaluate Water Quality in the Karasu River of Turkey," *Journal of Environment Biology*, Vol. 23, No. 3, 2002, pp. 239-246.

[15] M. Menachem, "The Jordan Valley and Eastern Sumaria," Bikat Hayarden Ve Mizrach Hashomron, Hebrew, 1992.

[16] T. Berman, U. Pollngher and T. Zohary, "A Short History of Stability and Change in Phytoplankton Populations in Lake Kinneret," *Israel Journal of Plant Science*, Vol. 46, No. 2, 1998, pp. 73-80.

[17] I. Dor, "Algues Des Sources Thermals de Tiberiade, Lake Tiberias Investigations," *The Sea Fisheries Research Station Bulletin*, Vol. 48, No. 4-5, 1967, pp. 3-29.

[18] I. Dor, "Considerations about the Composition of Benthic Algal Flora in Lake Kinneret," *Hydrobioogia*, Vol. 44, No. 2-3, 1974, pp. 255-264.

[19] A. Ehrlich, "Atlas of the Inland-Water Diatom Flora of Israel," *Israel Academic Science and Human*, Vol. 5, 1995, pp. 173-175.

[20] H. Hisoriev, A. F. Krahmalny and L. Krinitz, "Species Diversity of Algae in Water Bodies of Hula Valley (Northern Israel)," *Algologia*, Vol. 6, No. 2, 1996, pp. 49-56.

[21] H. Hisoriev, S. P. Wasser, E. Nevo and V. V. Stupina, "In Addition to the Flora of *Euglenophyta* of Israel," *International Journal of Algae*, Vol. 1, No. 2, 1999, pp. 63-75.

[22] B. Kimor and U. Pollingher, "The Plankton Algae of Lake Tiberias," *Sea Fish Research Station of Haifa*, ser. A78, Vol. 16, No. 7, 1965, pp. 1-72.

[23] B. Kimor, "The Phytoplankton of Lake Kinneret," *Monographiae Biologicae*, Vol. 32, No. 1, 1978, pp. 231-233.

[24] B. Komarovsky, "A Comparative Study of the Phytoplankton of Several Fish Ponds in Relation to Some of the Essential Chemical Constituents of the Water," *Bulletin Research of Council Israel*, Vol. 2, No. 4, 1953, pp. 379-410.

[25] A. F. Krakhmalny, S. P. Wasser and E. Nevo, "New Dinophyta Species for Israel," *Algology*, Vol. 6, No. 1, 1996, pp. 81-85.

[26] G. M. Palamar-Mordvintseva, "To Flora of Zygnematales (Conjugatophyceae) of Israel," *Algologia*, Vol. 6, No. 4, 1996, pp. 405-426.

[27] U. Polingher, "The Algae of the River Jordan," *Monographiae Biologicae*, Vol. 32, No. 2, 1978, pp. 223-228.

[28] U. Polingher, "Algae Found in the Plankton of Lake Kinneret," *Monographiae Biologicae*, Vol. 32, No. 2, 1978, pp. 236-242.

[29] U. Pollingher, T. Zohary and T. Fishbein, "Algal Flora in the Hula Valley – Past and Present," *Israel Journal of Plant Science*, Vol. 46, No. 3, 1998, pp. 155-168.

[30] M. Petit, "Liste des Diatomées du Lac de Tibériadé," In: L. Lortet, Ed., Études Zoo-Logiques sur la Fauna du lac de Tibériade suivies dén aperçu sur la fauna des lacs d'Antioche et de Homś," *Archieve Museum History Nature* (Lyon), Vol. 3, No. 11, 1883, pp. 191-192.

[31] M. Rahat and I. Dor, "The Hidden Flora of a Lake," *Hyrobiologia*, Vol. 31, No. 2, 1968, pp. 186-192.

[32] T. Rayss and E. Katchalsky, "About the Plankton in Lake Hula," *Country and Nature Brochure*, Vol. 5, No. 10, December 1938, pp. 669-671.

[33] T. Rayss, "Materiaux Pour la Flore Algologique de la Palestine I. Les Cyanophycees," *Pakistan Journal of Botany*, Vol. 3, No. 1, 1944, pp. 94-113.

[34] T. Rayss, "Les Algaes des Aeux Continentals. Materiaux Paur la Flore Algologique de la Palestine," *Pakistan Journal of Botany*, Vol. 5, 1951, pp. 71-95,

[35] F. E. Round, "The Benthic Algae," In: C. Serruya, Ed., *Lake Kinneret*, Dr. W. Junk Publishers, Dordrecht, 1978, pp. 323-328.

[36] P. M. Tsarenko, V. V. Stupina, S. P. Wasser, E. Nevo, O. V. Kovalenko, E. S. Kondratiuk, H. H. Hisoriev, A. F. Krahmalny and L. Krinitz, "Species Diversity of algae in Water Bodies of Hula Valley (Northern Israel)," *Algologia*, in Russian, Vol. 6, No. 2, 1996, pp. 182-193.

[37] E. Swift, "Cleaning Diatom Frustules with Ultraviolet Radiation and Peroxide," *Phycologia*, Vol. 6, No. 2-3, 1967, pp. 161-163.

[38] S. S. Barinova, "Morphology of Connective Spines in Diatom Algae of the Genus *Aulacoseira* Thwaites," *Paleontological Journal*, Vol. 31, No. 2, 1997, pp. 239-245.

[39] M. D. Guiry and G. M. Guiry, "AlgaeBase," World-Wide Electronic Publication, National University of Ireland, Galway, December 2009. http://www.algaebase.org

[40] S. S. Barinova, L. A. Medvedeva and O. V. Anissimova, "Diversity of Algal Indicators in Environmental Assessment," *Pilies Studio* (*in Russian*), 2006.

[41] E. Lipkovsky, S. Barinova, B. Teltsch and E. Nevo, "Seasonal Influences on Algal Biodiversity in the Upper Jordan River by bioindication and Canonical Correspondence Analysis (CCA)," *Applied Ecology and Environmental Research*, in Press.

[42] N. V. Korde, "The Methods of Biological Studies for the Bottom Deposits of Lakes (The Field Methods of Biological Analysis)," In: *Freshwater Life in USSR*, *Russion Academic Science Press*, in Russian, Vol. 4, No. 1, 1956, pp. 383-413.

[43] F. Hustedt, "Systematisch und Okologische Untersuchungen Uber Die Diatomeenflora von Java, Bali und Sumatra," *Archieve Hydrobiology Supply*, Vol. 15, pp. 131-177, 393-506, 638-790; Vol. 16, pp. 1-155, 274-394, 1938-1939.

[44] F. Hustedt, "Die Diatomeenflora des Flußsystems der Weser im Gebiet der Hansestadt Bremen," *Abhandl Naturw Ver Bremen*, Vol. 34, No. 3, 1957, pp. 181-440.

[45] E. Pantle and H. Buck, "Die Biologische Uberwachung der Gewässer und Die Darstellung der Ergebnisse," *Gas- und Wasserfach*, Vol. 96, No. 18, 1955, pp. 1-604.

[46] V. Sládeček, "System of Water Quality from the Biological Point of View," *Achieves für Hydrobiologie - Beiheft Ergebnisse der Limnologie*, Vol. 7, No. 1, 1973, pp. 1-218.

[47] V. Sládeček, "Diatom as Indicators of Organic Pollution," *Achieves Hydrochemistry Hydrobiology*, Vol. 14, 1986, pp. 555-566.

[48] H. Van Dam, A. Mertens and J. Sinkeldam, "A Coded Checklist and Ecological Indicator Values of Freshwater Diatoms from the Netherlands," *Netherlands Journal of Aquatic Ecology*, Vol. 28, No. 1, 1994, pp. 117-133.

[49] P. Bourrelly, "Ecology of Freshwater Organisms. 2. Algae and Other Aquatic Plants," *Verhandlungen der Internationalen Vereinigung Limnologie*, Vol. 18, No. 1, 1973, pp. 1326-1337.

[50] A. B. Novakovsky, "Abilities and Base Principles of Program Module 'GRAPHS'," *Scientific Reports*, Komi Scientific Center, Ural Division of the Russian Academy of Sciences, Vol. 27, No. 1, 2004.

[51] M. Al Saud, "Watershed Characterization of Wadi Aurnah, Western Arabian Peninsula," *Journal of Water Resource and Protection*, Vol. 1, No. 5, 2009, pp. 316-324.

[52] B. C. Emerson and R. G. Gillespie, "Phylogenetic Analysis of Community Assembly and Structure over Space and Time," *Trends Ecology Evolution*, Vol. 23, No. 11, 2008, pp. 619-630.

[53] M. Cantonati, R. Gerecke and E. Bertuzzi, "Springs of the Alps – Sensitive Ecosystems to Environmental Chan- ge: From Biodiversity Assessments to Long-Term Studies," *Hydrobiologia*, Vol. 562, No. 1, June 2006, pp. 59-96.

[54] T. Pavliček and E. Nevo, "Local Species Richness Distribution at 'Evolution Canyon' Microsite," Mt. Carmel, Israel, Ecologia Mediterranean, Vol. 34, No. 6, 2008, pp. 25-34.

J. Water Resource and Protection, **2010, 2, 527-531**
doi:10.4236/jwarp.2010.26059 Published Online June 2010 (http://www.SciRP.org/journal/jwarp)

Influence of Carbon Source on Biological Nitrogen Removal by Immobilised Bacteria

Wilawan Khanitchaidecha[1], Tatsuo Sumino[2], Futaba Kazama[1]
[1]*Interdisciplinary Graduate School of Medicine and Engineering, University of Yamanashi, Yamanashi, Japan*
[2]*Matsudo Research Laboratory, Hitachi Plant Technologies, Chiba, Japan*
E-mail: *wilawank1@gmail.com, kfutaba@yamanashi.ac.jp, tatsuo.sumino.cj@hitachi-pt.com*
Received January 8, 2010; *revised March* 24, 2010; *accepted April* 20, 2010

Abstract

Acetate, ethanol, and hydrolysed rice were used as external carbon sources in an ammonium removal process employing immobilised bacteria. The influence of the carbon source on the occurrence of free cells and total nitrogen removal efficiency was examined at C/N ratios of 1.5 (low), 2.5 (medium), and 3.5 (high). At the low C/N ratio, no free cells were found in the reactors and the use of acetate as the carbon source resulted in the highest total nitrogen removal efficiency, followed by ethanol and hydrolysed rice. The occurrence of free cells in reactors fed with acetate and ethanol led to a negligible increase in the total nitrogen removal efficiency with increasing C/N ratio. The results suggest that acetate is the most appropriate carbon source for nitrogen removal and that the number of free cells should be minimized to achieve the highest efficiency during long-term operation.

Keywords: Nitrogen Removal, Nitrification and Denitrification, Carbon Sources

1. Introduction

During the past few decades, biological ammonium-nitrogen (NH_4-N) removal has emerged as one of the most interesting methods for water and wastewater treatment. The system consists of a nitrification process (NH_4-N $\rightarrow$ NO_3-N (nitrate-nitrogen)) followed by denitrification to produce non-toxic nitrogen gas (NO_3-N $\rightarrow$ N_2). In general, nitrification is an aerobic process and denitrification is an anaerobic process. A source of organic carbon is an important component of the denitrification process. Several sources of carbon have been used including acetate [1-3], methanol [2,4], ethanol [1,3], glucose [3], peptone [3], glycerol [5], and lactic acid [5]. Additionally, solid waste-derived carbon sources such as molasses [6], corncobs [7], and excess sludge [8] have also been used. **Table 1** provides a comparison of the nitrogen removal efficiency obtained using various carbon sources. Of these, acetate and ethanol are attractive and versatile substrates due to biodegradability, low consumption (mg-C/mg-N), and low toxicity. Despite the effort invested in exploring biological nitrogen removal, there are few reports on the influence of the carbon source on N removal efficiency, particularly acetate vs. ethanol [9,10], and no research on the occurrence of free cells when using various carbon sources. Free cells are commonly found in immobilised sludge systems, and result in ineffective NH_4-N removal. The present work examines the influence of external carbon sources including acetate, ethanol, and hydrolysed rice (representing a solid waste source) on nitrogen removal. The use of hydrolysed rice in NH_4-N removal provides a potential means of waste reduction.

2. Materials and Methods

2.1. Solution Preparation

Simulated wastewater influent solution containing 40 mg/L of NH_4-N was prepared by mixing 0.19 g/L of $(NH_4)_2SO_4$, 0.48 g/L of $NaHCO_3$, 0.05 g/L of KCl, 0.11 g/L of $CaCl_2 \cdot 2H_2O$, 0.1 g/L of $MgSO_4 \cdot 7H_2O$, and 0.02 g/L of $Na_2HPO_4 \cdot 12H_2O$. The carbon concentration of acetate and ethanol feed solutions was fixed at 7.1 g/L.

Hydrolysed rice was prepared by adding 35 g of rice and 18 mL of 6 M HCl to 1L of tap water. The solution was heated to 90ºC for 24 hours. The resulting carbon concentration of the hydrolysed rice solution was 6.5-7.0 g/L of total organic carbon (TOC) and ~0.1 g/L of volatile organic carbon (VOC).

Table 1. Nitrogen removal efficiency and C/N ratio requirement observed using various carbon sources.

Carbon source	C/N ratio (mg-C/mg-N)	Nitrogen removal efficiency (%)	Reference
Acetate	1.5	90-100	[2]
Methanol	1.5	90-100	
Acetate	5.0	~100	[3]
Glucose	5.0	~100	
Acetic acid	1.1	~100	[9]
Ethanol	0.6	~100	
Acetic acid	4.3	98	[10]
Ethanol	2.35	91	
Methanol	2.9	93	
Ethanol	2.5	~100	[11]
Succinate	2.5		
Molasses	6[a]	92	[6]
Corncobs	1.5[a]	90	[7]

[a] mg-COD/mg-N ratio

2.2. Polyethylene Glycol (PEG) Pellet Preparation

Sludge was collected from the first sedimentation tank of a drinking water plant in Kofu, Japan. A 34.5 mL portion of 10% concentrated sludge was mixed with 10.5 mL of a solution containing PEG pre-polymer and promoter, and 5 mL of potassium persulfate ($K_2S_2O_8$) was added to initiate polymerization. The polymerized gel was cut into 3 mm cubes referred to as PEG pellets.

2.3. Reactor Set-up

A 3L acrylic reactor (12.5 × 16 × 20 cm) was separated into two identical chambers (the aeration and non-aeration chambers) by an acrylic plate perforated by a number of small holes (**Figure 1**). The aeration chamber contained 8 g of support material (polyester textile, Networking of Engineering and Textile Processing (NET) Company, Japan) and 0.05 L of 10% concentrated sludge. The bulk dissolved oxygen (DO) concentration was maintained at 5-6 mg/L, and the NH_4-N solution (influent) was continuously supplied at a rate of 0.2 L/h. The non-aeration chamber contained 0.6 L of PEG pellets, and the bulk DO concentration ranged from 4-5 mg/L. In order to investigate the effect of carbon source at various C/N ratios, the carbon source solution was fed to the non-aeration chamber for 10 min every 4 hours at a rate of ~42 mL/h (for the 1.5 C/N ratio), ~70 mL/h (for the 2.5 C/N ratio), or ~98 mL/h (for the 3.5 C/N ratio). The hydraulic retention time of the reactors was approximately 12 hours.

2.4. Analytical Methods

The influent and effluent were analysed for NH_4-N, NO_2-N, and NO_3-N concentrations using standard methods [12]. The total suspended solids (TSS) and VOC contents were measured at irregular intervals in accordance with standard methods [12]. The organic carbon concentration was analysed using an organic carbon analyser (Shimadzu *TOC*-5050*A*). The temperature, pH, and DO concentration of the reactor were measured onsite.

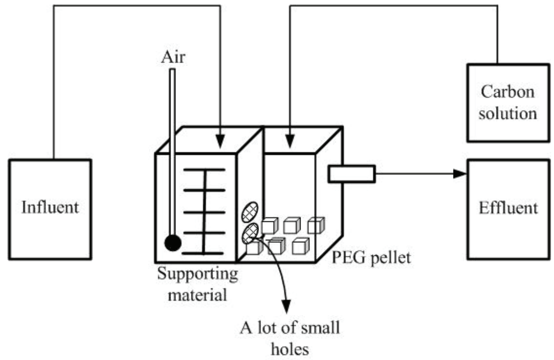

Figure 1. Schematic diagram of reactor design and operation.

3. Results and Discussion

In the aeration chamber of all reactors, the complete liquid recirculation produced by continuous aeration resulted in attachment of the sludge bacteria to the supporting material. The conditions in this chamber included a high DO concentration and continuous influent NH_4-N feed, resulting in nitrification being the main process in this chamber. Cultivation of nitrifying bacteria was indicated by a change in colour of the attached bacteria from dark to light brown. Nitrification was not the rate-limiting step in the process, since the zero concentration of NH_4-N in the effluent indicated complete nitrification (**Figures 2(a-d)**).

The non-aeration chamber directly communicated with the aeration chamber through the perforated divider, and the water containing high concentrations of NO_3-N and DO was immediately introduced to the non-aeration chamber. The DO concentration in the non-aeration chamber was 4-5 mg/L. Although this concentration is somewhat higher than usual for denitrification, the limited oxygen diffusion into the pellet and oxygen consumption by bacteria near the pellet surface led to formation of an anaerobic zone in the pellet core where denitrification could occur. The NO_3-N and added carbon (*i.e.* acetate, ethanol) diffused into the core as explained by Jun *et al.* [13]. The denitrifying bacteria were concentrated in the pellet core, while the region near the surface predominantly contained competing aerobic heterotrophic bacteria. In the present work, the denitrification process was the rate-limiting step of NH_4-N removal and the efficiency of the denitrification process depended on the growth rate of competitive bacteria, the carbon consumption, and the carbon source. The effect of carbon

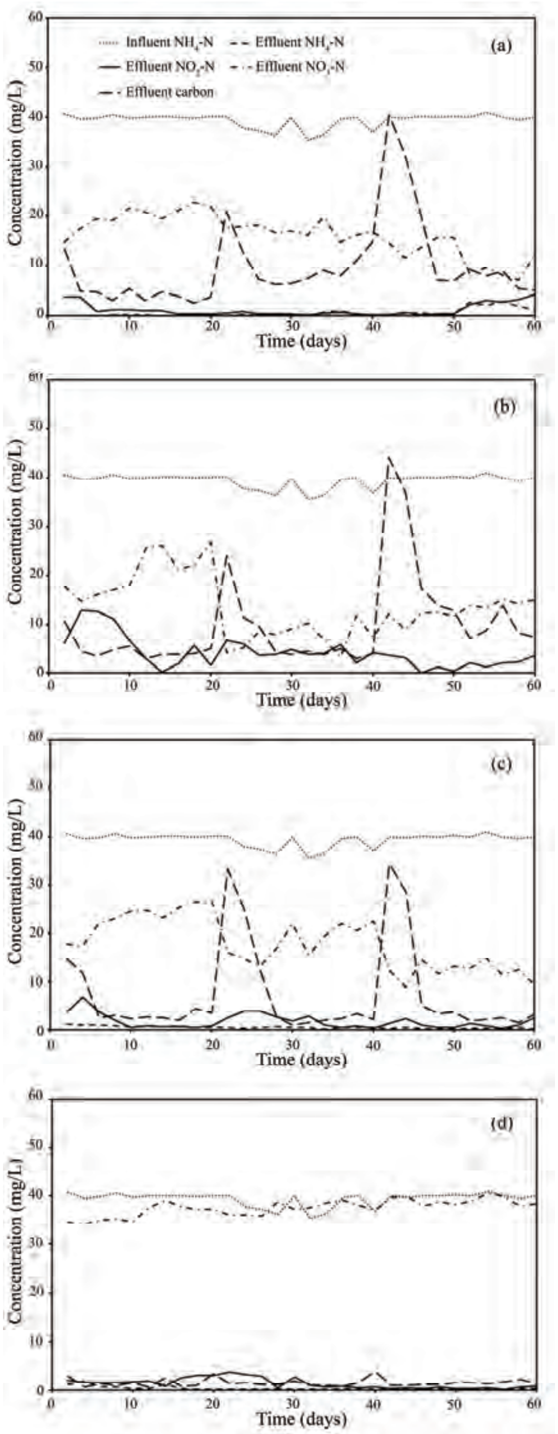

Figure 2. Nitrogen time course for (a) acetate-fed reactor; (b) ethanol-fed reactor; (c) hydrolysed rice-fed reactor, and (d) zero carbon feed reactor.

source on denitrification and growth of competing bacteria was examined during long-term operation (60 days).

Figure 3 depicts the total N (NH_4-N + NO_2-N + NO_3-N) removal efficiency for reactors fed with various carbon sources. It is not helpful to compare the efficiency be-

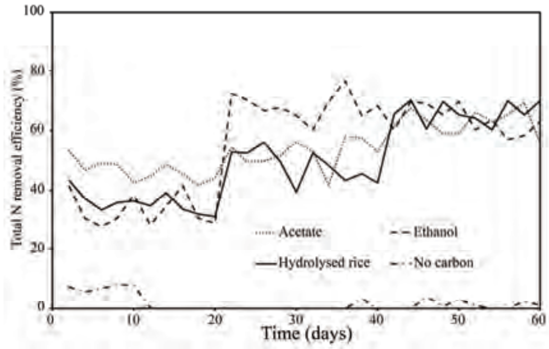

Figure 3. Total nitrogen removal efficiency of acetate-fed reactor, ethanol-fed reactor, and hydrolysed rice-fed reactor at C/N ratios of 1.5, 2.5, and 3.5, and zero carbon feed reactor.

-tween different C/N ratios, because the reactors were continuously operated with step-wise increases in C/N ratio. However, the effects of C/N ratio and carbon source on the growth of competitive bacteria were evident, and the increase in competitive bacteria might eventually affect the NH_4-N removal efficiency.

3.1. Low C/N Ratio

The NH_4-N removal efficiency of reactors operated under different carbon feed conditions is illustrated in **Figure 3**, and the results are summarised in **Table 2.** The efficiency of the acetate-fed reactor was 46.5%, higher than the ethanol-fed reactor at 33.1% or the hydrolysed rice-fed reactor at 35.5%. Acetate is a readily biodegradable carbon source and is directly incorporated into the Krebs cycle to release energy for bacterial metabolism, while ethanol and hydrolysed rice require preliminary processing to convert them to acetic acid or pyruvic acid [14]. The utilization of acetate, ethanol, and hydrolysed rice for energy production in heterotrophic bacteria (*i.e.* denitrifying bacteria) is sketched in **Figure 4**. Constantin and Fick [9] reported that approximately 25% of the added carbon is expended during this preliminary conversion process, resulting in a decrease in the net carbon feed for the ethanol and hydrolyzed rice-fed reactors. The required energy (expressed as the Gibbs free

Table 2. Summary of average total nitrogen removal efficiency from Figure 3.

Carbon Source	Total N removal efficiency (%)		
	C/N ratio of 1.5	*C/N ratio of* 2.5	*C/N ratio of* 3.5
Acetate	46.5 ± 3.5	52.4 ± 4.8	63.1 ± 4.4
Ethanol	33.1 ± 5.4	68.3 ± 4.8	63.6 ± 4.8
Hydrolysed rice	35.5 ± 3.7	48.2 ± 5.5	66.2 ± 3.9
No carbon		1.7 ± 2.5	

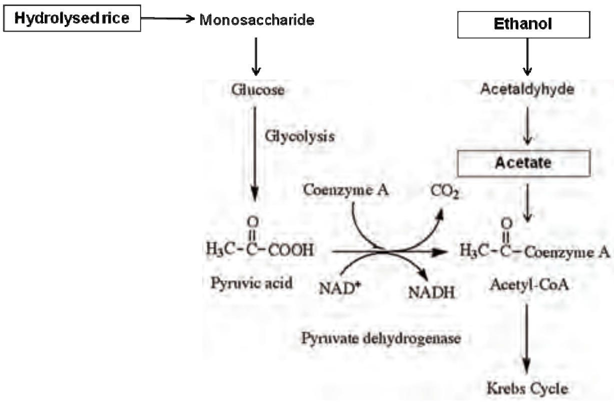

Figure 4. Process for carbon utilization by heterotrophic bacteria (modified from Akunna *et al.* [14]).

energy ΔG) for bacterial metabolism via acetate, ethanol, and glucose (the monomer of rice starch) consumption are 1110.5, 1325, and 2825 kJ/mol [15]. The consumption of acetate requires the least energy, supporting the preceding explanation that acetate is more easily utilized by heterotrophic bacteria.

The similar efficiency when using ethanol and hydrolysed rice as carbon sources reflects the incomplete hydrolysis (low $\frac{VOC}{DOC}$) of the rice used as the carbon source, and the effective use of hydrolysed rice for NH_4-N removal will require further study. In the reactor operated without a carbon source, the N removal efficiency was approximately 10% for 10 days, and eventually decreased to zero. Some nitrogen was removed during startup as stored carbon (*i.e.* Poly-β-hydroxybutyrate, PHB) was consumed as an energy source for denitrification [16]. The denitrification process ceased when the stored carbon was exhausted after 10 days of operation.

3.2. Medium C/N Ratio

At a C/N ratio of 2.5, the total N removal efficiency was highest in the ethanol-fed reactor, followed by the acetate and hydrolysed rice-fed reactors (**Table 2**). Suspended free cells were found in the non-aeration chamber of the acetate-fed reactor, but not in the other reactors. The occurrence of free cells in the acetate-fed reactor is due to a rapid increase in the number of competitive bacteria with increasing acetate concentration, followed by release from the pellet surface to the bulk solution. As discussed earlier, acetate is the most efficient carbon source for heterotrophic bacteria including denitrifying and other competitive bacteria. The free cells were pre- sent in the acetate-fed reactor at a concentration of ~800 mg/L after 40 days.

In the acetate-fed reactor, some added carbon was consumed by the free cells, leaving less carbon available for denitrifying bacteria. Therefore, the total N removal efficiency was slightly decreased compared to the lower C/N ratio, in contrast to the increased efficiency of the other two reactors. Further, the carbon concentration of 5-10 mg/L remaining in the effluent was higher than under low C/N ratio operation (**Figure 2(a)**). This might be an effect of free cells on the activity of the denitrifying bacteria and their carbon consumption. The free cells in the non-aeration chamber of acetate-fed reactor were removed after 40 days, and the remaining concentration was < 100 mg-TSS/L at that time.

The total N removal efficiency of the hydrolysed rice-fed reactor was approximately 20% lower than that of the ethanol-fed reactor. Two possible reasons are suggested to explain this difference: 1) the low net carbon content of hydrolysed rice due to the initial conversion reactions, and 2) the slow diffusion rate of hydrolysed rice into the pellet core. The diffusion rate is slow because hydrolysed rice is composed of glucose polymer, which is much larger than the molecular structure of ethanol. However, at a low C/N ratio, the differences in net carbon and diffusion rate on the total N removal efficiency could not be seen.

3.3. High C/N Ratio

At a high C/N ratio, the total N removal efficiency for all reactors was similar, ranging from 63-66% (**Table 2**). However, large quantities of free cells were found in the acetate- and ethanol-fed reactors (~1000 mg-TSS/L in the acetate-fed reactor and ~700 mg-TSS/L in the ethanol-fed reactor after 60 days). The explanation for the occurrence of free cells in the ethanol-fed reactor is the same as that previously postulated for the acetate-fed reactor. In the presence of a large number of free cells, the carbon source has no effect on the total N removal efficiency.

No free cells were found in the reactor when hydrolysed rice was used as the carbon source, indicating that most of the carbon was consumed by denitrifying bacteria. This is confirmed by the step-wise increase in efficiency with increasing C/N ratio (**Figure 3**). The slow increase in competitive bacteria (entrapped in the pellet) in this reactor is one advantage of using hydrolysed rice as the carbon source. However, hydrolysed rice requires the addition of more carbon to achieve nitrogen removal in comparison with acetate or ethanol.

In comparison to the literature cited in **Table 1**, the nitrogen removal efficiency in the present work was quite low. The primary reason is the inappropriate reactor design and set-up resulting in a high DO concentration in the non-aeration chamber. Although denitrification occurred, it was not effective. Moreover the high DO concentration and frequent organic carbon feed in the non-aeration chamber induced the rapid growth of competitive bacteria, which was not reported in other investigations.

4. Summary

1) Acetate is the most efficient carbon source for nitrogen removal as indicated by the efficiency at a C/N ratio of 1.5 (no free cells were observed). However, at higher ratios free cells (competitive bacteria) appeared in the acetate-fed reactor. Free cells tend to reduce the efficiency of the denitrification process.

2) Hydrolysed rice is a satisfactory alternative carbon source for nitrogen removal. No free cells were found in the rice-fed reactor. However, further study (including the hydrolysis process) will be required to obtain high nitrogen removal efficiency.

5. Acknowledgements

The authors are grateful for the financial support of GCOE program (University of Yamanashi, Japan), which has allowed this and other developmental work to be undertaken, and Ms. Yuki Hiraka for her assistance in operating the bioreactors.

6. References

[1] Y. Mokhayeri, R. Riffat, I. Takacs, P. Dold, C. Bott, J. Hinojosa, W. Bailey and S. Murthy, "Characterizing Denitrification Kinetics at Cold Temperature Using Various Carbon Sources in Lab-Scale Sequencing Batch Reactors," *Water Science and Technology*, Vol. 58, No. 1, January 2008, pp. 233-238.

[2] T. Osaka, K. Shirotani, S. Yoshie and S. Tsuneda, "Effects of Carbon Source on Denitrification Efficiency and Microbial Community Structure in a Saline Wastewater Treatment Process," *Water Research*, Vol. 42, No. 2, June 2008, pp. 3709-3718.

[3] Y. Otani, K. Hasegawa and K. Hanaki, "Comparison of Aerobic Denitrifying Activity among Three Cultural Species with Various Carbon Source," *Water Science and Technology*, Vol. 50, No. 8, April 2004, pp. 15-22.

[4] M. P. Ginige, J. C. Bowyer, L. Foley, J. Keller and Z. Yuan, "A Comparative Study of Methanol as a Supplementary Carbon Source for Enhancing Denitrification in Primary and Secondary Anoxic Zones," *Biodegradation*, Vol. 20, No. 2, September 2009, pp. 221-234.

[5] J. C. Akuna, C. Bizeau and R. Moletta, "Nitrate and Nitrite Reductions with Anaerobic Sludge Using Various Carbon Sources: Glucose, Glycerol, Acetic Acid, Lactic Acid and Methanol," *Water Research*, Vol. 27, No. 2, April 1993, pp. 1303-1312.

[6] Z. Quan, Y. Jin, C. Yin, J. J. Lee and S. Lee, "Hydrolyzed Molasses as an External Carbon Source in Biological Nitrogen Removal," *Bioresource Technology*, Vol. 96, No. 15, February 2005, pp. 1690-1695.

[7] Z. Xu, L. Shao, H. Yin, H. Chu and Y. Yao, "Biological Denitrification Using Corncobs as a Carbon Source and Biofilm Carrier," *Water Environment Research*, Vol. 81, No. 3, March 2009, pp. 242-247.

[8] V. Aravinthan, T. Mino, S. Takizawa, H. Satoh and T. Matsuo, "Sludge Hydrolysate as a Carbon Source for Denitrification," *Water Science and Technology*, Vol. 43, No. 1, January 2001, pp. 191-199.

[9] H. Constantin and M. Fick, "Influence of C-Sources on the Denitrification Rate of a High-Nitrate Concentrated Industrial Wastewater," *Water Research*, Vol. 31, No. 3, February 1997, pp. 583-589.

[10] A. Mohseni-Bandpi and D. J. Elliott, "Groundwater Denitrification with Alternative Carbon Sources," *Water Science and Technology*, Vol. 38, No. 6, March 1998, pp. 237-243.

[11] K. Heylen, B. Vanparys, L. Wittebolle, W. Verstraete, N. Boon and P. de Vos, "Cultivation of Denitrifying Bacteria: Optimization of Isolation Conditions and Diversity Study," *Applied and Environmental Microbiology*, Vol. 72, No. 4, April 2006, pp. 2637-2643.

[12] American Public Health Association, "Standard Methods for the Examination of Water and Wastewater," 19th Edition, APHA, AWWA, WEF, Am Public Health Assoc Byrd Progress, Springfield, New York, 1995.

[13] B. Jun, K. Miyanaga, Y. Tanji and H. Unno. "Removal of Nitrogenous and Carbonaceous Substrates by a Porous Carrier - Membrance Hybrid Process for Wastewater Treatment," *Biochemical Engineering Journal*, August 2003, Vol. 14, No. 1, pp. 37-44.

[14] J. C. Akunna, C. Bizeau and R. Moletta, "Denitrification in Anaerobic Digesters: Possibilities and Influence of Wastewater COD/N-NO_x Ratio," *Environmental Technology*, Vol. 13, No. 1, April 1992, pp. 825-836.

[15] D. R. Lide, "CRC Handbook of Chemistry and Physics," 81st Edition, CRC Press, Boca Raton, 2000.

[16] K. A. Third, N. Burnett and R. Cord-Ruwisch, "Simultaneous Nitrification and Denitrification Using Stored Substrate (PHB) as the Electron Donor in an SBR," *Biotechnology and Bioengineering*, Vol. 83, No. 6, June 2003, pp. 706-720.

J. Water Resource and Protection, **2010, 2, 532-539**
doi:10.4236/jwarp.2010.26060 Published Online June 2010 (http://www.SciRP.org/journal/jwarp)

Multiphase Flow Simulations through Tarbela Dam Spillways and Tunnels

Muhammad Abid, Muftooh Ur Rehman Siddiqi
Faculty of Mechanical Engineering GIK Institute of Engineering Sciences & Technology, Topi, Pakistan
E-mail: *abid@giki.edu.pk, engr.m.rehman@gmail.com*
Received March 12, 2010; *revised April* 1, 2010; *accepted May* 4, 2010

Abstract

Tarbela dam is one of the largest earth filled dam in the world used for power generation and irrigation purposes. Like all reservoirs the sediments inflow in the Tarbela reservoir has resulted in reduction in water storage capacity and is also causing damage to the tunnels, power generating units and ultimately to the plant equipment. This numerical study was performed to predict the flow patterns and characteristics in Tarbela dam. Tunnel 3 and 4 inlets; originally on the bed level were raised in the 3-D model and meshed. Analysis was performed using multiphase flow (water and air) for maximum inflow in the reservoir, *i.e.*, considering summer season and discharging water through different locations, *i.e.*, tunnels and spillways. Pressure, velocities, flow rate and free surface height results obtained were found in good agreement with the analytical and existing results where available. Results show uneven discharge through each gate due to maximum velocity near exits and overall stagnant phenomena of water within the reservoir. Maximum velocity was observed along the spillways outlet. Strong vortex motion was observed near the spillways outlet and tunnel inlets. New design of Tunnels 3 and 4 were suggested to WAPDA in order to decrease the sediment inflow and improvements in design of the spillways were suggested.

Keywords: Tarbela Dam, Reservoir Flow Simulation, Multiphase Flow, Spillways, Tunnels

1. Introduction

Tarbela dam was constructed in 1970's to regulate seasonal flows of the upper Indus for irrigation of the plains downstream and for hydro power generation. Reservoir length is 96.6 km with catchment area of 250 km^2 and storage capacity of 13.69 km^3. Even after 39 years it is the only major storage reservoir on the Indus. In addition to the irrigation releases exceeding 6.4 MAF it generates up to 3478 MW of electricity, and provides 32% of Pakistan's power needs. It is an asset of Pakistan and is one of the largest lakes of the world. Tarbela is located within the Indus Basin. The lake consists of main embankment dam with a length of 9000 ft and height of 470 ft and two auxiliary dams. It has two spillways *i.e.*, the service spillways and the auxiliary spillways and six tunnels. Service spillways have 7 Gates (50 feet wide × 58 feet high), auxiliary spillway has 9 Gates (50 feet wide × 58 feet high). Three tunnels in the right abutment are used for irrigation and power generation. Other three are used only for irrigation purposes [1].

1.1. Sedimentation

It was recommended by Rust that the principal parameters which govern sedimentation in lakes and rivers can be divided into three categories: physical, chemical and biological [2]. Due to sediment deposition and formation of delta, flow at mouth of small tributaries was blocked. Pools, thus created, further reduce capacity of reservoirs [3]. Tarbela Lake seizes the water of Indus which contains a heavy sedimentation load. During spring and summer season, melting of snow in the Himalayan and Karakorum region causes erosion of the upland catchment. Average sediment inflow in Tarbela Lake was approximately 265 Mt (Metric Ton) per year [4] hence; reduced capacity of the reservoir due to sedimentation delta profile is given in **Table 1** [5], and sedimentation delta profile till 2006 is shown in **Figure 1** [6]. Keeping in view the sediment flows in the reservoir, the aim was to study and analyze different parameters of hydrology.

Table 1. Reduced capacity of Tarbela lake.

Year	Capacity	Reduction MAF
2004	Gross	3.205
	Live	2.568
	Dead	0.630
2006	Gross	3.428
	Live	2.748
	Dead	0.696
2008	Gross	7.990
	Live	6.850
	Dead	0.657

2. Methodology

2.1. Material Selection, Modeling and Meshing

A 3-D model of the Tarbela Dam was made using data and drawings collected from WAPDA including original reservoir base, auxiliary spillways, service spillways, main embankment dam and six tunnels [6-9]. As per recommendations given in [6] tunnel 3 and 4 inlets which originally were on the base were modified and were raised to height of 46.8 m. **Table 2** shows the details of the materials used in the study [10-11].

Initially 117701 tetrahedral elements were generated using ICEM CFD® with maximum element size of 30.5 m, keeping in view the refinement along the spillways and tunnels (**Figures 2(a-c)**). Later on using adaptive meshing, 2589215 elements were used in CFX® for predicting free surface accurately (**Figures 2(d-e)**) [10].

2.2. Boundary Conditions and Solution

Sediment particles were not included during analysis. Homogeneous model was used to model the free surface. $k-\varepsilon$ turbulence model was used during analysis [12]. Domain was considered as isothermal and incompressible [10]. Analysis was performed using volume of fluid method for the maximum inflow of 116×10^5 kg/sec in the reservoir during the summer flood season. Average velocities given in **Table 3** were taken on the tunnels inlets [13]. Along free-surface, service spillways and auxiliary spillways zero Pascal pressure was applied as they were exposed to the atmospheric pressure. No slip conditions were applied on the walls of the reservoir. **Table 4** defines detailed boundary conditions.

3. Results and Discussion

Two case studies were performed

1) Four tunnels and both spillways were open.
2) Service spillways and Auxiliary spillways were open.

Table 2. Material model details.

Property	Water	Air
Thermodynamic State	Liquid	Gas
Dynamic Viscosity	8.899×10^{-4} kg/m.s	1.831×10^{-5} kg/m.s
Density	997.0 kg/m^3	1.185 kg/m^3
Molar Mass	18.02 kg/kmol	28.96 kg/kmol
Reference pressure	1 atm	1 atm
Reference Temperature	25°C	25°C
Gravity	9.8 m/sec^2	9.8 m/sec^2

Table 3. Velocities on tunnels.

Tunnel Number	Velocity (m/sec)
1	8.433
2	8.382
3	11.278
4	11.278

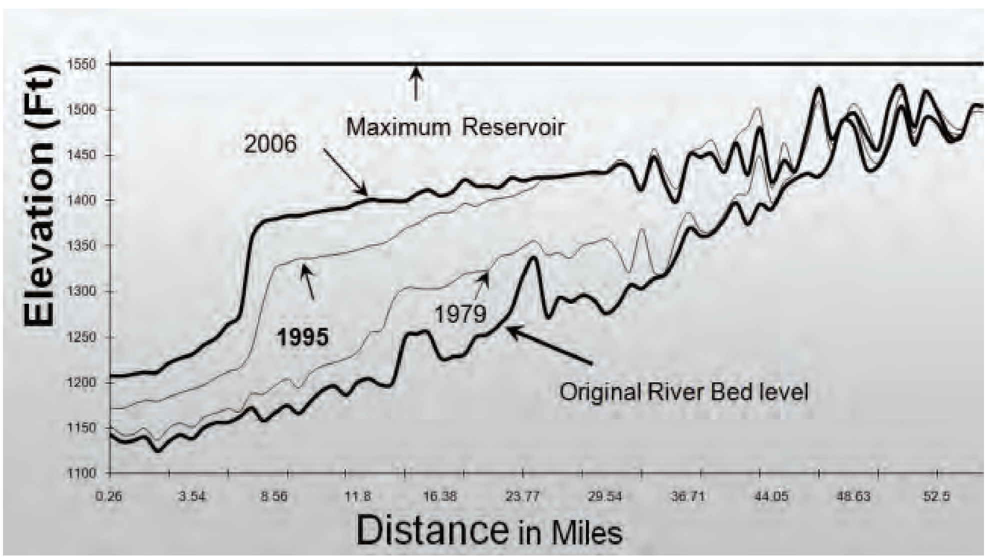

Figure 1. Sedimentation profile for 1974 to 200.

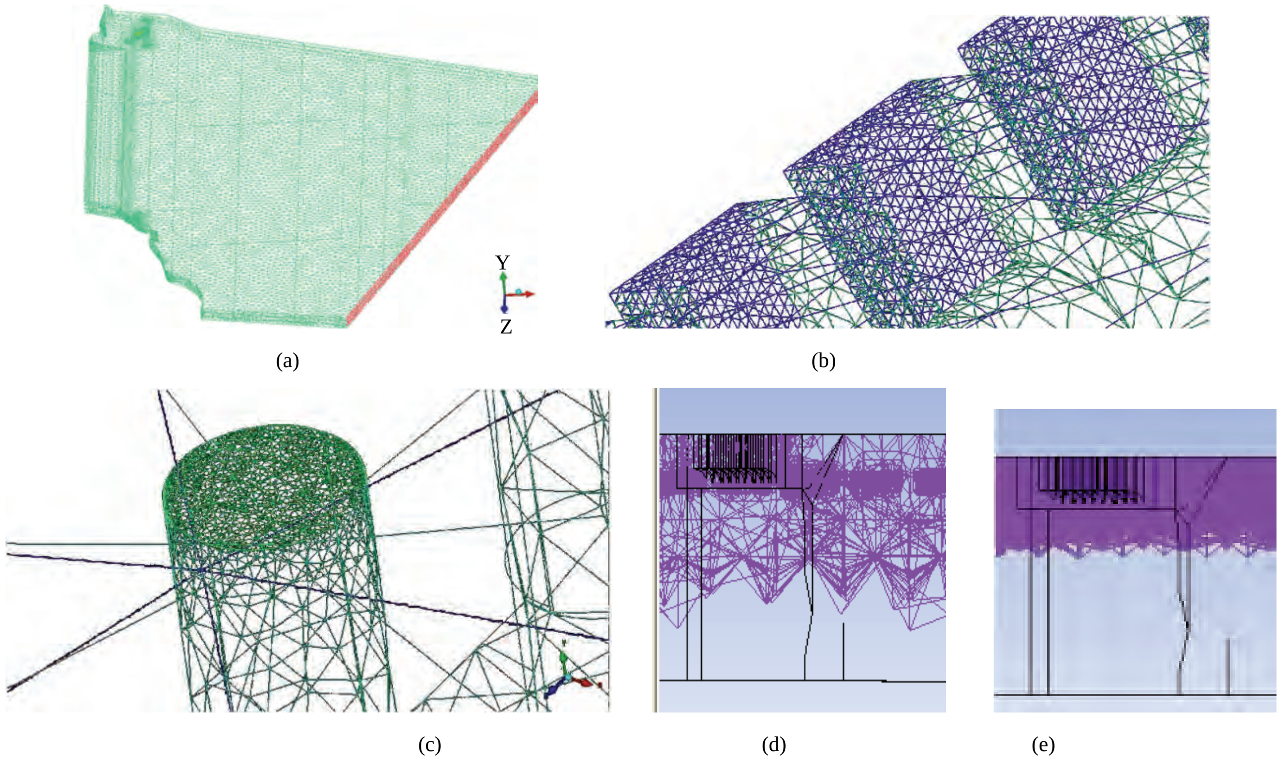

Figure 2. Initial mesh generation using ICEM. (a) Meshed geometry, fine mesh around; (b) Service Spillways; (c) Tunnel 1, mesh refinement using CFX; (d) first refinement level; (e) second refinement level.

3.1. Velocity

3.1.1. Case-1

A velocity of 1.3 m/sec was observed in the reservoir. Due to low level of free-surface, water was only flowing through the tunnels and not spillways. Velocity vectors showing vortices produced due to the suction of water in the tunnels as shown in **Figure 3(a)**. Each tunnel had an area of influence; from where it sucked water and produced chaotic effects in the water. This was observed by the streamlines of each of the four tunnels and the plane collectively. Four tunnels were located between the right bank and main Embankment dam; so disturbance was also produced in the same location, *i.e.*, top right corner of the domain as shown in **Figure 3(b)**.

Production of vortices was common in both the case studies. In current case study where all the tunnels were open; water was mostly sucked from the free stream and strong vortex motion was observed close to the inlets of the tunnels (**Figure 3(c)**, **Figure 3(d)** and **Figure 5(a)**).

Tunnel 1 sucked water mainly from three locations of the free stream over the tunnel, near the main embankment dam and middle of the reservoir approximately 1.13 km from the main embankment dam. Tunnel 2 showed same behavior as tunnel 1; but sucked more water from free stream just above it. Tunnel 3 sucked almost all the water from free stream above it and some from the right corner from the direction of the flow. Tunnel 4 sucked almost all of the water from the free stream above it (**Figure 3(b)**). Therefore it is concluded for current case study that as tunnel inlets move away from the boundaries of the reservoir; water is sucked from the free stream above it. When tunnels took in water from the free stream it did not revolve around the tunnel much. Revolving water would displace sediment from the bed of the reservoir to the tunnel inlets; which would damage turbines, gates and tunnels. So it was reasoned that tunnels inlets should be far away from the reservoir boundary. Appropriate Distance between tunnels and boundary can be calculated by analyzing the flow field of that particular domain (**Figure 3**).

3.1.2. Case-2

Water showed similar stagnant behavior in the reservoir. It speeded up when it came near the spillways. Water flowed smoothly towards both the spillways. Reason was that water got larger area to flow out of the domain which decreased the flow rate through each gate. So there was less chaotic effect observed than notified in case studies where only one of the spillways was open.

Auxiliary spillways have good design due to which water velocity remained near 1.25 m/sec in the moorage

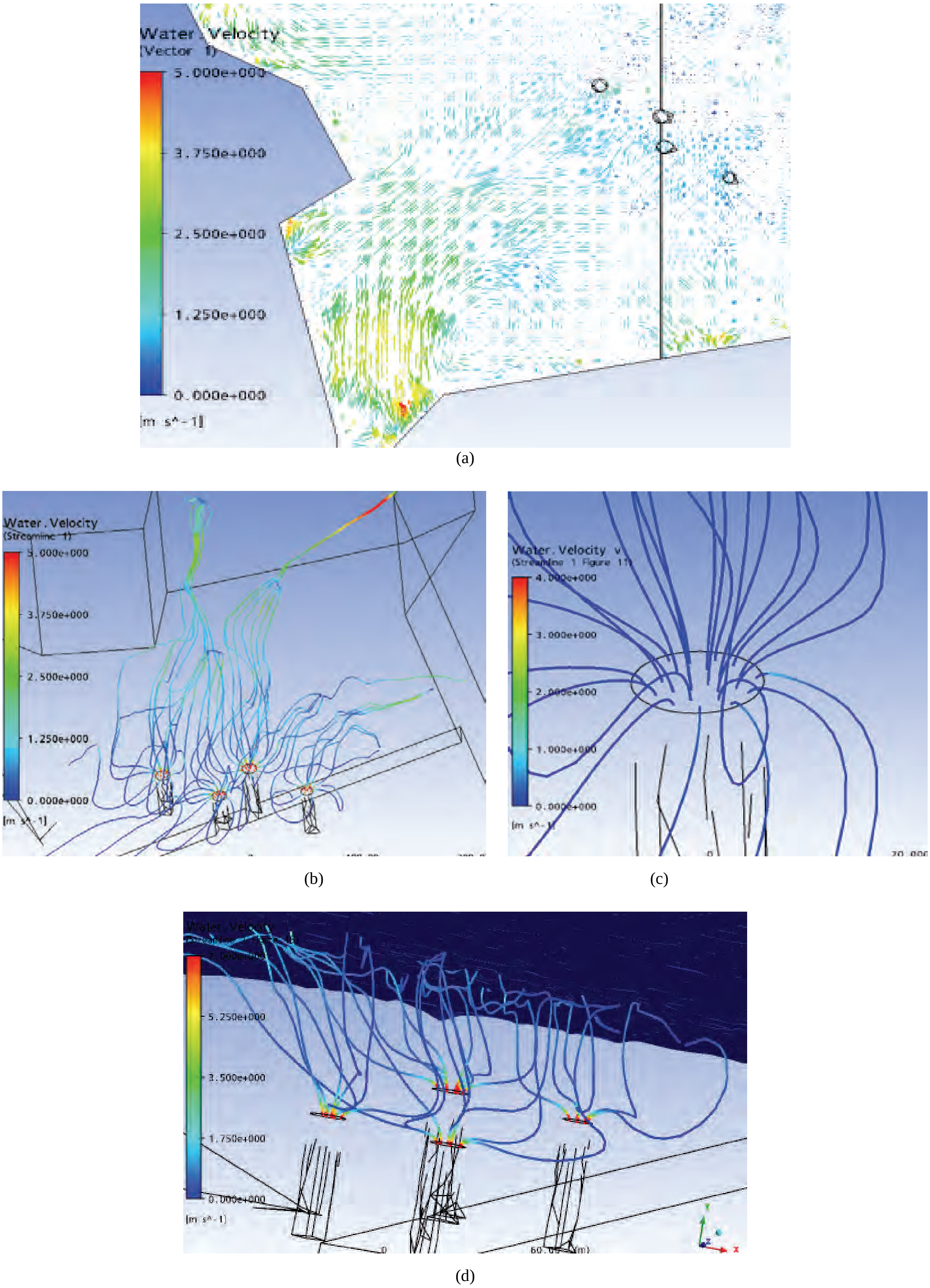

Figure 3. Case study 1 results. (a) velocity vectors; (b) Stream lines of all tunnels; (c) Stream lines through Tunnel1; (d) Tunnels sucking water from free surface.

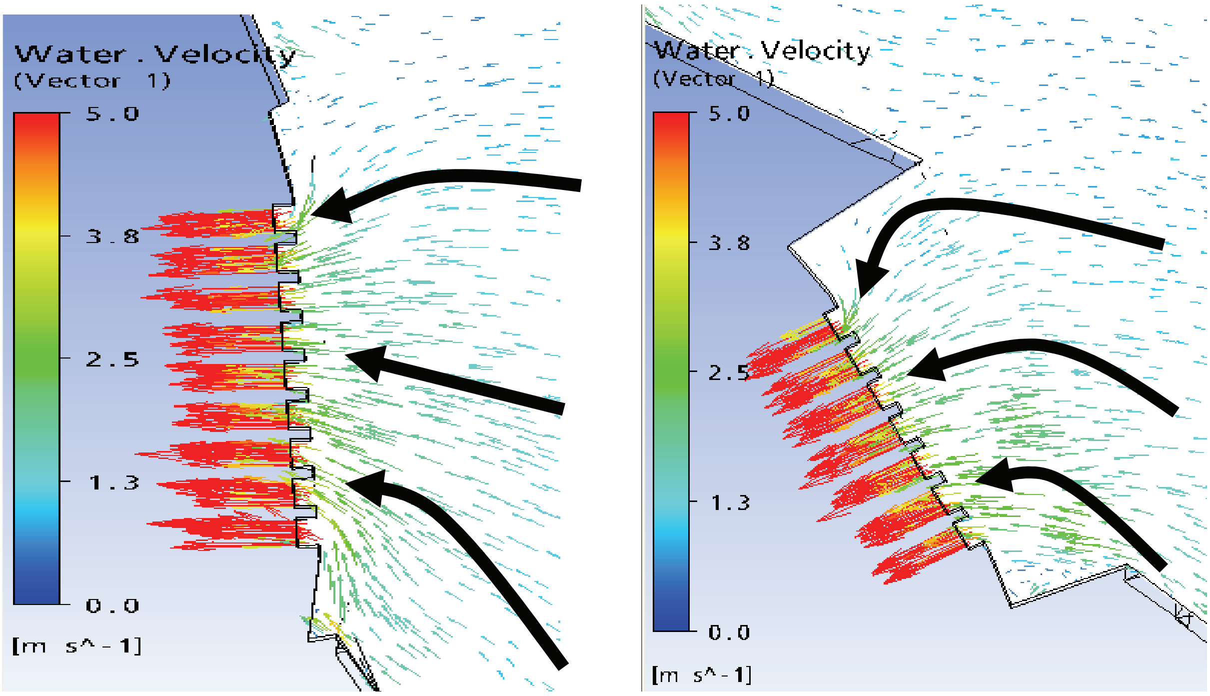

(a) (b)

Figure 4. Velocity vectors through. (a) Auxiliary spillways; (b) Service spillways.

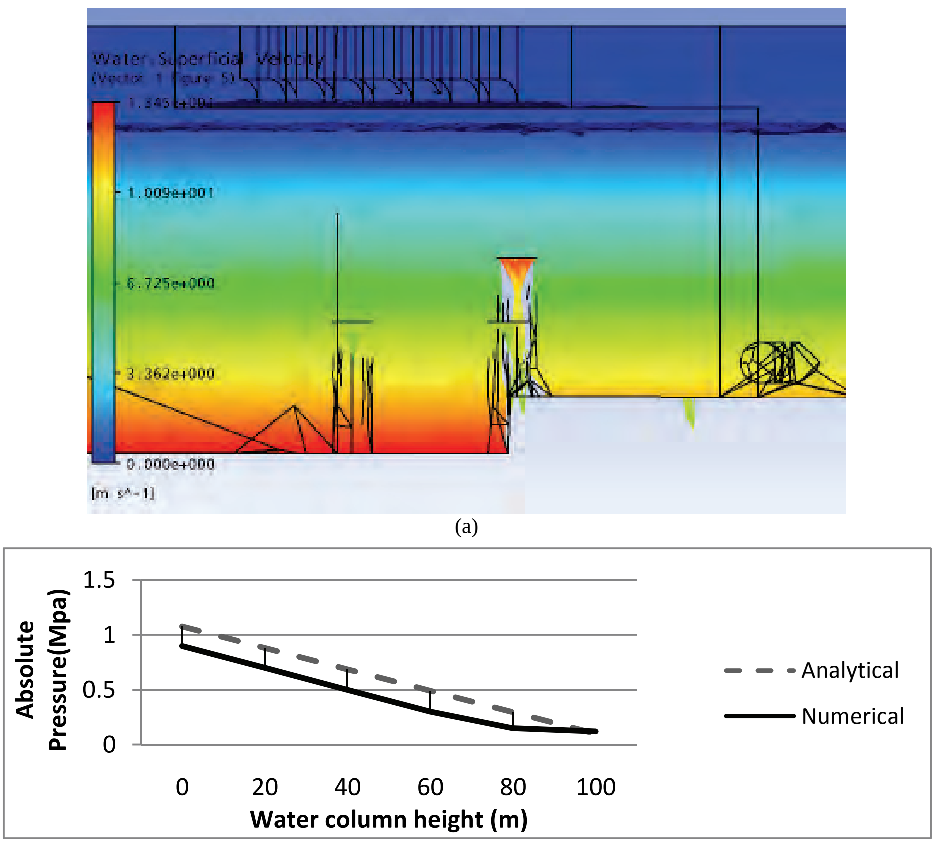

(a)

(b)

Figure 5. Pressure distribution. (a) with free surface; (b) with respect to surface height.

area but crossed 5 m/sec as it reached the domain boundary. Water discharge was not uniform through all the gates of the spillways (**Figure 4(a)**). Although both the spillways shows speedy swimmingly flow of water but near the service spillways the water speeded up to 2.5 m/sec and exceeds 5 m/sec before it exited the domain. Vortices were generated at the corners of the service spillways structure (**Figure 4(b)**). Corner gates of both the spillways showed non-uniformity in flow compared to the central gates.

A similar flow field was observed by Sungyul for Soyang dam, Korea. Water in the reservoir showed a stagnant behavior and velocity was observed up-to 5 m/sec with strong vortex effect near the exit [14].

3.2. Pressure Distribution

Pressure distribution obtained by the Navier Stokes equation was compared with the analytical results using $p = \gamma h$ [15] and were observed in good agreement. From this it could be concluded that other results predicting different behaviors will also agree with the original reservoir flow patterns. Pressure distribution was hydrostatic for both the cases and thus absolute pressure increased directly proportionally to the depth of the water column. Maximum pressure obtained numerically for the case study 1 was 1.17 MPa and for case 2 was 1.33 MPa (**Figures 5** and **6**). In current problem water was moving so potential energy of water was converted into kine-

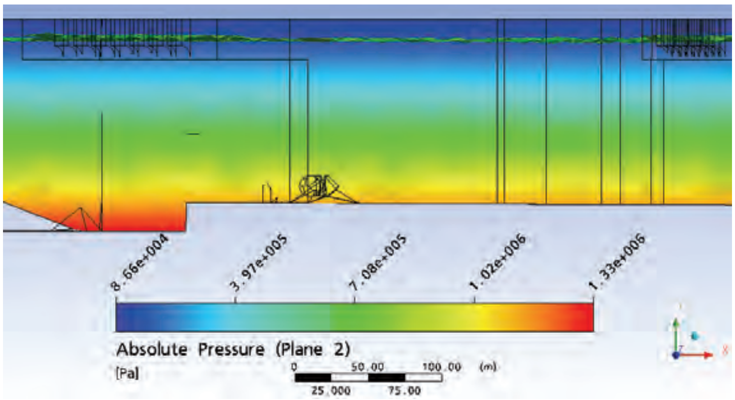

(a)

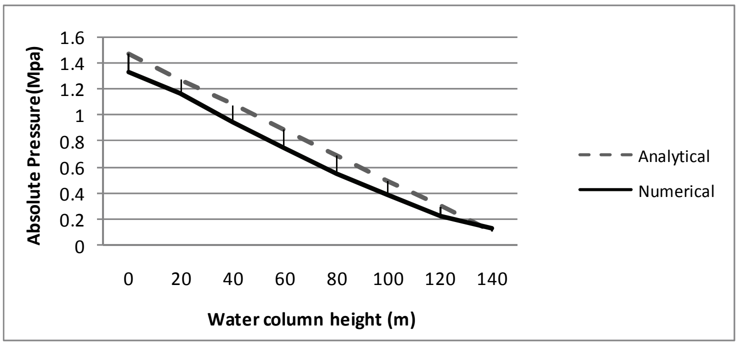

(b)

Figure 6. Pressure distribution. (a) with free surface; (b) with respect to surface height.

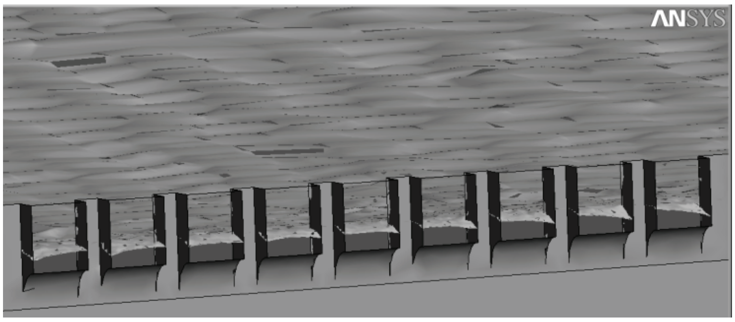

Figure 7. Free surface profile through auxiliary spillways.

tic energy resulting in a difference between the results.

3.3. Free Surface

Step function was used to define air and water volumes. Number '0' and '1' represented water and air respectively. An iso-surface was plotted on '0.5' representing free surface. Ripples on the iso-surface showed air flowing over free-surface of water (**Figure 7**). If water surface was at a lower level; delta of sediment was exposed to free atmospheric conditions and there were more chances of sediment to flow towards main embankment dam. For both the case studies free surface was maintained above the minimum pool level (76 m). Free surface height varied throughout the domain with an average value of 110 m for case 1 and 123 m for case 2 which was good for the reservoir capacity, tunnels and equipments installed on them [5]. For case 2 inclined free-surface from the corners gates to the central gates was observed due to non-uniform flow through the spillways gates discussed earlier in velocity. Similar behavior of the free-surface was predicted for Soyang Dam [14].

4. Conclusions

1) Areas of water exits *i.e.* at spillways and tunnels were very small compared to the reservoir so dynamic behavior of water was observed along spillways and tunnels and almost static behavior was observed in the reservoir.
2) Due to slow movement of water sediment should move very slowly in the reservoir.
3) If sediment particles accelerate towards the main embankment dam and choked the tunnels; reason would be other than water movement towards the main embankment.
4) Water flow was chaotic within the moorage area near both the spillways.
5) Service spillways produced more chaotic flows than the auxiliary spillways.
6) Spillways should be designed such that they are facing the water flow in perpendicular direction for easy flow.
7) Spillways should be placed at locations where there is deep water reservoir with no sharp edges on the corners. This will avoid chaotic flow of the water.
8) Spillways design should be such that water is not constrained into a structure before discharge; as this is observed in the case of service spillways design.
9) Auxiliary spillways should be opened instead of service spillways for discharge because more maintenance will be required for service spillways due to chaotic flows.
10) The water at corner gates in both spillways showed very strong vortex motion, resulting in non-uniform discharge through each gate.
11) Moorage area around spillways should be strengthened to avoid washing away of sand from the mountains/hills.
12) Central gates of both the spillways have relatively uniform discharge.
13) Water flow through spillways did not affect the sedimentation in bed of Tarbela dam reservoir.
14) Tunnel 3 and 4 at the current location, *i.e.*, at the base of the reservoir took in large amount of sediment particles, damaging not only the tunnels but also equipment installed on it [5].
15) Both these tunnels must be modified and inlet must be raised 47 m from the bed level.
16) Water produced vortices as it entered the tunnels; this effect should be considered during structural design of tunnels.
17) If only single tunnel was opened; due to swirling of water around the tunnel base; sediment particles were picked up and sucked into the tunnel damaging the tunnel and equipments installed on it.

More than one tunnel should be opened at any time to increase discharge from the location. For such case water will be taken directly from the free stream eliminating chances of sediment entering from the tunnel base.

5. References

[1] E. L. Tate and F. A. K. Farquharson, "Simulating Reservoir Management under the Threat of Sedimentation: The Case of Tarbela Dam on the River Indus," *Water Resources Management*, Vol. 14, No. 3, 2000, pp. 191-208.

[2] B. R. Rust, "Sedimentation in Fluvial and Lacustrine Environments," *Hydrobiologia*, Vol. 91, 1982, pp. 59-70.

[3] T. S. Fuat entürk, "Hydraulics of Dams and Reservoirs," Water Resources Publications, Littleton, 1994.

[4] C. T. Yang, "Applications of GSTARS Computer Models for Solving River and Reservoir Sedimentation Problems," Tianjin University and Springer-Verlag, Tianjin, 2008.

[5] Water and Power Development Authority, "Periodic Inspection Report of Pakistan," Pakistan, 2007.

[6] Department of Survey, "Report on Sedimentation Profiles Pakistan," Water and Power Development Authority, 2007.

[7] Consultants, TAMS, "Tarbela Dam Project," *Drawings*, Water and Power Development Authority, Vol. 4, 1968.

[8] Consultants, TAMS, "Tarbela Dam Project," *Drawings*, Water and Power Development Authority, Vol. 5, 1968.

[9] Consultants, TAMS, "Tarbela Dam Project," *Drawings*, Water and Power Development Authority, Vol. 6, 1968.

[10] M. Francisco, A. M. G. Lopes and V. A. F. Costa, "Optimization of a Sanitary Discharge Valve Using a Numerical Approach," *Proceedings of the* 5*th WSEAS International Conference on Simulation, Modeling and Optimization*, Tenerife, 2005.

[11] ANSYS Europe, Ltd, “ANSYS CFX Solver Modeling Guide,” ANSYS CFX Release 11.0. © 1996-2006.

[12] G. Iaccarino, “Prediction of a Turbulent Seperated Flow Using Commercial CFD Codes,” *Journal of Fluids Engineering*, Vol. 123, 2001, pp. 819-828.

[13] Hydraullics Department, “Tarbela Dam Hydrology Report,” Water and Power Development Authority, 2008.

[14] S. Yoo, K. Hong and M. Hwang, “A 3-Dimensional Numerical Study of Flow Patterns around a Multipurpose Dam,” *Proceedings of the* 5*th International Conference on Hydroinformatics*, Cardiff, 2002.

[15] J. H. Ferziger and M. Peric “Computational Methods for Fluid Dynamics,” Springer, 3rd Edition, 2001.

J. Water Resource and Protection, **2010, 2, 540-544**
doi:10.4236/jwarp.2010.26061 Published Online June 2010 (http://www.SciRP.org/journal/jwarp)

Transport of Suspended Solids in Dammam (Saudi Arabia) Coastal Areas: Fish Market Works

Hussam Al-Rabai'ah
Department of Mathematics, Tafila Technical University, Tafila, Jordan
E-mail: *hussam@ttu.edu.jo*
Received February 23, 2010; *revised April* 15, 2010; *accepted May* 4, 2010

Abstract

Some new projects are considered in the eastern coasts of Dammam city, Saudi Arabia Dredging operations would significantly alter coast hydrological and sediment transport processes. It is important that the project areas must keep flushing the fresh sea water in and out with good water quality parameters, which are currently facing increased pressure from urbanization and navigation requirements in conjunction with industrial developments. A suspended solids or sediments are expected to affect the flora and fauna in that area. A numerical modeling study in needed to study the effect of dredging and in particular the suspended sediments concentrations (mg/L) changed in the region. The results were obtained using finite element method and Newton-Raphson iterations.

Keywords: Numerical Modeling, TSS, Arabian Gulf, Sediment Transport

1. Introduction

Dredging is critical to maritime trade and many recreational pursuits. Extensive dredging and gravel extraction in those coastal areas are for the purpose of extending the coasts, to build a new fish market, and for other purposes. Effective sediment management tools are of fundamental importance for coastal and water authorities to reduce the costs for maintenance dredging and waterway building activities. In this context reliable in situ data of siltation rates and suspended solid concentrations are a precondition to understand the mechanisms that control sediment transport and to optimize for example strategies for dredging and dumping material. Also for numerical computer models the availability of appropriate validation datasets is essential.

During dredging and disposal operations, there is an increase in the total suspended solids (TSS) in the area of activity. TSS, is sometimes referred to as suspended solids, is a simple measure of the dry-weight mass of non-dissolved solids suspended per unit volume of water (usually expressed in mg/L). TSS includes inorganic solids such as clay, silt, sand, etc. as well as organic solids such as algae, zooplankton, and detritus [1]. These resuspended sediments can adverse impact biota. To study the effects of sediment transport in the Dammam coastal areas, it is necessary to understand and predict the sediment concentration and fate of these sediments using numerical models.

Following the progress in surveying technology for field data and computer application, models in 1-D, 2-D and 3-D for sediment transportation have been developed in the cases of rivers, estuaries, lakes and reservoirs (e.g., [2-4]). Fassnacht (1997, [5]) listed a table containing eight suspended sediment models with various applications. These models were applied to various settings; each model has its own pros and cons resulted from particular waterbody, specific boundary conditions and affecting factors; and a universal one may not be applicable in other cases. An integrated modeling study was completed to assess the magnitude of the potential impacts of suspended sediment plumes. The model was validated against previous dredging works in Dammam coastal areas [6] and then used to simulate the fish market dredging works. This research maybe used in other areas of new projects that require massive dredging works.

2. Methods

The proposed fish market location at the eastern part of Dammam city coasts is shown in **Figure 1**, while the study area is divided into 241 nodes that made finite-element mesh as described in **Figure 2**. Sediment transportation in estuary is influenced by many factors such as source of sand, tidal flow, wave, and particles flocculation

Figure 1. Study area; proposed fish market at the eastern coast of Dammam city.

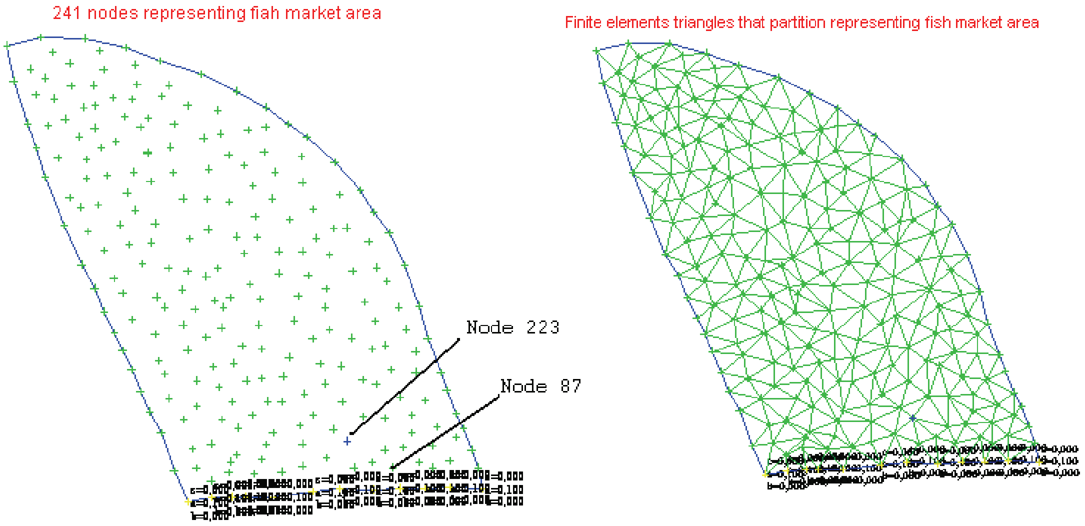

(a) (b)

Figure 2. 241 nodes representing fish market area (left) and finite element triangles of that area (right).

culation, deposition/re-suspension and erosion [7]. It is not practical to cover all the factors in one model. This research is the first attempt to build up a dynamical 2D model for the transportation of suspended solids in Dammam coastal areas. A two-dimensional sediment transport model was applied to the shallow coastal areas of Damman due to dredging operations was developed. The shallow-water hydrodynamic equations used for one-dimensional depth average flow consist of the equations for the conservation of mass, momentum, and energy. For most applications, the conservation of momentum and conservation of energy equation produce identical results. Sediment transportation in estuary is influenced by many factors such as source of sand, tidal flow, wave, particles flocculation, deposition/re-suspension and erosion. Every estuary has particular dominant agent among all the factors controlling the sediment transportation there. It is not practical to cover all the factors in one model.

The equation of continuity is given by Kolar *et al.* 1994, [8]:

$$\frac{\partial}{\partial x}(uH)+\frac{\partial}{\partial y}(vH)+\frac{\partial \eta}{\partial t}=Q$$

where

$$H=h+\eta$$

h is mean water depth, m is change in water level, m
H is total water depth, m
U is velocity component in x-direction, m/s
V is velocity component in y-direction, m/s
T is time, s
Q is injected water, m^3/s.

As the continuity equation includes three unknown variables *u*, *v*, and *h*, we need two more equations to complete the solution of the problem. These are given by the momentum equations in two directions

$$\frac{\partial u}{\partial x}+u\frac{\partial u}{\partial x}+v\frac{\partial u}{\partial y}=-g\frac{\partial \eta}{\partial x}+fv-$$

$$\frac{g}{HC^2}(u^2+v^2)^{1/2}u+\frac{k}{H}W_x|W|-\frac{Q}{H}(u-u_0)$$

$$\frac{\partial v}{\partial t}+u\frac{\partial v}{\partial x}+v\frac{\partial v}{\partial y}=-g\frac{\partial \eta}{\partial y}+fu-$$

$$\frac{g}{HC^2}(u^2+v^2)^{1/2}v+\frac{k}{H}W_y|W|-\frac{Q}{H}(v-v_0)$$

The Coriolis parameter *f*, is defined as

$$f=2\omega\sin\phi$$

where is the latitude and is the Earth's rate of rotation equal to 7.2722 × 10^{-5} s^{-1}. The wind shear stress parameter, *k*, is defined as:

$$k=\frac{\rho_a C_D}{\rho}$$

and:

Change in water level, m
H Total water depth, m
u Velocity in x-direction, m/s
v Velocity in y-direction, m/s
t Time, s
g Acceleration of gravity, m/s^2
The Earth's rate of rotation, s^{-1}
Latitude, deg
C Chézy bottom friction coefficient, $m^{1/2}$/s
$_a$ Density of air, kg/m^3
C_D Wind drag coefficient
Fluid density, kg/m^3
W_x Wind velocity in x-direction, m/s
W_y Wind velocity in y-direction, m/s
W Wind speed, m/s
u_o Velocity of injected water in x-direction, m/s
v_o Velocity of injected water in y-direction, m/s.

The momentum equations together with the equation of continuity complete the specification of the shallow water flow problem.

The area of study is divided into small regions of finite elements consisting of 241 nodes (**Figure 2(a)**). A mesh is generated using the aquasea software to obtain this mesh (**Figure 2(b)**).

Two types of inputs exist; either input for each node or input on areal regions. Inputs at boundary nodes were given values so that we obtain a wave fluctuation of 0.5 m mean sea level (MSL). Each node has two unknowns, the flow rate *Q* and the water surface elevation *z*.

For N nodes in an inlet system, the total numbers of unknowns are 2N, thus, 2N equations are needed to determine values of the unknowns. The finite difference representations of the shallow-water equations with the boundary conditions and the junction conditions constitute a system of 2N nonlinear algebraic equations. To solve these equations we use the generalized Newton-Raphson iteration method [9]. Iteration is continued until the differences in water surface elevation and discharge between successive iterations at any node fall below specified tolerance values. Areal data such as wind speed, wind direction, chezy coefficient and others were also taken into consideration.

3. Results and Discussions

Initial results of the model regarding flow directions show that it depends mostly on wind direction and geometry of the region bed (**Figure 3**). The dredged area –the proposed fish market - will result in concentrations of suspended solids. Two nodes were picked for studying total suspended solid concentration in a time-series manner. Nodes number 223 and 87 were chosen at the exit of area of study **Figure 2(a)**.

The model was verified by measured data of TSS contents at sites Dammam eastern coasts [10]. Model results for both selected nodes show that TSS will come back to normal levels within a maximum period of 6 days in the dredged area (**Figures 4** and **5**). This shows that dredging operations have no effect on the long terms on water quality in the area. This is consistent with results that dredging activities often generate no more increased suspended sediments than commercial shipping operations, bottom fishing or generated during severe storms [11]. Furthermore, natural events such as storms, floods and large tides can increase suspended sediments over much larger areas, for longer periods than dredging operations. It is therefore often very difficult to distinguish the environmental effects of dredging from those

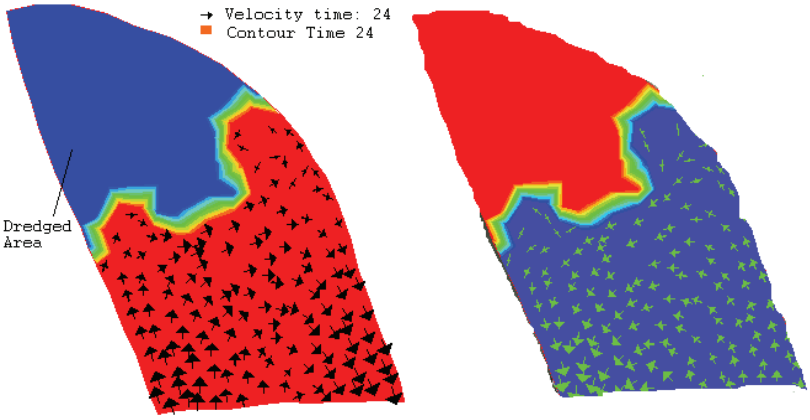

Figure 3. Flow direction within 1 day (left) and 10 days (right) of simulation.

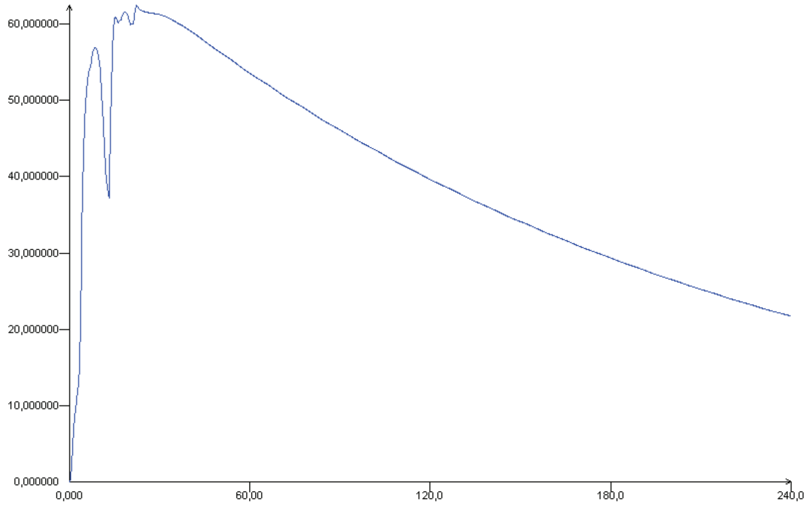

Figure 4. Suspended sediments concentration (mg/L) during 10 days after dredging operations at node 223.

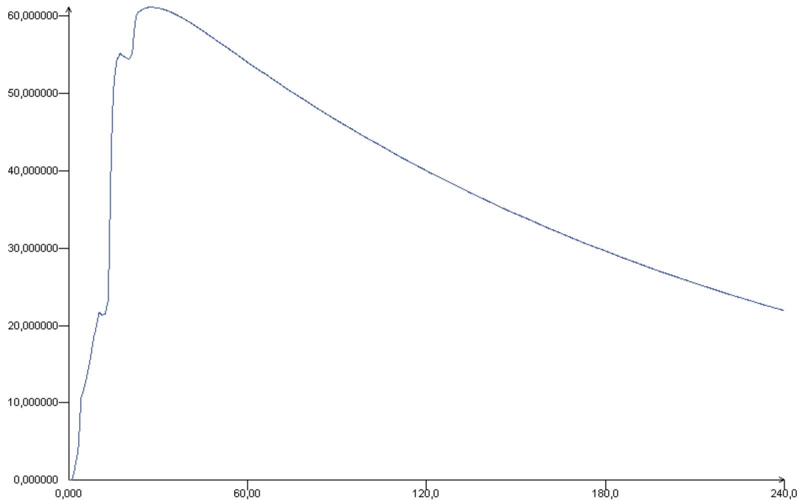

Figure 5. Suspended sediments concentration (mg/L) during 10 days after dredging operations at node 87.

resulting from natural processes or normal navigation activities [12].

4. Conclusions

The transportation of suspended solids Dammam coastal areas are jointly controlled by region inflow, tidal current and bottom vertical shear near the seabed. In this work, a 2D model to simulate the transportation of suspended solids was developed in which the mechanisms of advection, diffusion, flocculation settling of particles, scouring and silting of the seabed and the carrying capacity of wave and tide were involved. The model was run for 10 executive days to simulate sediment transportation and was verified with normal field data. The results showed that the modeled contents of suspended solids matched well with the existing readings. Modeled distributions of suspended reflected basically the overall behaviors of sediment transportation.

5. References

[1] APHA, "Standard Methods for the Examination of Water and Wastewater," 18th Edition, American Public Health Association, American Water Works Association, Water Pollution Control Federation, Washington, DC, 1992.

[2] E. Hayter and A. J. Metha, "Modeling Cohesive Sediment Transport in Estuary Waters," *Applied Mathematical Modelling*, Vol. 10, No. 4, August 1986, pp. 294-303.

[3] L. C. van Rijn, H. van Rossum and P. Termes, "Field Verification of 2-D and 3-D Suspended-Sediment Models," *Journal of Hydrologic Engineering*, *ASCE*, Vol. 116, No. 10, 1990, pp. 1270-1288.

[4] R. A. Falconer and B. Lin, "Three-Dimensional Modeling of Water Quality in the Humber Estuary," *Water Research*, Vol. 31, No. 5, 1997, pp. 1092-1102.

[5] S. R. Fassnacht, "A Multi-Channel Suspended Sediment Transport Model for the Mackenzie Delta, Northwest Territories," *Journal of Hydrologycal*, Vol. 197, No. 1-4, 1997, pp. 128-145.

[6] H. A. Al-Rabai'ah, "Numerical Modelling of Water Flow in a Dead-End Tidal Inlet at Dammam Coastal Areas, Saudi Arabia," *Journal of Applied Science and Environmental Sanitation*, Vol. 3, No. 3, 2008, pp. 127-136.

[7] X. H. Chen, Y. Q. Chen and G. Y. Lai, "Modeling Transportation of Suspended Solids in Zhujiang River Estuary, South China," *Chinese Journal of Ocean and Lim*, Vol. 23, No. 1, 2005, pp. 1-10.

[8] R. L. Kolar, J. J. Westerink, M. E. Cantekin and C. A. Blain, "Aspects of Nonlinear Simulations Using Shallow Water Models Based on the Wave Continuity Equation," *Computers and Fluids*, Vol. 23, No. 3, 1994, pp. 523-538.

[9] A. M. Cialone, M. Amein and 1. Dynlet, "Model Formulation and User's Guide," U.S. Department of Transportation, Federal Highway Administration, Atlanta, 1993.

[10] H. A. Nasr-El-Din, A. M. Al-Mohammad, A. A. Al-Shurei, N. K. Merwat, M. M. Erbiland and M. Samuel, "Restoring the Injectivity of Water Disposal Wells Using a Viscoelastic Surfactant-Based Acid," *Journal of Petroleum Science and Technology*, Vol. 54, No. 1-2, 2006, pp. 10-24.

[11] W. Parr, S. J. Clarke, P. Van Dijk and N. Morgan, "Turbidity in English and Welsh Tidal Waters," 1998, WRc Report No. CO 4301/1 to English Nature.

[12] J. G. S. Pennekamp, R. J. C. Epskamp, W. F. Rosenbrand, A. Mullie, G. L. Wessel, T. Arts and I. K. Deibel, "Turbidity Caused by Dredging: Viewed in Perspective," *Terra et Aqua*, Vol. 64, 1996, pp. 10-17.

J. Water Resource and Protection, **2010, 2, 545-554**
doi:10.4236/jwarp.2010.26062 Published Online June 2010 (http://www.SciRP.org/journal/jwarp)

Fuzzy Approach Based Management Model for Irrigation Planning

Dattatray Gangaram Regulwar[1], Jyotiba Bhalchandra Gurav[2,3]
[1]*Department of Civil Engineering, Government College of Engineering, Aurangabad, India*
[2]*Government College of Engineering, Aurangabad, India*
[3]*Department of Civil Engineering, Amrutvahini College of Engineering, Sangamner, India*
E-mail: *dgregulwar@rediffmail.com, jyotiba.gurav@rediffmail.com*
Received March 5, 2010; *revised April* 6, 2010; *accepted May* 4, 2010

Abstract

The objective of this paper is to develop the irrigation planning model and to apply the same in the form of Multi Objective Fuzzy Linear Programming (MOFLP) approach for crop planning in command area of Jayakwadi Project Stage I, Maharashtra State, India. To formulate MOFLP model various Linear Programming (LP) models are developed to optimize the Net Benefits (NB), Crop/Yield Production (YP), Employment Generation (EG) and Manure Utilization (MU) for which the objective function and constraints are crisp in nature. From the results of these LP models the linear membership function for each individual objective function has been developed. Considering the decision makers satisfaction level (λ), all the four objectives are maximized simultaneously. The results of the MOFLP and LP are compared. The MOFLP model concentrates on satisfying four objectives simultaneously. The present model will be helpful for the decision maker to take decision under conflicting situation when planning for different objectives simultaneously. The degree of satisfaction λ, works out to be 0.58. Compromised solution provides Net Benefits 1503.73 Million Rupees, Crop Production 319563.50 Tons, Employment Generation/Labour Requirement 29.74 Million Man days and Manure Utilization 154506.50 Tons respectively.

Keywords: Linear Programming (LP), Multi Objective Fuzzy Linear Programming (MOFLP), Optimal Cropping Pattern

1. Introduction

Water resources systems planning development and management is the area in which irrigation planning problem involves with multiple possible and valuable planning objectives. Some of them, one can represent in terms of monetary returns and a few which one cannot, are social upliftment, environmental status, ecological balance, conservation of natural resources etc. The objectives expressed in terms of monetary returns can be easily imposed in the form of objective functions. Irrigation planning is the area which is associated with many monetary and nonmonetary objectives. Some of the monetary objectives are crop production, total net benefits, manure utilization, labour requirement, water utilization and land utilization. The crop planning study is normally practiced for the determination of type of crops that should be taken and the area to be utilized for those crops. To decide these two parameters various other parameters are influencing such as type of crop suitable to particular soil, water availability, land availability, labour availability, manure requirement, etc. Crop planning problem is formulated in the form of linear programming model with number of objective functions and set of constraints. Focusing on only one objective does not satisfy the different desires of people/farmers of region. Some of the multiple objectives in crop planning problem may conflict with one another. This may be because of all these objectives share the same type of resources which used for any one objective it may not available for other objectives [1]. Single optimal solutions do not yield in case of multiple objective analyses, but which are more useful for the determination of the trade-offs among noncommensurabe objectives. The crop production study that provides the maximum net benefits is not likely to generate the highest employment of labour, nor it may produce the maximum yield or return in terms of foreign exchange from agricultural exports. Considering the case of developing countries these objectives may be more important than the maximization of net benefits. Every development objective uses the same available resources, but not in equal amount [2]. Irrigation planning problem becomes more complicated, if uncertainty is included in the form of drought and floods, fluctuations in the market price of crops and its yields, non availability of right type of labour at right time and inflow variation from season to season. To tackle such kind of vagueness in planning with multiple objectives and the imprecision involved in the parameter values; the fuzzy set theory is considered as an alternative approach. Many advantages of the Fuzzy Linear Programming (FLP) are considered over the other existing multiobjectvie optimization methods, especially constraint and weighting methods. When the numbers of objectives are greater than three these two methods may become computationally disadvantages. Also in case of weighting method, the specification of weight plays a vital role which is difficult to quantify and sometimes the solution is sensitive to weights. However the nondominated alternatives are generated in case of constraint method. To make the selection of suitable alternative the existing Multi Criterion Decision Making (MCDM) tools are used and which does not yield the same alternative. To check the robustness of ranking, an extensive sensitivity analysis is required. On the other hand, in case of FLP for each additional objective function only one constraint is required. The flexibility of converting the fuzzy model into existing optimization software makes the approach more useful.

Morales *et al.* [3] have developed a simulation model for planning the conjunctive use of irrigation water from a single multipurpose reservoir and an aquifer and allocation of cropped areas within an irrigation district. Raman *et al.* [4] have developed a decision support for planning of crop during droughts for Bhadra reservoir command area of Karnataka state, India. Mannocchi and Mecarelli [5] have discussed the optimization criteria for deficit irrigation of a farm. Srinivasa Raju and Nagesh Kumar [6] have discussed linear programming (LP) irrigation planning model for evaluation of irrigation development strategy for the case study of Sri Ram Sagar project, in Andhra Pradesh of India. Srinivasa Raju and Nagesh Kumar [7] developed the Fuzzy Linear Programming (FLP) for three conflicting objectives of Sri Ram Sagar project, in Andhra Pradesh of India. Sethi *et al.* [8] developed optimization model to find optimal cropping pattern and area allocation in relation with availability of water resources for different season. Itoh *et al.* [9] have presented crop planning problem with profit coefficients for agricultural products as discrete random variable. Sonmez and Altin [10] have developed the optimum cropping pattern for adequate and deficit water supply for mid size farm in Harran Plain Firat irrigation district. Sahoo *et al.* [11] have developed the linear programming and fuzzy optimization models for three conflicting objectives of irrigation planning in Mahanadi-Kathajodi delta in eastern India. Regulwar and Anand Raj [12] have presented the monthly Multi Objective Genetic Algorithm Fuzzy Optimization (MO-GA-FUOPT) for two conflicting objectives of Multireservoir in Godavari Sub basin, in Maharashtra state of India. Mohaddes and Mohayidin [13] have developed fuzzy mathematical programming model for tackling three objectives simultaneously, which are maximization of profit, maximization of employment and minimization of soil erosion. A monthly Multi Objective Multireservoir operation model solved by Genetic algorithm under Fuzzy environment has been developed by Regulwar and Anand Raj [14].

The objective of this paper is to develop the irrigation planning model and to apply the same in the form of Multi Objective Fuzzy Linear Programming (MOFLP) approach for crop planning in command area of Jayakwadi Project Stage I, Maharashtra State, India. The objective of MOFLP model is to develop an optimal cropping pattern that maximizes Net Benefits, Yield/Crop production, Employment Generation/Labour Requirement and Manure Utilization simultaneously.

2. Description of the Case Study Area

The lower Godavari River Basin, Maharashtra State, India is taken under consideration. The Jayakwadi project stage-I is located across eastward flowing river Godavari, Maharashtra state, India. The irrigable command area is 1416.40 km^2. The catchment area of the reservoir is up to the dam site 21774 km^2. The length of the dam is 10280m and its maximum height is 37.73 m. The gross storage of the reservoir is 2909 Mm^3 and live storage is 2170 Mm^3.Total installed capacity for power generation is 12 MW (Pumped storage plant). **Figure 1** shows index map of Jayakwadi project, Maharashtra state, India.

3. Methodology and Model Development

The objective is to find out optimal cropping pattern for 75% dependable yield in command area. The problem has been formulated as an optimization model based on deterministic inflows. In the formulation of the problem the following assumptions have been made:

Crops are considered to be grown throughout the year. The irrigation intensity adopted is 22% in Kharif season, 45% in Rabi season and 28% in two seasonal, H. W. crop 3%, Perennial 4.5% and that becomes a total irrigation intensity of 102.5%. Ground water usage is not considered in the command area. Only surface water has been considered for irrigation. The soil of the study area is homogeneous in nature. Various relationships within the models are based on the framework of leneariry.

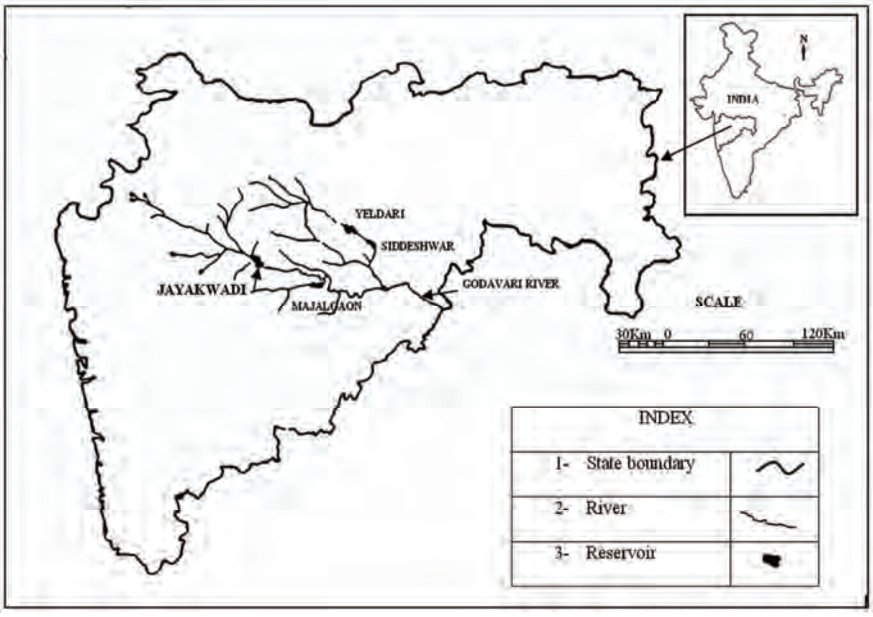

Figure 1. Index map of Maharashtra State of India.

Same management practice has been applied for a particular crop event under each land and hence, the crop/yield production, net benefits, labour/employment generation and manure utilization under particular crop activity is constant. The duration and timings of the cropping activity are considered as a constant and do not vary over years. There are three seasons for growing crops (viz. Kharif, Rabi, and two seasonal) without any overlapping. Under certain overlapping situations, care is taken by adding specific constraints. The input cost for each crop is considered as twenty percent of the total gross benefits to be gained.

3.1. Objective Function

The four objectives are considered in the present study.

3.1.1. Maximization of Net Benefits (NB)

Maximization of Net benefits can be expressed as; (canonical form of LP)

$$\text{Maximize } NB = \left[\left(\sum_{i=1}^{K_1} A_i^K + \sum_{i=1}^{R_1} A_i^R + \sum_{i=1}^{T_1} A_i^{TS} + \sum_{i=1}^{P_1} A_i^P + \sum_{i=1}^{H_1} A_i^{HW}\right) BC_i - \left(\sum_{i=1}^{K_1} A_i^K + \sum_{i=1}^{R_1} A_i^R + \sum_{i=1}^{T_1} A_i^{TS} + \sum_{i=1}^{P_1} A_i^P + \sum_{i=1}^{H_1} A_i^{HW}\right) IC_i\right] \quad (1)$$

[In which i = crop index. 1 = Sugarcane (P), 2 = Banana (P), 3 = Chilies (TS), 4 = L S Cotton (TS), 5 = Sorghum (K), 6 = Paddy (K), 7 = Sorghum (R), 8 = Wheat (R), 9 = Gram (R) and 10 = Groundnut (HW) and ha = 10000 m^2]

The net benefits (NB) coefficients from the irrigated area under various crops are obtained by subtracting the input cost (20% of gross benefit) from gross benefit for different crops. The Gross benefits are calculated by multiplying the average yield of a crop per ha and current market price of that crop. The crop production (CP) coefficients are taken as the average yield of a crop per ha. (Commissionerate of Agriculture Maharashtra State, 2006, Agricultural Statistical Information Maharashtra State, India part-II [15]).

3.1.2. Maximization of Yield or Crop Production (CP)

Focusing on the food sufficiency of the region, the crop production is to be maximized and can be expressed in canonical form as follows;

$$\text{Maximize } (CP) = \left[\left(\sum_{i=1}^{K_1} A_i^K + \sum_{i=1}^{R_1} A_i^R + \sum_{i=1}^{T_1} A_i^{TS} + \sum_{i=1}^{P_1} A_i^P + \sum_{i=1}^{H_1} A_i^{HW}\right) AY_i\right] \quad (2)$$

3.1.3. Maximization of Employment Generation (EG) or Labour Requirement

Keeping in mind the socio-economic development, the policy maker has to concentrate on the maximization of employment generation or labour requirement.

$$\text{Maximize } (EG) = \left[\left(\sum_{i=1}^{K_1} A_i^K + \sum_{i=1}^{R_1} A_i^R + \sum_{i=1}^{T_1} A_i^{TS} + \sum_{i=1}^{P_1} A_i^P + \sum_{i=1}^{H_1} A_i^{HW}\right) MD_i\right] \quad (3)$$

The labour requirement or numbers of Man Days (MD) for a particular crop per ha are considered through discussion with farmers and experts from agricultural fields.

3.1.4. Maximization of Manure Utilization (MU)

In order to maintain the fertility and nutrient sufficiency of soil in proper manner, one should concentrate on maximization of use of manures.

$$Maximize\ (MU) = \left[\left(\sum_{i=1}^{K_1} A_i^K + \sum_{i=1}^{R_1} A_i^R + \sum_{i=1}^{T_1} A_i^{TS} + \sum_{i=1}^{P_1} A_i^P + \sum_{i=1}^{H_1} A_i^{HW}\right) MU_i\right] \quad (4)$$

The Requirement of Manure (MU) for a crop per ha are considered through discussion with farmers and experts from agricultural fields.

3.2. Constraints

3.2.1. Sowing Area Constraint

3.2.1.1. Total Sowing Area Constraint

The total area constraint for various crops for the present study is considered to take care of total area available for cultivation in command area during different crop seasons. The total sowing area constraint is given by,

$$\left(\sum_{i=1}^{K_1} A_i^K + \sum_{i=1}^{R_1} A_i^R + \sum_{i=1}^{T_1} A_i^{TS} + \sum_{i=1}^{P_1} A_i^P + \sum_{i=1}^{H_1} A_i^{HW}\right) \le CA \quad (5)$$

3.2.2. Maximum Sowing Area Constraint (According to Existing Cropping Pattern)

The maximum sowing area constraint for various crops is defined to account for maximum sowing area available for cultivation during various crop seasons according to existing cropping pattern of the project. The maximum sowing area constraint is given by,

Kharif

$$\left(\sum_{i=1}^{K_1} A_i^K + \sum_{i=1}^{P_1} A_i^P\right) \le CA_i^K + CA_i^P \quad (6)$$

Rabi

$$\left(\sum_{i=1}^{R_1} A_i^R + \sum_{i=1}^{P_1} A_i^P\right) \le CA_i^R + CA_i^P \quad (7)$$

Hot Weather and Perennial

$$\left(\sum_{i=1}^{P_1} A_i^P + \sum_{i=1}^{H_1} A_i^{HW}\right) \le CA_i^P + CA_i^{HW} \quad (8)$$

3.2.3. Affinity Constraint

The farmers of the region are having a tendency to grow cash crops and other crops according to their interest and benefits. To safeguard the interest of the food requirement of the region according to the storage capacity of the reservoir the following limitation (upper limit using the existing cropping pattern) for various crops are incorporated as constraints,

Perennial

$$A_1^P \le CA_i^p \quad (9)$$

A_1^P = Area under perennial crop Sugarcane in ha

$$A_2^P \le CA_i^p \quad (10)$$

A_2^P = Area under perennial crop Banana in ha

Two Seasonal

$$A_3^{TS} \le CA_i^{TS} \quad (11)$$

A_3^{TS} = Area under two seasonal crop Chilies in ha

$$A_4^{TS} \le CA_i^{TS} \quad (12)$$

A_4^{TS} = Area under two seasonal crop L S Cotton in ha

Kharif

$$A_5^K \le CA_i^K \quad (13)$$

A_5^K = Area under kharif crop Sorghum in ha

$$A_6^K \le CA_i^K \quad (14)$$

A_6^K = Area under kharif crop Paddy in ha

Rabi

$$A_7^R \le CA_i^R \quad (15)$$

A_7^R = Area under rabi crop Sorghum in ha

$$A_8^R \le CA_i^R \quad (16)$$

A_8^R = Area under rabi crop Wheat in ha

$$A_9^R \le CA_i^R \quad (17)$$

A_9^R = Area under rabi crop Gram in ha

Hot Weather

$$A_{10}^{HW} \le CA_i^{HW} \quad (18)$$

A_{10}^{HW} = Area under hot weather crop Groundnut in ha

3.2.4. Labour Availability

To tackle the problem of uncertainty of avoiding the labour from outside the region, the labour requirement should not exceed the total labour availability during that interval,

Kharif

$$\left(\sum_{i=1}^{K_1} A_i^K + \sum_{i=1}^{P_1} A_i^P\right) RMD_{ij} \le \sum_{i=1}^{K_1+P_1} LA_{ij} \quad (19)$$

Rabi

$$\left(\sum_{i=1}^{R_1} A_i^R + \sum_{i=1}^{P_1} A_i^P\right) RMD_{ij} \le \sum_{i=1}^{R_1+P_1} LA_{ij} \quad (20)$$

Perennial and hot weather

$$\left(\sum_{i=1}^{P_1} A_i^P + \sum_{i=1}^{H_1} A_i^{HW}\right) RMD_{ij} \le \sum_{i=1}^{P_1+H_1} LA_{ij} \quad (21)$$

3.2.5. Manure Availability

In order to keep the fertility of soil in rich condition, the total manure requirement should not exceed the total availability of the manure in that season.

Kharif

$$\left(\sum_{i=1}^{K_1} A_i^K + \sum_{i=1}^{P_1} A_i^P\right) RMU_{ij} \le \sum_{i=1}^{K_1+P_1} MA_{ij} \quad (22)$$

Rabi

$$\left(\sum_{i=1}^{R_1} A_i^R + \sum_{i=1}^{P_1} A_i^P\right) RMU_{ij} \le \sum_{i=1}^{R_1+P_1} MA_{ij} \quad (23)$$

Perennial and Hot Weather

$$\left(\sum_{i=1}^{P_1} A_i^P + \sum_{i=1}^{H_1} A_i^{HW}\right) RMU_{ij} \le \sum_{i=1}^{P_1+H_1} MA_{ij} \quad (24)$$

3.2.6. Water Availability Constraint

The total water requirement of different crop should not exceed the total water availability in the reservoir,

$$\left(\sum_{i=1}^{K_1} A_i^K + \sum_{i=1}^{R_1} A_i^R + \sum_{i=1}^{T_1} A_i^{TS} + \sum_{i=1}^{P_1} A_i^P + \sum_{i=1}^{H_1} A_i^{HW}\right) IWR_{ij} \le TWA_{ij} \quad (25)$$

3.2.7. Non Negativity Constraint

$$A_i^K, A_i^R, A_i^{TS}, A_i^P, A_i^{HW}, AY_i, MD_i, MU_i, CA, CA_i^K, CA_i^R, CA_i^P, CA_i^{HW}, LA_j, MA_j, RMD_{ij}, LA_{ij}, RMU_{ij}, MA_{ij}, IWR_{ij}, TWA_{ij} \ge 0 \quad \forall i, j \quad (26)$$

3.3. Fuzzy Linear Programming Algorithm (FLP Algorithm)

In brief it is divided into following steps:

1) Considering only one objective at a time, solve the problem as a linear programming problem.

2) Focusing on the results obtained in the step 1, work out the corresponding values of each objective from the solution obtained.

3) Comparing the values of objective function obtained in step 2; find out (Z_U) and (Z_L) for each objective under consideration.

4) Keeping in view the values of (Z_U) and (Z_L) for each objective; establish the linear membership function.

5) Introducing the dummy variable (λ), now the objective function changes to maximize the dummy variable (λ) subjected to the additional constraints due to the fuzziness in the value of the objective functions and original constraints.

6) Develop the equivalent Linear Programming (LP) model as a Multiobjective Fuzzy Linear Programming model (MOFLP).

7) With degree of truth (λ) work out compromised solution.

The schematic representation of fuzzy approach model for compromised solution is as shown in **Figure 2**.

4. Result Analysis

The objective function of the present study considering the Equations (1) to (4) of the linear programming planning (LPP) model are to maximize the net benefits, yield/crop production, employment generation and ma-

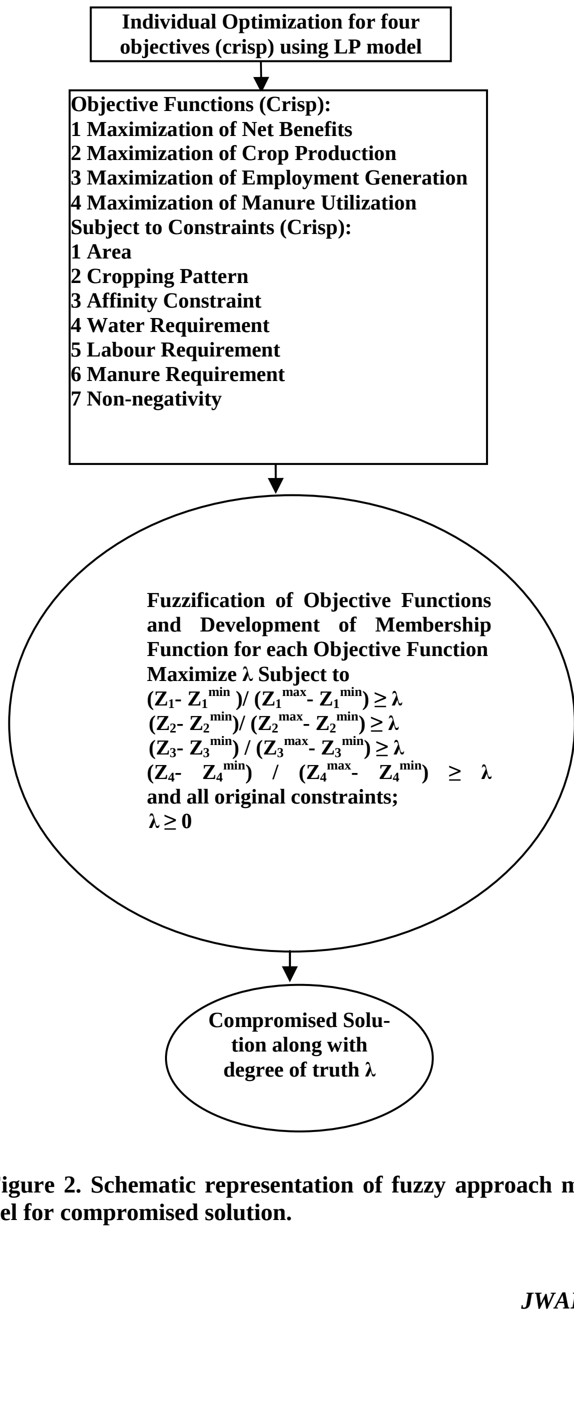

Figure 2. Schematic representation of fuzzy approach model for compromised solution.

nure utilization for the command area of the Jayakwadi Project stage-I. These objective functions are maximized separately subjected to constraints (Equations (5) to (26)) using the LINGO (Language for INteractive General Optimization). The results of this individual maximization of the four different objectives are used to develop the membership function for each objective taking the help of the best (+) and worst (-) value of the same. The membership functions are shown graphically in **Figures (3-6)**. The same membership functions are written in the form of mathematical Equations (27) to (30). The results are shown in **Table 1**. Also the results are shown graphically in **Figures (7-11)**.

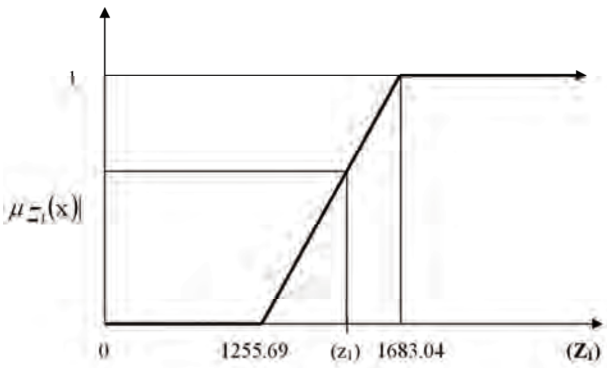

Figure 3. Membership function for Z_1 (in Million Rupees).

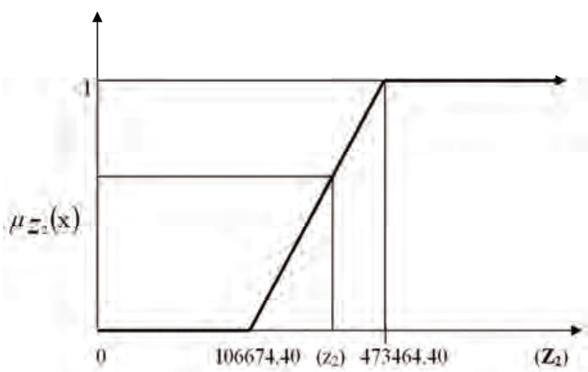

Figure 4. Membership function for Z_2 (in Tons).

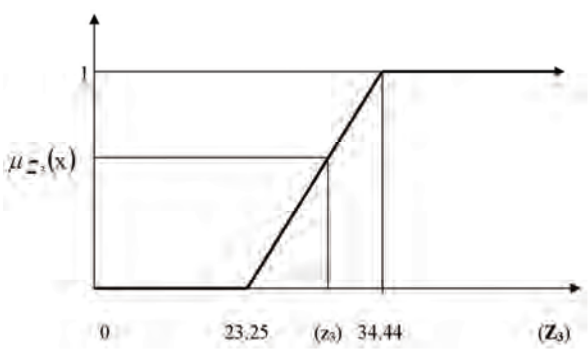

Figure 5. Membership function for Z_3 (in Million Man days).

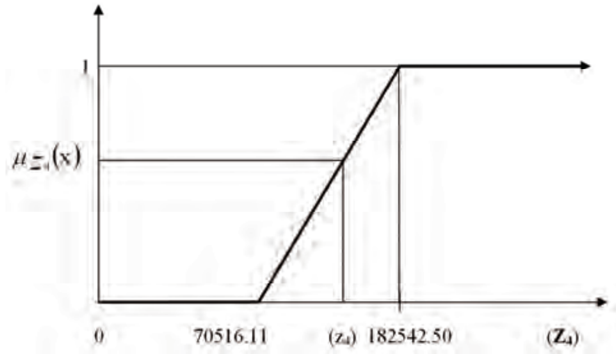

Figure 6. Membership function for Z_4 (in Tons).

The membership functions $\mu_1(X)$, $\mu_2(X)$, $\mu_3(X)$ and $\mu_4(X)$ of the fuzzy sets characterizing the objective functions rise linearly from 0 to 1 at the highest achievable value of $Z_1 = 1683.04$ Million Rs, $Z_2 = 473464.40$ tons, $Z_3 = 34.44$ Million Man days and $Z_4 = 182542.50$ tons respectively. The level of satisfaction associated with net benefits rises from 0 if the net benefit is 1255.69 million Rs or less to 1 if the total net benefits is $Z_1 = 1683.04$ Million Rs or more. The level of satisfaction with respect to crop/yield Production rises from 0 if the crop/yield production is 106674.40 Tons or less to 1 if the crop/yield production is $Z_2 = 473464.40$ tons or more and the satisfaction level associated with employment generation rises from 0 for 23.25 million man days or less to 1 for employment generation $Z_3 = 34.44$ Million Man days and more. Similarly the level of satisfaction associated with manure utilization rises from 0 if the manure utilization is 70516.11 tons or less to 1 if the manure utilization is $Z_4 = 182542.50$ tons or more. The maximum satisfaction level from the membership functions of four participating/conflicting objectives has been designated as the 'best' achieved/compromised solution.

$$\mu_{Z_1}(x) = \begin{cases} 1 & z_1 \geq 1683.04 \\ \dfrac{(z_1 - 1255.69)}{(1683.04 - 1255.69)} & 1255.691 \leq z_1 \leq 1683.04 \\ 0 & z_1 \leq 1255.69 \end{cases} \quad (27)$$

$$\mu_{Z_2}(x) = \begin{cases} 1 & z_2 \geq 473464.40 \\ \dfrac{(z_2 - 106674.40)}{(473464.40 - 106674.40)} & 106674.4 \leq z_2 \leq 473464.40 \\ 0 & z_2 \leq 106674.40 \end{cases} \quad (28)$$

$$\mu_{Z_3}(x) = \begin{cases} 1 & z_3 \geq 34.44 \\ \dfrac{(z_3 - 23.25)}{(34.44 - 23.25)} & 23.25 \leq z_3 \leq 34.44 \\ 0 & z_3 \leq 23.25 \end{cases} \quad (29)$$

$$\mu_{Z_4}(x) = \begin{cases} 1 & z_4 \geq 182542.50 \\ \dfrac{(z_4 - 70516.11)}{(182542.50 - 70516.11)} & 70516.11 \leq z_4 \leq 182542.50 \\ 0 & z_4 \leq 70516.11 \end{cases} \quad (30)$$

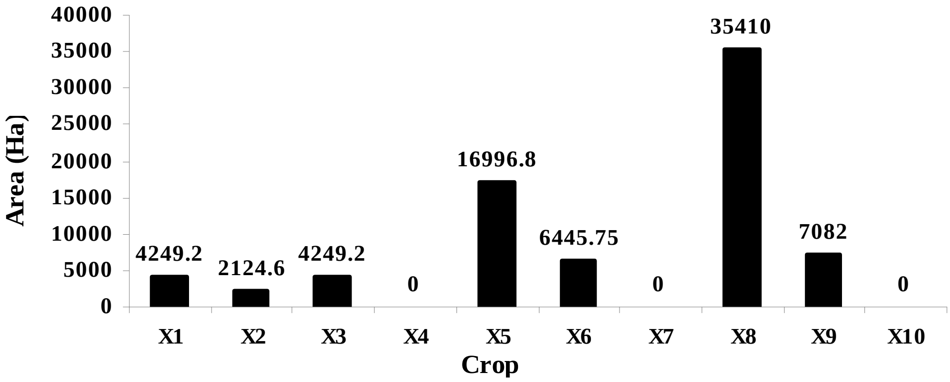

Figure 7. Cropping pattern for maximization of net benefits.

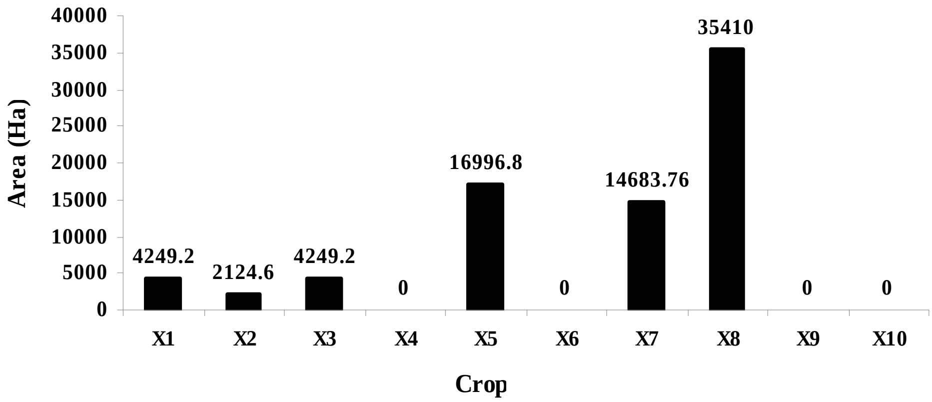

Figure 8. Cropping pattern for maximization of crop production.

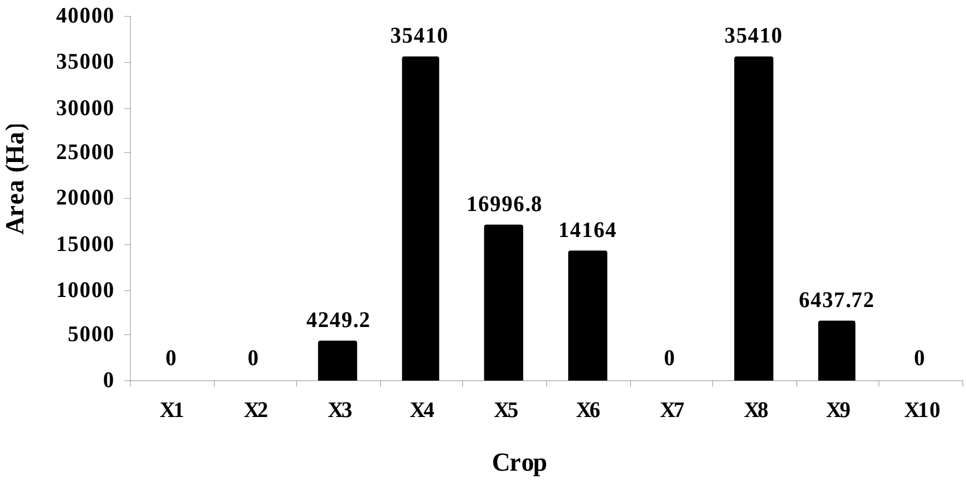

Figure 9. Cropping pattern for maximization of employment generation.

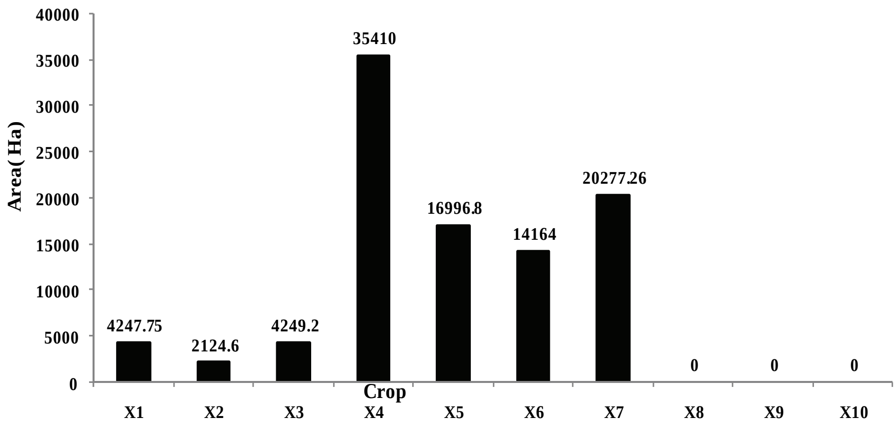

Figure 10. Cropping pattern for maximization of manure utilization.

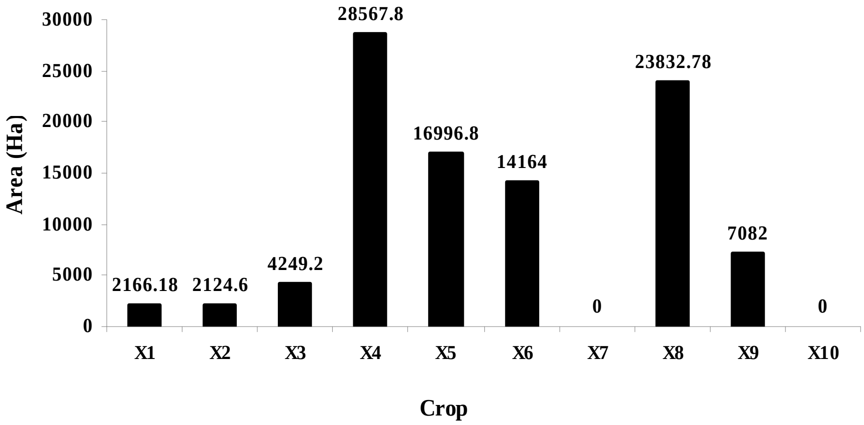

Figure 11. Cropping pattern in the form of compromised solution for four conflicting objectives under fuzzy environment.

Finally the modified form of the optimization problem (MOFLP) by introducing the dummy variable λ = min [$\mu_1(X)$, $\mu_2(X)$, $\mu_3(X)$, $\mu_4(X)$] such that the objective is to

Maximize λ

Subject to,

$(Z_1–1255.69 \times 10^6) / (1683.04 \times 10^6–1255.69 \times 10^6) \geq \lambda$

$(Z_2–106674.40) / (473464.40–106674.40) \geq \lambda$

$(Z_3–23.25 \times 10^6) / (34.44 \times 10^6–23.25 \times 10^6) \geq \lambda$

$(Z_4–70516.11) / (182542.50–70516.11) \geq \lambda$

and all other original constraint given (Equations (5) to (26)) in the model; $\lambda \geq 0$.

The solution of MOFLP is presented in **Table 1**. From this solution it is observed that the area to be irrigated is constant in case of Chilies (TS) and Sorghum (K) under LP model and MOFLP model solution. When the Net Benefit is to be maximized then the area under irrigation is zero for LS Cotton (TS), Sorghum (R) and Groundnut (HW) because the benefit coefficient is low for these crops. Similarly when the Crop Production is to be maximized then the area under irrigation is zero for LS Cotton (TS), Paddy (K), Gram (R) and Groundnut (HW).

Also when the Employment Generation/Labour Requirement is to be maximized then the area under irrigation is zero for sugarcane (P), Banana (P), Sorghum (R) and Groundnut (HW). This is due to the labour requirement per ha is low and also due to the limited area under existing cropping pattern. On the other hand when manure utilization is to be maximized then the area under irrigation is zero for wheat (R) ,Gram (R) and Groundnut (HW) as manure requirement per ha is low and also due to the limited area under existing cropping pattern. Area under irrigation is zero for Sorghum (R) and Groundnut (HW) if four conflicting objectives are considered simultaneously under MOFLP environment.

In case of individual optimization for four objectives separately the irrigation intensity is 54.05%, 54.86%, 79.54% and 68.81% respectively, while in case of MOFLP it is 70.02%. In case of MOFLP the irrigation intensity is more by 15.97%, 15.15%, 1.21% if we compare with individual optimization for net benefits, crop production and manure utilization respectively and less by 9.52% if we compare with individual optimization for employment generation.

The degree of truth for compromised solution for four

Table 1. Solution for the net benefits, crop yield/ production, employment generation and manure utilization crop areas of LPP model and MOFLP.

Sr No	Crop and Season	Solution for Maximization of				Compromised Solution for four Conflicting Objectives under Fuzzy Environment (**λ=0.58**)
		Net Benefits (Z_1) (Area of Crop) (ha)	Crop Production (Z_2) (Area of Crop) (ha)	Employment Generation (Z_3) (Area of Crop) (ha)	Manure Utilization (Z_4) (Area of Crop) (ha)	Area of Crop (ha)
1	Sugarcane (P)	4249.20	4249.20	0.00	4247.75	2166.18
2	Banana (P)	2124.60	2124.60	0.00	2124.60	2124.60
3	Chilies (TS)	4249.20	4249.20	4249.20	4249.20	4249.20
4	L S Cotton (TS)	0.00	0.00	35410.00	35410.00	28567.80
5	Sorghum (K)	16996.80	16996.80	16996.80	16996.80	16996.80
6	Paddy (K)	6445.75	0.00	14164.00	14164.00	14164.00
7	Sorghum (R)	0.00	14683.76	0.00	20277.26	0.00
8	Wheat (R)	35410.00	35410.00	35410.00	0.00	23832.78
9	Gram (R)	7082.00	0.00	6437.72	0.00	7082.00
10	Groundnut (HW)	0.00	0.00	0.00	0.00	0.00
Net Cropped Area (ha)		76557.55	77713.56	112667.72	97469.61	99183.36
Net Benefits (Million Rs)		1683.04 ($\mathbf{Z_1^+}$)	1654.75	1255.69 ($\mathbf{Z_1^-}$)	1459.84	1503.73
Crop Production (Tons)		472166.50	473464.40 ($\mathbf{Z_2^+}$)	106674.40 ($\mathbf{Z_2^-}$)	446120.20	319563.50
Employment Generation (Million Man days)		24.72	23.25 ($\mathbf{Z_3^-}$)	34.44 ($\mathbf{Z_3^+}$)	26.17	29.74
Manure Utilization (Tons)		76554.09	70516.11 ($\mathbf{Z_4^-}$)	159485	182542.50 ($\mathbf{Z_4^+}$)	154506.50
Irrigation Intensity (%)		54.05	54.86	79.54	68.81	70.02

conflicting objectives under fuzzy environment is works out to be λ=0.58. MOFLP compromise solution provides Net Benefits 1503.73 (Million Rupees), Crop Production 319563.50 (Tons), Employment Generation/Labour Requirement 29.74 (Million Man days) and Manure Utilization 154506.50 (Tons) respectively.

5. Conclusions

The irrigation planning and their environmental and social aspects are focused under the present case study. The objective of the study is to develop an optimal cropping pattern that maximizes Net Benefits, Crop Production, Employment Generation/Labour Requirement and Manure Utilization simultaneously. For this, MOFLP approach has been developed and applied to Jayakwadi Project Stage I, Maharashtra State, India. This study proposes a basis for irrigation planning as an integrated approach. The degree of truth for compromised solution for four conflicting objectives under fuzzy environment is works out to be λ = 0.58. MOFLP compromised solution provides Net Benefits 1503.73 Million Rupees, Crop Production 319563.50 Tons, Employment Generation/ Labour Requirement 29.74 Million Man days and Manure Utilization 154506.50 Tons respectively. The present model will be helpful for the decision maker to take decision under conflicting situation when planning for different objectives simultaneously. This model is capable to trace out an integrated irrigation planning with prime consideration for economic, social and environmental issue. The results obtained under the present study are sensitive to the changes in the market price of crop, cost of crop production, unit labour cost, and unit manure cost and water availability.

6. Acknowledgements

The authors would like to express their sincere thanks to Command Area Development Authority, Aurangabad, Maharashtra State, India and Mahatma Phule Krishi Vidyapeeth Rahuri, Ahmednagar, Maharashtra State, India for providing necessary data for analysis.

7. References

[1] S. Vedula and P. P. Mujumdar, "Water Resources Systems Modelling Techniques and Analysis," Tata-McGraw Hill, New Delhi, 2005.

[2] D. P. Loucks, J. R. Stedinger and D. A. Haith, "Water Resources Systems Planning and Analysis," Prentice-Hall, Englewood Cliffs, New Jersey, 1981.

[3] J. C. Morales, M. A. Marino and E. A. Hozapfel, "Planning Simulation Model of Irrigation District," *Journal of Irrigation and Drainage Engineering*, Vol. 118, No. 1, 1992, pp. 74-87.

[4] H. Raman, S. Mohan and N. C. V. Rangacharya, "Deci-

sion Support System for Crop Planning during Droughts," *Journal of Irrigation and Drainage Engineering*, Vol. 118, No. 2, 1992, pp. 229-241.

[5] F. Mannocchi and P. Mecarelli, "Optimization Analysis of Deficit Irrigation Systems," *Journal of Irrigation and Drainage Engineering*, Vol. 120, No. 3, 1994, pp. 484-503.

[6] K. S. Raju and D. N. Kumar, "Optimum Cropping Pattern for sri Ram Sagar Project: A Linear Programming Approach," *Journal of Applied Hydrology*, Vol. 8, No. 1-2, 2000, pp. 57-67.

[7] K. S. Raju and D. N. Kumar, "Irrigation Planning of sri Ram Sagar Project Using Multi Objective Fuzzy Linear Programming," *ISH Journal of Hydraulic Engineering*, Vol. 6, No. 1, 2000, pp. 55-63.

[8] L. N. Sethi, D. Nagesh Kumar, S. N. Panda and B. C. Mal, "Optimal Crop Planning and Conjunctive Use of Water Resources in a Coastal River Basin," *Water Resource and Management*, Vol. 16, No. 3, 2002, pp. 145-169.

[9] T. Itoh, H. Ishii and T. Nanseki "A Model of Crop Planning under Uncertainty in Agricultural Management," *International Journal of Production Economics*, Vol. 81-82, 2003, pp. 555-558.

[10] F. K. Sonmez and M. Altin, "Irrigation Scheduling and Optimum Cropping Pattern with Adequate and Deficit Water Supply for Mid-Sized Farms of Harran Plain," *Pakistan Journal of Biological Sciences*, Vol. 7, No. 8, 2004, pp. 1414-1418.

[11] B. Sahoo, A. K. Lohani and R. K. Sahu, "Fuzzy Multiobjective and Linear Programming Based Management Models for Optimal Land-Water-Crop Systems Planning," *Water Resource and Management*, Vol. 20, 2006, pp. 931-948.

[12] D. G. Regulwar and P. Anand Raj, "Development of 3-D Optimal Surface for Operation Policies of a Multireservoir in Fuzzy Environment Using Genetic Algorithm for River Basin Development and Management," *Water Resource and Management*, Vol. 22, No. 5, 2008, pp. 595-610.

[13] S. A. Mohaddes and M. G. Mohayidin, "Application of the Fuzzy Approach for Agricultural Production Planning in a Watershed, a Case Study of the Atrak Watershed Iran," *American-Eurasian Journal of Agriculture & Environment Science*, Vol. 3, No. 4, 2008, pp. 636-648.

[14] D. G. Regulwar and P. Anand Raj, "Multi Objective Multireservoir Optimization in Fuzzy Environment for River Basin Development and Management," *Journal of Water Resource and Protection*, Vol. 1, No. 4, 2009, pp. 271-280.

[15] Commissionerate of Agriculture Maharashtra State, "Agricultural Statistical Information Maharashtra State," *India Part*-II, 2006.

Notations

The following symbols are used in this paper

A_i^K	Area of i^{th} crop in kharif season (ha);
A_i^R	Area of i^{th} crop in rabi season (ha);
A_i^{TS}	Area under two seasonal crop (ha);
A_i^P	Area under perennial crop (ha);
A_i^{HW}	Area under hot weather crop (ha);
BC_i	Benefit coefficient for i^{th} crop;
AY_i	Average yield of i^{th} crop;
MD_i	Number of man days for i^{th} crop per ha;
MU_i	Manure utilization/Requirement of manure in tons for i^{th} crop per ha;
CA	Total command area for all season for i^{th} crop (ha);
CA_i^K	Command area for kharif season for i^{th} crop (ha);
CA_i^P	Command area under perennial crop (ha);
CA_i^{HW}	Command area under hot weather crop (ha);
CA_i^R	Command area for rabi season for i^{th} crop (ha);
IC_i	Input cost for i^{th} Crop;
RMD_{ij}	Requirement of man days or labour for i^{th} crop in j^{th} interval;
LA_{ij}	Labour availability for i^{th} crop in j^{th} interval;
RMU_{ij}	Requirement of manure utilization for i^{th} crop in j^{th} interval;
MA_{ij}	Manure availability for i^{th} crop in j^{th} interval;
IWR_{ij}	Irrigation water requirement for i^{th} crop in j^{th} interval;
TWA_{ij}	Total water availability for i^{th} crop in j^{th} interval;
i	Crop index;
H_1	Hot weather crops;
R_1	Crops under rabi season;
R	Rabi;
T_1	Two seasonal crops;
P_1	Perennial crops;
K_1	Crops under kharif season;
$X_1 \ldots X_{10}$	Area under cultivation of a particular crop '*i*' (ha);
μ (X)	Membership function;
λ	Degree of truth/Level of satisfaction

J. Water Resource and Protection, 2010, 2, 555-559
doi:10.4236/jwarp.2010.26063 Published Online June 2010 (http://www.SciRP.org/journal/jwarp)

Flood Reduction Function of Paddy Rice Fields under Different Water Saving Irrigation Techniques

Joko Sujono
Department of Civil and Environmental Engineering, Faculty of Engineering, Gadjah Mada University, Yogyakarta, Indonesia
E-mail: *jsujono@tsipil.ugm.ac.id*, *jsujono@yahoo.com*
Received March 9, 2010; *revised April* 11, 2010; *accepted May* 4, 2010

Abstract

This study is conducted to investigate the function of paddy fields for flood reduction under different water saving irrigation techniques. A daily water balance component data including rainfall, percolation, and overflow through the paddy field levee were collected from experimental paddy rice fields during rainy season cultivation. Results show that paddy field was very effective in flood reduction. More than 40% of rainfall could be stored in the paddy fields. However, the effectiveness of paddy fields in flood reduction was highly depends on the WSI technique used. Semi dry cultivation technique was the most effective one in terms of flood reduction. It retained the rainfall up to 55.7% (365 mm) of the total rainfall (636 mm) without reducing the yield. In terms of flood volume reduction, the alternate wetting and drying performed similarly with traditional continuous flooding, *i.e.*, 37.2% and 40.8%, respectively.

Keywords: Flood Reduction Function, Water Saving Irrigation, Paddy Field

1. Introduction

Paddy rice cultivation with paddy field irrigation has multi-functional roles not only to provide food securely but also to maintain other functions such as economic, culture and environment [1-3]. One of the important functions related to environment issues is flood prevention and water conservation. A number of studies of these functions have been carried out mainly in Japan from the early 1980s. The studies described the functions of paddy fields to increase the water storage capacity of river basins, lower the peak flow of rivers, and increase groundwater recharge [2].

Recently, a number of studies have been done to investigate the function of paddy fields in storing rainfall water [3-6]. Unami and Kawachi [4] studied a flood simulation method to investigate the effect of irrigation tanks and paddy fields in flood reduction of drainage canals. It is easy to understand the function of paddy fields in detaining floods in their field systems as they temporary store rainfall. Kim *et al.* [5] mentioned that the paddy field has a flood reduction function more scattered compared with dam. The large amount of water stored in paddy fields has a function as many small reservoirs or dams [3]. Kim *et al.* [6] developed a daily paddy water balance model at two field experimental locations. The study indicated that on average the amount of paddy storage during flood period is 333 mm to rainfall ranging from 425 mm to 851 mm. Sujono [7] mentioned that flood routing analysis indicated that paddy fields is also very effective in flood reduction both flood peak and volume. This paper presents the effect of water irrigation management technique used in the paddy rice cultivation on flood reduction.

2. Water Saving Irrigation

Traditionally, a lot of water is needed for the paddy rice growing, since rice is grown under continuously flooded condition in paddy fields except for a short period of sun drying at the late stage of rice tiller [8]. The method has also been reported only yields a low of rice or low water productivity [9]. There is a major challenge for paddy rice cultivators to increase the productivity of water used to grow rice. To grow rice with much less water in the scarce water condition due to increasing demand of water for domestic and industry is necessary and possible [10]. Efforts have been conducted to increase the water productivity for growing rice [8,10,11].

The formal research on water saving irrigation (WSI) techniques for rice in China was started around 1985. The impetus came from different aspects such as shortages of food, electricity and water demand for industrial, domestic increased sharply. The research on improvement of water management for paddy rice was given priority for funding from the Government [9]. Since then, a number of WSI techniques in China have been studied [9,12]. Recently, another WSI technique, called the system of rice intensification (SRI) has been attracting more attention following the reports of its dramatic yield and water productivity advantages in Madagascar. Among the available WSI techniques are presented as the following.

2.1. System of Rice Intensification

The SRI technique has been evaluated at a number of countries outside Madagascar. Great results of the SRI practice have been reported [13,14]. In Sri Lanka, a team of IWMI researchers surveyed 60 farmers using the SRI method and 60 farmers not using it, randomly selected in two districts. There was a 44% increase in yield/ha and that water productivity was increase by 90% [13]). In Indonesia, Nippon Koei [14] has promoted the SRI practice in eastern Indonesia, *i.e.*, South Sulawesi and West Nusa Tenggara provinces. By using the SRI method, the yield are 9.5 t/ha. It was increase by 93% compare with non SRI yields of 4.9 t/ha. Water saving with the SRI is 40%. McDonald *et al.* [15] compiled a database of experiments where SRI was evaluated against accepted best management practices (BMP). Among 40 experimental reports/papers that applying SRI, five from Madagascar and the others from Asian countries, there was no evidence outside of Madagascar that SRI produced remarkable yield when compared to the accepted BMP.

2.2. Alternate Wetting and Drying

The alternate wetting and drying (AWD) has spread and widely practiced in China [16]. By 2002 the AWD irrigation technique was applied in 40% of the rice production areas or 12 million ha in China [8]. The AWD practice increases the water productivity on-farm level remarkable up to 1.52 kg/m^3 of water compare with the traditional one, *i.e.*, 1.04 kg/m^3 of water on average in the four provinces in China [9]. The AWD increased the water productivity by 46% and grain yield marginally by 6% compared to traditional method. Application the AWD in Tuanlin Irrigation Experimental Station from 1991 to 2000 showed that the yield difference between the AWD and the traditional method was not statistically significant. However, under the AWD the water productivity was much higher (average 27%) than under the traditional practice [16].

2.3. Semi-dry Cultivation

Comparing the SRI and AWD, semi-dry cultivation (SDC) is the most high water efficiency. The water productivity could reach 70% higher than traditional method whereas the yield could increase by 9%. SDC can be used in different soils, and it deserves further studying and spreading due to high water use efficiency, beneficial environmental impact and high yield [9].

3. Materials and Methods

3.1. Study Location

The research was carried out at the Environmental Engineering Laboratory, Department of Civil and Environmental Engineering, Faculty of Engineering, Gadjah Mada University, Yogyakarta, Indonesia. The paddy plot consists of 5 blocks with equal size, *i.e.*, 2 m × 3 m and 0.8 m depth, as shown in **Figure 1**.

The paddy plots were constructed as impermeable as possible to avoid leakage and percolation water flow out from the plots. At the bottom of the plot, a porous pipe (ϕ10 cm) was installed to collect the percolation water. The pipe was connected with a tap, so that the percolation water can be measured from outside the plot. To store water used for water irrigation, a small storage was

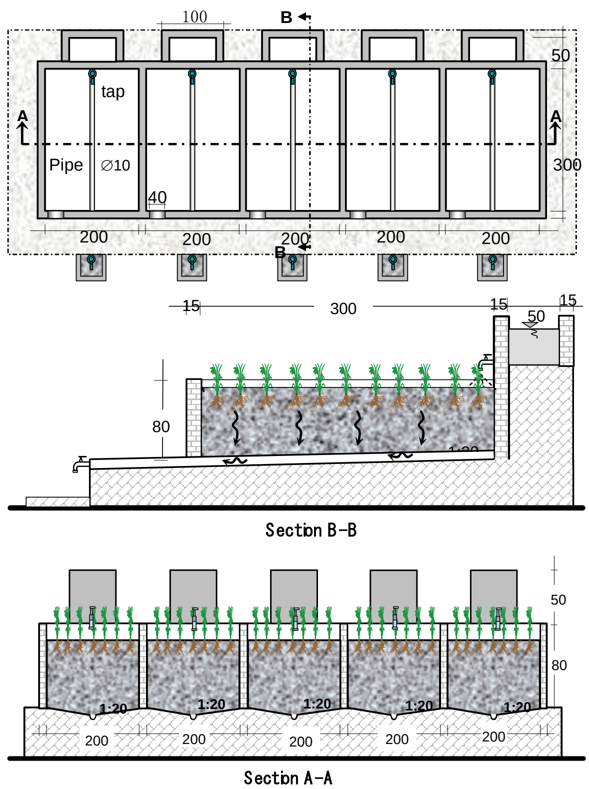

Figure 1. Experimental plots.

also constructed. In addition, pan-evaporation and rainfall gage were installed near the plots. The research was done from March 2007 until mid of June 2007 starting from land preparation up to harvesting.

3.2. Paddy Rice Cultivation

Paddy rice called IR-64 variety was selected for the experiments. This variety was released in 1986, a medium duration variety (100-115 days). Transplanting rice in plots was done following the SRI method, *i.e.*, young seedling (10 days) and wide spacing (25 cm × 25 cm).

3.3. Nutrient Control

Following the guideline from Nippon Koei [14] fertilizer was applied three times as follows: 1) first fertilizer at rate of 125 kg Urea/ha, 100 kg SP36/ha and 25 kg KCl/ha was given at 7 DAT (days after transplanting); 2) second fertilizer was applied at 25 DAT using 125 kg Urea/ha and 3) last fertilizer as a top dressing was given at 40 DAT using 100 kg ZA/ha.

3.4. Water Management Technique

Four water management irrigation techniques namely traditional continuous flooding (TRI), SRI, AWD and SDC were applied in the research as shown in **Figure 2**.

The amount of water and when it should be irrigated vary among the techniques. In the TRI, after transplanting the standing water depth in paddy plot was kept at 30 mm depth. For all the WSI techniques, except the SDC, the upper limit water depth in the plot was 2 cm. There was no water depth on paddy field under the SDC technique after 10 DAT. The minimum water depth was set up at 70% soil moisture capacity (SMC) for the AWD and SDC, whereas for the SRI the minimum was at 0 mm depth. The extra limit levels for all water management techniques used were set up to 8 cm for storing more rainfall and spill occurred when the water level goes beyond the extra limit level. When the depth of water in the plot or average moisture content in the root zone falls to the lower limit level, the plot was filled to the upper limit level by irrigation.

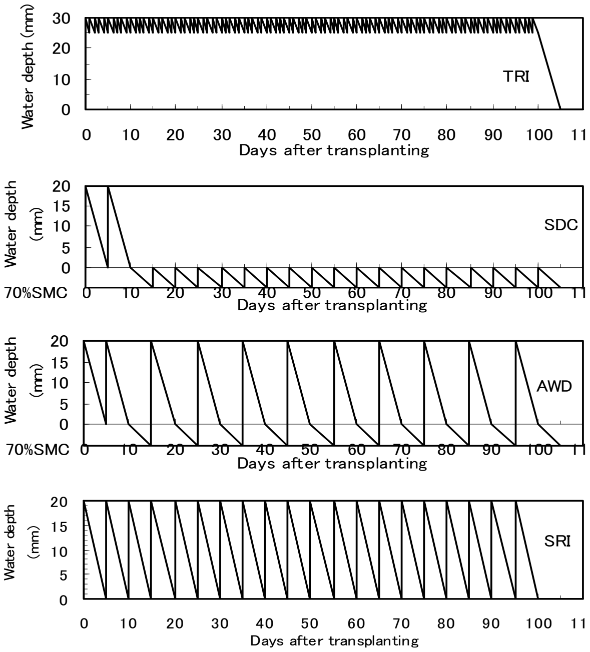

Figure 2. Water management irrigation technique.

4. Results and Discussion

4.1. Effects of Water management Technique on Yield

Table 1 shows the effect of water management technique on yield. The maximum rice production was obtained under SDC technique with 2.06 kg/6 m^2 (3.43 ton/ha) followed by AWD with 1.83 kg/6 m^2 (3.05 ton/Ha). The production reduced almost 50% compared with dry season cultivation [17]. The lower production was affected by lower number of tillers due to high rainfall intensity during growing period. The average productive tiller for all the water management studied was only 12-15 tillers for each hill. During growing period, rainfall almost occurred every day and up to 40 DAT the amount of rainfall was 572 mm as shown in **Figure 3.**

4.2. Effects of Water management Technique on Irrigated Water

Irrigated water requirement varied depending on WSI

Table 1. Yield production during rainy season cultivation.

Water management technique	Yield (ton/ha)	% difference to control
TRI (control)	1.53	0
AWD	3.05	99.3
SDC	3.43	125.2
SRI	2.02	32.2

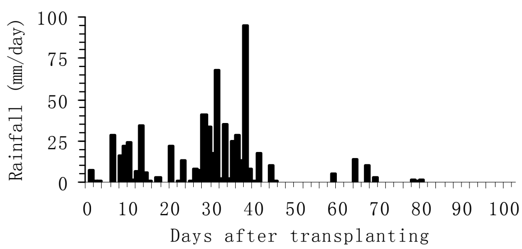

Figure 3. Rainfall during paddy rice cultivation.

technique used as presented in **Table 2**. The amount of irrigated water needed during rainy season cultivation was much less than dry season cultivation that required 885 mm for TRI, 735 mm for AWD, and 631 mm for SDC [17]. This condition might be happened due to high rainfall occurred during rainy season cultivation (635 mm), whereas at dry season cultivation there was no rainfall at all. The table shows that WSI techniques reduce significantly the amount of water needed for paddy rice cultivation compared to TRI. Using SDC and AWD techniques, the irrigated water reduction reached 55.4% and 38.5%, respectively. The SRI technique seems required much water due to leakage occurred during the experiment as indicated with much higher percolation (384 mm) than others.

4.3. Effects of Water management Technique on Flood Reduction

Flood reduction under different water irrigation techniques were given at **Table 3**. The table shows that paddy field (plot) was very effective in storing rainfall in the paddy field and it has a potential function for flood reduction both volume and peak. Flood reduction of paddy plots varied among the water management techniques in the range between 37.2% up to 55.7%. The SDC technique was the most effective one in flood reduction that retained rainfall at the paddy field up to 55.7%. This phenomenon occurred due to the upper limit of water depth at the plots was kept at 0 mm, whereas for the other techniques such as AWD and SRI the maximum water depth was maintained at 2 cm. It means the storage capacity of paddy field for storing rainfall using the SDC technique was higher than other techniques.

Table 2. Water parameters during rainy season cultivation.

Water parameters	Water management technique			
	TRI	AWD	SDC	SRI
(1) irrigated water (mm)	194	119	128	319*
(2) rainfall (mm)	536	635	635	635
(3) percolation (mm)	215	154	156	384*
(4) spill (mm)	318	399	282	320
% irrigated water compared to control	0	–38.5	–55.4	97.0*

*leakage was occurred in the SRI plot

Table 3. Flood reduction under different water management technique.

Time	Rainfall	Spill over the plots (mm)			
	(mm)	TRI	AWD	SDC	SRI
6-26 April 2007	332	292	302	254	262
% reduction		–12.1	–9	–23.6	–21.2
1 season	635	318	399	282	320
% reduction		–40.8	–37.2	–55.7	–49.7

5. Conclusions

Three water saving irrigation (WSI) management techniques, *i.e.*, alternate wetting and drying (AWD), semi dry cultivation (SDC) and system of rice intensification (SRI) for paddy rice cultivation and traditional continuous flooding (TRI) were applied in the experimental paddy plots. Some important results are summarized as follows.

- Paddy fields were very effective in flood reduction/ retaining rainfall. Flood reduction of paddy plots varies among the water management techniques used in the range between 37.2% up to 55.7%. The semi-dry cultivation technique was the most effective one in flood reduction that retained rainfall up to 55.7%.
- Based on the experiment, to increase the function of paddy fields for flood reduction the semi-dry cultivation technique should be applied for paddy rice cultivation especially during rainy season.
- The amount of irrigated water during rainy season cultivation varies among the water management techniques in the range of 128 mm to 195 mm. It means that rainfall was fully utilized or higher effective rainfall was obtained under WSI without hindering rice production.
- Study on the effectiveness of water saving irrigation techniques on flood reduction at basin scale may be needed to get the whole picture performance of the techniques.

6. Acknowledgements

This research was supported by Faculty of Engineering, Gadjah Mada University. The author thanks the students for field work and data collection.

7. References

[1] J. W. Ahn, “Rice Farming and Strategy to Rural Development,” *Paddy and Water Environment*, Vol. 3, No. 2, 2005, pp. 73-77.

[2] Y. K Matsuno, K. Nakamura, T. Masumoto, H. Matsui, T. Kato and Y. Sato, “Prospects for Multi-Functionality of Paddy Rice Cultivation in Japan and Other Countries in Monsoon Asia,” *Paddy and Water Environment*, Vol. 4, No. 4, 2006, pp. 189-197.

[3] C. C. Huang, M. H. Tsai, W. T. Lin, Y. F. Ho and C. H. Tan, “Multifunctionality of Paddy Fields in Taiwan,” *Paddy and Water Environment*, Vol. 4, No. 4, 2006, pp. 199-204.

[4] K. Unami and T. Kawachi, “Systematic Assessment of Flood Mitigation in a Tank Irrigated Paddy Fields Area,”

Paddy and Water Environment, Vol. 3, No. 4, 2005, pp. 191-199.

[5] T. C. Kim, U. S. Gim, J. S. Kim and D. S. Kim, "The Multi-Functionality of Paddy Farming in Korea," *Paddy and Water Environment*, Vol. 4, No. 4, 2006, pp. 169-179.

[6] S. J. Kim, G. A. Park and H. J. Kwon, "Evaluation of Paddy Water Storage Dynamics during Flood Period in South Korea," *Water Engineering*, Vol. 11, No. 5, 2007, pp. 269-276.

[7] J. Sujono, "Water Saving Irrigation on Paddy Fields for Increasing Productivity and for Flood Reduction," *IASTED International Conference on Water Resources Management*, Hawaii, 2007.

[8] Y. Li and R. Barker, "Increasing Water Productivity for Paddy Irrigation in China," *Paddy and Water Environmental*, Vol. 2, No. 4, 2004, pp. 187-193.

[9] M. Zhi, "Water Efficient Irrigation and Environmentally Sustainable Irrigated Rice Production in China," International Commission on Irrigation and Drainage, 2002. http://www.icid.org/wat_mao.pdf

[10] F. Rijsberman, "Growing more Rice with less Water," *Paddy and Water Environmental*, Vol. 2, No. 4, 2004, pp. 181-183.

[11] R. Barker, T. P. Tuong, Y. Li, E. G. Castillo and B. A. M. Bouman, "Growing more Rice with less Water: Research Findings from a Study in China," *Paddy and Water Environmental*, Vol. 2, 2004, pp. 185-194.

[12] Y. Li, "Water Saving Irrigation in China," *Irrigation and Drainage*, Vol. 55, No. 3, 2006, pp. 327-336.

[13] R. E. Namara, P. Weligamage and R. Barker, "Prospects for Adopting System of Rice Intensification in Sri Lanka: A Socio-Economics Assessment," *Research Report* 75, International Water Management Institute, Colombo, 2003.

[14] N. Koei, "The System of Rice Intensification in East Indonesia," Nippon Koei Co., Ltd., Nippon Koei, 2005.

[15] A. J. McDonald, P. R. Hobbs and S. J. Riha, "Does the System of Rice Intensification Outperform Conventional Best Management? A Synopsis of the Empirical Record," *Field Crops Research*, Vol. 96, No. 1, 2006, pp. 31-36.

[16] B. Dong, R. Loeve, Y. H. Li, C. D. Chen, L. Deng and D. Molden, "Water Productivity in the Zhanghe Irrigation System: Issues of Scale," *Proceedings of an International Workshop on Water Saving Irrigation for Rice*, Wuhan, 2001, pp. 97-115.

[17] J. Sujono, F. Nurrochmad and R. Jayadi, "Growing more Rice with less Water," *Research Report*, Department of Civil and Environmental Engineering, Faculty of Engineering, Gadjah Mada University, Gadjah Mada, 2006.

J. Water Resource and Protection, **2010, 2, 560-568**
doi:10.4236/jwarp.2010.26064 Published Online June 2010 (http://www. SciRP.org/journal/jwarp)

Differential Evolution Algorithm with Application to Optimal Operation of Multipurpose Reservoir

Dattatray Gangaram Regulwar[1], Sumant Anant Choudhari[2], Pallakury Anand Raj[3]
[1]*Department of Civil Engineering, Government College of Engineering, Aurangabad, India*
[2]*Research Scholar, National Institute of Technology, Warangal, India*
[3]*Department of Civil Engineering, National Institute of Technology, Warangal, India*
E-mail: {*dgregulwar, sumantchoudhari*}*@rediffmail.com, a_raj_p@yahoo.co.in*
Received March 12, 2010; *revised April* 7, 2010; *accepted May* 4, 2010

Abstract

This paper includes an application of Differential Evolution (DE) for the optimal operation of multipurpose reservoir. The objective of the study is to maximize the hydropower production. The constraints for the optimization problem are reservoir capacity, turbine release capacity constraints, irrigation supply demand constraints and storage continuity. For initializing population, the upper and lower bounds of decision variables are fixed. The fitness of each vector is evaluated. The mutation and recombination is performed. The control parameters, *i.e.*, population size, crossover constant and the weight are fixed according to their fitness value. This procedure is performed for the ten different strategies of DE. Sensitivity analysis performed for ten strategies of DE suggested that, De/best/1/bin is the best strategy which gives optimal solution. The DE algorithm application is presented through Jayakwadi project stage-I, Maharashtra State, India. Genetic algorithm is utilized as a comparative approach to assess the ability of DE. The results of GA and ten DE strategies for the given parameters indicated that both the results are comparable. The model is run for dependable inflows. Monthly maximized hydropower production and irrigation releases are presented. These values will be the basis for decision maker to take decisions regarding operation policy of the reservoir. Results of application of DE model indicate that the maximized hydropower production is 30.885×10^6 kwh and the corresponding irrigation release is 928.44 Mm^3.

Keywords: Optimization, Hydropower Production, Differential Evolution, Reservoir Operation

1. Introduction

Water for drinking purpose, for use in industry, irrigation and hydropower production, is main factor for hindering developments in many parts of the globe. Hence, proper management of available water resources is essential. Reservoir operation forms an important role in water resources development. Yeh [1] reviewed reservoir management and operation models. Algorithms and methods surveyed include linear programming (LP), dynamic programming (DP), nonlinear programming (NLP), and simulation. Oliveira and Loucks [2] have presented operating rules for multireservoir systems by using genetic search algorithms. Simulation was used to evaluate each policy by computing performance index for a given flow series. Wardlaw and Sharif [3] have presented several alternative formulations of a genetic algorithm for reservoir system. Later on, multi-reservoir systems optimization has been studied by Sharif and Wardlaw [4]. Nagesh Kumar *et al.* [5] have studied optimal reservoir operation for hydropower production which involved constrained nonlinear optimization. Earlier to that Srinivasa Raju and Nagesh Kumar [6] have discussed application of genetic algorithms for irrigation planning. GA was used to determine optimal cropping pattern for maximizing benefits for an irrigation project. Regulwar and Anand Raj [7] have presented A Multi objective, Multireservoir operation model for maximization of irrigation releases and hydropower production using Genetic Algorithm. A monthly Multi Objective Genetic Algorithm Fuzzy Optimization (MOGAFUOPT) model has been developed. From the relationships developed amongst irrigation releases, hydropower production and level of satisfaction, a three dimensional (3-D) surface covering the whole range of policies has been developed.

Storn [8] has represented a heuristic approach for minimizing nonlinear and non differentiable continuous space function. The proposed method which requires few control variables is robust, easy to use and lends itself very well to parallel computation. Lampinen [9] has proposed differential evolution algorithm for handling nonlinear constraint functions. Differential Evolution (DE) algorithms claimed to be very efficient when they are applied to solve multimodal optimal control problems (Lopez Cruz *et al.* [10]). Differential evolution was used for the optimization of non-convex Mixed Integer Nonlinear Programming (MINLP) problems. The results of DE were compared with simplex, simulated annealing and genetic algorithm (Babu and Angira [11]). Vasan and Srinivasaraju [12] have demonstrated application of differential evolution to Bilaspur project in Rajasthan, India. The objective was to determine suitable cropping pattern for maximum benefits. Ranjithan [13] has presented the role of evolutionary computation in environmental and water resources systems analysis and discussed various methods such as Simulated Annealing, Tabu Search, GA, Evolutionary strategies, Particle swarm and Ant colony optimization. Janga Reddy and Nagesh Kumar [14] have studied Multi Objective Differential Evolution (MODE) with an application to a reservoir system optimization. The evolutionary operators used in differential evolution algorithms are very much suitable for problems having interdependence among the decision variables.Vasan and Komaragiri Srinivasa Raju [15] have demonstrated the applicability of DE to a case study of Mahi Bajaj Sagar project (MBSP), India. Ten different strategies of DE were employed to assess the ability of DE for solving higher dimensional problems as an alternative methodology for irrigation planning. The results were compared with LP.

In Genetic Algorithm (GA) low mutation rate is required to get global optimum [16]. The low mutation rate may get trouble with problems having interdependent relationships between variables and may require more number of function evaluations [17]. In reservoir operation the interdependence relationship may exist among decision variables. Interdependencies among variables can be tackled by properly rotating the co-ordinate system of the given function as it is done in Differential Evolution. DE has all properties necessary to handle complex problems with interdependencies between parameters [18]. DE maintains correlated self-adopting mutation step sizes in order to make timely progressive optimization. There is interdependence among variables therefore the evolutionary operators of DE are suitable to tackle these problems. This paper presents the applicability of DE for determining operation policies of a multipurpose reservoir.

2. Methodology

Differential evolution is a recent evolutionary optimization technique. It is simple, faster convergent and robust. The main difference between GA and DE is that GA depends on crossover while DE uses mutation as primary search mechanism. DE uses weighted differences between solution vectors to perturb the population. Unlike genetic algorithms, no binary coding of the population members is necessary. The general convention used for different variants of DE is DE/a/b/c. Here DE is for Differential evolution, ‘a’ is a string which denotes the vector to be perturbed, ‘b’ denotes the number of difference vectors taken for perturbation of ‘a’ and ‘c’ is the crossover method. According to Price and Storn [19] different strategies of DE are DE/rand/1/bin, DE/best/1/bin, DE/best/2/bin, DE/rand/2/bin, DE/rand-to-best/1/bin, DE/rand/1/exp, DE/best/1/exp, DE/best/2/exp, DE/rand/2/exp, and DE/rand-to-best/1/exp.

DE holds D-dimensional real valued vectors of *Np* population in pair. The current population $P_{\mathbf{x}}$, includes vectors $\mathbf{x}_{i,g}$ added or created randomly or by comparison with other vectors.

$$\begin{aligned} P_{\mathbf{x},g} &= \left(\mathbf{x}_{i,g}\right) \quad i = 0,1,\ldots,Np-1, \quad g = 0,1,\ldots,g_{\max}, \\ \mathbf{x}_{i,g} &= \left(x_{j,i,g}\right) \quad j = 0,1,\ldots,D-1. \end{aligned} \tag{1}$$

The index, $g = 0, 1,\ldots g_{\max}$, shows the generation of a vector. A population index i is assigned to each vector which ranges from 0 to Np-1. The index ‘j’ indicates parameter within vector ranges from 0 to D-1. After initialization, an intermediary population $P_{v,g}$, of *Np* mutant vectors, $\mathbf{v}_{i,g}$ produced by random mutation.

$$\begin{aligned} P_{\mathbf{v},g} &= \left(\mathbf{v}_{i,g}\right) \quad i = 0,1,\ldots Np-1, \quad g = 0,1,\ldots,g_{\max}, \\ \mathbf{v}_{i,g} &= \left(v_{j,i,g}\right) \quad j = 0,1,\ldots,D-1. \end{aligned} \tag{2}$$

Each vector in the current population is then recombined with a mutant to produce a trial population, $P_{\mathbf{u}}$ of *Np* trial vectors, $\mathbf{u}_{i,g}$

$$\begin{aligned} P_{\mathbf{u},g} &= \left(\mathbf{u}_{i,g}\right) \quad i = 0,1,\ldots,Np-1, \quad g = 0,1,\ldots,g_{\max}, \\ \mathbf{u}_{i,g} &= \left(u_{j,i,g}\right) \quad j = 0,1,\ldots,D-1. \end{aligned} \tag{3}$$

During crossover, trial vectors overwrite the mutant population, so a single array can hold both populations. Then the cost of the trial vector is compared with the cost of the target vector, the vector having low cost will go into the next generation.

2.1. Case Study

The Jayakwadi project stage-I is taken as a case study. It is built across river Godavari, in Maharashtra State, India. The gross storage of reservoir is 2909×10^6 m^3 and live storage is 2171 × 10^6 m^3. Total installed capacity for power generation is 12.0 MW (Pumped storage plant). Irrigable command area is 1416.40 km^2. The schematic representation of the physical system showing Jayakwadi project stage-I is shown in **Figure 1**. Monthly historical flow data for 73 years is collected and 75% dependable monthly flows are estimated using the Weibull plotting position formula. The inflow, irrigation demand, turbine capacity are presented in **Table 1**.

2.2. Model Formulation

The objective of the study is to maximize the hydropower production and present operation policy of a case study reservoir. Mathematically it can be expressed as:

$$\text{Max} \quad Z = \sum_{t=1}^{12} P_t \qquad (4)$$

where P_t = Hydropower produced in kwh during month '*t*'. If the monthly releases for hydropower (*RP*) are

Table 1. Inflow, irrigation demand and power demand.

Sr no.	Months	Maximum irrigation demand in Mm^3	Turbine Capacity in Mm^3	75% dependable inflow in Mm^3
1.	June	18.55	33.96	148.762
2.	July	26.7	33.96	408.25
3.	August	25.43	33.96	610.66
4.	September	85.79	33.96	600.0
5.	October	267.86	33.96	287.75
6.	November	228.74	33.96	196.46
7.	December	210.88	33.96	125.53
8.	January	230.34	33.96	37.65
9.	February	85.23	33.96	21.462
10.	March	70.06	33.96	19.562
11.	April	85.49	33.96	25.5
12.	May	58.20	33.96	46.587
	Total	1393.27	407.52	2528.173

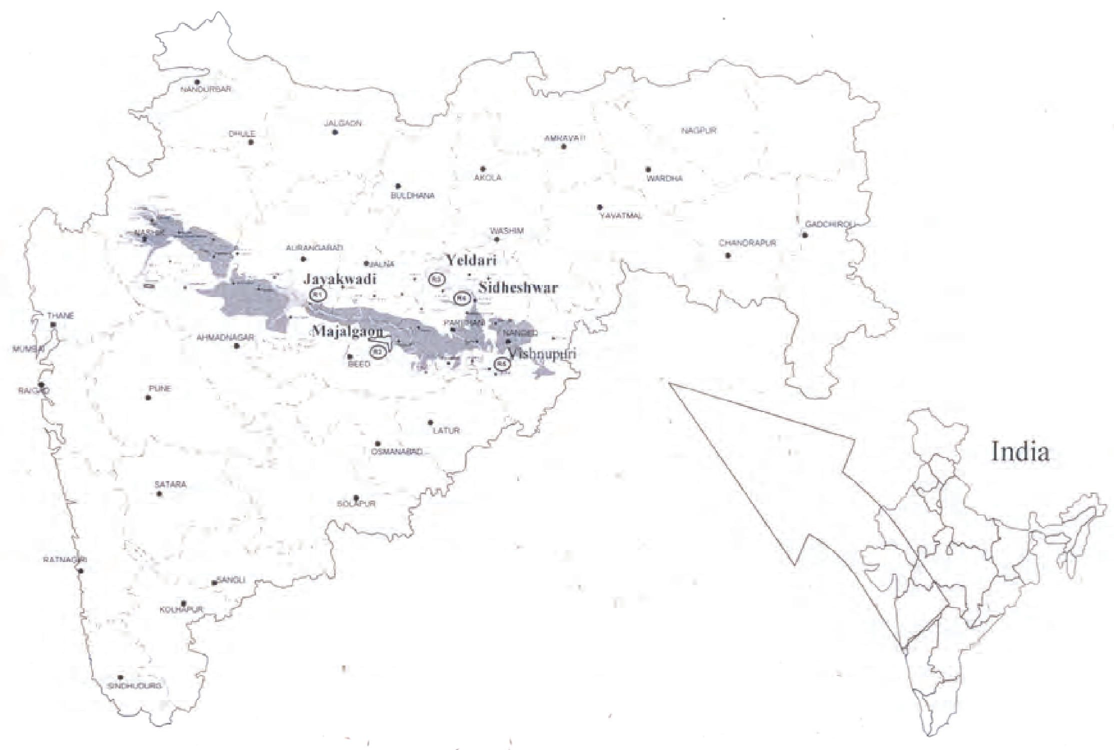

Figure 1. Sketch showing Jayakwadi project stage-1, Maharashtra state, India.

expressed in Mm^3, head (h) in meters, then power produced P in KW hours for a 30 day month is given by P = 2725 × (RP) × (h). The model is subjected to the following constraints.

2.2.1. Releases into Turbine and Capacity Constraints

The releases into turbines for power production, should be less than or equal to the flow through turbine capacity (TC) for all the months. Also, power production in each month should be greater than or equal to the firm power (FP). These constraints can be written as:

$$RP(t) \le TC \quad \forall \quad t = 1,2,3.....12. \tag{5}$$

$$RP(t) \ge FP \quad \forall \quad t = 1,2,3,.....12. \tag{6}$$

2.2.2. Irrigation Supply-Demand Constraints

The releases into canals for irrigation (*RI*) should be less than or equal to the maximum irrigation demand ($ID_{\max}$) for all the months. Also, the releases into the canals for irrigation should be greater than or equal to the minimum irrigation demand ($ID_{\min}$). The irrigation release-demand constraint, can, therefore be written as:

$$RI(t) \le ID_{\max}(t) \quad \forall \quad t = 1,2,3,.....12. \tag{7}$$

$$RI(t) \ge ID_{\min}(t) \quad \forall \quad t = 1,2,3.......12 \tag{8}$$

2.2.3. Reservoir Storage-Capacity Constraints

The storage in the reservoirs (*S*) should be less than or equal to the maximum storage capacity (*SC*) and greater than or equal to the minimum storage capacity ($S_{\min}$) for all months. These constraints can be written as:

$$S(t) \le SC \quad \forall \quad t = 1,2,3......12. \tag{9}$$

$$S(t) \ge S_{\min} \quad \forall \quad t = 1,2,3......12 \tag{10}$$

2.2.4. Reservoir Storage-Continuity Constraints

This constraint relate to the turbine releases (RP), irrigation releases (RI), release for drinking and industrial water supply (RWS) which is taken as a constant, reservoir storage (S), inflows into the reservoirs (IN), Losses from the reservoirs for all months. The losses from the reservoirs are taken as function of storage as given by Loucks *et al.* [20]. Let A_o is reservoir water surface area corresponding to the dead storage volume and e_t is evaporation rate corresponding to the time period t (in depth units). A_a is the reservoir water spread area per unit volume of active storage. Then the actual evaporation during the time period 't' is given by

$$\text{Evaporation loss} = A_0 e_t + A_a e_t \frac{(S_t + S_{t+1})}{2}$$

$$\text{Put } a_t = \frac{A_a e_t}{2} = 0.5 A_a e_t \quad \text{then,}$$

$$\text{Evaporation loss} = A_0 e_t + a_t (S_t + S_{t+1})$$

Then the hydrologic continuity constraint can be written as:

$$(1+a_t)S(t+1) = (1-a_t)S(t) + IN(t) - RP(t) - RI(t) \\ -SP(t) - WS(t) - FCR(t) + \beta RP(t) - A_0 e_t(t) \tag{11}$$

3. Results and Discussion

Differential Evolution (DE) has ten strategies. The model is run with DE parameters, *i.e.*, crossover constant and weight for each strategy. The population is fixed by running the model for different population sizes in combination with crossover constants and weight. For deciding crossover constant and weight for each strategy, the model is run for different crossover constants, *i.e.*, 0.7, 0.75, 0.8, 0.85, 0.9, 0.95 with the combination of weight ranging from 0.2 to 0.9 with the increment of 0.05. For every combination fitness is calculated and compared with population. Based on this approach population is fixed as 400. For getting optimal solution, generation is fixed as 500. The DE parameters, *i.e.*, crossover constants and weight are decided for each strategy and presented in **Table 2**. The relationships between weight and hydropower releases corresponding to crossover constant are presented graphically in **Figures 2** to **11**. By considering these DE parameters, the optimization model is run and optimized values of objective function are presented for all strategies in **Table 2**. The random seed should be greater than one. So for seed also the model is run for various seed values, *i.e.*, 1 to 90, and 77 is fixed from the comparison of results.

Table 2 presents comparison of strategies of DE. In this table, the crossover constant, weight, optimal hydropower production and annual irrigation releases are presented corresponding to each strategy. The comparison of strategies for maximum objective function value is shown graphically in **Figure 12**. From the **Table 2**, it is clear that the strategy number 6, *i.e.*, DE/best/1/bin gives the optimal results. For this strategy, the DE parameters are crossover 0.85, and weight 0.9. The optimized hydropower production is worked out to be 30.89 × 10^6 kwh. The release for irrigation corresponding to the optimal fitness of objective function is 928.44 Mm^3. Monthly optimal releases for irrigation are shown graphically in **Figure 13**. Monthly optimal hydropower production is shown graphically in **Figure 14**. For comparison of DE results, the genetic algorithm approach is utilized in this study. The proposed reservoir operation model is solved using GA. Stochastic remainder selection; one point crossover and binary mutation are used as GA operators in this study. For selection of population size, crossover probability, mutation probability and optimal generations, a thorough sensitivity analysis is carried out. The system performance is estimated by taking crossover probability between 0.6 to 1.0 with a increment of 0.05 and mutation probabilities between 0.4 to 0.001 with a decrement of 0.1 up to 0.01 and then the decrement is taken as 0.001. The population size is var-

Table 2. Comparison of strategies of differential evolution.

Sr. No.	Strategy	CR	F	Annual hydropower produced kwh	Annual Irrigation releases Mm^3
1	DE/best/1/exp	0.85	0.70	29651500	927.271
2	DE/rand/1/exp	0.95	0.70	30365652	827.383
3	DE/rand-to-best/1/exp	0.80	0.90	27208474	872.191
4	DE/best/2/exp	0.95	0.50	29268860	976.005
5	DE/rand/2/exp	0.85	0.60	29380314	881.820
6	DE/best/1/bin	0.85	0.90	30885738	928.442
7	DE/rand/1/bin	0.95	0.80	28513356	853.046
8	DE/rand-to-best/1/bin	0.85	0.90	27368522	862.894
9	DE/best/2/bin	0.85	0.90	29247944	906.402
10	DE/rand/2/bin	0.95	0.80	30099228	947.816

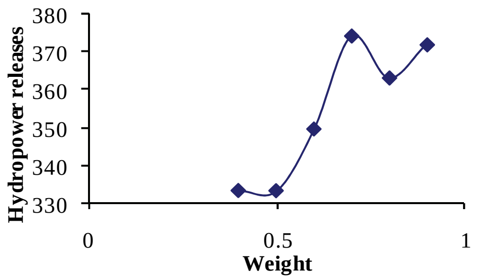

Figure 2. Relationship between weight and strategy No. 1 for crossover 0.85.

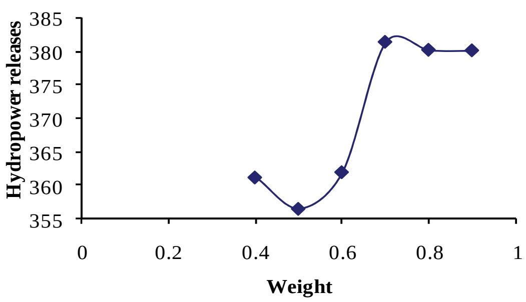

Figure 3. Relationship between weight and strategy 2 for crossover 0.95.

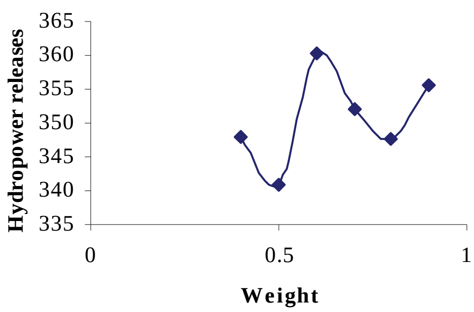

Figure 4. Relationship between weight and strategy No. 3 for crossover 0.8.

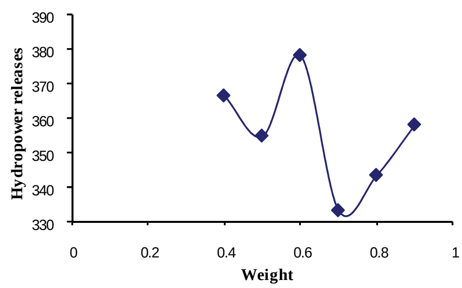

Figure 5. Relationship between weight and strategy No. 4 for crossover 0.95.

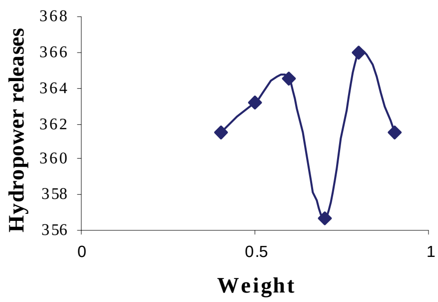

Figure 6. Relationship between weight and strategy No. 5 for crossover 0.85.

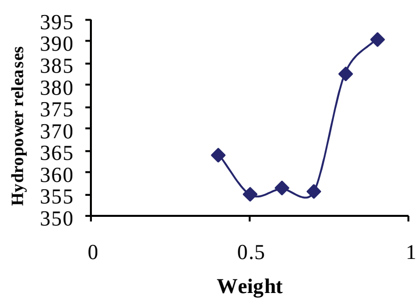

Figure 7. Relationship between weight and strategy No. 6 for crossover 0.85.

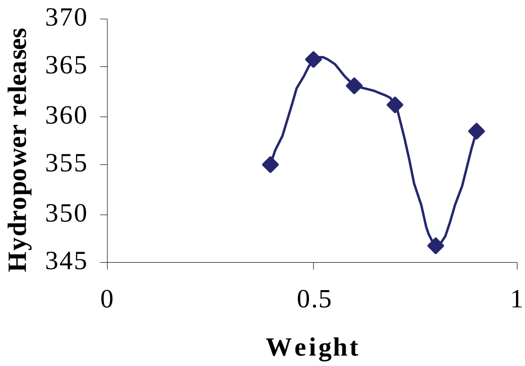

Figure 8. Relationship beween weight and strategy No. 7 for crossover 0.95.

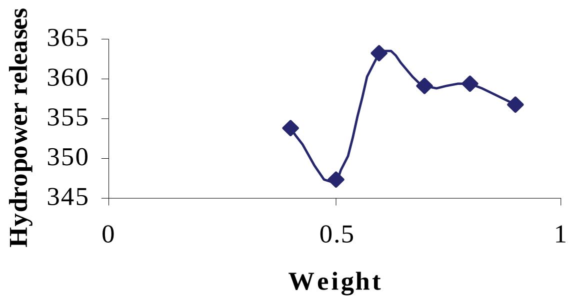

Figure 9. Relationship between weight and strategy No. 8 for crossover 0.85.

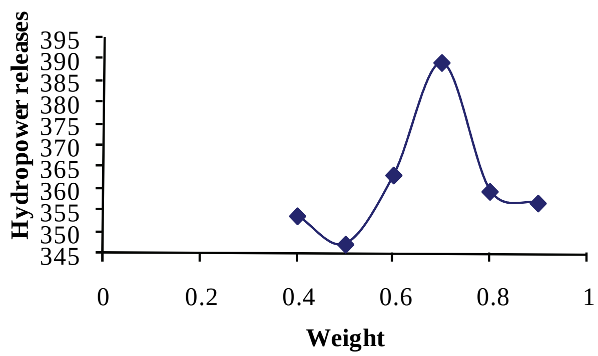

Figure 10. Relationship between weight and strategy No. 9 for crossover 0.85.

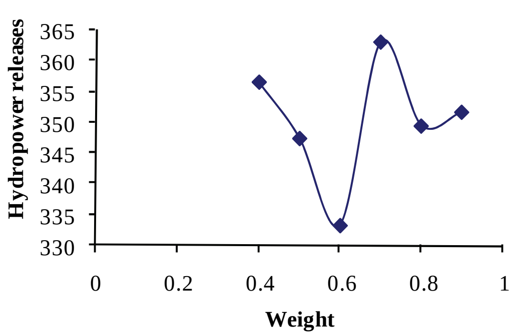

Figure 11. Relationship between weight and strategy No. 10 for crossover 0.95.

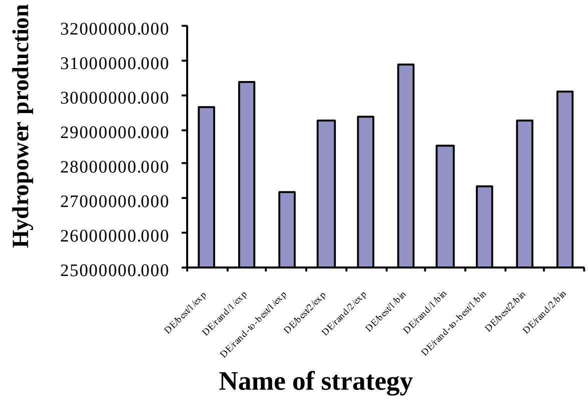

Figure 12. Comparison of strategies.

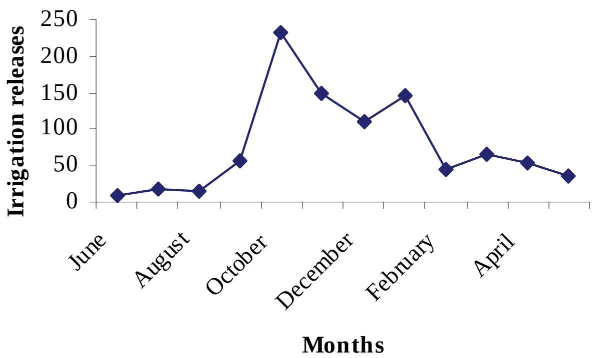

Figure 13. Optimal releases for irrigation (DE/best/1/bin).

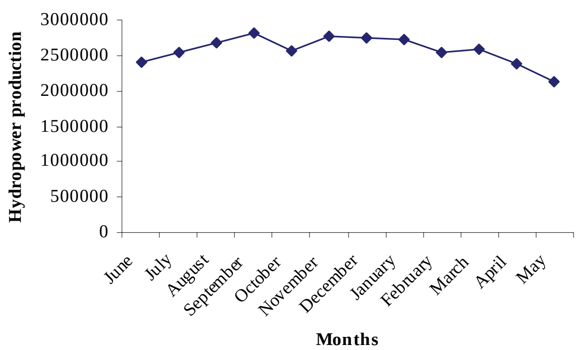

Figure 14. Optimal hydropower production (DE/best/1/bin).

ied from 50 to 150 and generation from 20 to 500. Based on the system performance the optimal population size and optimal number of generations are 100 and 500 respectively. For crossover probability of 0.95 and mutation probability of 0.01, the maximization is achieved. The monthly optimized irrigation releases and hydropower production by using GA are obtained and presented in **Table 3**. The comparison of DE and GA results for irrigation releases and hydropower production are presented for best strategy in the same table. Also **Table 4** represents the monthly optimal irrigation releases obtained by DE strategies and GA. **Table 5** represents the

Table 3. Comparison of optimal releases for irrigation and hydropower production by DE and GA.

Month	Release for irrigation Mm^3 By DE	Release for irrigation Mm^3 By GA	Hydropower produced $\times 10^6$ kwh By DE	Hydropower produced $\times 10^6$ kwh By GA
June	9.65	14.20	2.405	2.581
July	16.58	16.94	2.552	2.548
August	13.47	16.63	2.671	2.571
September	55.10	58.14	2.811	2.56
October	232.55	178.05	2.575	2.562
November	148.90	146.51	2.776	2.576
December	109.42	145.18	2.738	2.571
January	144.63	129.31	2.717	2.552
February	44.38	55.59	2.544	2.559
March	64.87	48.87	2.577	2.564
April	52.12	54.67	2.384	2.572
May	36.76	38.09	2.137	2.553
TOTAL	928.442	902.19	30.887	30.769

Table 4. Irrigation releases obtained by the DE strategies and GA in Mm^3.

Month	DE1	DE2	DE3	DE4	DE5	DE6	DE7	DE8	DE9	DE10	GA
June	9.7	9.7	9.7	9.7	9.7	9.7	9.7	9.7	9.7	9.7	14.20
July	16.6	16.6	16.6	16.6	16.6	16.6	16.6	16.6	16.6	16.6	16.94
August	13.5	13.5	13.5	13.5	13.5	13.5	13.5	13.5	13.5	13.5	16.63
September	57.4	34.8	56.2	56.2	52.3	55.1	49.7	46.3	72.9	62.5	58.14
October	232.6	138.9	162.4	162.4	138.8	232.6	140.6	162.4	162.4	162.4	178.05
November	148.9	149.6	157.9	209.1	151.7	148.9	160.3	193.9	118.5	117.9	146.51
December	109.4	127.9	109.3	109.3	85.4	109.4	123.2	109.3	85.4	109.3	145.18
January	134.9	145.2	145.8	211.8	195.1	144.6	147.7	151.9	176.6	223.7	129.31
February	51.9	44.3	34.6	51.9	74.5	44.4	52.7	34.6	74.5	34.6	55.59
March	63.1	64.9	53.2	67.4	46.0	64.9	55.6	66.9	63.6	67.8	48.87
April	44.5	34.7	74.8	44.5	62.0	52.1	34.7	34.7	56.0	74.8	54.67
May	44.5	47.4	38.3	23.7	36.4	36.8	48.9	23.2	56.8	55.0	38.09
Total	927.0	827.4	872.2	976.0	881.8	928.4	853.0	862.9	906.4	947.8	902.19

*DE*1 DE/best/1/exp, *DE*2 DE/rand/1/exp, *DE*3 DE/rand-to-best/1/exp, *DE*4 DE/best/2/exp, *DE*5 DE/rand/2/exp, *DE*6 DE/best/1/bin, *DE*7 DE/rand/1/bin, *DE*8 DE/rand-to-best/1/bin, *DE*9 DE/best/2/bin, *DE*10 DE/rand/2/bin

Table 5. Hydropower production obtained by the DE strategies and GA in kwh ($\times 10^6$).

Month	DE1	DE2	DE3	DE4	DE5	DE6	DE7	DE8	DE9	DE10	GA
June	2.41	2.42	2.11	2.35	2.32	2.40	2.37	2.29	2.41	2.30	2.58
July	2.35	2.52	2.18	2.52	2.48	2.55	2.23	2.17	2.57	2.80	2.55
August	2.61	2.61	2.14	2.26	2.51	2.67	2.56	2.19	2.41	2.53	2.57
September	2.36	2.72	2.02	2.73	2.67	2.81	2.16	2.08	2.78	2.87	2.56
October	2.86	2.58	2.54	2.53	2.82	2.58	2.53	2.46	2.79	2.63	2.56
November	2.76	2.83	2.48	2.72	2.76	2.78	2.01	2.41	2.62	2.65	2.58
December	2.80	2.36	2.46	2.29	2.23	2.74	2.71	2.23	2.36	2.41	2.57
January	2.69	2.62	2.38	2.48	2.68	2.72	2.32	2.56	2.67	2.79	2.55
February	2.63	2.45	1.99	2.36	2.22	2.54	2.52	2.32	2.44	2.26	2.56
March	1.79	2.58	2.41	2.38	2.46	2.58	2.55	2.13	2.62	2.19	2.56
April	2.21	2.45	2.41	2.36	2.00	2.38	2.40	2.44	1.85	2.37	2.57
May	2.18	2.22	2.08	2.27	2.23	2.14	2.15	2.09	1.73	2.30	2.55
Total	29.65	30.37	27.21	29.27	29.38	30.89	28.51	27.37	29.25	30.10	30.77

monthly optimal hydropower production by DE strategies and GA. **Tables 4** and **5** gives exhaustive comparison of all DE strategies and GA for irrigation releases and hydropower production. This comparison among all strategies of DE and GA provides applicability of differential evolution for optimal operation of multi-purpose reservoir.

4. Conclusions

In the present study a multipurpose reservoir in Godavari River sub basin in Maharashtra State, India is considered. A multiobjective operation model for maximization of hydropower production is proposed using differential evolution algorithm. Results of application of DE model indicate that the maximized hydropower production is 30.885×10^6 kwh and the corresponding irrigation release is 928.44 Mm^3. From the results it can be seen that the monthly maximized irrigation release and hydropower production can be the basis for decision maker to take decision for reservoir operation. Genetic algorithm is utilized as a comparative approach. The results of GA and different DE strategies for irrigation releases and hydropower production show that both the results are close and comparable. Therefore it can be said that DE can be used as an alternative methodology for optimal operation of multipurpose reservoir. Differential evolution algorithm works with numerical values. Therefore highly complex objective functions do not introduce any difficulties and even discontinuous functions are acceptable. From the results, it can be said that the DE can be effectively applied to multi-objective operation problem and the reservoir can be operated for optimal reservoir releases for irrigation and hydropower production after meeting the other demands from the reservoir.

5. Acknowledgements

The authors are thankful to Rainer Storn, K. Price and J. Lampinen for their guidance during the work. Also, the authors are thankful to Command Area Development Authority, Aurangabad, Maharashtra state, India for providing necessary data for the analysis.

6. References

[1] W. W.-G. Yeh, "Reservoir Management and Operations Models: A State-of-the-Art Review," *Water Resources Research*, Vol. 21, No. 12, 1985, pp. 1797-1818.

[2] R. Oliveira and D. P. Loucks, "Operating Rules for Multi-Reservoir Systems," *Water Resource Research*, Vol. 33, No. 4, 1997, pp. 839-852.

[3] R. Wardlaw and M. Sharif, "Evaluation of Genetic Algorithm for Optimal Reservoir System Operation," *Journal of Water Resource, Planning and Management*, Vol. 125, No. 1, 1999, pp. 25-33.

[4] M. Sharif and R. Wardlaw, "Multireservoir Systems Optimization Using Genetic Algorithms: Case Study," *Journal of Computer in Civil Engineering*, Vol. 14, No. 4, 2000, pp. 255-263.

[5] D. Nagesh kumar, A. Kumar and K. S. Raju, "Application of Genetic Algorithms for Optimal Reservoir Operation," *Proceedings of X World Water Congress*, Melbourne, 2000.

[6] K. S. Raju and D. Nagesh Kumar, "Irrigation Planning Using Genetic Algorithms," *Water Resource Management*, Vol. 18, No. 2, 2004, pp. 163-176.

[7] D. G. Regulwar and P. A. Raj, "Development of 3-D Optimal Surface for Operation Policies of a Multireservoir in Fuzzy Environment Using Genetic Algorithm for River Basin Development and Management," *Water Resource and Management*, Vol. 22, No. 5, 2008, pp. 595-610.

[8] R. Storn and K. Price, "Differential Evolution a Simple Evolution Strategy for Fast Optimization," *Dr Dobb's Journal*, Vol. 22, No. 4, 1997, pp. 18-24.

[9] J. Lampinen, "Multiconstraint Nonlinear Optimization by Differential Evolution Algorithm," *Technical Report*, Lappeenranta University of Technology, Laboratory of Processing, 1999. http://www.lut.fi/~jlampine/debiblo.htm

[10] I. L. Lopez Cruz, L. G. Van Willigenburg and G. Van Straten, "Efficient Differential Evolution Algorithms for Multimodal Optimal Control Problems," *Journal of Applied Soft Computing*, Vol. 3, No. 2, 2003, pp.97-122.

[11] B. V. Babu and R. Angira, "A Differential Evolution Approach for Global Optimization of MINLP Problems," *Proceedings of* 4*th Asia Pasific conference on Simulated Evolution and Learning* (*SEAL*2002), Vol. 2, Singapore, 2002, pp. 880-884.

[12] A. Vasan and K. Srinivasa Raju, "Optimal Reservoir Operation Using Differential Evolution," *International Conference on Hydraulic Engineering*: *Research and Practice* (*ICON-HERP*-2004), Indian Institute of Technology Roorkee, India, 2004.

[13] S. R. Ranjithan, "Role of Evolutionary Computation in Environmental and Water Resources Systems Analysis," *Journal of Water Resources Planning and Management*, *ASCE*, Vol. 131, No. 1, 2005, pp.1-2.

[14] M. J. Reddy and D. N. Kumar, "Multiobjective Differential Evolution with Application to Reservoir System Optimization," *Journal of Computing in Civil Engineering*, ASCE, Vol. 21, No. 2, 2007, pp.136-146.

[15] A. Vasan and K. S. Raju, "Application of Differential Evolution for Irrigation Planning: An Indian Case Study," *Water Resources Management*, Vol. 21, No. 8, 2007, pp. 1393-1407.

[16] D. E. Goldberg, "Genetic Algorithms in Search, Optimization and Machine Learning," Addison-Wesley, Reading, Massachusetts, 1989.

[17] R. Salomon, "Re-Evaluating Genetic Algorithm Performance under Coordinate Rotation of Benchmark Func-

tions: A Survey of Some Theoretical and Practical Aspects of Genetic Algorithms," *Biology Systems*, Vol. 39, No. 3, 1996, pp. 263-278.

[18] K. V. Price, "An Introduction to Differential Evolution, New Ideas in Optimization," McGraw-Hill, London, 1999, pp. 79-108.

[19] K. Price and R. Storn, "Home Page of Differential Evolution," 2005. http://www.icsi.Berkeley.edu/~storn/code.html

[20] D. P. Loucks, J. Stedinger and D. Haith, "Water Resources Systems Planning and Analysis," Prentice-Hall, Eaglewood Cliffs, New Jersey, 1981.

Appendix: Notation

The following symbols are used in this paper

RP(t):	Monthly releases for power generation during month t
TC:	Flow corresponding to maximum capacity of turbine
FP:	Flow corresponding to firm power.
RI(t):	Releases for irrigation during month t.
IDmax(t):	Maximum irrigation requirement of command area during month t.
IDmin (t):	Minimum irrigation requirement of command area during month t
S(t):	Storage volume in the reservoir during month t
SC:	Maximum storage volume of reservoir
Smin:	Dead storage volume of reservoir
SP(t):	Spills during month t
FCR(t):	Feeder Canal Releases during month t
β:	Constant.
NP:	Number of Population
CR:	Crossover Constant
F:	Weight

J. Water Resource and Protection, 2010, 2, 569-576
doi:10.4236/jwarp.2010.26065 Published Online June 2010 (http://www. SciRP.org/journal/jwarp)

Relationship between Reduction of Summer Precipitation in North China and Atmospheric Circulation Anomalies

Lisheng Hao[1,2,3], Jinzhong Min[1], Yihui Ding[4], Ji Wang[5]
[1]*Nanjing University of Information Science & Technology, Nanjing, China*
[2]*Hebei Climate Center, Shijiazhuang, China*
[3]*Hebei Province Meteorological and Ecological Environment Laboratory, Shijiazhuang, China*
[4]*National Climate Center, Beijing, China*
[5]*Climate Center of Beijing Area, Beijing, China*
E-mail: *HLS*54515@163.*com*
Received March 18, 2010; *revised April* 23, 2010; *accepted May* 6, 2010

Abstract

Based on Reanalysis datasets from National Centers for Environmental Prediction/National Center for Atmospheric Research (NCEP/NCAR) and summer rainfall datasets from China National Climate Center (NCC), by using trend analysis and composite analysis methods, the relationship between the reduction of summer precipitation in North China and northern hemispheric circulation changes was investigated. The results show that summer rainfall in North China had a significant decreasing tendency, especially true since 1965 in which an abrupt change occurred. The northern hemisphere atmospheric circulation at 500 hPa had a remarkable change after 1965, from outstanding meridional circulation to outstanding zonal circulation, leading to upper trough activity to decrease, resulting in the rainfall weather processes caused by upward motion behind trough significantly to reduce. At 500 hPa in Mongolian region, air temperature decreased, resulting in lower troposphere pressure to increase, leading to low pressure activity significantly to decrease and rainfall weather processes influencing North China to reduce. At the same time, the decreased air temperature in 500 hPa would caused the upper troposphere geopotential height to reduce, resulting in high–altitude jet southerly location, the East Asian summer monsoon to weaken, then it was difficult for water vapor transport to cross the Yangtze River valley and reach the North China region, with a southerly summer monsoon rainfall zone. The summer precipitation reduction in North China had a good correlation with the northern hemispheric circulation changes.

Keywords: North China, Summer Precipitation, Reduction, Atmospheric Circulation, Anomalies

1. Introduction

Since late 1960s, summer precipitation in North China has shown a significantly decreasing trend with the drought trend being more obvious [1] especially since the 1970s, leading to the deficit of water resources which has a great influence on local industrial, agricultural production and the lives of residents. Recent research conducted by Ding and Zhang [2] shows that abrupt changes happened in the 1970s, leading to summer precipitation decline in North China. Through analyzing 86 stations summer rainfall data of 1951–2007, Xu *et al*. [3] declared that summer precipitation in North China is more than normal, with the precipitation having decreased significantly since 1965. Although the drought trend in North China had eased in the early 1970s, the regional drought continued to intensify in the late 1970s, and extended to the late 1980s and early 1990s. With a brief interruption of increasing precipitation in North China in the early 1990s, the precipitation in North China once again has reduced significantly since 1996 and the drought worsens.

The reasons for summer precipitation reduction in North China and its future trend are widely concerned by scientists and policy–makers [4,5]. Through analyzing a climate abrupt change in the summer precipitation in North China around 1965, Huang *et al*. [6] pointed out that such a climate abrupt change is due to increasing sea surface temperature in eastern tropical Pacific in the mid-1960s. Zhang [7] argued that the summer precipitation reduction in North China is related to the subtropical high anomalies in Western Pacific. After investigating the relationship between snow cover over Tibetan Plateau and China's summer precipitation, Peng *et al.* [8] found a decadal climate jump in accumulated snow amount in the late 1970s, on the basis of which there is a good correlation between North China summer precipitation reduction and the amount of snow cover. The numerical simulation study conducted by Zhu *et al.* [9] further proves the point that snowy winter in Tibetan Plateau would lead to a weakening Tibetan Plateau heat source, which thereby continued into the summer season, causing the East Asian summer monsoon to weaken and as a result, the "South floods and North drought" situation occurs in China with North China even drier. Yu *et al*. [10,11] found that the upper troposphere air temperature in summer was declining since the late 1980s and this had led to the reduction of summer precipitation in North China and an increase in the Yangtze River basin. More studies showed that the reduction of summer rainfall in North China was closely related to weakening East Asian summer monsoon [12-17].

In spite of the fact that many scholars have studied the reasons of summer precipitation reduction in North China, the reasons for North China summer precipitation reduction and the impact factors still remain uncertain, and further investigation is still essential. Herein we will investigate the factors causing North China summer rainfall reduction by means of comparative analysis of the northern hemisphere atmospheric circulation changes since 1965 when an abrupt change occurred.

2. Data and Methods

The data sets for this study are from two sources. Summer precipitation data from 20 stations (**Figure 1**) located in North China during the period of 1951–2008 was provided by the Climate Diagnostics and Prediction Division of China National Climate Center. Atmospheric circulation data were taken from National Centers for Environmental Prediction/National Center for Atmospheric Research (NCEP/NCAR) reanalysis monthly data with a horizontal resolution of 2.5° × 2.5° in 1951–2008, *provided by the NOAA–CIRES Climate Diagnostics Center, Boulder, Colorado, USA, from their Web site at* http://www.cdc.noaa.gov/ [18].

Abnormal changes in summer precipitation in North China are investigated by means of trend analysis, Mann-Kendall test. Atmospheric circulation anomaly analyses were conducted in terms of composite averaged fields of height, temperature, pressure and wind.

3. Changes of Summer Precipitation in North China

First we analyze the changes in summer precipitation in North China during the period of 1951-2008 (**Figure 2**). **Figure 2** shows that summer rainfall has a great interannual variability, trend curve reflecting an obvious interdecadal change feature. Taking the minimum precipitation year for node, it can be divided into three major stages, namely 1951–1969, 1969–1983, 1983–2008, with a gradually declining trend in average rainfall in the three stages. Linear analysis conducted on precipitation change pass through 95% significant level, indicating that linear decline is significant during recent 58 years, with an average reduction of 14.9 mm every ten years.

Then, we analyze whether there are abrupt changes in summer precipitation in North China. Mann-Kendall test has special advantages in depicting abrupt changes [19], and in particular, it can determine the time period when the abrupt changes occur. Herein we will use this method to investigate whether there are abrupt changes occurring in summer precipitation in North China. **Figure 3** is the results of Mann-Kendall tests. We can find an abrupt change in 1965, and since then summer precipitation has

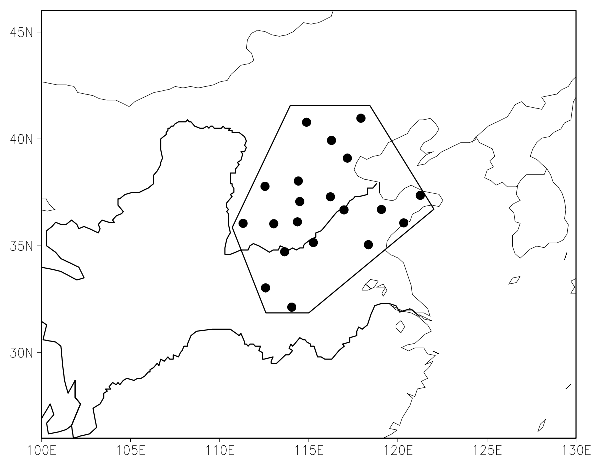

Figure 1. Spatial distribution of stations in North China.

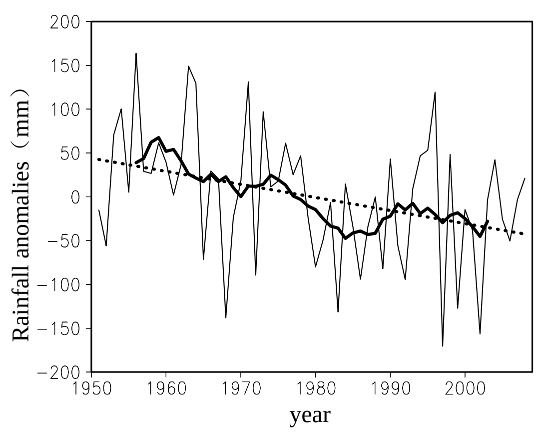

Figure 2. Variation of 1951–2008 summer precipitation in North China (thin solid for annual variation, thick solid for running-11yr mean, dashed for linear tendency).

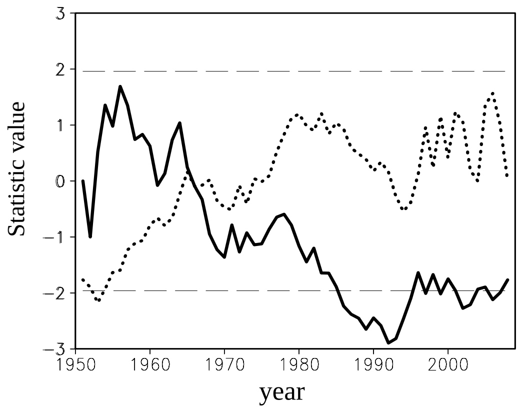

Figure 3. *Mann–Kendall* test of summer precipitation in North China (solid for C_1, dotted for C_2, dashed for 95% significant level).

significantly reduced.

4. Circulation Changes

For the precipitation is closely related with water vapor conditions (summer monsoon water vapor transport), upward motion conditions (surface low pressure, upper–level trough, upper–level jet) and the strength of the summer monsoon. Based on the abrupt change occurring in 1965 for summer precipitation reduction in North China, we take 1965 as the boundary. Then we conduct comparative analyses of 500 hPa height fields and air temperature fields, 850 hPa wind fields, sea-level pressure fields between 1951-1965 and 1966-2008 respectively , in order to understand the relationship between reduction of summer precipitation in North China and changes in atmospheric circulation.

4.1. 500 hPa Geopotential Height Field Changes

At 500 hPa height field the trough and ridge activities often resulted in upward motion after the upper-level trough, causing more precipitation weather processes. In order to understand the circulation changes after 1965, we make a comparative analysis of 500 hPa height field in the summer of 1951–1965 and 1966–2008 respectively (**Figure 4**).

The positive polar anomaly in **Figure 4(a)** indicates a shallower polar vortex during 1951–1965. The North Atlantic coast of Europe negative anomaly, the Urals positive anomaly, Lake Baikal to the Tibetan Plateau negative anomaly, so from Europe, the Urals to Central Asia formation a "–,+, –" Eurasian teleconnection pattern, showing that the European long-wave trough, the trough from Lake Baikal to the northern part of Tibetan Plateau are deeper, a stronger ridge of high pressure over the Urals. This distribution leads to a lot of activities of troughs and ridges, outstanding performance of meridional circulation. As a result, there will be more upward motions in North China with the Lake Baikal trough shifting frequently southeastward. **Figure 4(b)** opposite with **Figure 4(a)**, but anomaly value is obviously smaller. Polar negative anomaly shows a bit deeper polar vortex. Positive anomaly over the European coast of the North Atlantic, negative anomaly of the Urals, and positive anomaly from Lake Baikal to the Tibetan Plateau, form a "+,–,+" Eurasian teleconnection pattern from Europe, the Ural Mountains to the Central Asia, which shows that European long-wave trough, and the trough at Lake Baikal to the northern part of Tibetan Plateau are

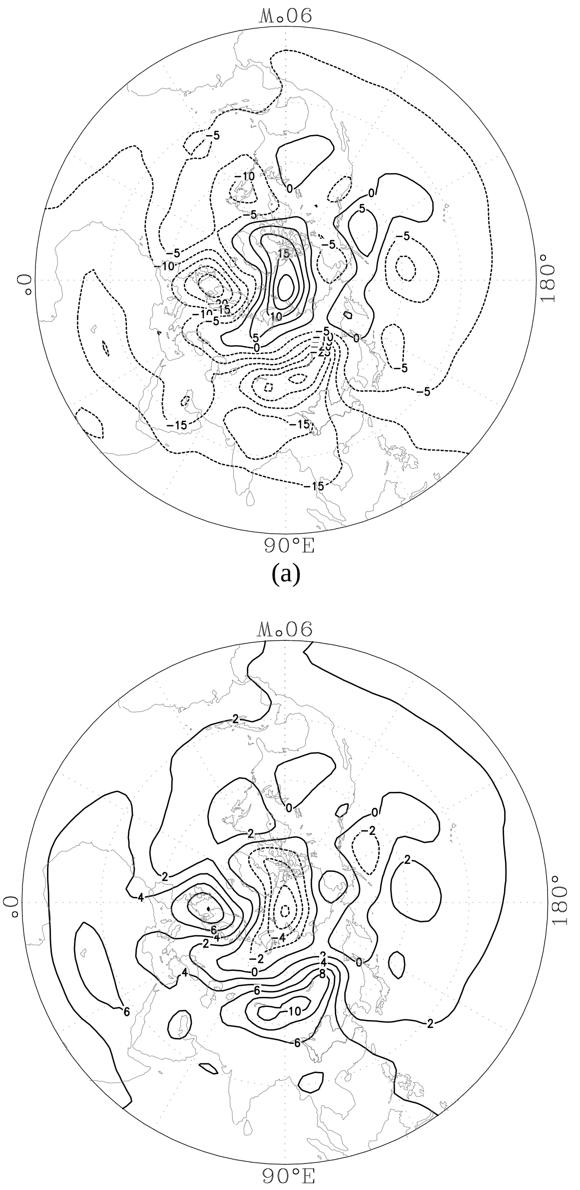

(a) (b)

Figure 4. Difference of summer 500 hPa height field, light-colored line for terrain boundary, unit: gpm. (a) 1951–1965 minus 1951–2008; (b) 1966–2008 minus 1951–2008.

shallower, weak ridge of high pressure over the Urals. This distribution makes activities of troughs and ridges very weak, outstanding performance to zonal circulation. As a result, upward motion in North China caused by the Lake Baikal trough has significantly reduced. It can be seen that Eurasian teleconnection pattern at 500 hPa height field is significant during the summer months, whose changes can affect zonal index circulation over the East Asia, alter the frequency and intensity of the trough and ridge activities over Mongolian and Yellow River Loop area, and then affect summer precipitation in North China.

4.2. 500 hPa Air Temperature Field Changes

As is know, the rising or declining air temperatures at upper–level can affect not only the lower troposphere pressure, but also the location of upper-level westerly jet. Next, we make a comparative analysis of air temperature changes at 500 hPa layer (**Figure 5**). As is shown in **Figure 5(a)**, we can see North Atlantic Ocean subtropical region with positive anomaly, the high latitude regions from North Atlantic Ocean to Europe, North America coast with negative anomaly, high latitude Europe with positive anomaly, Ural Mountains with small positive anomaly, northwestern Mongolia to Yellow River Loop with positive anomaly. This reveals that in the summer of 1951–1965 at the 500 hPa level, air temperature over Mongolian area is higher, causing the lower troposphere pressure to reduce, resulting in more low pressure weather processes activity, leading to an increase in precipitation. Meanwhile, the pressure of the upper troposphere over the region increases, leading to the pressure gradient to reduce in the south side of the region and to increase in the north side of the region, resulting in upper–level jet with northerly location, then the summer monsoon rainfall area northerly. **Figure 5(b)** is contrary to **Figure 5(a)**, but the anomalous value is smaller. From Mongolia to the northwest to Yellow River Loop with the maximum intensity, broadly area negative anomaly. This shows a significantly lower air temperature over the Mongolian region in 1966–2008. At 500 hPa layer, the dropping air temperature lead to a rise of the lower troposphere pressure in the region, resulting in both low–pressure activity and precipitation weather processes to decrease, thereby reducing precipitation. At the same time, the upper troposphere geopotential height decreases over the region, causing the south side pressure gradient of the region to increase and the north side pressure gradient to decrease, resulting in upper–level westerly jet with southerly location, then the summer monsoon rainfall area southerly.

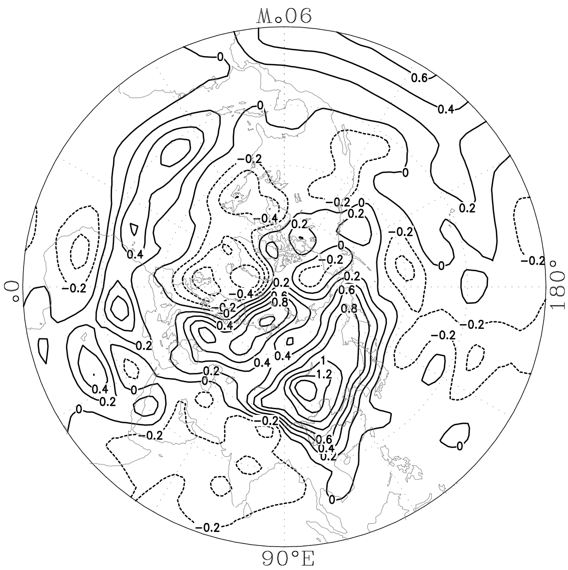

(a)

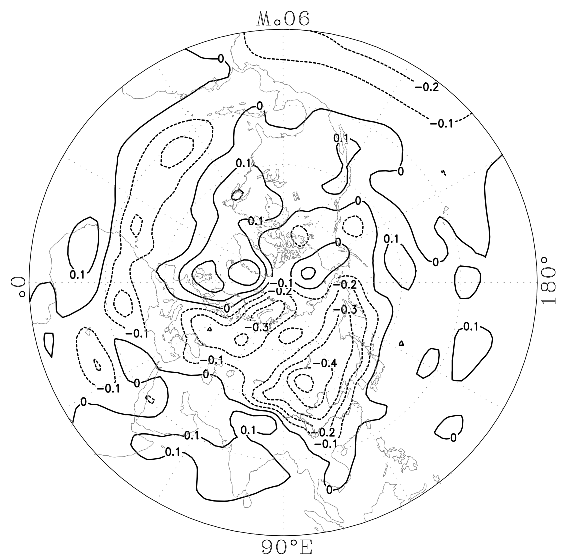

(b)

Figure 5. Same as Figure 4, except for 500 hPa air temperature (unit:℃).

4.3. Changes in 850 hPa Wind Field

Now that the 850 hPa wind field plays a key role in transferring water-vapor which may has a remarkable influence on precipitation. Herein we conduct a comparison analysis to the 850 hPa wind field (**Figure 6**).

Comparing **Figure 6(a)** with **Figure 6(b)**, we find that the Indian summer monsoon blows mainly from west to east. Moreover, comparing that in 1966–2008 with 1951–1965, we find Indian summer monsoon wind speed exhibits almost no change, being consistent with India summer precipitation reduction tendency not obviously [20]. The East Asian summer monsoon blows mainly from the South China Sea to North China, Northeast. **Figure 6(a)** shows that the East Asian summer monsoon wind speed is the same as the Indian summer monsoon in 1951–1965, extending to the Northeast China area from the South China Sea. Besides, in Mongolian area exists an obvious cyclone circulation, which produces the wind direction convergence nearby Yellow River loop. **Figure 6(b)** is obviously different from **Figure 6(a)**. First, the East Asian summer monsoon wind speed has remarkably decreased after crossing 30ºN, with a very small value compared with Indian summer monsoon wind speed, indicating that east Asian summer monsoon very rarely crossed the Yangtze River and arrived in North China in 1966–2008, which, in turn, produced a wind speed convergence in the Yangtze valley. Second, the cyclone circulation in the Mongolian region vanished, and the wind direction convergence nearby Yellow River loop was very weak. Therefore, rainy in the summer of 1951–1965 in North China were possibly due to the effective water vapor transportation by East Asia summer monsoon and the wind direction convergence nearby Yellow River loop, while rainy in the summer of 1966–2008 in Yangtze valley were possibly due to the wind speed convergence over there created by the East Asian summer monsoon. So there are different characteristics in the two places. In 1966–2008, less precipitation in North China was possible because of the shortage of effective water vapor transportation and the weakness of the wind direction convergence nearby the Yellow River loop.

In order to further analyze 850 hPa wind anomaly changes, we calculated the difference field of horizontal wind speed during 1951–1965, and 1966–2008 respectively, shown in **Figure 6(c)**, and **Figure 6(d)**. **Figure 6(c)** shows that the Indian summer monsoon basically has no exceptional changes, but the East Asian summer monsoon presents an obvious southerly wind anomaly, with cyclone circulation in the Mongolian area, weak anticyclone circulation in the northwest Pacific Ocean, and an obvious wind direction convergence circulation nearby Yellow River loop. **Figure 6(d)** is basically opposite to **Figure 6(c)**. That is to say, the Indian summer monsoon has no exceptional changes, but the East Asia monsoon presents a northerly wind anomaly, with anticyclone circulation in Mongolian area, weak cyclone circulation in the northwest Pacific, and wind direction divergence circulation nearby the Yellow River loop.

The facts added together, the 1966–2008 relative to the 1951–1965, though variation of the intensity and position of the northwest Pacific Ocean subtropical high is not remarkable, and changes of intensity of the Indian summer monsoon is not too obvious, but the East Asian summer monsoon weakens remarkably. In 1951–1965, East Asia summer monsoon is stronger, with prevailing southerly wind anomaly in the mid-latitude area of East Asia, which extending to the Northeast China area. The stronger southerly air stream of the East Asian summer monsoon and the stronger southeast air stream of the Subtropical High can effectively transport water vapor to the North China, which meets with northwest cold air flow near the Yellow River loop from Mongolia region, producing convergence upward motion, resulting in more summer precipitation in North China. In 1966–2008, the east Asian summer monsoon weakens remarkably after crossing 30ºN, which made it difficult for the water-vapor to be transported across 30°N by south wind and arrive in North China. Meanwhile, the Mongolian western cold air flow also becomes weaker. These two factors cause the summer precipitation to reduce in North China.

4.4. Changes in the Sea Level Pressure Field

The change in sea surface pressure field is the very important indicator in prediction of summer precipitation, thus, we conduct a comparison analysis with the pressure changes before and after 1965 (**Figure 7**). On the mean map of the sea level pressure field in the summer of 1951–2008 (figure omitted), the Arabian Peninsula to India, Mongolia was a low pressure center respectively, the North Pacific and North Atlantic is a stronger high pressure. The low pressure in Arabian Peninsula to India plays an important role in the formation of the Indian summer monsoon and the Mongolian low pressure plays an important role in the formation of the East Asian summer monsoon.

Comparison of **Figure 7(a)** and **Figure 7(b)** indicates that Mongolian region was an obviously negative anomaly during 1951–1965 which changed into a positive anomaly during 1966–2008, with the atmospheric pressure field in the Arabian Peninsula to India having no changes. These indicate that in the summer of 1951–1965, the Mongolian low pressure was stronger, having a good correlation with higher upper–level air temperature over the Mongolian area. The lower Mongolian low pressure caused more low-pressure activities in North China, resulting in more precipitation weather processes, which has a good corresponding relationship with more precipitation days in North China in the past. But in the summer of 1966–2008, the Mongolian low pressure significantly weakened, having a good correlation with dropping upper–level air temperature over the Mongolian area. The weaker Mongolian low pressure caused low–pressure activities in North China to reduce, resulting in reduction of precipitation weather processes, which has a good correlation with the reduction of the number of precipitation days in North China in recent years.

5. Summaries

Summer precipitation in North China shows a significant linear decreasing trend from 1951 to 2008, with an average reduction of 14.9 mm for every 10 yr. An abrupt change occurred in 1965, since then, the precipitation decreased more significantly. The atmospheric circulation

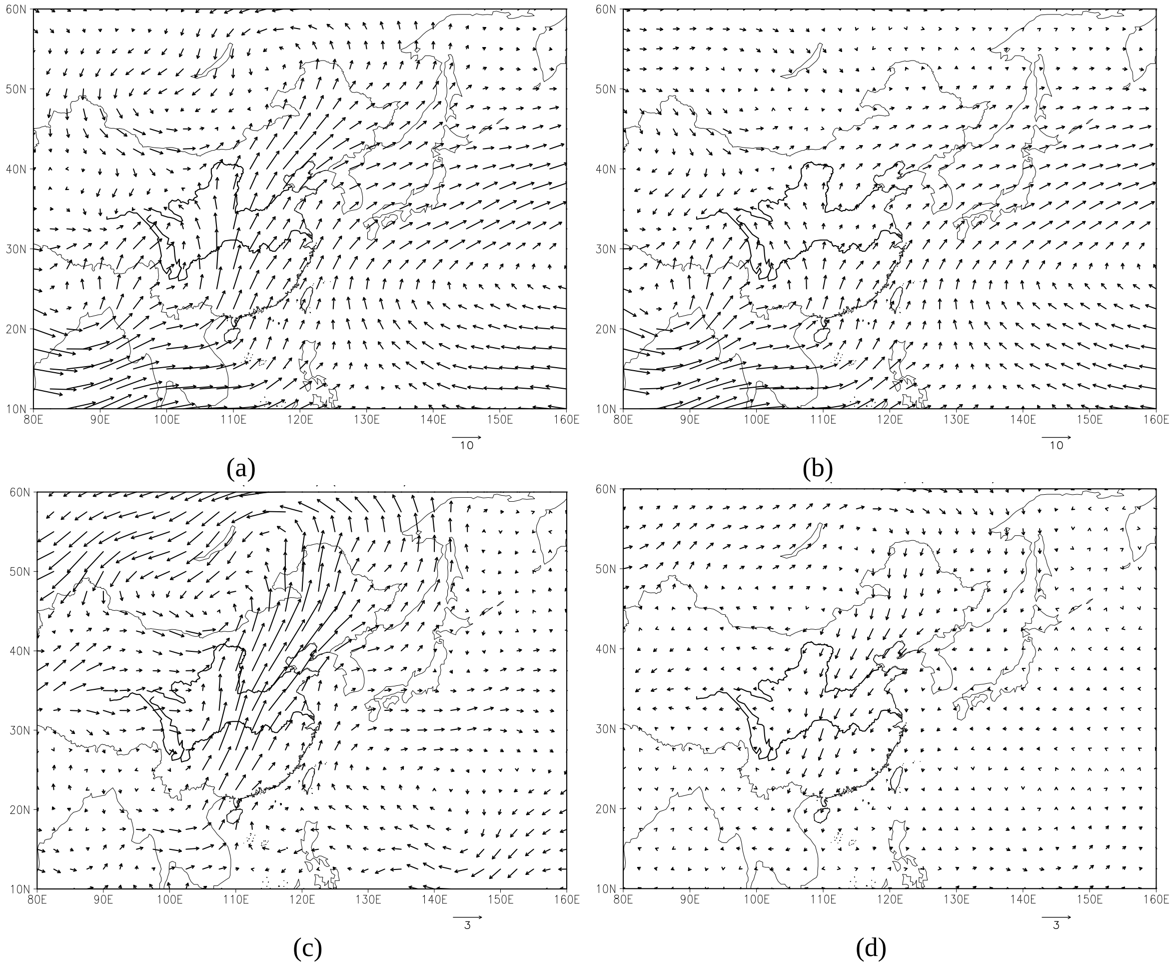

Figure 6. Difference of summer 850hPa wind field (unit: m.s^{-1}). (a) Composite distribution of 1951–1965; (b) Composite distribution of 1966–2008; (c) 1951–1965 minus 1951–2008; (d) 1966–2008 minus 1951–2008.

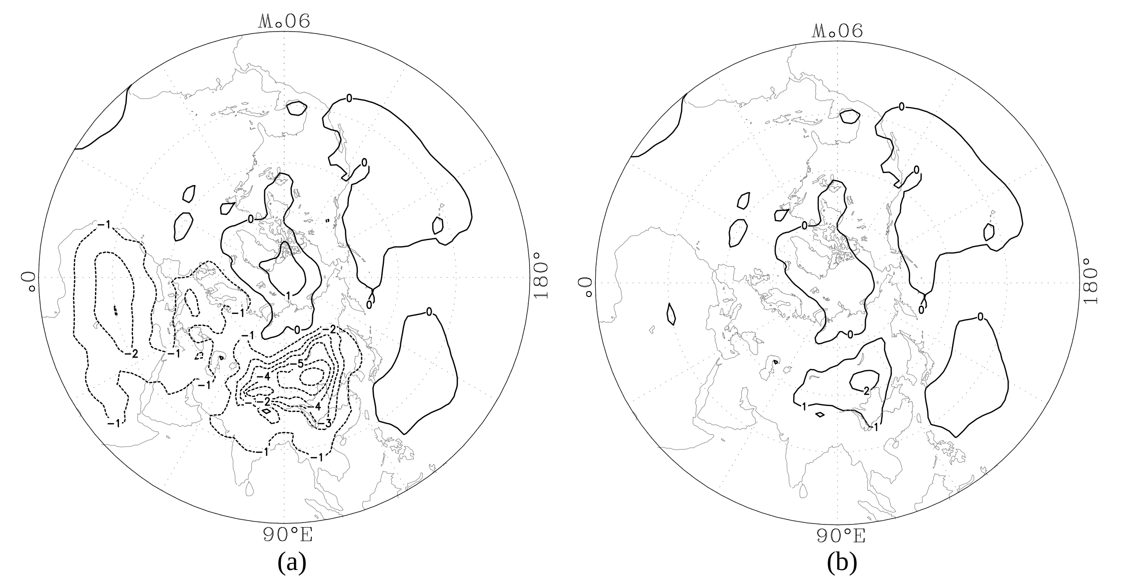

Figure 7. Same as Figure 4, except for sea lever pressure fields, unit: hPa.

has notable changes after 1965.

As in the summer 500 hPa height field, it is found that since 1965, the European trough, Lake Baikal trough have become shallower, Ural mountain high-pressure ridge weaker, the atmospheric circulation converted from prominent meridional circulation to prominent zonal circulation, leading to trough and ridge activities reduction, resulting in the precipitation weather processes caused by the upward motion behind trough significantly to decline. At 500 hPa, air temperature dropped in Mongolia area, which caused the lower troposphere pressure in the region to increase and low pressures activities in North China to reduce, thus resulting in reduction of the precipitation weather processes in North China. Meanwhile, lower air temperature caused the upper troposphere geopotential height to reduce in the region, resulting in the south side pressure gradient to increase and the north side pressure gradient to decrease in cooling zone, leading to the upper–level jet with southerly location, associated with southerly summer monsoon rainfall area.

In response to the dropping air temperature at 500 hPa in Mongolian areas, the Mongolian low pressure on the ground significantly weakened, leading to low pressure activities to reduce, resulting in reduction of the precipitation weather processes in North China. Meanwhile, in response to the lower air temperature, the upper–level jet with southerly location, and the East Asian summer monsoon weakened. So in the 850 hPa wind field, the East Asian summer monsoon wind speed decreased rapidly when reaching 30ºN, thus making it difficult for the monsoon wind to cross the Yangtze River and arrive in North China. However, a wind speed convergence was created in the Yangtze River basin, resulting in more precipitation in this region.

In conclusion, summer precipitation reduction in North China has a good correlation with the changes of the Northern Hemispheric circulation. The reasons for the circulation changes would be explored further in-depth study.

6. Acknowledgements

NCEP/NCAR Reanalysis data provided by the NOAA/OAR/ESRL PSD, Boulder, Colorado, USA, from their Web site at http://www.cdc.noaa.gov/. The authors gratefully acknowledge Science and Technology Department of Hebei Province for financial support. The first author is grateful to Prof. Ding Yihui and Min Jinzhong for their detailed supervision and Dr. Wang Ji for his help. The authors would like to thank reviewers for their constructive suggestions.

7. References

[1] D. Z. Ye and R. H. Huang, "Studies on Regularity and Cause of Droughts and Floods in the Yangtze River Valley and the Yellow River Valley," Chinese Shan-dong Science and Technology Press, Jinan, 1996, pp. 1-387.

[2] Y. H. Ding and L. Zhang, "Intercomparison of the Time for Climate Abrupt Change between the Tibetan Plateau and Other Regions in China [J]," *Chinese Journal of Atmospheric Sciences* (*in Chinese*), Vol. 32, No. 4, 2008, pp. 794-805.

[3] K. Xu, J. H. He and C. W. Zhu, "The Interdecadal Relationship Linkage between Summer Monsoon Rainfall in Eastern China and the Surface Air Temperature Warming over Lake Baikal in over the Past 50 Years [J]," *Acta Meteorological Sinica* (*in Chinese*), 2010, in Press.

[4] G. Y. Xu, X. Q. Yang and X. G. Sun, "Interdecadal and Interannual Variation Characteristics of Rainfall in North China and its Relation with the Northern Hemisphere Atmospheric Circulations [J]," *Chinese Journal of Geophysics* (*in Chinese*), Vol. 48, No. 3, 2005, pp. 511-518.

[5] X. Q. Yang, Q. Xie, Y. M. Zhu, *et al*., "Decadal-to-Interdecadal Variability of Precipitation in North China and Associated Atmospheric and Oceanic Anomaly Patterns [J]," *Chinese Journal of Geophysics* (*in Chinese*), Vol. 48, No. 4, 2005, pp. 789-797.

[6] R. H. Huang, Y. H. Xu and L. T. Zhou, "The Interdecadal Variation of Summer Precipitations in China and the Drought Trend in North China [J]," *Plateau Meteorology* (*in Chinese*), Vol. 18, No. 4, 1999, pp. 465-476.

[7] Q. Y. Zhang, "The Variation of the Precipitation and Water Resources in North China since 1880 [J]," *Plateau Meteorology* (*in Chinese*)**,** Vol. 18, No. 4, 1999, pp. 486-495.

[8] J. B. Peng, L. T. Chen and Q. Y. Zhang, "Multi-Scale Variations of Snow Cover over QXP and Tropical Pacific SST and Their Influences on Summer Rainfall in China [J]," *Plateau Meteorology* (*in Chinese*), Vol. 24, No. 3, 2005, pp. 366-377.

[9] Y. X. Zhu, Y. H. Ding and H. W. Liu, "Simulation of the Influence of Winter Snow Depth over the Tibetan Plateau on Summer Rainfall in China [J]," *Chinese Journal of Atmospheric Sciences* (*in Chinese*), Vol. 33, No. 5, 2009, pp. 903-915.

[10] R. C. Yu, B. Wang and T. J. Zhou, "Tropospheric Cooling and Summer Monsoon Weakening Trend over East Asia [J]," *Geophysical Research Letters*, Vol. 31, No. L22212, 2004.

[11] R. C. Yu, T. J. Zhou, J. Li, *et al.*, "Progress in the Studies of Three-Dimensional Structure of Interdeadal Climate Change over Eastern China," *Chinese Journal of Atmospheric Sciences* (*in Chinese*), Vol. 32, No. 4, 2008, pp. 893-905.

[12] R. H. Zhang, "The Role of Indian Summer Monsoon Watervapor Transportation on the Summer Rainfall Anomalies in the Northern Part of China during the El NINO Mature Phase [J]," *Plateau Meteorology* (*in Chinese*), Vol. 18, No. 4, 1999, pp. 567-574.

[13] F. Li and J. H. He, "Interdecadal Variations of Interaction between North Pacific SSTA and East Asian Summer

Monsoon [J],” *Journal of Tropical Meteorology*, Vol. 7, No. 1, 2001, pp. 41-52.

[14] X. G. Dai, P. Wang and J. F. Chou, “Multiscale Characteristics of the Rainy Season Rainfall and Interdecadal Decaying of Summer Monsoon in North China,” *Chinese Science Bulletin*, Vol. 48, No. 12, 2003, pp. 2730-2734.

[15] Y. H. Ding, Z. Y. Wang and Y. Sun, “Interdecadal Variation of the Summer Precipitation in East China and its Association with Decreasing Asian Summer Monsoon. Part I: Observed Evidences [J],” *International Journal of Climate*, Vol. 28, No. 9, 2007, pp. 1139-1161.

[16] Y. H. Dind and Y. Y. Liu, “A Study of the Teleconnection in the Asian-Pacific Monsoon Region,” *Acta Meteorologica Sinica* (*in Chinese*), Vol. 66, No. 5, 2008, pp. 670-682.

[17] W. G. Sun, B. Y. Cheng and Q. Guo, “Influence of East Asian Monsoon Circulation on Precipitation-Evaporation Difference in North China [J],” *Chinese Journal of Agrometeorology* (*in Chinese*), Vol. 30, No. 3, 2009, pp. 327-334.

[18] E. Kalnay, M. Kanamitsu, R. Kistler, *et al*., “The NCEP/NCAR 40-Year Reanalysis Project,” *Bulletin of American Meteorological Society*, Vol. 77, No. 3, 1996, pp. 437-472.

[19] C. B. Fu and Q. Wang, “The Definition and Detection of the Abrupt Climatic Change [J],” *Chinese Journal of Atmospheric Sciences* (*in Chinese*), Vol. 16, No. 4, 1992, pp. 482-493.

[20] L. S. Hao, J. Z. Min and X. X. Yao, “Comparison of Summer Monsoon Rainfall Changes between North China and Indian,” *Advances in Climate Change Research* (*in Chinese*), Vol. 3, No. 5, 2007, pp. 271-275.

J. Water Resource and Protection, 2010, 2, 577-584
doi:10.4236/jwarp.2010.26066 Published Online June 2010 (http://www. SciRP.org/journal/jwarp)

Statistical Analysis of Groundwater Table Depths in Upper Swarnamukhi River Basin

Ismail Jasmin[1], Talagam Murali[2], Perugu Mallikarjuna[1]
[1]*Department of Civil Engineering, Sri Venkateswara University College of Engineering, Tirupati, India*
[2]*Department of Civil Engineering, N.B.K.R. Institute of Science and Technology, Vidyanagar, India*
E-mail: *jasmin_i@rediffmail.com*
Received January 17, 2010; *revised March* 3, 2010; *accepted April* 20, 2010

Abstract

Development and effective utilization of groundwater resources is essential in semi-arid regions for activities such as water supply and irrigation. The present study aims to analyze statistically the groundwater data at the Chinnagottigallu, Yerravaripalem, Chandragiri, Sriramapuram, Tirupati, Renigunta, Karvetinagaram and Yerpedu piezometric stations of upper Swarnamukhi river basin in the drought prone Rayalaseema region of Andhra Pradesh, India and to develop models through multiple linear correlation and regression analysis. The monthly rainfall and groundwater data at the raingauge and piezometric stations of the basin for the period 2001-2006 were collected from the Groundwater and Irrigation Departments of the region. It is observed from the analysis that the groundwater table depth in any period is influenced by the rainfall in the period and, the rainfall and groundwater table depth in the previous period. The study also reveals that the effect of antecedent groundwater table depth is more pronounced than that of rainfall and antecedent rainfall. The models proposed may be adopted for the estimation of groundwater table depths to effectively plan and efficiently manage groundwater resources of the basin.

Keywords: Multiple Linear Correlation, Partial Correlation Coefficient, Root Mean Square Error, Efficiency Coefficient

1. Introduction

Groundwater constitutes the largest available source of water for water supply and irrigation in semi-arid regions and therefore the development and utilization of groundwater resources is of great interest to meet these requirements. As rainfall is the primary source of recharge for many aquifers, variations of rainfall and groundwater table depth are closely related. However, the correlation may sometimes be imperfect because differences in rainfall intensity and distribution produce different amounts of recharge for the same amount of rainfall. Therefore proper understanding of the groundwater status is important in order to meet the increasing demand due to growing population and urbanization, and to formulate future development and management strategies.

Satistical analysis of water table data carried out at Powarkheda in Hoshangabad District of Madhya Pradesh, India [1] suggested the optimum utilization of open wells, putting the area to high water requiring crops and minimizing canal seepage and other losses to prevent water logging. A water balance and groundwater flow model [2] was proposed to develop groundwater draft/recharge maps for planning groundwater development of Ponnaiyar river basin of Karnataka state, India. The studies [3,4] carried out on the rejuvenation of Swarnamukhi basin suggested the construction of rainwater harvesting structures for improving the groundwater potential of the basin. The groundwater development studies in the Koyna river basin in Maharashtra, India [5] suggested artificial recharge measures for water scarce areas. The pattern of water level fluctuations in different physiographic regions of Nileshwar river basin in Kasargod District of Kerala state, India was studied [6] and concluded that the Nileshwar basin is 'SAFE' for future groundwater development. The study conducted on the groundwater status in Dhund river basin in Jaipur District of Rajasthan, India [7] recommended proper groundwater management strategies to stabilize the declining trend of water levels.

2. Study Area and Data

The Swarnamukhi, an ephemeral river, spreading over a catchment area of 3092 km^2 is bounded by latitudes 13^{0}25'30" N and 14^{0}08'30" N and longitudes 79^{0}07'39"E and 80^{0}11'E in Chittoor and Nellore Districts of Andhra

Pradesh, India as shown in **Figure 1**. It originates at the Pakala Mandal of Chittoor District, flows in a northeasterly direction and finally joins the Bay of Bengal. The upper Swarnamukhi basin covering an area of 2217 km^2 lying in Chittoor District has been selected for the present groundwater study. The area falls under semi-arid climate. The maximum, minimum and mean temperatures are 44^0.18C, 12^0.48C and 27^0.49C respectively. The maximum, minimum and mean wind speeds at 3 m height are 18.15 kmph, 5.14 kmph and 9.72 kmph respectively. The average annual rainfall is about 920 mm. The drainage pattern is dendritic to subdendritic.

The area under irrigation in Chittoor District, drought prone area of Rayalaseema region of Andhra Pradesh, is about 2.02 lakh hectares which mainly depends on groundwater as there are no major irrigation projects. The groundwater in the basin over a period of time has been overexploited leading to water scarcity and deterioration of its quality. Degradation of catchment area, indiscriminate groundwater use, erratic rainfall and sand quarrying are some of the causes for the present status. The present study aims to analyze the groundwater table depths statistically and develop models through multiple linear correlation and regression analysis to estimate the groundwater table depths for better planning and management of groundwater resources.

The monthly groundwater table depth and rainfall data at Chinnagottigallu (Cgg), Yerravaripalem (Yvp), Chandragiri (Cgr), Sriramapuram (Srp), Tirupati (Tpt), Renigunta (Rng), Karvetinagaram (Kvt) and Yerpedu (Ypd) piezometric and rainguage stations located in the basin as shown in **Figure 1** for the period 2001-2006 were collected from the Groundwater and Irrigation Departments respectively, and used for the model development. **Tables 1** and **2** present the rainfall and groundwater table depths at the raingauge and piezometric stations respectively. The groundwater table depth data showed that there is no systematic trend with rainfall as the processes are complex exhibiting high degree of both spatial and temporal variability. The model coefficients, however, may be updated to obtain the refined models for better forecasting accuracy.

3. Model Development

An association of three or more variables is best investigated by multiple regression and correlation analysis. Since linear equations are easier to treat than nonlinear equations, variables of nonlinear relations in hydrology are often transformed to linear relations for the purpose of development of a multiple regression model. If there are m variables to correlate, including one dependent and (m-1) independent variables, the multiple linear regression model is generally expressed as (1).

$$X_1 = b_1 + b_2 X_2 + b_3 X_3 + \ldots + b_i X_i + \ldots + b_m X_m \quad (1)$$

in which b_1 is the intercept and b_i (i = 2,3, …, m) are the multiple regression coefficients of the dependent variable X_1 on the independent variable X_i (I = 2,3, …, m) with all other variables kept constant.

Applying the least squares method of the sum of residuals, the m partial differential equations in b_1, b_2, …, and b_m yield m linear equations. The solution of these equations facilitates determination of m parameters.

3.1. Linear Regression Model

In the present study, the monthly groundwater table depth model at a piezometric station is developed using the rainfall, antecedent rainfall and antecedent ground water table depth data of the piezometric station under consideration and also the piezometric stations upstream. The steps in the modeling include 1) identification of influencing parameters 2) development of a model and 3) performance evaluation of the model developed.

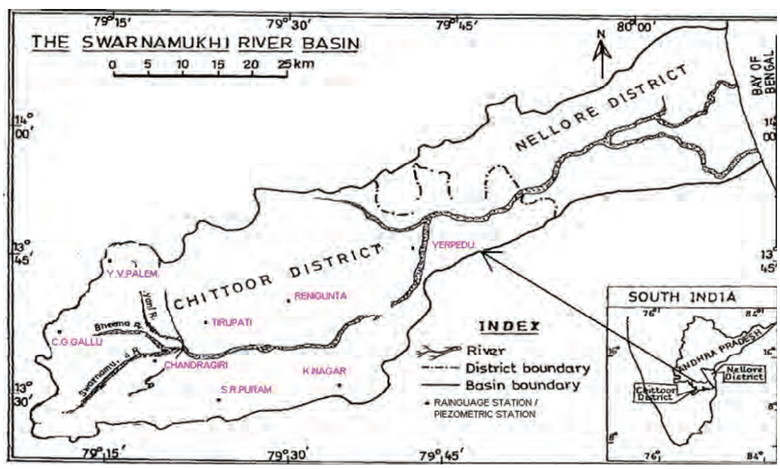

Figure 1. Location map of Swarnamukhi river basin.

Table 1. Monthly rainfall in mm at piezometric stations.

Raingauge Station	Month / Year	Jan	Feb	Mar	Apr	May	Jun	Jul	Aug	Sep	Oct	Nov	Dec
Yvp	2001	1.8	0.0	0.0	52.6	19.8	12.0	84.4	66.8	166.8	455.2	21.6	42.4
	2002	0.0	0.0	0.0	0.8	7.4	162.4	8.0	54.0	77.4	183.6	9.8	5.2
	2003	0.0	0.0	2.2	10.0	0.0	48.0	258.2	230.4	111.2	171.6	0.0	0.0
	2004	0.0	30.0	28.0	30.2	169.4	48.8	139.1	19.8	169.6	36.4	40.0	0.0
	2005	0.0	0.0	0.0	63.0	46.2	93.8	93.2	130.4	73.0	232.6	192.2	244.8
	2006	0.0	0.0	80.4	4.4	10.8	93.2	2.2	142.0	77.8	82.6	60.4	10.2
Cgg	2001	0.0	0.0	0.0	88.9	43.8	7.2	70.4	51.6	153.7	366.5	29.3	53.1
	2002	1.8	0.0	0.0	0.0	29.1	55.0	0.0	64.9	49.3	169.2	16.4	10.4
	2003	0.0	0.0	0.0	0.0	0.0	61.2	202.4	178.8	139.8	171.4	0.0	0.0
	2004	0.0	0.0	20.0	14.6	177.4	39.4	108.2	21.2	118.4	80.7	50.8	0.0
	2005	0.0	15.2	0.0	67.2	56.2	109.6	117.0	207.8	111.2	209.8	208.6	133.4
	2006	0.0	0.0	58.8	65.9	94.6	53.0	18.0	127.2	82.6	95.2	82.8	11.2
Kvt	2001	3.2	0.0	0.0	131.2	40.6	9.2	76.6	60.8	207.4	180.8	58.2	43.2
	2002	0.0	0.0	0.0	0.0	25.6	160.1	8.6	50.2	89.8	156.3	54.5	14.6
	2003	0.0	0.0	26.6	0.0	0.0	108.1	381.1	149.2	107.0	116.2	19.6	5.4
	2004	0.0	0.0	0.0	61.4	207.5	45.3	63.1	5.2	300.8	93.0	88.6	0.0
	2005	0.0	0.0	0.0	64.6	54.3	83.4	129.8	114.2	144.9	458.7	240.3	228.1
	2006	0.0	0.0	0.0	0.0	71.1	117.7	9.8	152.2	220.7	177.6	21.0	61.4
Srp	2001	0.0	0.0	5.2	138.0	19.1	52.6	87.4	173.6	156.0	343.3	53.0	52.4
	2002	0.0	0.0	0.0	0.0	8.6	140.2	65.0	54.6	71.0	129.1	59.0	13.6
	2003	0.0	0.0	50.0	0.0	0.0	50.0	325.9	125.8	126.6	135.2	31.0	0.0
	2004	0.8	0.0	0.0	20.0	258.2	15.0	95.4	0.0	173.0	156.7	85.8	0.0
	2005	0.0	0.0	0.0	50.4	4.2	55.5	114.5	116.3	162.5	314.1	158.0	167.4
	2006	0.0	0.0	0.0	2.0	68.2	48.0	28.0	58.2	175.2	108.2	41.5	25.8
Cgr	2001	0.0	0.0	0.0	97.8	45.4	24.8	116.6	46.0	144.7	304.8	59.8	66.1
	2002	37.4	0.0	0.0	0.0	29.4	89.7	13.6	68.5	111.1	222.4	53.6	19.4
	2003	0.0	0.0	16.3	15.3	9.6	140.1	190.9	149.0	125.7	157.8	17.6	9.7
	2004	0.0	0.0	0.0	53.3	146.6	87.8	107.0	34.6	239.7	68.4	74.2	0.0
	2005	0.0	0.0	0.0	69.1	36.5	18.3	152.3	132.5	180.4	282.9	324.4	241.9
	2006	0.0	0.0	16.4	1.7	114.2	31.0	7.2	132.5	117.0	243.6	110.6	21.8
Tpt	2001	0.0	0.0	0.0	69.6	17.2	45.3	137.4	22.8	168.3	297.0	84.8	130.7
	2002	25.8	0.0	0.0	1.0	77.2	196.7	8.2	106.6	188.5	267.7	89.0	27.8
	2003	0.0	0.0	22.2	11.8	23.0	222.0	289.0	98.7	145.4	146.7	19.7	13.4
	2004	0.0	3.2	0.0	81.4	207.9	60.5	100.2	35.4	279.5	163.4	132.4	0.0
	2005	0.0	9.8	0.0	27.0	22.7	66.4	153.5	73.4	134.2	332.8	517.9	164.0
	2006	0.0	0.0	38.6	19.4	142.2	126.2	4.8	75.6	108.0	165.2	150.2	14.2
Rng	2001	3.1	0.0	0.0	75.7	46.0	37.5	88.7	62.4	185.6	318.8	147.1	149.7
	2002	17.3	0.0	0.0	0.0	83.9	121.2	33.9	91.8	267.5	313.6	196.9	74.7
	2003	0.0	0.0	35.3	0.0	0.0	94.5	373.1	131.2	177.1	174.3	35.7	14.4
	2004	0.0	0.0	0.0	39.6	195.2	66.2	103.6	65.6	425.2	198.6	232.0	0.0
	2005	0.0	8.2	0.0	38.0	21.6	50.0	171.4	157.8	116.0	454.3	592.6	202.0
	2006	0.0	0.0	54.3	0.0	13.9	27.8	4.2	17.8	20.8	162.5	204.2	26.2
Ypd	2001	22.3	0.0	0.0	61.3	83.2	20.0	69.9	42.3	110.4	400.1	187.2	136.3
	2002	62.2	0.0	0.0	4.2	13.8	125.7	54.3	64.9	138.2	292.6	216.4	80.5
	2003	0.0	0.0	13.4	0.0	3.6	89.6	288.5	163.3	154.8	155.8	26.0	29.6
	2004	0.0	2.6	0.0	75.8	198.3	45.0	70.4	25.4	219.4	213.3	162.8	0.0
	2005	0.0	35.8	10.6	23.8	34.8	77.2	142.0	64.8	115.0	474.6	550.1	341.8
	2006	5.6	0.0	0.0	0.0	38.0	41.4	75.8	304.1	262.2	74.2	5.2	0.0

3.1.1. Identification of Influencing Parameters

The identification of influencing parameters is based on multiple correlation analysis. The values of multiple and partial correlation coefficients indicate the degree of influence of independent variables on the dependent one.

3.1.2. Development of Model

The linear regression model in terms of influencing parameters is expressed as a simple linear model as (2).

$$G_t = b_1 + b_2R_t + b_3R_{t-1} + b_4G_{t-1} + b_5G_{t-1(us1)} + b_6G_{t-1(us2)} + \ldots \quad (2)$$

where G_t is the groundwater depth in m in the t^{th} month, b_1, b_2, … are empirical constants, R_t is the rainfall in mm in the t^{th} month, R_{t-1} is the antecedent rainfall in mm and G_{t-1} is the antecedent groundwater depth in m at the stations. $G_{t-1(us1)}$, $G_{t-1(us2)}$, … are the groundwater table depths at the piezometric stations on the upstream of the

Table 2. Monthly groundwater table depth in m at piezometric stations.

Piezometric Station	Month / Year	Jan	Feb	Mar	Apr	May	Jun	Jul	Aug	Sep	Oct	Nov	Dec
Yvp	2001	30.0	-	-	-	29.50	30.00	30.00	30.0	30.0	15.80	11.05	11.70
	2002	11.0	13.27	15.15	16.75	19.25	20.19	21.02	18.01	20.15	20.62	18.26	18.70
	2003	20.13	20.57	21.09	21.95	23.61	21.95	23.32	20.09	16.93	13.93	10.77	7.55
	2004	11.55	12.58	14.20	15.40	15.45	16.06	16.71	17.76	17.50	16.80	15.27	15.55
	2005	16.32	20.58	21.45	21.85	21.89	22.41	22.52	22.36	20.48	18.85	13.31	6.12
	2006	6.0	17.40	17.77	10.55	10.72	11.79	13.53	14.52	14.65	12.79	11.26	10.96
Cgg	2001	40.0	-	-	-	13.05	13.93	14.25	14.56	15.0	14.01	11.94	12.17
	2002	11.74	12.28	13.06	13.77	14.20	14.68	14.95	15.37	15.75	15.53	14.52	14.45
	2003	14.70	15.04	15.79	16.12	16.47	16.48	16.78	16.46	16.0	15.54	14.86	15.18
	2004	15.63	16.08	16.61	17.31	17.90	17.33	17.91	18.64	19.06	18.01	17.55	18.15
	2005	18.96	18.96	18.93	19.77	21.01	22.23	21.62	21.33	18.64	17.96	15.12	5.88
	2006	4.58	4.77	5.07	5.22	5.70	6.07	6.57	9.98	9.93	9.95	9.62	9.16
Kvt	2001	9.0	-	-	-	-	9.95	9.95	10.01	10.44	8.9	7.14	7.07
	2002	6.57	6.8	7.39	8.10	8.63	9.26	9.44	9.74	10.13	10.5	9.58	9.67
	2003	10.76	11.25	12.34	14.78	16.41	17.16	15.42	10.17	9.79	10.44	10.21	11.04
	2004	11.77	12.45	14.15	15.61	15.72	14.92	16.0	16.58	16.67	12.7	11.74	12.04
	2005	13.07	13.27	14.30	15.85	16.73	17.17	18.75	20.18	7.99	12.98	6.86	1.20
	2006	1.99	2.89	3.33	4.09	4.95	4.09	4.91	5.54	4.56	9.99	4.02	4.25
Srp	2001	10.1	-	-	-	21.66	23.32	24.86	26.65	27.57	27.32	21.99	19.21
	2002	16.62	16.35	16.87	17.84	18.92	21.01	21.88	21.64	22.95	23.94	23.78	23.83
	2003	24.69	25.25	26.06	27.81	29.28	30.45	31.18	30.49	30.07	29.99	29.34	29.17
	2004	29.53	29.93	30.85	31.78	32.15	31.96	32.49	33.13	33.69	34.21	33.79	32.88
	2005	33.0	33.56	34.50	36.12	36.19	36.19	36.19	36.19	36.19	36.19	36.19	30.11
	2006	22.46	19.1	18.35	18.69	19.77	20.43	21.70	23.07	24.08	24.66	24.89	24.74
Cgr	2001	14.3	-	-	-	-	17.76	17.76	17.28	18.20	14.08	13.35	13.2
	2002	12.45	12.80	13.74	14.37	14.89	15.31	15.59	15.86	16.39	16.18	14.24	14.42
	2003	16.0	16.71	17.34	18.02	18.32	18.6	17.21	16.46	16.25	15.68	14.96	16.22
	2004	16.23	16.45	17.16	18.13	17.08	16.74	16.77	16.03	14.67	14.94	14.48	14.55
	2005	15.10	15.80	16.57	17.05	17.32	17.69	17..73	16.46	14.58	13.92	9.99	6.83
	2006	7.86	8.0	8.06	8.43	9.03	9.97	9.48	8.75	8.13	8.20	5.86	5.70
Tpt	2001	6.5	-	-	-	17.81	18.38	19.34	19.8	20.13	20.13	19.65	19.66
	2002	19.12	19.44	19.78	19.94	20.18	20.53	20.56	20.77	21.08	21.09	20.77	20.72
	2003	20.86	21.21	21.33	21.64	21.92	22.32	22.52	22.59	22.48	22.33	22.21	22.36
	2004	22.42	22.54	22.66	22.73	22.67	22.95	23.13	23.35	23.66	23.92	24.02	24.10
	2005	24.31	24.43	24.31	25.30	25.59	25.93	26.25	26.55	26.79	26.86	24.10	22.74
	2006	21.9	21.2	20.66	20.16	16.84	19.65	19.53	19.57	19.58	19.45	19.22	19.05
Rng	2001	2.5	-	-	-	-	8.4	8.4	8.67	11.92	4.71	2.94	3.21
	2002	2.15	3.49	3.76	4.50	5.31	5.81	6.44	6.85	7.25	6.76	4.99	2.94
	2003	3.92	5.26	6.11	7.02	9.80	8.63	4.18	3.55	4.34	3.95	4.95	5.51
	2004	4.9	6.55	7.43	7.35	6.26	5.62	6.19	7.29	6.58	6.76	3.67	4.45
	2005	6.93	5.59	6.77	7.56	9.54	9.30	9.79	9.71	11.65	4.03	0.56	0.64
	2006	1.69	3.01	3.66	5.27	7.11	7.38	7.88	8.45	8.88	7.15	2.82	2.88
Ypd	2001	3.4	-	-	-	13.36	18.80	19.09	18.76	18.65	13.96	9.59	8.61
	2002	7.15	8.41	8.87	9.98	11.19	14.25	15.20	16.11	16.41	16.66	11.86	11.89
	2003	12.89	14.41	16.59	16.78	17.78	17.78	17.78	13.98	13.65	13.84	13.18	15.75
	2004	16.05	16.95	16.95	16.95	16.95	16.95	16.95	15.98	15.98	15.95	11.85	10.67
	2005	12.11	13.35	15.25	15.95	16.24	15.95	15.95	15.95	15.85	15.85	6.73	3.42
	2006	4.82	6.87	7.05	8.1	9.17	10.62	14.26	15.76	15.76	15.76	15.62	14.25

piezometric station under consideration.

3.1.3 Performance Evaluation Criteria

The performance of the model is verified through selected performance evaluation criteria as explained below. Out of the several numerical model performance indicators, the coefficient of determination (R^2), root mean square error (RMSE) and efficiency coefficient (EC) are chosen for the present study. The scatter plot of the observed versus estimated groundwater table depths is selected as a graphical indicator.

Coefficient of Determination (R^2): It is the square of the correlation coefficient (R) and the correlation coefficient is expressed as (3).

$$R = \frac{\sum_{i=1}^{n} (y_i - \bar{y})(\hat{y}_i - \bar{\hat{y}})}{\left[\sum_{i=1}^{n} (y_i - \bar{y})^2 \sum_{i=1}^{n} (\hat{y}_i - \bar{\hat{y}})^2\right]^{1/2}} \times 100 \quad (3)$$

where y_i and $\hat{y}_i$ are the observed and estimated values respectively and, $\bar{y}$ and $\bar{\hat{y}}_i$ are the means of observed and estimated values.

Root Mean Square Error (RMSE): It yields the residual error in terms of the mean square error and is expressed as (4).

$$\text{RMSE} = \sqrt{\frac{\sum_{i=1}^{n} (y_i - \hat{y}_i)^2}{n}} \quad (4)$$

where n = number of observations.

Efficiency Coefficient (EC): It is used to assess the performance of the models and is given by (5).

$$\text{EC} = 1 - \left(\frac{F}{Fo}\right) \times 100 \quad (5)$$

where

$$F_0 = \sum_{i=1}^{n} (y_i - \bar{y})^2 \quad \text{and } F = \sum_{i=1}^{n} (y_i - \hat{y}_i)^2$$

A value of EC of 90% generally indicates a very satisfactory model performance while a value in the range 80-90%, a fairly good model. Values in the range 60-80% would indicate an unsatisfactory model fit.

4. Results and Discussion

The groundwater table depth in any month at a piezometric station of upper Swarnamukhi basin is correlated with the rainfall of the month, antecedent rainfall and antecedent groundwater table depth at the station and also at the stations upstream. The measures of correlation such as multiple correlation coefficients and partial correlation coefficients have been computed and presented in **Table 3**. The high multiple correlation coefficients (**Tables 3** and **4**) indicate that the monthly groundwater table depth at any station can better be correlated with rainfall, antecedent rainfall and groundwater table depths of the station and the upstream stations. The partial correlation coefficients, which measure the extent of association of independent variable with the dependent one indicate that the effect of antecedent groundwater table depth at the station is more pronounced than that of rainfall and antecedent rainfall. This may be due to the fact that the groundwater in the basin may be overexploited at the rates of withdrawal more than critical, because of scanty rainfall and degradation of catchment during the period. It may also be observed from **Table 4** that there is only marginal improvement in the correlation when the effect of groundwater table depths at the piezometric stations upstream of the station under investigation is also included in the analysis due to local dyke formations.

The linear regression models in terms of influencing parameters are presented in **Table 5**. The scatter plots of observed versus estimated groundwater table depths are shown in **Figure 2**.

The results of the study have been evaluated through R^2, RMSE and EC as presented in **Table 6**. The higher values of R^2 and EC and, low values of RMSE indicate that the regression models developed are fairly good and yield satisfactory results. Therefore the regression models developed may be adopted for the reasonable estimation of groundwater table depths at the piezometric station based on rainfall, antecedent rainfall and antecedent groundwater table depth for effective planning and management of groundwater resources of the basin.

Table 3. Measures of multiple linear correlation.

Piezometric Station	Multiple Correlation Coefficient				Partial Correlation Coefficient		
	Independent Variable Omitted				Independent Variable Omitted		
	-	R_t	R_{t-1}	G_{t-1}	R_t	R_{t-1}	G_{t-1}
Yerravaripalem (Yvp)	0.902	0.884	0.872	0.291	0.199	0.256	0.947
Chinnagottigallu (Cgg)	0.964	0.964	0.947	0.194	0.000	0.187	0.980
Karvetinagaram (Kvt)	0.914	0.914	0.877	0.272	0.000	0.282	0.955
Sriramapuram (Srp)	0.967	0.965	0.959	0.324	0.064	0.128	0.942
Chandragiri (Cgg)	0.980	0.972	0.974	0.337	0.128	0.110	0.939
Tirupati (Tpt)	0.980	0.980	0.976	0.155	0.000	0.090	0.987
Renigunta (Rng)	0.820	0.759	0.817	0.477	0.379	0.086	0.813
Yerpedu (Ypd)	0.922	0.918	0.888	0.464	0.093	0.269	0.864

Table 4. Measures of multiple linear correlation (Effect of groundwater table depths of upstream piezometric stations also considered).

Piezometric Station	Multiple Correlation Coefficient												
	Independent Variable Omitted												
Yerravaripalem	-	R_t	R_{t-1}	G_{t-1}									
	0.902	0.884	0.872	0.291									
Chinnagottigallu					$R_{t(Yvp)}$	$R_{t-1(Yvp)}$	$G_{t-1(Yvp)}$						
	0.969	0.966	0.966	0.190	0.965	0.969	0.967						
Karvetinagaram					$R_{t(Cgg)}$	$R_{t-1(Cgg)}$	$G_{t-1(Cgg)}$						
	0.923	0.923	0.919	0.270	0.923	0.920	0.918						
Sriramapuram					$R_{t(Kvt)}$	$R_{t-1(Kvt)}$	$G_{t-1(Kvt)}$	$R_{t(Cgg)}$	$R_{t-1(Cgg)}$	$G_{t-1(Cgg)}$	$R_{t(Yvp)}$	$R_{t-1(Yvp)}$	$G_{t-(Yvp)}$
	0.983	0.983	0.983	0.321	0.983	0.983	0.982	0.983	0.983	0.983	0.983	0.981	0.981
Chandragiri													
	0.980	0.972	0.974	0.337									
Tirupati					$R_{t(Cgr)}$	$R_{t-1(Cgr)}$	$G_{t-1(Cgr)}$	$R_{t(Srp)}$	$R_{t-1(Srp)}$	$G_{t-1(Srp)}$			
	0.991	0.990	0.991	0.154	0.991	0.991	0.991	0.991	0.990	0.987			
Renigunta					$R_{t(Tpt)}$	$R_{t-1(Tpt)}$	$G_{t-1(Tpt)}$						
	0.839	0.802	0.838	0.475	0.831	0.835	0.833						
Yerpedu					$R_{t(Rng)}$	$R_{t-1(Rng)}$	$G_{t-1(Rng)}$	$R_{t(Tpt)}$	$R_{t-1(Tpt)}$	$G_{t-1(Tpt)}$	$R_{t(Cgr)}$	$R_{t-1(Cgr)}$	$G_{t-1(Cgr)}$
	0.951	0.950	0.949	0.460	0.950	0.948	0.951	0.951	0.950	0.951	0.950	0.950	0.951

Piezometric Station	Partial Correlation Coefficient											
	Independent Variable Omitted											
Yerravaripalem	R_t	R_{t-1}	G_{t-1}									
	0.199	0.256	0.947									
Chinnagottigallu				$R_{t(Yvp)}$	$R_{t-1(Yvp)}$	$G_{t-1(Yvp)}$						
	0.079	0.079	0.981	0.091	0	0.064						
Karvetinagaram				$R_{t(Cgg)}$	$R_{t-1(Cgg)}$	$G_{t-1(Cgg)}$						
	0	0.093	0.956	0	0.081	0.104						
Sriramapuram				$R_{t(Kvt)}$	$R_{t-1(Kvt)}$	$G_{t-1(Kvt)}$	$R_{t(Cgg)}$	$R_{t-1(Cgg)}$	$G_{t-1(Cgg)}$	$R_{t(Yvp)}$	$R_{t-1(Yvp)}$	$G_{t-1(Yvp)}$
	0	0	0.945	0	0	0.045	0	0	0	0	0.064	0.064
Chandragiri												
	0.128	0.110	0.939									
Tirupati				$R_{t(Cgr)}$	$R_{t-1(Cgr)}$	$G_{t-1(Cgr)}$	$R_{t(Srp)}$	$R_{t-1(Srp)}$	$G_{t-1(Srp)}$			
	0.045	0	0.988	0	0	0	0	0.045	0.090			
Renigunta				$R_{t(Tpt)}$	$R_{t-1(Tpt)}$	$G_{t-1(Tpt)}$						
	0.294	0.049	0.824	0.138	0.098	0.119						
Yerpedu				$R_{t(Rng)}$	$R_{t-1(Rng)}$	$G_{t-1(Rng)}$	$R_{t(Tpt)}$	$R_{t-1(Tpt)}$	$G_{t-1(Tpt)}$	$R_{t(Cgr)}$	$R_{t-1(Cgr)}$	$G_{t-1(Cgr)}$
	0.046	0.065	0.875	0.046	0.079	0	0	0.079	0	0.079	0.079	0

Table 5. Regression equations.

Piezometric Station	Regression equation
Yerravaripalem	$G_t = 3.303 – 0.013R_t – 0.015R_{t-1} + 0.906\ G_{t-1}$
Chinnagottigallu	$G_t = 0.887 – 0.011\ R_{t-1} + 0.987\ G_{t-1}$
Karvetinagaram	$G_t = 1.920 – 0.012\ R_{t-1} + 0.901\ G_{t-1}$
Sriramapuram	$G_t = 1.049 + 0.005\ R_t – 0.01\ R_{t-1} + 0.975\ G_{t-1}$
Chandragiri	$G_t = 0.866 + 0.006\ R_t – 0.006\ R_{t-1} + 0.992\ G_{t-1}$
Tirupati	$G_t = 0.680 – 0.002\ R_{t-1} + 0.981\ G_{t-1}$
Renigunta	$G_t = 2.100 + 0.008\ R_t – 0.002\ R_{t-1} + 0.809\ G_{t-1}$
Yerpedu	$G_t = 3.246 + 0.004\ R_t – 0.01\ R_{t-1} + 0.860\ G_{t-1}$

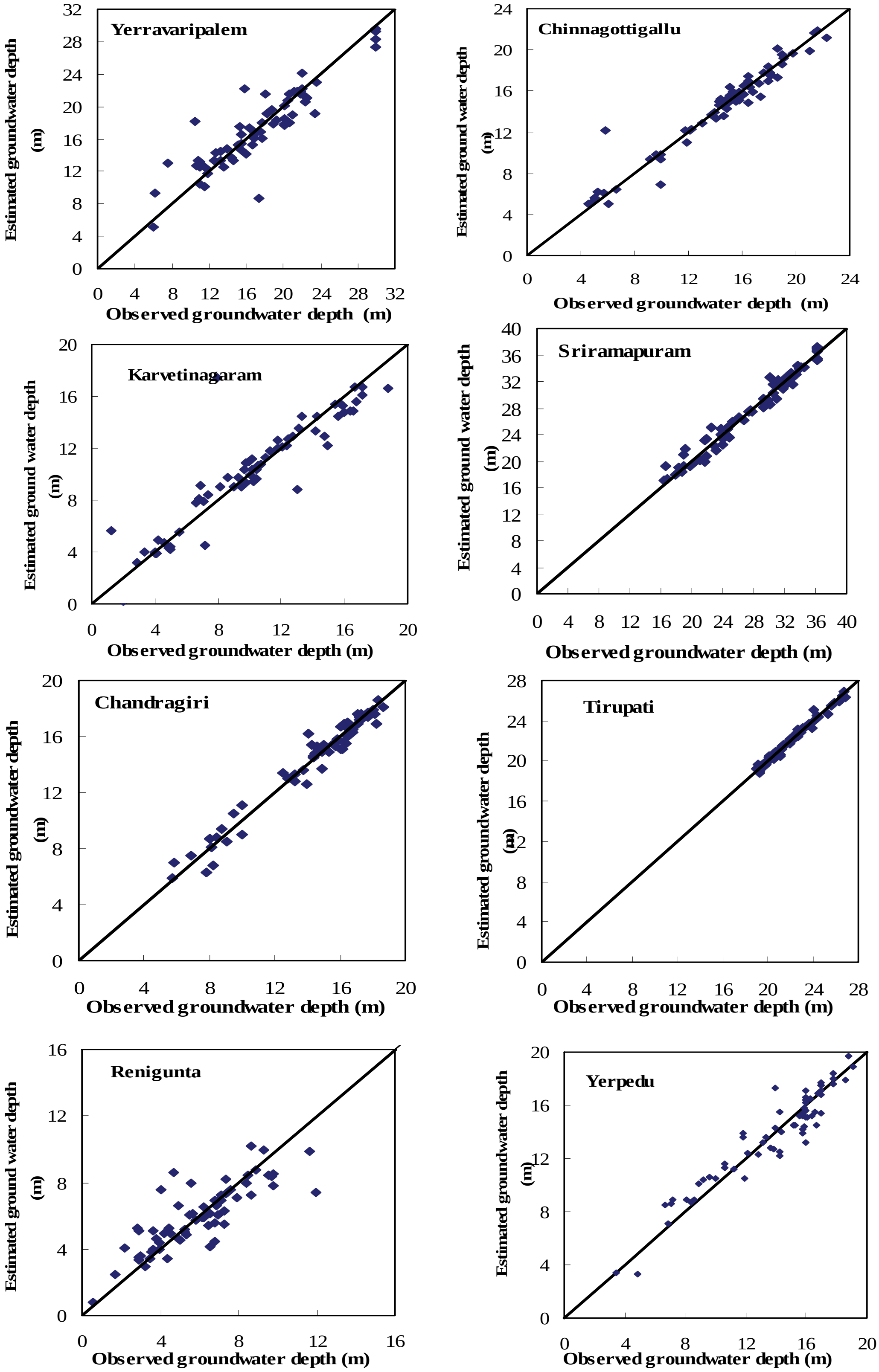

Figure 2. Comparison of observed and estimated groundwater table depths.

Table 6. Performance evaluation indicators.

Piezometric station	R^2	RMSE (m)	EC (%)
Yerravaripalem	0.83	2.29	82.78
Chinnagottigallu	0.93	1.16	93.01
Karvetinagaram	0.84	1.81	83.60
Sriramapuram	0.94	1.51	93.60
Chandragiri	0.96	0.69	95.70
Tirupati	0.96	0.42	96.29
Renigunta	0.68	1.40	67.68
Yerpedu	0.85	1.43	84.95

5. Conclusions

The multiple linear correlation analysis has been carried out to study the influence of rainfall, antecedent rainfall and antecedent groundwater table depth on groundwater depth in the upper Swarnamukhi river basin. The influencing variables have been selected based on the measures of multiple linear correlations. It is observed that the rainfall, antecedent rainfall and antecedent groundwater table depth influence the groundwater table depth significantly. Further, the effect of antecedent groundwater table depth is more pronounced than that of rainfall and antecedent rainfall. The relationships proposed may be adopted to predict the groundwater table depths to a reasonable degree of accuracy for better planning and management of groundwater resources of the basin.

6. Acknowledgements

One of the authors, I. Jasmin, thanks Council of Scientific and Industrial Research, New Delhi, India for granting Senior Research Fellowship to pursue research on groundwater.

7. References

[1] K. K. Mishra, "Statistical Analysis of Water Table Data at Powarkheda," *Journal of the Institution of Engineers, India*, Vol. 74, No. FEV, February 1994, pp. 213-215.

[2] S. V. N. Rao and K. S. Ramasastri, "Estimation of Groundwater Draft and Recharge in Coastal Aquifers Using Field Data," *The Indian Society for Hydraulics, Journal of Hydraulic Engineering*, Vol. 6, September 2000, pp. 9-17.

[3] H. D. Singh, P. Munirathnam, V. K. Chetty and T. V. K. Reddy, "A Study on the Rejuvenation of Swarnamukhi River through Water Harvesting Structures (Subsurface Dams)," *Proceedings of International Groundwater Conference on Sustainable Development and Management of Groundwater Resources in Semi-Arid Region with Special Reference to Hard Rock*, Dindigul, Tamil Nadu, February 2002, pp. 239-248.

[4] N. J. Raju, T. V. K. Reddy and P. Munirathnam, "Subsurface Dams to Harvest Rainwater - A Case Study of the Swarnamukhi River Basin, Southern India," *Hydrogeology Journal*, Vol. 14, No. 4, April 2006, pp. 520-531.

[5] P. K. Naik and A. K. Awasthi, "Groundwater Resources Development in the Koyna River Basin," *Journal of India Water Resources Society*, Vol. 25, July 2005, pp. 25-32.

[6] N. B. N. Prasad, E. A. Hameed, B. Sivakumar and S. Michael, "Groundwater Development Status in Lakshadweep - A Case Study," *The Indian Society for Hydraulics, Journal of Hydraulic Engineering*, Vol. 12, No. 1, September 2006, pp. 25-36.

[7] A. K. Sinha, R. P. Singh and A. Kumar, "Groundwater Status in Dhund River Basin, Jaipur District, Rajasthan," *Journal of Geological Society of India*, Vol. 68, No. 5, November 2006, pp. 809-818.

J. Water Resource and Protection, 2010, 2, 585-591
doi:10.4236/jwarp.2010.26067 Published Online June 2010 (http://www. SciRP.org/journal/jwarp)

A Novel Approach for Groundwater Budgeting Using GIS in a Part of Pondicherry Region, India

Sivaraman Pethaperumal[2], Sabarathinam Chidambaram[1], Kandasamy Vijayaragavan[1], Mohan Viswanathan Prasanna[3], Kannan Anandavel[2], Ulaganathan Karmegam[1], Ramachandran Manivannan[1], Paluchamy Anandhan[1], Kesari Tirumalesh[4]
[1]*Department of Earth Sciences, Annamalai University, Annamalai Nagar, India*
[2]*State Groundwater Unit and Soil Conservation, Department of Agriculture, Pondicherry, India*
[3]*School of Engineering and Science, Department of Applied Geology, Curtin University of Technology, Sarawak, Malaysia*
[4]*Scientist D, Isotope Hydrology Division, BARC, Mumbai, India*
E-mail: *chidambaram_s@rediffmail.com*
Received March 23, 2010; *revised April* 23, 2010; *accepted May* 6, 2010

Abstract

The over extraction of groundwater from the coastal aquifers, result in reduction of groundwater resource and lowering of water level. In general, the depletion of groundwater level enhances the landward migration of saltwater wedge. Pondicherry is one such region with recent alluvium as the major formation. Since the study area forms a part of the coastal aquifer system this behaves as a fragile ecosystem. The present study has been attempted to calculate the extraction of water and to estimate the amount of recharge into this alluvial aquifer by using groundwater level variations. The monthly water level fluctuation was observed during the study period (2000-2002) in eighteen locations. The maximum rise in groundwater level observed during 2000 was considered as the initial water level for the study and the subsequent decline in water level (draw down) was monitored monthly until the rising trend was noted. This indicates the fall in water level due to extraction. Later keeping the deepest draw down as the initial value increasing water level trend was studied until there was a notice of decline in groundwater level. This indicates as the rise in water level due to recharge. This method of observation carried out at a single location was adopted for all eighteen locations. The spatial representation of these data for eighteen locations were carried out by using GIS and the area occupied by different groundwater level contours were calculated and the amount of water withdrawn/recharged was estimated. The maximum recharge was noted in the central and the northern part of the study area when compared to the other regions. Similarly, the maximum discharge was noted in the northern and the southern part of the study area during the study period.

Keywords: Water Level, Recharge, Groundwater Budget, GIS

1. Introduction

Groundwater is one of the most important and scarce commodity. Groundwater exists in the geological formations through which it can penetrate, be transmitted and stored beneath the surface. When the rate of infiltration is sufficient and the rocks are saturated to an appreciable thickness, then the groundwater becomes usable enough to yield useful supplies of water to wells, springs and stream. At present nearly 1/5th of all the water used in the world are obtained from the groundwater. Land use/ land cover pattern of Pondicherry and its surroundings were studied by using IRS 1C LISS III data [1]. The land use/land cover patterns were visually interpreted and digitized using ERDAS IMAGINE software. The study observed that agriculture area (52.89%) is dominant in Pondicherry and its surroundings, followed by settlement with vegetation (18.35%). The dependency of groundwater for the agricultural purpose has considerably increased in the recent past. Nearly about 80% of groundwater is used for agriculture. The quantification of the groundwater resources has become essential for water management. There are differebt methods for assessing the rate of recharge e.g., by using stable isotope, tra- cer techniques, groundwater modeling (thangarajan *et al.*) etc. Aquifer recharge studies using different isotopes for determination of infiltration capacities, permeability and in delineation of aquifer, inter connection were studied by several authors [2-10]. An Indicator based model was described to assess and quantify the significance of vulnerability to salt water intrusion due to excessive groundwater withdrawal and also to analyze the impact of artificial recharge in minimizing the salt water intrusion for coastal aquifers [11]. A detailed study on the Pondicherry groundwater was also done by National Geophysical Research Institute Hyderabad [12] to estimate the areas of over exploitation and to derive water balance using geo-hydrological data. Groundwater utilization for agricultural intensification in the Pondicherry region was studied by CGWB [13]. A detailed study was also carried out by the State Groundwater Unit of Agriculture Department, Pondicherry [14] to augment the available groundwater resource. Since the available methods are sophisticated, time consuming and costly an alternate method for the assessment of groundwater recharge and discharge was attempted by using the available groundwater level and GIS technique. Visualization is a convenient and effective way to communicate complex information. Greater importance is being put on data visualization today, GIS is a leading technology in this movement. It has tremendous potential to affect a wide variety of fields in present day. Hence, an attempt has been made in this study to handle GIS technique for groundwater budgeting in this shallow alluvial aquifer of Pondicherry region using water level data.

Figure 1. Location map of the study area.

2. Study Area

The study area is located 28 km in the North West part of Pondicherry region, it lies between latitudes of 11^0 50'N to 12^0 59'N and longitude of 70^0 35'E to70^0 45'E (**Figure 1**). The study area falls in the survey of Indian top sheets of 58 M/10. It geographically covers an extent of nearly 85 Sq.km. Groundwater of the study area occurs in alluvial aquifer under un-confined to semi-confined condition. The depth of the tube wells tapping this aquifer ranges between 25 m and 50 m bgl (below ground level). The average annual fluctuation is around 7.50 m. The studies [15] indicate that the transmissivity values of the aquifers is 275.4 m^2/d at Madukarai in the west and is 770 m^2/d at Thirukanji in the east.

2.1. Geology

The results of the shallow drilling in north of Pondicherry [16,17] reveals the geology of the region. Later the Central Groundwater Board, Governement of India [18] brought out a detailed report on the groundwater survey and exploration in the Union Territory of Pondicherry. In general the geology of Pondicherry region ranges from Archean to recent alluvium. The recent formation in the region is represented by Laterite and alluvium, Laterite occurs as thin cap over the Cuddalore formation. Thickalluvial deposits are built up along the course of Pennaiar and Gingee rivers. The study area falls in this region and is completely covered by alluvium.

3. Methodology

Water level data for the past 14 years were observed and the study was conducted for a period of three years (2000-2002).

3.1. Discharge

In the year 2000 the monthly water level data was studied and the minimum drawdown level of groundwater was noted. This is taken as the initial reading (I_L). Similarly, in the simultaneous year (2001) the maximum drawdown level of groundwater is noted (D_L). The difference between this two groundwater levels gives the discharge in region ($I_{L\sim}D_L$), using this phenomenon difference in water level was calculated for the different location in the study area. The rate of discharge (D_R) can be calculated by the difference between the initial water level (I_L) and maximum drawdown level (D_L) divided by the time taken for discharge (D_T).

$$D_R = \frac{I_L \sim D_L}{D_T}$$

3.2 Recharge

In the year 2001, the maximum drawdown level of groundwater level (D_L) was noted and the subsequent rise in monthly water level was noted till the deviation of water level decrease was identified. This level of risen water table (R_L) is the recharge level. The difference between this two groundwater levels gives the recharge (R). The time taken for the recharge water level from the maximum draw down level can be calculated (R_T). The rates and recharge (R_R) is given by,

$$R_R = \frac{R}{R_T}$$

$$R = (D_{L} \sim R_{L})$$

The study pertains to a part of Pondicherry region covered by unconfined aquifers in alluvial formation. The water level data for the three years were analyzed as per the methodology mentioned above.

3.3. GIS

Map info (Ver.7.8) GIS software along with Vertical Mapper was used to spatially distribute the water level data in order to locate the region of maximum discharge and recharge. The rate of recharge and discharge were also calculated and spatially plotted on the map. GIS helps to approximately calculate the area of recharge and discharge falling in different contour intervals.

4. Result and Discussion

The initial (shallow) and maximum (deeper) water levels for each location were identified (**Table 1**). The shallow water table was identified during February in most of the locations. Similarly, the maximum draw down (DD) level was noted during the period of September. The maximum discharge (**Table 1**) was noted at the Kodukkur region, it lies in the northern part of the study area. The rate of the discharge is 13.97 m in 7 months, *i.e.*, about 1.99 m/month. In general the subsurface water flow is from the north to the south, more over there are number of agricultural fields located in this region and the main crop cultivated is paddy. The alluvial plain here is generally a monotonous with slope ranging from 1m to 3 m. The lands in this plain are intensively cultivated throughout the year. The minimum discharge was noted at the V. Nerkunam region it is located in the eastern part of study area, the discharge rate is 0.69 m in 7 months, *i.e.*, about 0.098 m/month. The average discharge level of the study area is 6 m and the average rate of discharge is 0.45 m. The maximum time taken for the discharge in the study area is 19 months. Assessment of groundwater resources of Pondicherry region by Sukhija [19] estimated the groundwater inputs and annual recharge is due to rainfall, return flow from agricultural fields, seepage from tanks, canals and groundwater in-flow. The general overview of groundwater and the water level changes were discussed in the CGWB report [20]. Besides the rivers and major canals, there are depressions acting as storage tanks which are spread all over the terrain to serve as surface water reservoirs.

From the recharge status (**Table 2**) of the study area, the maximum recharge is noted at the Kodukkur region, it lies in the northern part of the study area. The recharge is 14.19 m for the particular year and the rate of recharge is 1.18/month., the minimum recharge is noted at the Sompet region, it is located in the western part of the study area. The recharge of this region is about 0.4 m for four months; the rate of recharge is 0.10 m/month. A study of the distribution of rainfall reveals (Pethaperuaml 2008) that there is a decrease in the rainfall from east to west, about 1300 mm near the coast to 1100 mm in the west. The average recharge level is 2.6 m, in the Vampupet, Kalitheampattu and Rajaputhrapallayam region. The average rate of recharge of the study area is 0.58 m/month. The northern part of the study area shows high rate of recharge due to three reasons; 1) agricultural return flow; 2) direct recharge from the river Gingee and 3) flow of groundwater from the adjacent areas.

4.1. Spatial Distribution of Discharge

Initially the difference between the shallow and deeper water level of the study area helps to identify the discharge level. A contour map (**Figure 2**) was derived out for this discharge level data (**Table 3**), depicting three categories of discharge as maximum, minimum and moderate. All categories discussed in this paper are in order to differentiat the available data. The contour interval ranging form 10.69 m to 13.97 m indicates maximum discharge region in the study area, which falls near Kodukkur, the spatial extent of this maximum discharge covers 1.79 sq.km. The contour interval ranging from 0.69m to 5.69 m, indicates minimum discharge regions in the study area, with a spatial extent of 51.22 sq.km. The medium discharge level was identified to have a spatial extent of 31.99 sq.km lying between contours 5.69–10.69 m.

4.1.1. Spatial Distribution of Rate of Discharge

The contour map for rate of discharge (**Figure 3**) shows four different categories (**Table 4**) of which the very high discharge rate is noted in Kodukkur covering an area of about 1.28 sq.km. The low discharge rate covers about 90% of the study area with a spatial extent of about

Table 1. Discharge status by using relative water level (2000–2001).

Village	Water Level		Difference		Rate	Location	
	initial (m)	MAX.DD (m)	**Level**	Month	Month	X	Y
Mannadipet	22.8 (Feb. 2k)	29.95 (Sep. 01)	7.15	19	0.3763	79.6251	11.9865
Thirukkanur	23.65 (Feb.2k)	28.7(Sep.01)	5.05	**19**	0.2658	79.6357	11.9871
Sompet	23.6 (Feb.2k)	29.1 (Dec. 01)	5.5	**22**	0.2500	79.6328	11.9731
Kudathur	22 (Jan. 2k)	29.1 (Dec. 01)	7.1	**12**	0.5917	79.66	11.9913
Vambupet	17.75 (Feb.2k)	22.2 (Sep. 01)	4.45	**19**	0.2342	79.6803	11.9646
Sellipet	11.1 (Feb. 2k)	18.1 (Sep.01)	7	**19**	0.3684	79.7004	11.9507
Sagadapet	22.15 (Oct. 2k)	27.75 (Sep. 01)	5.6	**11**	0.5090	79.6552	11.9444
Kalitheerthalkuppam	8.65 (Feb. 2k)	15.95 (Sep. 01)	7.3	**19**	0.3842	79.6281	11.9233
Madagadipet	8.5 (Feb. 2k)	17.45 (Sep. 01)	8.95	**19**	0.4711	79.6363	11.9192
Thirubuvanai	6.2 (Feb. 2k)	12.85 (Sep. 01)	6.65	**19**	0.3500	79.6506	11.9161
Thiruvandarkoil	7.85 (Oct. 2k)	17.3 (Sep. 01)	9.45	**11**	0.8591	79.6591	11.9171
Sorapet	28.35 (Jan.2k)	33.3 (Dec. 01)	4.95	**12**	0.4125	79.6648	11.9537
Rajaputrapalaym	20.13 (Feb.2k)	24.47 (Sep. 01)	4.34	**7**	0.6200	79.6877	11.9343
Azhiyur	17.52 (Sep.2k)	22.21 (Sep. 01)	4.69	**12**	0.3908	79.6672	11.9121
Kalithirampattu	17.8 (Feb.2k)	21.42 (Sep. 01)	3.62	**7**	0.5171	79.6878	**11.6596**
V. Nerkunam	21.33 (Feb.2k)	22.02 (Spe. 01)	0.69	**7**	0.0986	79.6724	11.9766
Kodukkur	10.23 (Feb.2k)	24.15 (Sep. 01)	13.97	**7**	1.9957	79.6514	11.9962
Madurapakkam	22.25 (Sep.2k)	25.64 (Sep. 01)	3.39	**12**	0.2825	79.621	11.9951

Table 2. Recharge status by using relative water level (2001–2002).

Village	Water Level		Difference		Rate	Location	
	Max (m)	Min (m)	Level	Month	Month	X	Y
Mannadipet	29.95 (Sep. 01)	28.3 (Ap.02)	1.65	7	0.2357	79.6251	11.9865
Thirukkanur	28.7 (Sep.01)	27 (Feb.02)	1.7	5	0.3400	79.6357	11.9871
Sompet	29.1 (Dec. 01)	28.7 (Ap. 02)	0.4	4	0.1000	79.6328	11.9731
Kudathur	29.1 (Dec. 01)	23.65 (Feb. 02)	5.45	2	2.725	79.66	11.9913
Vambupet	22.2 (Sep. 01)	19.6 (Feb. 02)	2.6	5	0.52	79.6803	11.9646
Sellipet	18.1 (Sep.01)	14.9 (Feb. 02)	3.2	5	0.64	79.7004	11.9507
Sagadapet	27.75 (Sep. 01)	26.65 (Feb. 02)	1.1	5	0.22	79.6552	11.9444
K.kuppam	17 (Sep. 01)	15.95 (Feb. 02)	1.05	5	0.21	79.6281	11.9233
Madagadipet	17.65 (Sep. 01)	17.45 (Feb. 02)	0.2	5	0.04	79.6363	11.9192
Thirubuvanai	13.8 (Sep. 01)	12.85 (Feb. 02)	0.95	5	0.19	79.6506	11.9161
Thiruvandarkoil	17.3 (Sep. 01)	16.3 (Feb. 02)	1	5	0.2	79.6591	11.9171
Sorapet	33.3 (Dec. 01)	29.4 (Feb. 02)	3.9	2	1.95	79.6648	11.9537
Rajaputrapalaym	24.47 (Sep. 01)	21.87 (Feb. 02)	2.6	5	0.52	79.6877	11.9343
Azhiyur	22.21 (Sep. 01)	18.71 (Feb. 02)	3.5	5	.7	79.6672	11.9121
Kalithirampattu	21.42 (Sep. 01)	18.8 (Feb. 02)	2.62	5	0.524	79.6878	11.6596
V. Nerkunam	22.02 (Spe. 01)	21.54 (Feb. 02)	0.48	5	0.096	79.6724	11.9766
Kodukkur	24.15 (Sep. 01)	9.96 (Sep. 02)	14.19	12	1.1825	79.6514	11.9962
Madurapakkam	26.35 (Sep. 01)	25.64 (Feb. 02)	0.71	5	0.142	79.621	11.9951

Table 3. Area occupied by difference rang of for discharge level relative water level.

Categories	Ranges (m)	Area (Sq. Km)
Minimum	0.6961 – 5.6962	51.2173
Moderate	5.6962 – 10.6962	31.9969
Maximum	10.6962 – 13.9696	1.7923

Table 4. Area occupied by different ranges of for rate of discharge relative water level.

Categories	Ranges (m)	Area (Sq. Km)
Low	0.0988 – 0.5989	73.4384
Medium	0.5989 – 1.0989	9.0898
High	1.0989 – 1.5989	1.2029
Very high	1.5989 – 1.9956	1.2768

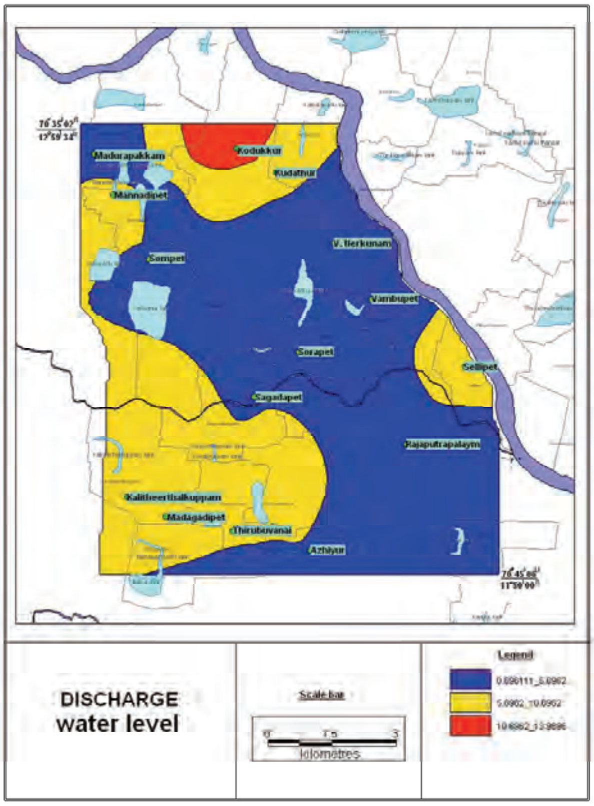

Figure 2. Contour map of discharge water level.

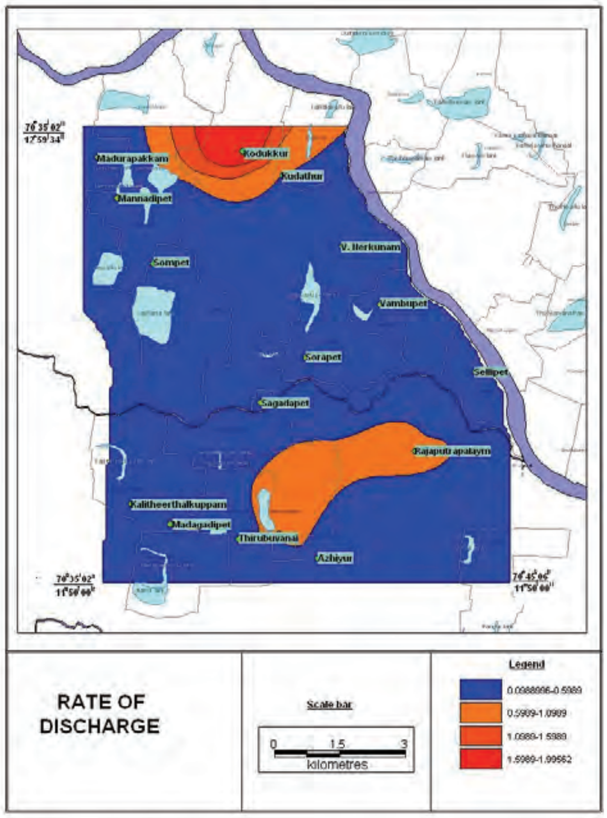

Figure 3. Contour map for rate of discharge.

73.43 sq.km. The rate of discharge of the remaining part of the study area falls in medium (0.59-1.09 m/month) and high (1.09-1.59 m/month) category.

4.2. Spatial Distribution of Recharge

Difference between the maximum and minimum water level (Water Level Difference) helps to find the recharge. By using the recharge level data (**Table 5**) a contour map was drawn (**Figure 4**) with three different categories as low, medium and high recharge. The high recharge was again noted at Kodukkur, it lies between 10.20-14.18 m contour. It is interesting to note that both high discharge and recharge are noted in the same region. Kodukkur region is dominated by groundwater dependent irrigation system for paddy cultivation. Hence higher rate of discharge is noted in this region but since the area is an alluvial terrain with good porosity the agricultural return

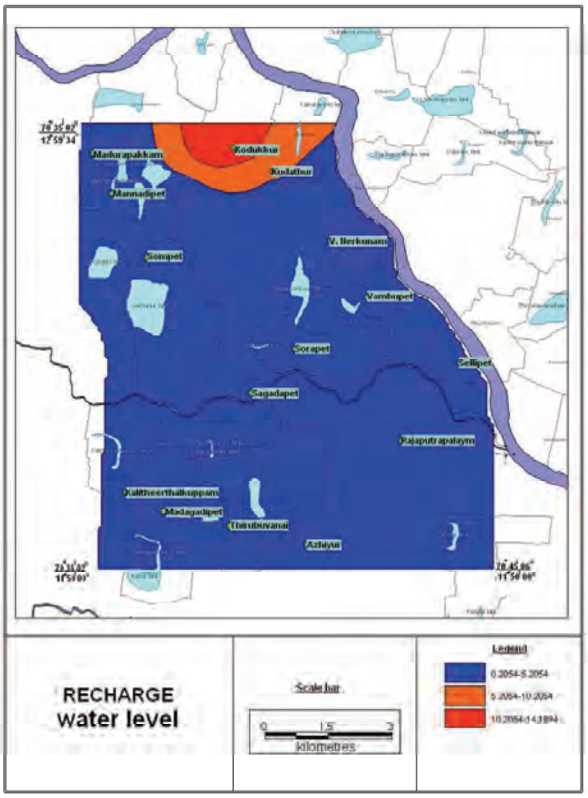

Figure 4. Map for recharged water level.

Table 5. Area occupied by different ranges of for recharge level relative water level (2002).

Categories	Ranges (m)	Area (Sq. Km)
Low	0.2054–5.254	80.0144
Medium	5.254 – 10.2054	3.3067
High	10.2054 – 14.1894	1.6844

flow enhances the rate of recharge in this region. The spatial extent of this high recharge is 1.68 sq.km, the low recharge (**Table 5**) the study area falls between 0.20 to 5.20 m category, which covers an area of about 80.91 sq.km. The rest is occupied by the medium recharge region.

4.2.1. Spatial Distribution of Rate of Recharge

The calculated recharge rate was spatially plotted on a contour map (**Figure 5**) with six different categories (**Table 6**) like excellent, very good, good, moderate, poor and very poor. The Excellent recharge rate range between 2.54 m/month and 2.72 m/month. This is noted in Kodukkur and Sorapet villages, covering an area of 0.71 sq.km. Similarly, the Very poor recharge rate was found near Sompet, K. Kuppum, V. Nerkunam, Sagadapet and Rajaputra palayam villages, ranging between 0.041 m/month and 0.54 m/month which cover an area of 44.13 sq.km. The poor category ranges between 0.54

Table 6. Area occupied by different ranges of for rate of recharge relative water level.

Categories	Ranges (m)	Area (Sq. Km)
Very poor	0.0411 – 0.5411	44.1351
Poor	0.5411 – 1.0411	28.2419
Moderate	1.0411 – 1.5411	6.4208
Good	1.5411 – 2.0411	3.36478
Very good	2.0411 – 2.5411	2.1276
excellent	2.5411 – 2.7229	0.7131

m/month and 1.04 m/month covering an area of 28.24 sq.km. Rest of the area falls in, moderate (1.04–1.0 m/month), good (1.54-2.04 m/month) and very good (2.04 –2.54 m/month) categories. The average rate of recharge in the study area is 1.38 m/month.

4.3. Volume Estimation

Based on the recharge and discharge contour maps, the mid point of the each contour range is multiplied with area lying between the contours, to derive the volume of the recharge/discharge area. This is in turn multiplied by the porosity of the formation (alluvium) to obtain the storage capacity of aquifer. If the porosity of the region is assumed to be 15%, the amount of water withdrawn is 67208.30 $\times 10^3 m^3$ and the quantity of water recharged is 39374.26 $\times 10^3 m^3$ .The rate of recharge was noticed to be higher in centre part of the study area at Sorapet.

The study shows that water level increases during monsoon period and decreases during post monsoon and summer. The discharge period is about 19 months on an average and the recharge is observed for a lesser interval of 5 month during the study period. Hence, it is noted that the duration of discharge is higher that the recharge. The estimated recharge volume also proves that the volume of the water recharged is almost half of the volume of discharge.

5. Conclusions

The variation in water level helps us to identify the difference in groundwater potential. The above study facilitates to spatially identify the regions with high discharge and good recharge. It also brings out the rate of recharge and discharge and therby to discriminate the regions with the above function. The study also reveals that the discharge and recharge is higher a one specific location which is mainly due to agricultural extraction and return flow respectively. This study also reveals a fact the though both the process takes place simultaneously in nature, there can be specific demarcation of period for discharge and recharge dominance. The discharge is noted for a longer period than the recharge is for a shorter period due the lesser availability of water. The spatial extent of the results will help the water managers to provide scientific solutions for the resource. So, the volume of the extraction and recharge in a particular area with the aid of GIS reduces the adhoc experimentation and this method is also less expensive. Hence the monthly water level data of a region along with GIS software can assist in evolving the maximum recharge and discharge regions along with the volume of the water recharged or discharged in a specific area.

6. Acknowledgements

The authors wish to express thank to the state groundwater unit and soil conservation, Pondicherry, BRNS for the financial support, and staff members in Department of Earth Sciences, Annamalai University for their cooperation.

7. References

[1] E. P. Nobi, R. Umamaheswari, C. Stella and T. Thangaradjou, "Land Use and Land Cover Assessment along Pondicherry and its Surroundings Using Indian Remote Sensing Satellite and GIS," *American-Eurasian Journal of Scientific Research*, Vol. 4, No. 2, 2009, pp. 54-58.

[2] V. P. Yakutseni, "Geology of Helium (Geologiya Geliya)," Nedra Publishing, Leningrad, 1968.

[3] T. Dincer, W. Almurin and V. Zimmerman, "Study of Infiltration and Recharge through the Sand Dunes in Arid Zones with Special Reference to the Stable Isotopes and Thermonuclear Tritium," *Journal of Hydrology*, Vol. 23, No. 12, 1974, pp. 79-109.

[4] V. I. Ferronsky, Ed, "Isotopes of Natural Waters," Nanka Publishing, Isotopiya Pairodnykhvod, Moscow, 1978.

[5] R. A. Downing, F. J. Pearson and D. D. Smith, "The Flow Mechanism in the Chalk Based on Radio-Isotope Analysis of Groundwater in the London Basin," *Journal of Hydrology*, Vol. 40, No. 1-2, 1979, pp. 67-83.

[6] C. Gaye and W. M. Edmunds, "Groundwater Recharges Estimation Using Chloride, Stable Isotopes and Tritium Profiler in the Sands of Northwestern Senegal," *Environmental Geology*, Vol. 127, 1996, pp. 246-251.

[7] G. B. Allison, "A Review of Some of the Physical, Chemical and Isotope Techniques Available for Estimating Groundwater Recharge," *Proceedings of NATO Workshop on Estimation of Natural Recharge of Groundwater*, Antalaya Turkey, 1987, pp. 49-72.

[8] V. S. Kovalevsky and V. L. Zlobina, "Helium Survey for Delineation Areas of Karst - Suffosion Processes Caused by High-Rate Groundwater Withdrawal," *Environmental Geology Water Sciences*, Vol. 10, No. 2, 1987, pp. 89-94.

[9] B. S. Sukhija, D. V. Reddy, P. Nagabushanam, S. Hussain and V. Y. Giri, "The Use of Environmental Isotopes and Chloride as Natural Tracers to Investigate the Effects of Depressurization of a Coastal Aquifer for Lignite Mining, India," *Hydrology Journal*, Vol. 4, No. 2, 1996, pp. 70-87.

[10] M. F. Abu-Taleb, "The Use of Infiltration Field Tests for Groundwater Artificial Recharge," *Environmental Geology*, Vol. 37, No. 1-2, 1999, pp. 64-71.

[11] V. Lenin, K. Sundaram, G. Dinesh, G. Ravikumar and D. Govindarajalu, "Vulnerability Assessment of Seawater Intrusion and Effect of Artificial Recharge in Pondicherry," *Indian Journal of Science and Technology*, Vol. 1, No. 7, 2008, pp. 7-125.

[12] B. S. Sukhija, D. V. Reddy and I. Vasanthakumar Reddy, "Study of Ground Water Resources of Pondicherry and its Environs," 1987, pp. 3-151.

[13] M. Suresh, "Ground Utilization for Agricultural Intensification, A Case Study from Pondicherry," India with Reference to Sustainability and Equity, Agricultural University of Norway, 1996.

[14] State Ground Water Unit of Agriculture Department, "Tank Rehabilitation Project Pondicherry," Technical and Administrative Provisions, Public Works Department, Government of Pondicherry, Pondicherry, 1996.

[15] Central Ground Water Board (CGWB), "Groundwater Resource and Development Prospects in Pondicharry Region," *Union Territory of Pondicherry*, Vol. 19, No. 1-2, 1993, pp. 59-63.

[16] K. M. Nair and V. P. Rao, "Result of Shallow Drilling in the Area North of Pondicherry," Unpublished, *Oil and Natural Gas Corporation Limited Field Season Report of* 1969-1970, 1971.

[17] V. P. Rao "Field Party," *Oil and Natural Gas Corporation Limited*, India, No. 6, 1972.

[18] K. V. Raghava Rao, K. V. J. R.Krupanidhi, G. Balasubramanian, P. R. Subramaninan and P. Natarajan, "Report on Groundwater Survey and Exploration in the Union Territory of Pondicherry and its Environs," *Central Ground Water Board Report*, India, 1976.

[19] B. S. Sukhija, D. V. Reddy and P. Nagabhushaman, "Isotopic Fingerprints of Paleoclimates during the Last 30000 Years in Deep Confined Groundwaters of Southern India," *Quartern Research*, Vol. 50, No. 3, 1998, pp. 252-260.

[20] P. Natarajan, "Ground Water Resources and Development Prospects in Pondicherry Region, Union Territory of Pondicherry," *Central Ground Water Board Report*, August 1993, pp. 1-41.

J. Water Resource and Protection, **2010, 2, 592-596**
doi:10.4236/jwarp.2010.26068 Published Online June 2010 (http://www. SciRP.org/journal/jwarp)

Observation on *Poterioochromonas* sp. (Chrysophyte)

Shengjuan Guo[1,2], Lirong Song[1*]
[1]*State Key Laboratory of Freshwater Ecology and Biotechnology, Institute of Hydrobiology Chinese Academy of Sciences, Wuhan, China*
[2]*CCCC Second Harbor Consultants Co. Ltd, Wuhan, China*
E-mail: *guoshj@gmail.com, lrsong@ihb.ac.cn*
Received March 10, 2010; *revised April* 25, 2010; *accepted April* 30, 2010

Abstract

Poterrioochromonas sp., isolated from *Microcystis* cultures in 2002, was described with LM, SEM, TEM. The grazing characteristics of this strain were also observed in laboratory experiments. The results showed that this strain has the representative features of the genus except for the lorica, and the most conspicuous feature of *Poterioochromonas* sp. was about the chromatophores.

Keywords: Microstructure, Ultrastructure, *Poterioochromonas* sp., Microcystis Aeruginosa

1. Introduction

Golden alga is an important component of plankton in the water ecology. Some species have characteristics of plant nutrition, such as chromatophore (chloroplast) or special product of assimilation (chrysolaminaran, *et al.*). So they are called as “chrysophytes” by botanists. However, some species have two flagella and can swim, and depend predominantly on phagotrophic nutrition without chromatophore which characterizes the phagotrophic nutrition. Thus some zoologists term them as “chrysomonads”, which is an important part of protozoa. Additionally, some species have both the characteristics of the plant nutrition (photosynthesis) and the phagotrophic nutrition, *i.e.*, they are mixotrophy. Although osmotrophy (dissolved) and phagotrophy (particulate), is observed in many algae, it is the use of particulate food that has generated most interest and to which the term mixotrophy usually applies [1].

Since Pringsheim [2] first reported that a *Ochromonas* ingested small algae, the phenomenon of ingestion of phytoplankters by chrysomonads has been widely recognized. Some genus of chrysomonads are capable of grazing blue-green algae (*Anacystis* and *Microcystis*) and green algae (*Chlorella*, *Chlamydomonas* and *Carteria*), and diatom (*Achnanthes*) [3-6]. These observations suggest that the ingestion of algae by mixotrophic chrysomonads is common. Our research group got a species of golden alga, isolated from *Microcystis* cultures in 2002. This alga could grow not only by ingestion and digestion of *Microcystis*, but also in phototrophic condition at the same time, which is described as mixotrophy. Mixotrophic algae are common in most aquatic ecosystems and, when numerically dominant, they depend significantly on phagotrophy [7,8]. Because of their small size and high metabolic rate they may also be important in the regeneration of nutrients [9], and thus an understanding of their nutritional characteristics is significant.

The golden alga we got was identified as *Poterioochromonas* sp., a strain that is phylogenetically close to *Poterioochromonas malhamensis* (99% similarity) by 18s rDNA (GenBank Accession No.AY699607) [10]. In this paper, we investigated the growth and ingestion characteristics of this strain, including the biological morphological features under different growth conditions.

This paper sponsored by National Hi-Tech Research and Development Program of China (2005AA60101005).

2. Materials and Methods

Poterioochromonas sp. was isolated from the mass culture of *Microcystis aeruginosa* in our lab in 2002. A clone culture was established by picking up single cells with micropipettes.

1) Cultures were grown in a flask with sterile BG-11 medium at 22℃ under an illumination of *ca.* 25 μmol photons·m^{-2}·s^{-1} with a photoperiod of 12 h : 12 h (Light: Dark) from daylight fluorescent lamps.

2) Feeding *Poterioochromonas* sp. in a relative low ratio of 3:1 (prey : predator) every two days for a week, the initial condition of the predator is 10^6 mL^{-1}.

3) Inoculating low densities (ca. 10^3 mL^{-1}) of *Poterioochromonas* sp. into the cultures containing approximately 10^6 or 10^7 mL^{-1} M. *aeruginosa* FACHB469.

We often sampled and observed the organism with an olympus CX 41 light microscope (LM).

2.1. Surface and Ultrastructure of *Poterioochromonas* sp.

For SEM (Scanning electron microscope), cells were fixed for 2 hours in 2.5% glutaraldehyde at room temperature, one drop of cells were placed on little glass slides, which coated with 0.1% poly-L-Lysine, dried for 30 min, and subsequently washed three times (10 min each) in 0.1 M phosphate buffer, pH 7.0. After three 10-min rinse in ultrapure water, samples were dehydrated through 50%, 70%, 80%, 90%, 95% and 100% ethanol (5 min each stage) and then 1:1 (ethanol : isoamyl acetate) for 10 min at room temperature, and used the critical point drying in a HITACHI HCP-2 apparatus after replaced by pure isoamyl acetate. The slides containing the algae were then mounted on stubs and coated with gold in a GIKO ID-3 sputter coater. Coated specimens were examined with HITACHI S-3000N SEM.

For TEM (Transmission Electron Microscopy), *Poterioochromonas* cells were harvested by gentle centrifugation. Cells were washed 2 times with PBS (pH = 7.0, 0.1 M), fixed with 2.5% glutaraldehyde, and then put in 1% OsO_4 for 2 hours at room temperature. After graded ethanol dehydration, samples were embedded in EPOXY epon-812 and polymerized at 70℃ for 8 hours. Sections were cut, stained with uranyl acetate and lead citrate, and then examined with a HITACHI H-600 TEM.

3. Results

The general appearance of *Poterioochromonas* sp., as observed with LM, is illustrated in **Figure 1** and **Figure 2**.

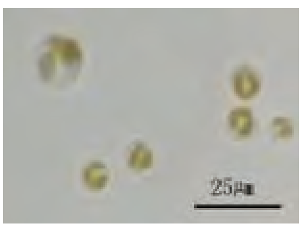

Figure 1. Photomicrographs of *Poterioochromonas* sp. in autotrophy.

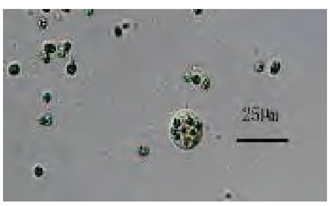

Figure 2. Photomicrographs of *Poterioochromonas* sp. in mixotrophy.

We found that the autotrophic cells, with two unequal long flagella and two yellow-green chromatophores, are spherical to elongate, and approximately 5-10 µm in di--ameter. We did not see any eye-spot. They could not only photosynthesize with chromatophores, but also efficiently digest the preys. And the volume of the predator could become larger when there were prey(s) in the cell. The diameter of the largest cells can reach 25 µm. The size and color of the chromatophores would change a lot during the *Poterioochromonas* cell ingested and digested preys. We only noted that the cells reproduce asexually by binary division, remaining motile, although it is reported that some chrysophyte can reproduce sexually. We did not see any lorica or scale outside the cell with LM.

From the pictures of the SEM, we noticed two kinds of cells: sphere or ellipse, as **Figure 3** shown.

The *Poterioochromonas* cells bear two heterodynamic flagella: pleuronematic flagellum with hair-like appendages (mastigonemes, 1.25 µm) and acronematic flagellum without any appendage (**Figure 4**). The two flagella are unequal in length: the longer is almost two times the body length; the shorter is half of the body's.

From the pictures of TEM, we observed that the cells are uninucleate, with a fine periplast but no rigid cell wall or spines or scales outside. The two chromatophores were oriented around the nucleus and lacked a pyrenoid. The single Golgi body is anterior to the nucleus and close to the flagellar bases. Mitochondrial cristae are tubular (**Figure 5**).

When added to the cultures of the *Poterioocromonas* sp., *M. aeruginosa* FACHB469 could be swallowed, and transported to a single membrane-bound food vacuole and digested there (**Figures 6**, **7** and **8**) by the predators. The

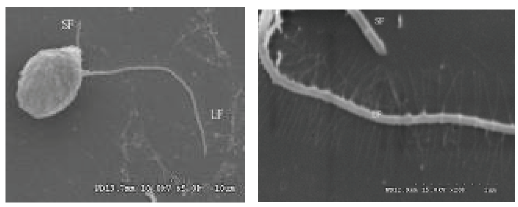

Figures 3-4. Scanning electron micrograph of *Poterioochromonas* sp.; SF: short flagellum; LF: long flagellum.

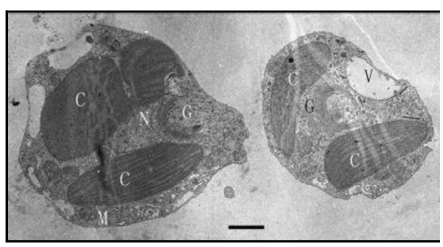

Figure 5. Transmission electron micrograph of *Poteriochromonas* sp. under autotrophy. C: chromatophore, G: golgi body, M: mitochondrion, N: nucleus, V : vacuole. Bar = 1 µm.

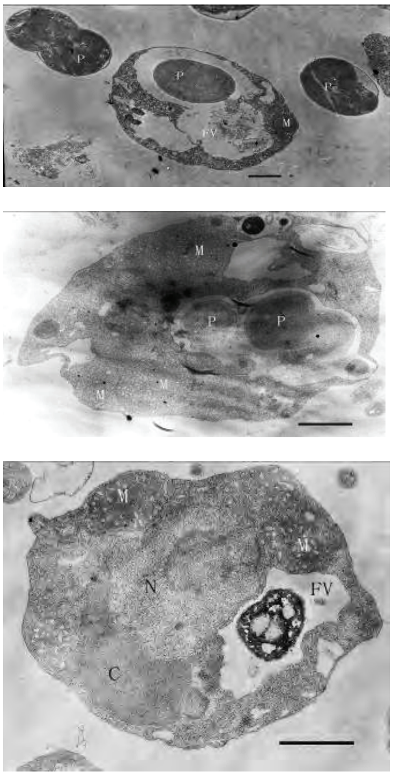

Figures 6-8. Transmission electron micrograph of *Poterioochromonas* sp.with prey(s). P : prey. Bar = 1 µm.

shape of the predator could be elongated, and the ultrastructure would change a lot. The most conspicuous feature of the predators was about the chromatophore.

When feeding *Poterioochromonas* sp. in a relative low ratio of 3:1 (prey: predator) every two days for a month, we could see no less than two swelling chromatophores with blurry or clear lamina around the nucleus (**Figures 9**, **10** and **11**). Some times the number of the chromatophores could reach six. At the same time there are many little osmiophilic globules in the interthylakoid spaces of the chromatophores. The predators could still move well and ingest preys.

When inoculating low densities (ca. 10^3 mL^{-1}) of *Poterioochromonas* sp. into the cultures containing approximately 10^6 or 10^7 mL^{-1} M. *aeruginosa* FACHB469, the predators could ingest preys very quickly and grow exponential rapidly. Meanwhile the chromatophores of most predators might become shrunken or missing in the first few days (**Figures 12**, **13** and **14**), and there were also many large osmiophilic globules located in the cytoplasm at the same time (**Figure 15**). Later when the most preys were nearly eaten off, the predators entered a "stationary growth phase", and chromatophores of *Poterioochromonas* sp. could appear again (**Figure 16**), and the large osmiophilic globules would disappear.

During the process of mixotrophic growth, the volumes of mitochondria become much larger (**Figures 8** and **12**) than those under autotrophy. We also observed a cell under the division (**Figure 17**).

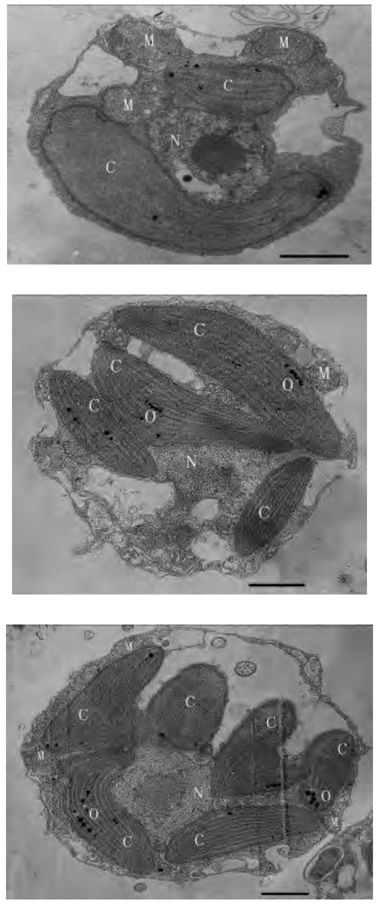

Figures 9-11. Transmission electron micrograph of *Poterioochromonas* sp. growth with low concentration of preys. O: osmiophilic globule. Bar = 1 µm.

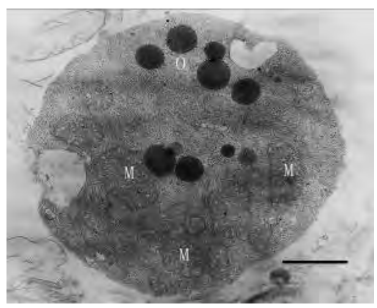

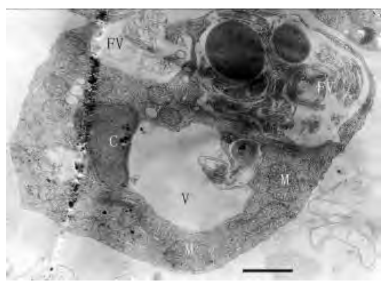

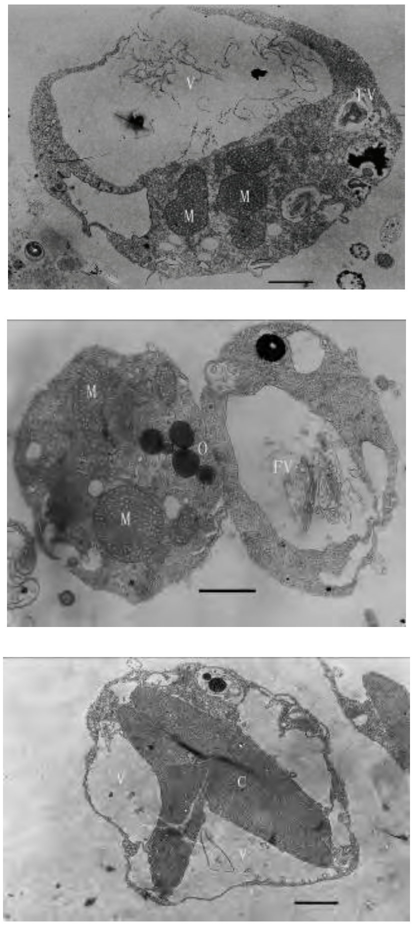

Figures 12-16. Transmission electron micrograph of *Poterioochromonas* sp. when adding with high concentration of preys. O: osmiophilic globule. Figures 12-15. Sampled within 3 days; Figure 16. Sampled after 7 days. Bar = 1 µm.

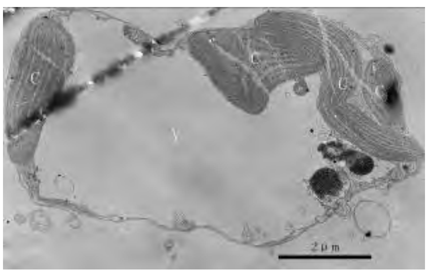

Figure 17. Transmission electron micrograph of *Poterioochromonas* sp. in division. Bar = 2 µm.

4. Discussion

Mixotrophy in algal flagellates is an interesting phenomenon from both cytological and ecological viewpoints [6]. However, as we know, there are few reports about such chrysomonas fed with algae in China. We isolated a strain Poterioochromonas and got the clone culture in 2002 [10]. We studied many morphological features and characteristics of this golden alga though we are not sure which species it was.

First, the most conspicuous feature of Poterioochromonas sp. was about the chromatophores. The morphology and number of chromatophore changed a lot during the mixotrophic growth. When the concentration of preys was relatively low, the number of chromatophores would increased obviously, and when much plentiful, the chromatophores would be shrunken or disappeared in the "exponential growth phase", while they would be observed again when the predators entered a "stationary growth phase" (**Figures 9-14** and **16**). Based on references [1,11], the reason for the shrunken and disappearance of chromotaphore appears to be the result of rapid mixotrophic growth as the flagellate division rate exceeds the assemblage of the cellular organelle, such as chromotaphore. The recovery of chromotaphore may be attributed to the effects of preys limitation and subsequent decrease in the predator growth rate and gave enough time for the assemblage of chromotaphore.

During the changes of chromatophores, osmiophilic globules changed similarly. The globules apparently formed from breakdown products of the chromophore membranes as well as from pigments synthesized during growth, and they are a reservoir of energy-rich components in the cell [12,13]. The appearance of osmiophilic materials seems to be the product of the digesting preys and the disorganized chromophore of the predator.

The giant mitochondria might indicate the metabolic utilization of the preys, which might provide more energy for the predators.

Additionally, from the preys' view, after being swallowed for a period of time, the prey(s) in the *Poterioochromonas* disappeared, it suggested that the predators not only ingest but also digest the prey organisms.

We could not observe any lorica outside *Poterioochromonas* sp. with TEM and LM, which was the special structure for the genus and difficult to identify [14]. More information should be explored to conclude whether this strain has lorica or not.

5. Conclusions

In conclusions, we investigated the morphological features and growth characteristics of *Poterioochromonas* sp., the results showed that the strain has the representative features of the genus except for the lorica. Mixotrophic chrysomonads can be found in many kinds of water bodied, including oligotrophic environments [15,16], mesotrophic and eutrophic waters [11,17]. It is an ecology strategy to control the harmful algae by using mixotrophy. Although we have done some research in the laboratory, there are many problems required further investigation before putting *Poterrioochromonas* sp. in the field.

6. References

[1] D. A. Holen, "Effects of Prey Abundance and Light Intensity on the Mixotrophic Chrysophyte *Poterioochromonas malhamensis* from a Mesotrophic Lake," *Freshwater Biology*, Vol. 42, No. 3, 1999, pp. 445-455.

[2] E. G. Pringsheim, "On the Nutrition of *Ochromonas*," *Quarterly Journal of Microscopical Science*, Vol. 93, No. 21, 1952, pp. 71-96.

[3] R. J. Daley, G. P. Morris and S. R. Brown, "Phagotrophic Ingestion of a Blue-Green Alga by *Ochromonas*," *Journal of Protozool*, Vol. 20, No. 1, 1973. pp. 58-61.

[4] G. T. Cole and M. J. Wynne, "Endocytosis of *Microcystis aeruginosa* by *Ochromonas danica*," *Journal of Phycology*, Vol. 10, No. 4, 1974, pp. 397-410.

[5] M. E. Boraas, K. W. Estep, P. W. Johnson and J. M. Sieburth, "Phagotrophic Phototrophs: The Ecological Significance of Mixotrophy," *Journal of Protozoology*, Vol. 35, No. 2, 1988, pp. 249-252.

[6] X. M. Zhang, M. M. Watanabe and I. Inouye, "Light and Electron Microscopy of Grazing by *Poterioochromonas Malhanmensis* (Chrysophyceae) on a Range of Phytoplankton Taxa," *Journal of Phycology*, Vol. 32, No. 1, 1996, pp. 37-46.

[7] D. F. Bird and J. Kalff, "Algal Phagotrophy: Regulating Factors and Importance Relative to Photosynthesis in Dinobryon (Chrysophyceae)," *Limnology and Oceanography*, Vol. 32, No. 2,1987, pp. 277-284.

[8] U.-G. Berninger, D. A. Caron and R. W. Sanders, "Mixotrophic Algae in Three Ice-Covered Lakes of the Pocono Mountains," U.S.A. *Freshwater Biology*, Vol. 28, No. 2, 1992, pp. 263-272.

[9] K. O. Rothhaupt, "Nutrient Turnover by Freshwater Bacterivorous Flagellates: Differences between a Hetero-Trophic and Mixotrophic Chrysophyte," *Aquatic Microbial Ecology*, Vol. 12, No. 1, 1997, pp. 65-70.

[10] D. Y. Ou, L. R. Song, N. Q. Gan and W. Chen, "Effect of Microcystins on and Toxin Degradation by *Poterioochromonas* sp.," *Environmental Toxicology*, Vol. **20**, No. 3, 2005, pp. 373-380.

[11] R. W. Sanders, U. G. Berninger, E. L. Lim, P. F. Kemp and D. A. Caron, "Heterotrophic and Mixotrophic Nanoplankton Predation on Picoplankton in the Sargasso Sea and on Georges Bank," *Marine Ecology Progress Series*, Vol. 192, No. 1, 2000, pp. 103-118.

[12] N. W. Withers and F. T. Haxo, "Isolation and Characterization of Carotenoid-Rich Lipid Globules from *Peridinium foliaceum*," *Plant Physiology*, Vol. 62, No. 1, 1978, pp. 36-39.

[13] B. Camara, P. Hugueney, F. Bouvier, M. Kuntz and R. Monéger, "Biochemistry and Molecular Biology of Chromoplast Development," *International Review of Cytology*, Vol. 163, No. 1, 1995, pp. 175-247.

[14] R. W. Sanders, K. G. Porter and D. A. Caron, "Relationship between Phototrophy and Phagotrophy in the Mixotrophic Chrysophyte *Poterioochromonas malhamensi*s," *Microbial Ecology*, Vol. 19, 1990, pp. 97-109.

[15] I. Domaizon, S. Viboud and D. Fontvieille, "Taxon Specific and Seasonal Variations in Flagellates Grazing on Heterotrophic Bacteria in the Oligotrophic Lake Annecy—Importance of Mixotrophy," *FEMS Microbiology Ecology*, Vol. 46, No. 3, 2003, pp. 3117-3329.

[16] A. Katechakis and H. Stibor, "The Mixotroph *Ochromonas tuberculata* may Invade and Suppress Specialist Phago- and Phototroph Plankton Communities Depending on Nutrient Conditions," *Oecologia*, Vol. 148, No. 4, 2006, pp. 692-701.

[17] J. Comte, S. Jacquet, S. Viboud, D. Fontvieille, A. Millery, G. Paolini and I. Domaizon, "Microbial Community Structure and Dynamics in the Largest Natural French Lake (Lake Bourget)," *Microbial Ecology*, Vol. 52, No. 1, 2006, pp. 72-78.

J. Water Resource and Protection, 2010, 2, 597-608
doi:10.4236/jwarp.2010.26069 Published Online June 2010 (http://www. SciRP.org/journal/jwarp)

Multifactorial Fuzzy Approach for the Assessment of Groundwater Quality

Natarajan Venkat Kumar, Samson Mathew, Ganapathiram Swaminathan
Civil Engineering Department, National Institute of Technology, Tiruchirappalli, S. India
E-mail: *venkatkumar.nit@gmail.com*
Received March 1, 2010; *revised April* 23, 2010; *accepted May* 4, 2010

Abstract

This paper describes the utility of fuzzy Simulink model to assess the groundwater quality levels in Tiruchirappalli city, S. India. Water quality management is an important issue in the modern times. The study aimed at examining the influence of multiple parameters of ground water on potable quality. The data collected for Tiruchirappalli city have been utilized to develop fuzzy Simulink approach. This is illustrated with seventy nine groundwater samples collected from Tiruchirappalli Corporation, S. India. The characteristics of the groundwater groundwater for this plain were monitored during the years 2006 and 2008. The quality of groundwater at several established stations within the plain were assessed using Fuzzy simulation. The results of the calculated fuzzy logic Simulink model and the monitoring study have yielded good agreement. Groundwater quality for potability indicated high to moderate water pollution levels at Srirangam, Ariyamangalam, Golden Rock and K. Abisekapuram depending on factors such as depth to groundwater, constituents of groundwater and vulnerability of groundwater to pollution. Fuzzy logic simulation approach was a practical, simple and useful tool to assess groundwater quality. This approach was capable of showing the water quality assessment for drinking on fuzzy Simulink model

Keywords: Groundwater, Potability, Fuzzy Simulation, GIS, Tiruchirappalli

1. Introduction

The quality, quantity and availability of drinking water are one of the most important environmental, social and political issues at global level. There are quality variation specifications of water for its intended use. Groundwater chemistry is affected from many factors such as movement through the rocks, recycling by irrigation practices, natural or artificial recharge and discharge.

Therefore, the determination of water quality is of primary prerequisite for public, agricultural and industrial supplies. Monitoring of water quality and qualitative decision-making on the basis of a data is challenge for environmental engineers and hydrologists as every step from sampling to analysis contains uncertainties. The regulatory limits for various pollutants/contaminants in drinking water proposed by various regulatory bodies like Bureau of Indian Standards (BIS) and World Health Organization (WHO) [1,2] are having limitations due to variation in intake to water by individuals during various seasons throughout the year. A prescribed limit from any regulatory body contains uncertainties as these are the extrapolated values from the data either from animal experiments or very trivial epidemiological studies [3-5].

The applications of artificial intelligence techniques have been used to convert human experience into a form of understandable by computers. Fuzzy logic provides a powerful and convenient formalism for classifying environmental conditions and for describing both natural and anthropogenic changes. Whereas traditional indices are based either on crisp sets with discontinuous boundaries between them, or on continuous variables whose values are only meaningful to experts, fuzzy sets make it possible to combine these approaches. From fuzzy logic it can be used to classify and quantify environmental effects of a subjective nature and it even provides formalism for dealing with missing data. The fuzzy memberships developed in this paper were used as water quality indices, but it is also possible to "defuzzify" them and to obtain a more traditional type of index [6].

A new groundwater modeling technique was developed in which fuzzy set theory is combined with finite difference modeling methods. Additionally, a rule based fuzzy-set approach to risk analysis of nitrate contaminated groundwater was presented in the study of Dahab [3]. Recently, neuro fuzzy techniques have been applied to predict groundwater vulnerability using GIS [4,7,8].

In this present paper, a fuzzy Simulink system was developed to assess the groundwater quality of Tiruchirappalli city corporation at previously selected seventy nine sampling stations. The applied water quality assessment system involves the selection of water quality parameters and index values to from BIS and WHO standards. Ranges of values were assigned to these parameters to form the input Membership Functions (MBF). In this application, twelve input variables, namely as pH, Ec, Ca^{++}, Mg^{++}, Na^{+}, Cl^{-}, Alkalinity, Total Hardness, SO_4, F, NO_3, and Coli forms were used to describe Water Quality Index (WQI) [9]. The input membership functions of the selected parameters have three linguistic terms defined as Acceptable, Non Acceptable and Rejected levels of groundwater.

The groundwater hydrochemistry records of the study area were used for the preparation of water quality maps. These maps were obtained by geostatistical (Kriging) methodology and the results are presented in the form of equal ion concentration lines [10]. The MATLAB V. 2008 (a) software was also used to analyse the data.

2. Study Area, Materials and Methods

2.1. Study Area

The Base map of Tiruchirappalli city was drawn from Survey of India Topo sheets Nos. 58 J/9, 10, 13 and 14 and satellite imagery (IRS-1C and LISS III) is lies between 10° 48' 18'' North: 78° 41' 7'' East. The general topology of Tiruchirappalli is flat and lies at an altitude of 78 m above sea level. Tiruchirappalli is fed by the ri- vers Cauvery and Kollidam. There are reserve forests along the river Cauvery. Golden Rock and the Rock Fort are the prominent hills. The southern/south-western part of the district is dotted by several hills which are thought to be an offset of the Western Ghats Mountain range and the soil is considered to be very fertile. For the sample collection, seventy nine bore well locations were identified. These locations were identified in such a way that the bore wells were evenly distributed over the study area.

The water samples were collected for periods between March 2006 and December 2008. The water from these bore wells were used for drinking, house hold utilities and bathing by the residents. The Laboratory tests were conducted on these samples for 16 different physicochemical potable water quality parameters as per the standard procedure [1,2,11] criteria are adopted for testing these samples.

2.2. Thematic Maps

The base map data used for the study included digitized data sets originally developed by Survey of India, the Tiruchirappalli city corporation. The data sets were originally digitized from 1:20,000 scale topographic maps. The work maps were prepared from 1 : 20,000 scale topographic paper maps using AutoCAD, Arc GIS 9.2 and Surfer V.7.

The groundwater hydrochemistry records of the study area were used for the preparation of maps. These maps are obtained by geostatistical (Kriging) methodology and the results were presented in the form of equal ion concentration lines [10,12,13].

The groundwater quality data were used as the hidden layer for the preparation of base maps. These features were the boundary lines between mapping units, other linear features (streets, rivers, roads, etc.) and point features (bore well points, etc.). The contours were developed for pH, EC, Cl^{-}, Na^{+}, Ca^{++}, Mg^{++}, Total Hardness, Alkalinity, F, SO_4^{-}, Coli form and NO^{-3} for the seasonal conditions of the study period between 2006 and 2008.

The monitoring and sampling program was initiated in 2006 and finalized the year 2008. A total of seventy nine monitoring stations were established of them represented groundwater conditions. The groundwater stations had different depths to groundwater. The sampling locations of all the stations are shown in **Figure 1**. A total of seventy nine separate ground water quality monitoring sessions were realized during the study period during the months of June, August, October and November of the year 2006-2008 and March, June and October of the year 2006-2008.

2.2.1. Potable Water Quality Maps

The data used for the mapping water quality assessment for potability were developed from the laboratory water quality analysis. Data for these studies were based on the sampling conducted by the first author for groundwater samples collected from predetermined locations of existing bore wells in Tiruchirappalli city. The data were linked to the sampling bore well locations using geodata base creation of Arc GIS 9.2 and surfer software.

The decision on the water quality assessment for potability gives that the water is desirable, acceptable and not acceptable as per the guidelines from BIS and WHO [1, 12] regulatory bodies. But, in the border line cases of water quality parameters, it becomes a Herculean task as different types of uncertainties are involved at various part of experimental and measurement process right from sampling, sample storage, processing and analysis. The sets of the monitored data and limits should not be as crisp set, but as fuzzy sets. One way of avoiding the difficulty in uncertainty handling in water quality assessment is to introduce a margin of safety or degree of precaution before applying a single value to drinking water quality standards as the same technique was also used by other workers in the field of environmental science [14-16]. These methodologies based on fuzzy set theory

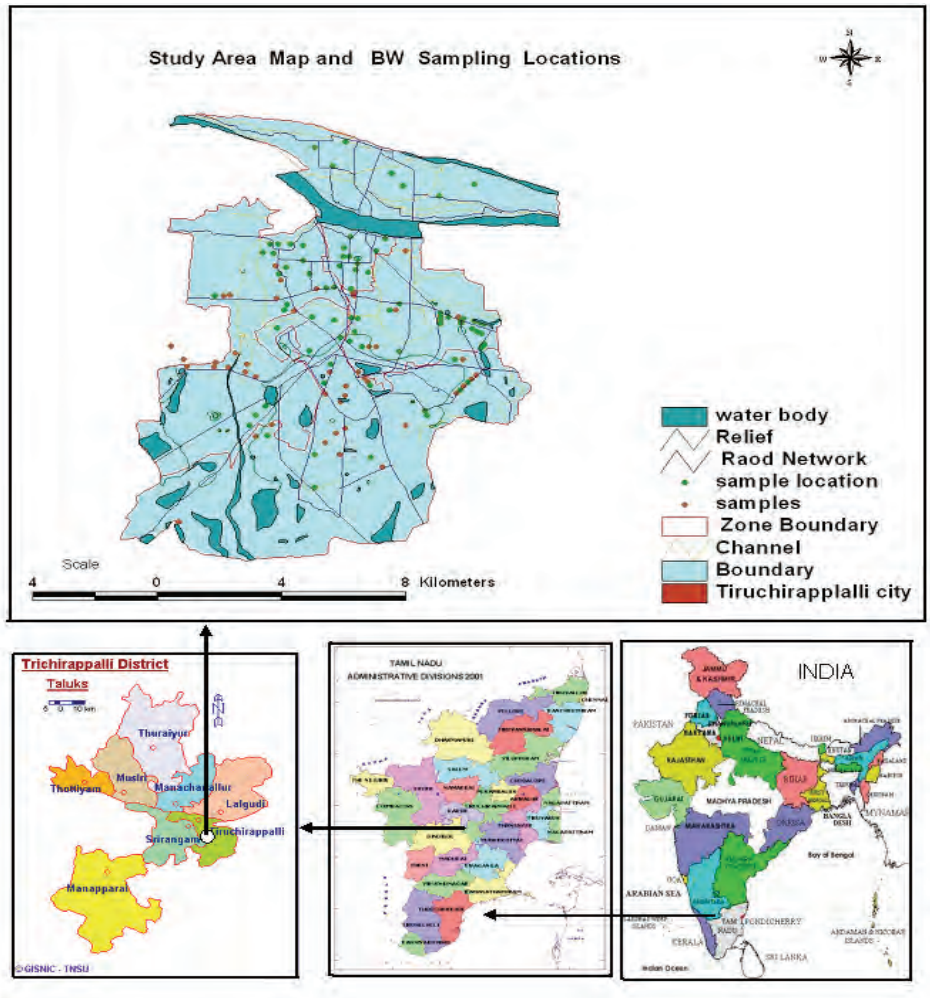

Figure 1. Study area map with sampling locations.

were utilized with real environmental water quality assessment to handle the uncertainties in imprecise environment in decision-making on the potability water quality can be handled. Keeping the importance of uncertainty handling in the drinking water quality assessment and versatility of the fuzzy set theory in decision-making. An attempt was made to classify the under ground water from Tiruchirappalli corporation, South India for the drinking purposes.

2.3. Fuzzy Sets

The theory of fuzzy sets was first introduced by [17] to model uncertainty in subjective information. Fuzzy sets are defined as sets whose members are vague objects. Data can generally be received in terms of linguistic judgments and beliefs (natural language), which can then be converted to the form of fuzzy sets in order to provide a base for logical and mathematical reasoning [18]. A fuzzy set is represented by a membership function defined on the universe of discourse. The universe of discourse is the space where the fuzzy variables are defined. The membership function gives the grade, or degree, of membership (μ) within the set, of any element of the universe of discourse. The membership function maps the elements of the universe on to numerical values in the interval (0, 1). A membership function value of zero implies that the corresponding element is definitely not an element of the fuzzy set, while a value of unit means that the element fully belongs to the set. A grade of membership in between corresponds to the fuzzy membership to set [13].

2.3.1. Fuzzy Rule Evaluation

Fuzzy rules appear no different to standard rules. They take the familiar form "IF x is a, THEN y is b", where x and y are linguistic variables, and where a and b are linguistic values. Under classical logic, the THEN *implication* is true of the IF condition, known as the *antecedent*, is evaluated as true. For fuzzy rules, the implication is set to be true to the same degree as the antecedent. Considering two linguistic variables *length* and *width*, and the rule "IF *length* is *a*, THEN *width* is *b*", If *a* is instantiated to a value then *b* is assigned to the value such that the membership of *b* is the same as that for *a*, each to their respective fuzzy sets. This process is known as monotonic selection. Antecedents with more than one statement are not a problem as the earlier rules for fuzzy union (disjunction, OR) and intersection (conjunction, AND) are applied. Similarly for consequents with multiple parts, the resultant antecedent membership is applied to all parts of the consequent.

2.3.2. Matching between Fuzzy Values

The fuzzy number for field data (A) on parameters and the fuzzy numbers (A') characterizing linguistic terms are matched together to arrive at a measure called a Degree of Match (DM) defined by: Erosy *et al.* (1992), [13]. DM ff (AA') = $\int \mu A \cap A' (x)\, dx / \int \mu A' (x) \Sigma\, dx$, $x \in X$. in which x denotes the universe, and $\mu A \cap A'$, x is membership grade for $A \cap A'$.

Furthermore, if A and A' are the discrete possibility distributions the measure is defined as:

$$DM\ ff\ (AA') = \Sigma\, \mu\, A \cap A' (x) / \Sigma\, \mu A' (x),\ x \in X.$$

2.4. Fuzzification

Fuzzification is the process of decomposing a system input and/or output into one or more fuzzy sets. Many types of curves can be used, but triangular or trapezoidal shaped membership functions are the most common. In this present study trapezoidal functions were used for the Input variables and triangular functions were utilized for output variables. Fuzzy sets span a region of input (or output) value graphed with the membership. Any particular input is interpreted from this fuzzy set and a degree of membership is interpreted. The membership functions should overlap to allow smooth mapping of the system. The process of fuzzification allows the system inputs and outputs to be expressed in linguistic terms so that rules can be applied in a simple manner to express a complex system.

2.4.1. Defuzzification

After fuzzy reasoning a linguistic output variable which needs to be translated into a crisp value. The objective is to derive a single crisp numeric value that best represents the inferred fuzzy values of the linguistic output variable. Defuzzification is such inverse transformation which maps the output from the fuzzy domain back into the crisp domain. Some defuzzification methods tend to produce an integral output considering all the elements of the resulting fuzzy set with the corresponding weights. Other methods take into account just the elements corresponding to the maximum points of the resulting membership functions [13]. The Mean of Maximum (MoM) method is used only in some cases where the Center of Maximum (CoM) approach does not work. In the CoM method, only the peaks of the membership functions are used. The defuzzified crisp compromise value is determined by finding the place where the weights are balanced. Thus the areas of the membership functions play no role and only the maxima are used. The crisp output is computed as a weighted mean of the term membership maxima, weighted by the inference results.

2.4.2. Fuzzy Logic Simulation System

In fuzzy logic system, the knowledge of the human is put in the form of a set of fuzzy linguistic rules. These rules would produce approximate decisions, just as a human would. The human expert observes quantities by observing the inputs, and leads to a decision or output using his judgment. The human expert can be replaced by a combination of a fuzzy rule-based system (FRBS) and a block called a defuzzifier. The inputs are fed into the FRBS, where physical quantities are represented into linguistic variables with appropriate membership functions. These linguistic variables are then used in a set of fuzzy rules within an inference engine, resulting in a new set of fuzzy linguistic variables. In defuzzification stage, the variables are combined and changed to a crisp output which represents an approximation to actual output [19].

Simulink models and sub models representing the complex interaction between various parameters are framed and used for twelve selected parameters. The grouping of parameters and rules designed for Simulink. A typical block diagram showing Simulink of first group water quality parameters viz. pH, EC, Cl^-, Na^+ is presented in **Figure 2**. Data collected from the study area for various seasons were used as the inputs for Fuzzy simulation model. The simulation was used for the collected data for seasonal variations. Based on Field experience, Delphi technique [20] and expert knowledge 66 rules are designed for physico-chemical water quality parameters in Group I as shown in **Figure 2**.

The parameters of the kind Total Alkalinity, Total Hardness, Calcium and Magnesium were the members of second group parameters and were selected with 73 design IF- THEN rules used in the Simulink process. The schematic block diagram is shown in **Figure 3**. The health concern parameters such as Sulphate, Fluoride [21], Nitrate and Coli forms were selected in group three and 42, IF – THEN rules were utilized based up on expert's knowledge and shown in **Figure 4**. Out puts from all the three groups that is the results obtained from first, second and third groups were combined and framed as final simulation model as shown in **Figure 5**. The quality assessment of groundwater of Tiruchirappalli city, a total of 27 rules was fired for the final assessment of ground-

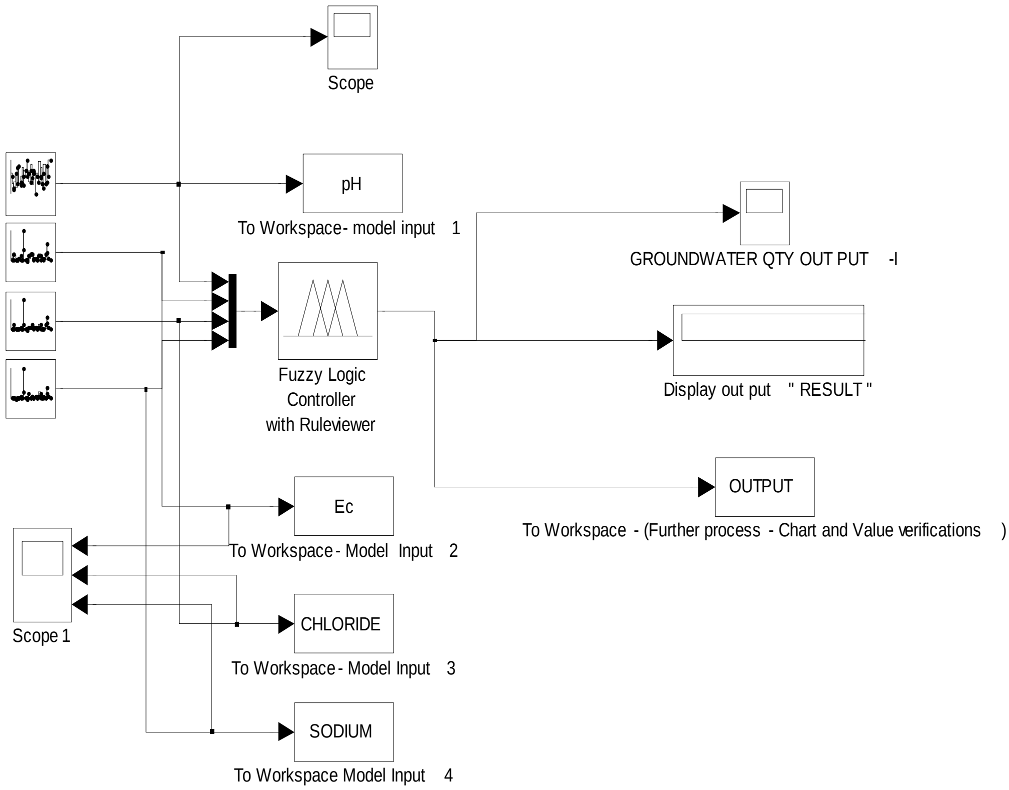

Figure 2. Block diagram for simulink process of FIP - First group water quality parameters.

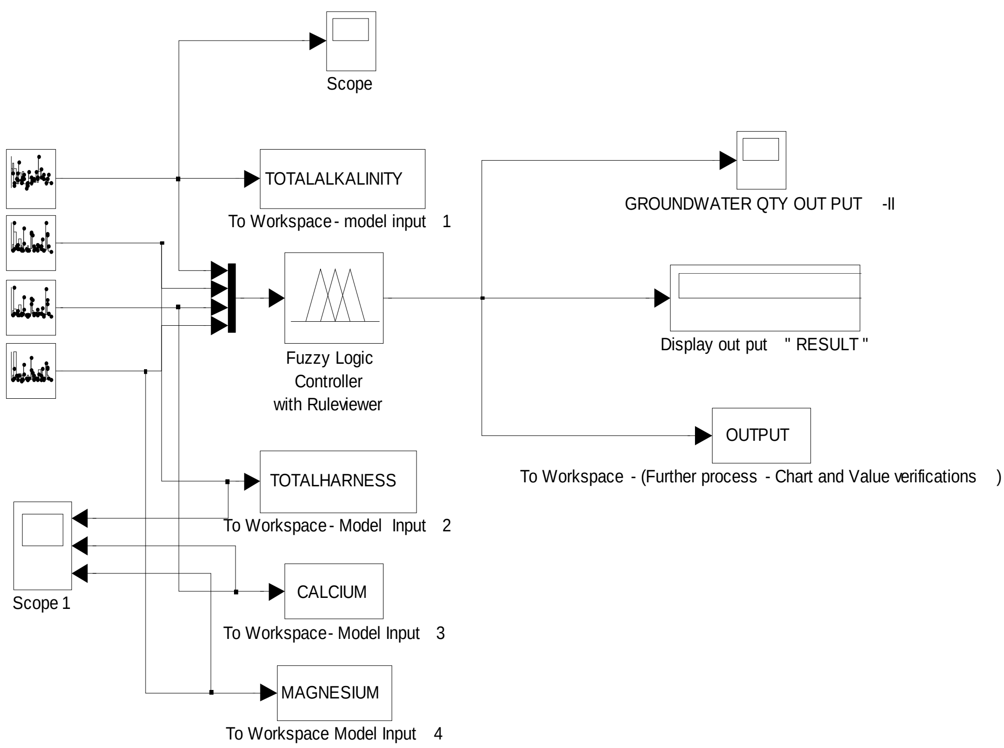

Figure 3. Block diagram for simulink process of FIP - Second group water quality parameters.

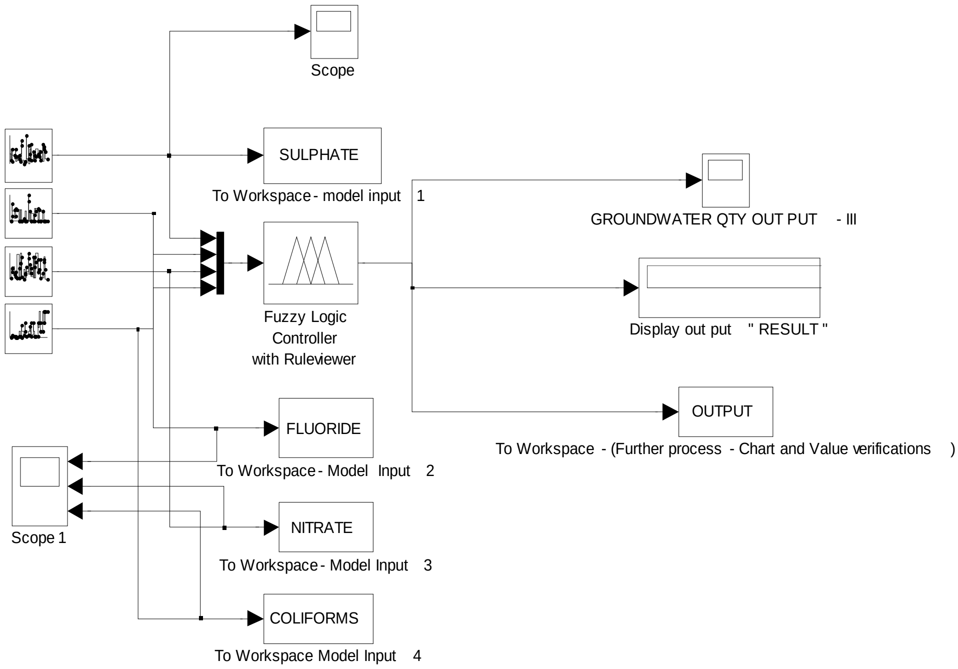

Figure 4. Block diagram showing simulink process of FIP - Third group water quality parameters.

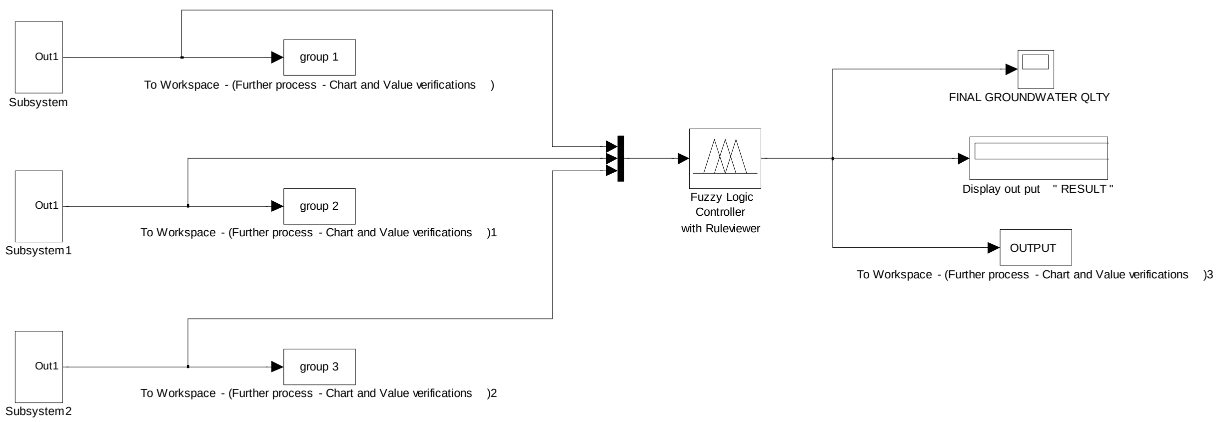

Figure 5. Block diagram for the fuzzy simulink process of FIP for water quality assessment.

water quality. The results from all the three groups are aggregated to assess the final classification of water as shown in block diagram **Figure 5**. The processes are applied to all the seasonal water samples and the results obtained are as shown in **Figure 6.**

The rule based decision on expert's perception was fired using Mamdani implification of maximum and minimum operator [22]. To assess the drinking water quality of the groundwater samples, 181 rules are fired.

2.5. Approach towards Groundwater Quality Assessment for Potability

A fuzzy rule based system is generated in which users classify the water according to given data in Desirable, Acceptable, Not acceptable, Rejected quality with respect to different parameters, all connected using AND operator [23]. The user's feedback is also taken with respect to overall quality for different parameters connected by AND operator. For example, one of the feedbacks taken may be like this, If TDS = good AND pH = medium and Sulphate = good then, overall water quality = High. After this, Delphi's technique [20] is applied to converge the feedback of various users to a single value; a degree of match is computed between the user's perception and field data for different parameters. For every type of water quality viz. good (Desirable) medium (Acceptable) or bad (Not Desirable). The water quality for which degree of match is the highest is considered to re-represent the quality of the water sample.

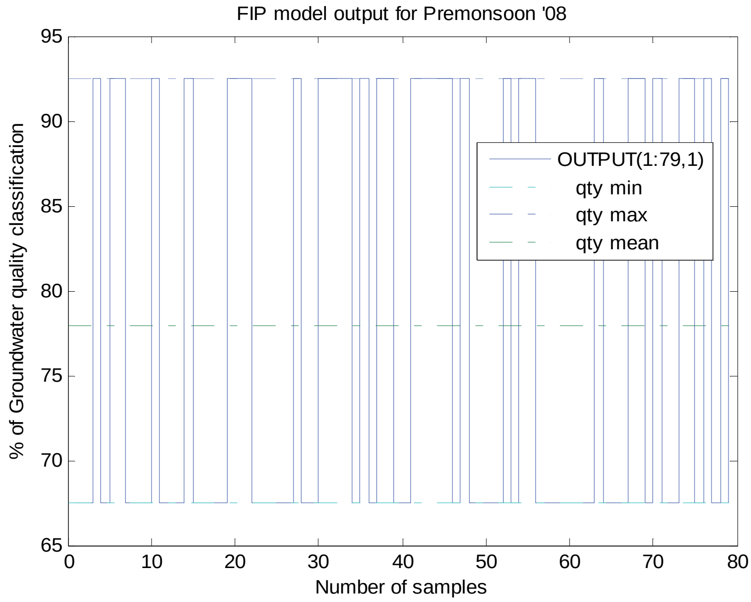

Figure 6. Subsurface water potable frequency showing Pre monsoon 2008.

3. Results and Discussions

Physio-chemical Groundwater quality assessment by deterministic method for drinking groundwater usage on the basis of 8 water quality parameters were compared with the concentration in the water with point value prescribed limits [21,23]. In case Groundwater quality model approach, these 8 parameters were divided in the four categories on the basis of expert opinion having their importance with respect to drinking water quality criteria.

The major findings of the research study are:

1) The accuracy of chemical analysis was verified by ionic balance errors and was found Minimal.

2)The hydro chemical analyses revealed that water samples in the study area was characterized by hard to very hard, fresh to brackish and alkaline in nature. The highly turbid water may cause health risk as excessive turbidity can protect pathogenic microorganisms from the effects of disinfectants and also stimulate the growth of bacteria during storage.

3) Characteristic by pH values, most of the water samples were alkaline in nature which are well within permissible limit (6.5 – 8.5) and some of the samples have been found acceptable for usage and the ranges are between 6.5 and 9.2 meeting BIS standards of IS: 10500: 1991 and WHO (2006) guidelines.

4) Based on Electrical Conductivity (Ec) values measured all water samples Zone-I (Srirangam) are desirable (< 1 mS/cm) for potability.

5) The microbial results indicated that all the samples exceeded the acceptable limit of drinking water. Presence of Salmonella and *Shigella* was also detected.

6) Although, the water samples contain significant concentrations of calcium, magnesium, sulphate, alkalinity ($HCO_3 + CO_3$) and potassium ions, predominant presence of two ions, sodium and chloride were found in the samples.

7) It was found that 60% of drinking water samples were found desirable for drinking purpose and the remaining samples could also acceptable for drinking in the absence of alternate water sources.

8) The groundwater quality assessment for potability using fuzzy logic controller has been estimated for Pre monsoon period (March to July) for the years 2006 to 2008. Potability indices show that the groundwater quality of bore well No. 25 of Zone–II (Ariyamangalam) was very low, as it is near to Municipal solid waste dumping yard. The lowest potability of 32.5% was found in bore well No. 73 of Zone–IV (K. Abisekapuram), located very near to sewer line and an open pond with stagnant water. The remaining bore wells in all the four zones records the potability between 67.5% and 92.5% and is illustrated in **Figure 7**.

9) The groundwater quality assessment for potability using fuzzy logic controller has been estimated for Post monsoon period (August to November) for the years 2006 and 2008. The potability of 32.5% for the bore well No. 59, 62, 63 and 73 of Zone–IV (K. Abisekapuram). The potability indices show that the groundwater qualities of these Bore wells were located very near to an open ponds and stagnant waste water during the rainy season. The remaining bore wells have the potability between 67.5% and 92.5% and are illustrated in **Figure 8**.

10) Digital Surface Model (DSM) diagrams were con-

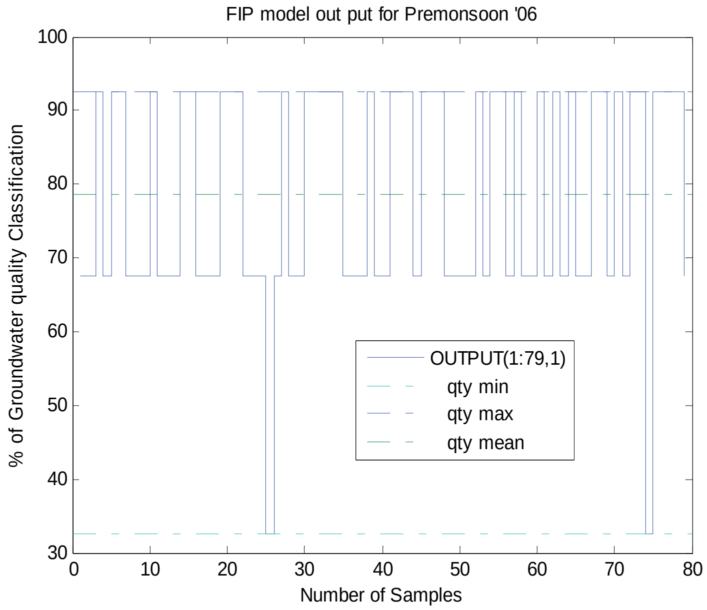

Figure 7. Subsurface water potable frequency during premonsoon periods 2006.

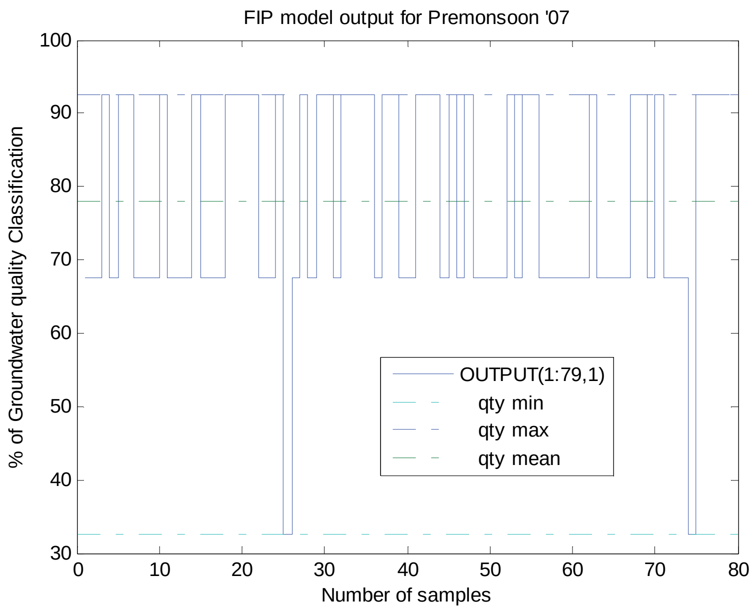

Figure 8. Subsurface water potable frequency during pre monsoon periods 2007.

structed directly from major anions and cations, so as to consider common behaviors within the study area. A typical DSM concentration based on Cl^- and HCO_3^- map is presented in **Figure 9**. There was high concentration in the Ariyamangalam zone makes the water non potable more than 50% of the sampled groundwater showed high chloride.

11) Pre-monsoon and post-monsoon contour potable water quality maps are constructed directly from major anions and cations from fuzzy Simulink model is shown in **Figure 10**. The contour maps of the equal concentrations based on standards is given in **Figure 10**.

The high risk was observed in the regions of Ariyamangalam zone consumption of ground water from the model during pre monsoon 2007. It was also noted that the market area and Ariyamangalam zone were the alarming zones of non potability regions during pre monsoon period 2006.

The high risks were noticed in some central parts of K. Abishekapuram towards Ariyamangalam due to the open pond and improper disposal of solid sluges.

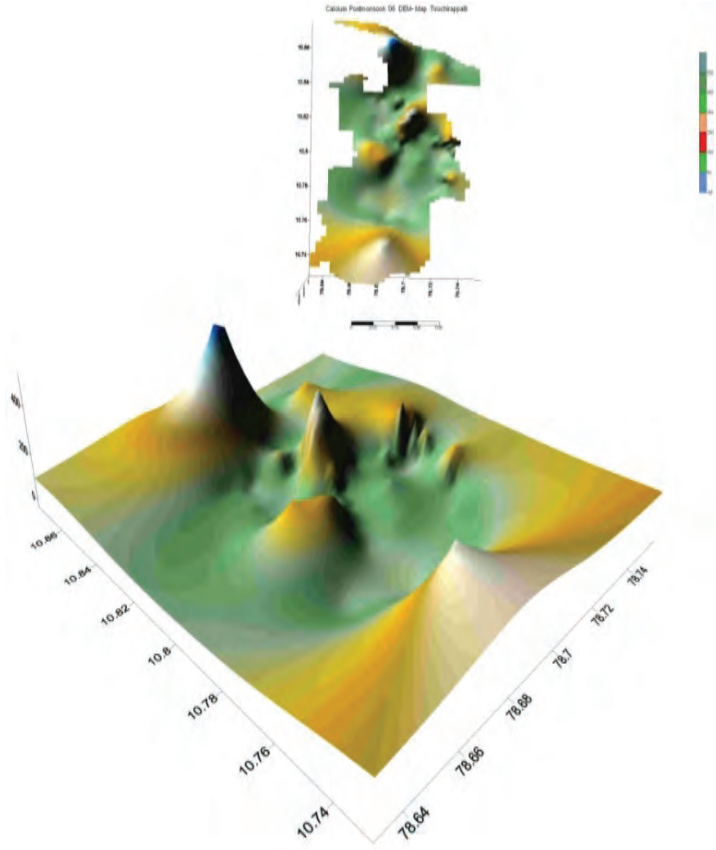

(a)

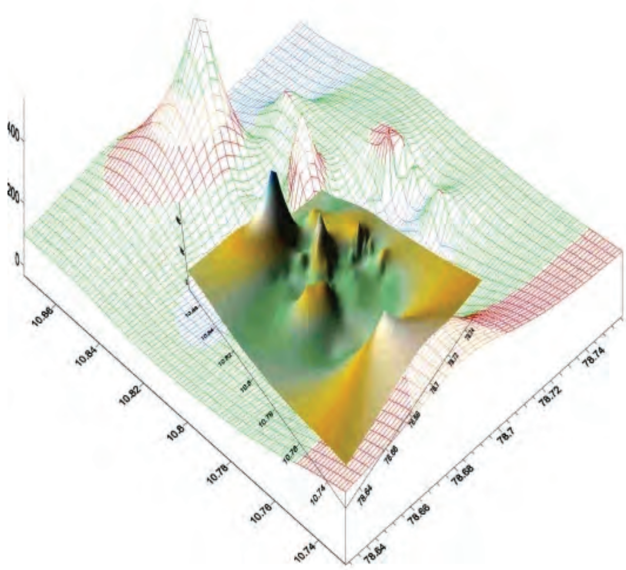

(b)

Figure 9. (a) DSM for chloride dispersion in Zone IV of Tiruchirappalli city; (b) DSM with Wire frame model for chloride dispersion in Zone IV of Tiruchirappalli city.

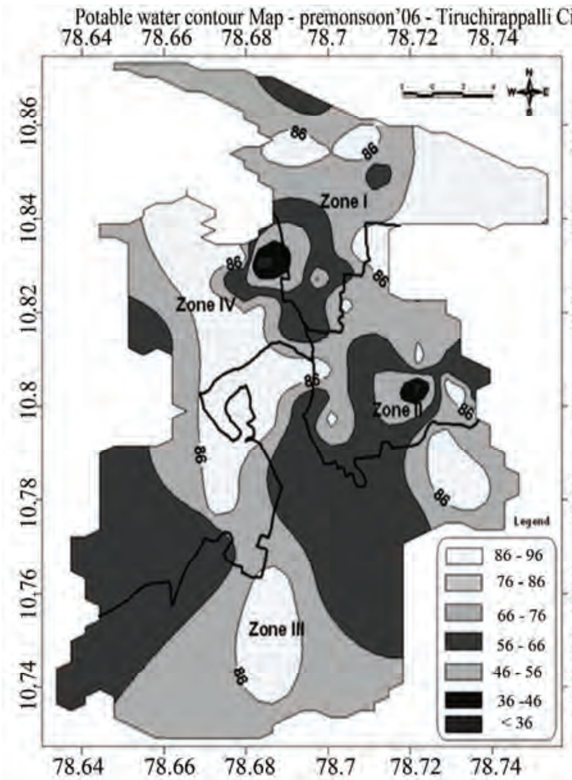

Potable Water Contour Map
Fuzzy Information Processing for
Groundwater Quality Assessment

Figure .Potable Water Contour Map (in %)

Duing Pre monsoon 2006

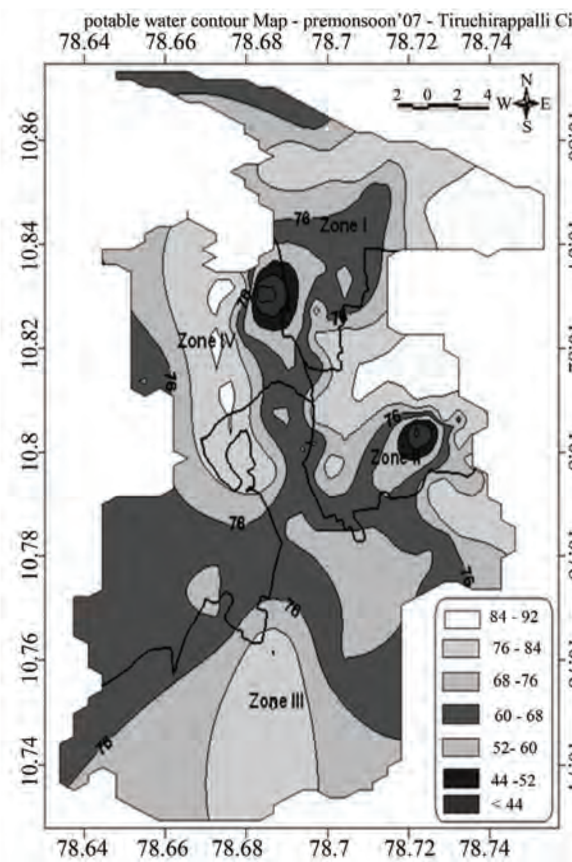

Potable Water Contour Map
Fuzzy Information Processing for
Groundwater Quality

Figure. Potable Water Contour Map (in %)

During Pre monsoon 2007

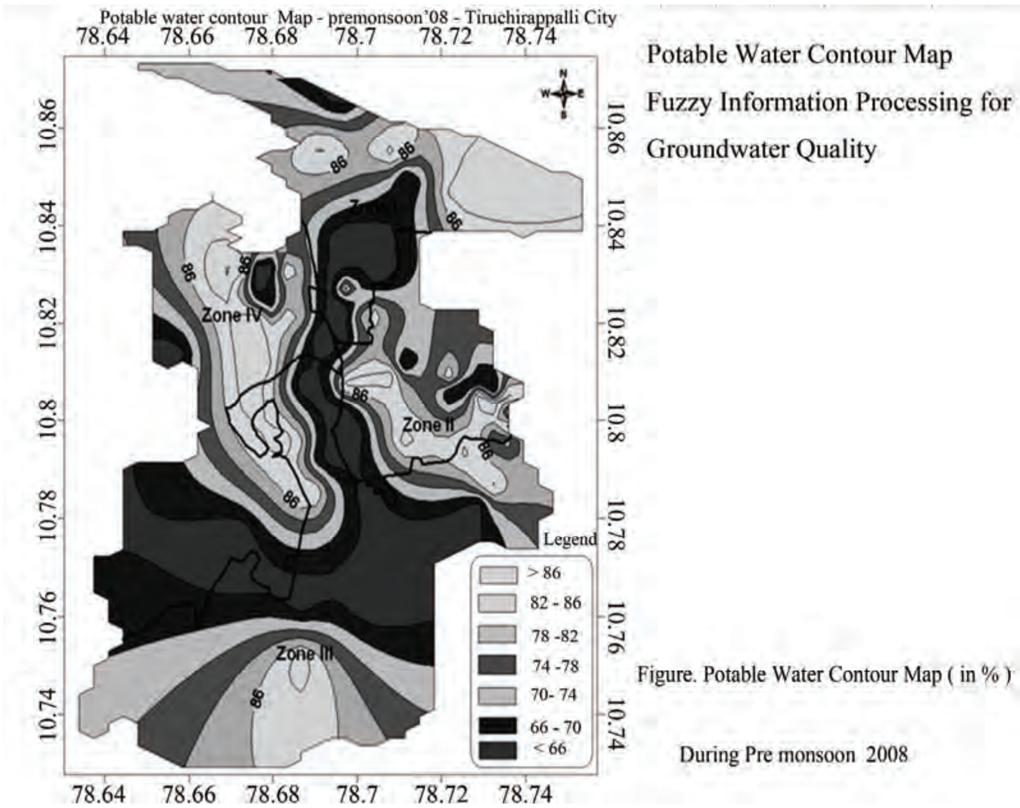

Figure 10. FIP potable water contour maps for pre monsoon 2006, 2007 and 2008.

4. Conclusions

The quality of the groundwater of the Tiruchirappalli city was monitored in 79 sampling wells for 3 years and major recorded data revealed that the concentrations of cations and anions were above the maximum, desirable for human consumption. The Electrical Conductivity was found to be the most significant parameter within input parameters used in the modeling. The developed model enabled well to test the data obtained from 79 samples of bore wells of Tiruchirappalli city.

- The groundwater in Tiruchirappalli meets all WHO drinking water standards with in the range of 67.5% to 92.5% for potable during pre monsoon condition of all the sampling durations.
- As the sampling station of 24 and 73 were found in non potable condition due to vicinity of wastewater discharging areas and solid waste dumping sites.
- During post monsoon all the sampling stations satisfies WHO [2] drinking water standards within in the range of 67.5% to 92.5%.
- At the stations 59, 62 and 72 were reported with non potablity of 32.5% due to unhealthy environmental conditions of wastewater and local waste dumps near by the sampling points.
- Solid wastes including sledges were disposed, and without any pre treatment before dumping and no protection towards the subsurface water for potability.
- In the previous study by the authors [13] the subsurface water quality in Ariyamangalam, Zone Tiruchirappalli City Corporation was seriously under threat by carbonates and sulphates near the sampling points of Ariyamangalam zone. Also contaminated by several pollutants as Ariyamangalam itself was currently polluted due to the waste dumping site and improper waste water vicinity.
- Without immediate response, the subsurface water is currently degrading its consumption quantity and will not be potable in near future if the proper steps have not been taken care.

5. Acknowledgements

The First author gratefully acknowledges the support by Fellowship under TEQIP, MHRD, and Govt. of India for his Doctoral study. The authors wish to express their sincere appreciation is also extended to the anonymous reviewers for their valuable comments to enhance the quality of this paper. Special thanks to Sarva Mangala Preveena for her constant support in preparation of this manuscript.

6. References

[1] Bureau of Indian Standard, "Indian Standard Specification for Drinking Water," BIS Publication No. IS (10501), New Delhi, 1991.

[2] World Health Organization, "Guidelines for Drinking Water Quality Recommendation," Vol. 2, World Health Organization, Geneva, 2008.

[3] M. F. Dahab, Y. W. Lee and I. Bogardi, "A Rule Based Fuzzy-Set Approach to Risk Analysis of Nitrate Contaminated Groundwater," *Water Sciences Technology*, Vol. 30, No. 7, 1994, pp. 45-52.

[4] B. Dixon, "Prediction of Groundwater Vulnerability Using an Integrated GIS Based Neuro-Fuzzy Techniques," *Journal of Spatial Hydrology*, Vol. 4, No. 2, 2004, pp. 38-41.

[5] R. Khaiwal and V. K. Garg, "Distribution of Fluoride in Groundwater and its Suitability Assessment for Drinking Purposes," *International Journal of Environmental Health Research*, Vol. 16, No. 2, 2006, pp. 163-166.

[6] K. Schulz and B. Howe, "Uncertainty and Sensitivity Analysis of Water Transport Modeling in a Layered Soil Profile Using Fuzzy Set Theory," *Journal of Hydroinformatics*, Vol. 1, No. 2, 1999, pp. 127-138.

[7] B. Dixon, H. D. Scott, J. C. Dixon and K. F. Steele, "Prediction of Aquifer Vulnerability to Pesticides Using Fuzzy-Rule Based Models of the Regional Scale," *Physical Geography*, Vol. 23, 2002, pp. 130-152.

[8] B. Dixon, "Application of Neuro-Fuzzy Techniques in Predicting Groundwater Vulnerability: A GIS Based Sensitivity Analysis," *Journal of Hydrology*, Vol. 309, No. 1-4, 2005, pp. 17-38.

[9] S. M. Preveena, M. H. Abdullah, A. Z. Aris and K. Bidin, "Groundwater Solution Techniques: Environmental Applications," *Journal of Water Resource and Protection*, Vol. 2, 2010, pp. 8-13.

[10] Z. K. Sen, "Fuzzy Groundwater Classification Rule Derivation from Quality Maps," *Water Quality Exposure Health*, Vol. 1, No. 1, 2009, pp. 115-112.

[11] American Public Health Association, "Standard Method for Examination of Water and Waste Water," 21st Edition, American Public Health Association, Washington, DC., 2005.

[12] B. Shomar, S. A. Fkher and Alfred Yahya, "Assessment of Groundwater Quality in the Gaza Strip, Palestine Using GIS Mapping," *Journal of Water Resource and Protection*, Vol. 2, No. 2, 2010, pp. 93-104.

[13] V. Kumar, N. S. Mathew and G. Swaminathan, "Fuzzy Information Processing for as Assessment of Groundwater Quality," *International Journal of Soft Computing*, Vol. 4, No. 1, 2009, pp. 1-9.

[14] Z. Chen, G. H. Huan and A. Chakma, "Hybrid Fuzzy-Stochastic Modeling Approach for Assessing Environmental Risks at Contaminated Groundwater Systems," *Journal of Environmental Engineering*, Vol. 129, 2003, pp. 79-88.

[15] S. Liou and S. A. L. Wang, "Generalized Water Quality Index for Taiwan," *Environmental Monitor Assessment*, Vol. 9635-52, 2004.

[16] S. Liou and S. L. Lo, "A Fuzzy Index Model for Tropic Status Evolution of Reservoir Waters," *Water Research*, Vol. 96, No. 1, 2004, pp. 35-52.

[17] L. A. Zadeh, "Fuzzy Set," *Information Control*, Vol. 8, No. 3, 1965, pp. 338-353.

[18] L. A. Zadeh, 'The Concept of a Linguistic Variable and its Application to Approximate Reasoning," *Information Science*, Vol. 8, 1975, pp. 199-249.

[19] M. Jamshidi, "Tools for Intelligent Control: Fuzzy Controllers, Neural Networks and Genetic Algorithms," *Philosophical Transactions of the Royal Society*, Vol. 361, No. 1809, 2003, pp. 1781-1808.

[20] C. Okoliand and S. D. Pawlowski, "The Delphi Method as a Research Tool an Example, Design Considerations and Applications," *Information and Management*, Vol. 42, No. 1, 2004, pp. 15-29.

[21] V. K. Garg, S. Dahiya, A. Chaudhary and Deepshikha "Fluoride Distribution in Underground Waters of Jind District, Haryana, India," *Ecology Environmental Conservation*, Vol. 4, No. 172, 1998, pp. 19-23

[22] E. M. Mamdani, "Advances in the Linguistic Synthesis of Fuzzy Controllers," *International Journal of Man-Machine Studies*, Vol. 8, No. 6, 1976, pp. 669-678.

[23] N. Chang, H. W. Chen and S. K. King, "Identification of River Water Quality Using the Fuzzy Synthetic Evaluation Approach," *Journal Environmental Management*, Vol. 63, 2001, pp. 293-305.

[24] C. O. Cude, "Water Quality Index: A Tool for Evaluation Water Quality Management Effectiveness," *Journal of the American Water Resources Association*, Vol. 37, No. 1, 2001, pp. 125-137.

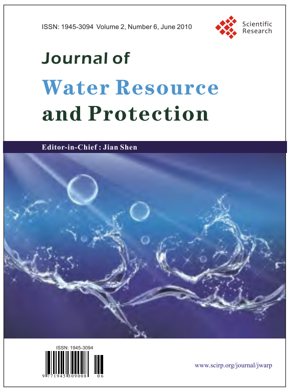

Call for Papers

Journal of Water Resource and Protection (JWARP)

http://www.scirp.org/journal/jwarp
ISSN:1945-3094 (Print), 1945-3108 (Online)

JWARP is an international refereed journal dedicated to the latest advancement of water resource and protection. The goal of this journal is to keep a record of the state-of-the-art research and promote the research work in these fast moving areas.

Subject Coverage

This journal invites original research and review papers that address the following issues in water resource and protection. Topics of interest include, but are not limited to:

- Water resources and quality assessment
- Rivers, lakes and estuary systems
- Wastewater treatment and sludge biotreatment
- Water purification and water supply
- Water source protection and sustainable use
- Modeling, measuring and prediction of water pollution
- Ground water pollution control
- Reactions and degradation of wastewater contaminants
- Other topics about water pollution

We are also interested in short papers (letters) that clearly address a specific problem, and short survey or position papers that sketch the results or problems on a specific topic. Authors of selected short papers would be invited to write a regular paper on the same topic for future issues of the *JWARP.*

Notes for Intending Authors

Submitted papers should not have been previously published nor be currently under consideration for publication elsewhere. Paper submission will be handled electronically through the website. All papers are refereed through a peer review process. For more details about the submissions, please access the website.

Website and E-Mail

http://www.scirp.org/journal/jwarp Email: jwarp@scirp.org

J. Water Resource and Protection, 2010, 2, 501-608.
Published Online June 2010 in SciRes (http://www.SciRP.org/journal/jwarp).

TABLE OF CONTENTS

Volume 2 Number 6 **June 2010**